AN ABSTRACT OF THE DISSERTATION OF

Trevor R. Tivey for the degree of Doctor of Philosophy in Integrative Biology presented on June 13, 2019.

Title: Cellular Recognition, Division, and Proliferation in the Cnidarian-Dinoflagellate Symbiosis.

Abstract approved: _____
Virginia M. Weis

Cnidarians and their symbiotic dinoflagellates form a productive mutualism that shapes marine environments. In this symbiosis, dinoflagellate species from the family Symbiodiniacea reside within cnidarian host gastrodermal cells and provide the host with photosynthetically fixed carbon in exchange for host metabolites. This nutritional exchange allows both partners to thrive in nutrient-limited tropical environments. One important consequence of this relationship is the formation of coral reef ecosystems, which serve as important marine habitats for biodiversity. As sea surface temperatures continue to warm as a result of anthropogenic climate change, these cnidarian-Symbiodiniaceae symbioses face physiological challenges that can result in cellular stress and changes in host-symbiont biomass ratios. The success of endosymbionts relies on (1) effective recognition and uptake by host cells, (2) population growth and distribution through cell proliferation of host and symbiont cells, and (3) resilience in the face of environmental stressors. This dissertation therefore examines these aspects of host-symbiont cellular regulation during the establishment, maintenance, and breakdown of symbiosis in the sea anemone *Exaiptasia pallida* (commonly referred to as Aiptasia).

In cnidarians, symbiont uptake is mediated through innate immune pathways of recognition. Glycan-lectin interactions are an important subset of these pathways, in which symbiont surface glycans are recognized by cnidarian host proteins known as lectins during the onset of symbiosis. In Chapter 2, the surface glycans of symbionts were experimentally manipulated and characterized to determine the effect of altered N-glycan

composition on uptake by Aiptasia. The biosynthesis pathway of N-glycans was characterized and inhibited in the Symbiodinacea species *Breviolum minutum*. Inhibition of the N-glycan biosynthesis pathway resulted in a significant increase in the proportion of high-mannose glycans but not in the abundance of N-glycans. Hosts experienced a decrease in the uptake of experimentally treated *Breviolum minutum*. This work reveals that glycan complexity plays a functional role during the establishment of symbiosis.

In Chapter 3, the examination of host-symbiont regulation continued during the proliferative colonization phase. The cell proliferation of Aiptasia was investigated in the symbiotic and aposymbiotic state, and the cell cycles of two *Breviolum* symbionts were analyzed from algal cultures and host isolates. Localized host cell proliferation was found to correlate with regions containing proliferating symbionts. Overall, hosts undergoing colonization had increased levels of cell proliferation compared to aposymbiotic hosts. The location of cell proliferation also significantly shifted from the epidermis in aposymbiotic hosts towards the gastrodermis in colonizing symbiotic hosts. In contrast to the relationship between proliferating host cells and their colonizing symbionts, the cell cycles of symbionts in fully symbiotic hosts appeared to be restricted. The cell cycles of *Breviolum* species *in hospite* exhibited increased S-phase populations but decreased G_2M-phase populations, which resembled their respective cell cycles in nutrient-limited cultures. *B. psygmophilum* appeared to have increased S-phase populations and wider G_1-phase population peaks than *B. minutum*. These cell cycle differences between species suggest a role for cell cycle regulation in mechanisms governing nutrition and host-symbiont specificity.

In Chapter 4, a noninvasive method was developed to monitor the patterns of symbiont proliferation during recolonization and thermal stress. Successful recolonization by symbiont populations consisted of local growth from symbiont clusters as well as the consistent establishment of new symbiont clusters during the first two weeks. Clusters with increased densities of symbionts declined immediately after thermal stress, whereas singlet symbiont populations persisted for a longer period. The importance of host-symbiont specificity was observed when comparing the rapid, consistent recolonization by homologous symbiont *B. minutum* to the slower, inconsistent

recolonization by heterologous symbionts *Symbiodinium microadriaticum* and *Durusdinium trenchii*. However, after recolonization was established, *B. minutum* colonization was more susceptible to bleaching from the effect of thermal stress. Symbionts *S. microadriaticum* and *D. trenchii* persisted longer in Aiptasia under thermal stress. These differences in the establishment and resilience of symbiont recolonization emphasize the need for understanding the underlying mechanisms that govern successful cnidarian-dinoflagellate associations.

In summary, the work presented in this dissertation details the cellular regulation of cnidarian-Symbiodiniaceae symbioses. Differences between symbiont species and the composition of their cell surfaces have an effect on the success and nature of their symbioses with their cnidarian hosts. The results of this dissertation underscore the importance of shared cellular mechanisms that control many aspects of these symbioses, including the establishment and homeostasis of the association.

Cellular Recognition, Division, and Proliferation in the Cnidarian-Dinoflagellate Symbiosis

by
Trevor R. Tivey

A DISSERTATION

submitted to

Oregon State University

in partial fulfillment of
the requirements for the
degree of

Doctor of Philosophy

Presented June 13, 2019
Commencement June 2020

Doctor of Philosophy dissertation of Trevor R. Tivey presented on June 13, 2019.

APPROVED:

Major Professor, representing Integrative Biology

Chair of the Department of Integrative Biology

Dean of the Graduate School

I understand that my dissertation will become part of the permanent collection of Oregon State University libraries. My signature below authorizes release of my dissertation to any reader upon request.

Trevor R. Tivey, Author

ACKNOWLEDGEMENTS

I consider myself extremely fortunate to have been surrounded by mentors, families, and friends who have all supported me through this process. First and foremost, I would like to thank my advisor, Virginia Weis, for believing in me and my work from the very beginning. When I first came to Oregon State University, she took the time to meet with me weekly to travel back in time through the literature to review fundamental questions regarding symbiosis. I immediately got the sense that she would support whatever path I chose to take through my doctoral studies. Looking back, Virginia has not only supported my decision-making but also helped me to develop into a better scientist and writer. She has always been warm-hearted and understanding, creative and funny, and most importantly encouraging and inspiring.

I would like to thank the members of my committee, Barb Taylor, Tom Sharpton, Eli Meyer, Mark Leid, and Jim Strother for their help throughout my Ph.D. Their conversation and comments and have guided the overall design and direction of this dissertation and my thought process through six years of scientific training. Thanks to Sandra Loesgen who provided critical help to my dissertation. I would also like to thank the faculty members of the SSIMBIO group for providing me with an opportunity to think about how symbiosis fits within the holistic approach of systems biology.

The Integrative Biology department has been incredibly supportive over the past six years. I especially thank the office staff past and present (Tara, Traci, Trudy, Tresa, Torri, and Jane) for keeping me on track and answering any questions I've ever had. In addition to this support, I feel incredibly fortunate for the teaching mentors and teaching experience I received from this department. I thank Lori Kayes for her amazing coordination of GTAs year to year, and for her belief in my teaching. I thank Jessica Beck for the number of opportunities she has provided me for mentorship. I also thank Devon Quick for her help and insightful conversations. I especially thank Lindsay Biga, who has been an inspiring mentor and ally for me over my last few years.

I wouldn't be where I am today without the past and present members of the Weis lab. When I came into the lab, Angela Poole, Cammie Crowder, Sheila Kitchen, and Nate Kirk were all incredibly welcoming. They are genuine and collaborative; the relationships

I have had with them have shaped how I do science. Thanks also to our current graduate students. Thanks to Val Lapacek for heeding Virginia's advice to make sure I have space to focus, but being available to chat when I needed a break. Thanks to Shumpei Maruyama who has helped me challenge my way of thinking while also making me laugh. A special thanks is needed for John Parkinson and Jason Presnell, who have served as fantastic mentors and friends. Additional thanks are needed for Morgan and Allie, who have helped to provide some levity over this past year. Finally, I especially thank Jack Koch for his friendship and advice. From the time he came into the Weis lab, he has been an unstoppable force and a great friend. I thank him and his wife Morgan for bringing me into their lives.

I'd like to show my appreciation for the support from all of my friends I've made during my time at Oregon State University and all of my friends from my past that have continued to support me through this process, with a special thanks to Stephanie, Dave, and Danny. Thanks to my graduate cohort, who established the EBC in 2013 and never looked back. Thanks to David Taylor for our much-needed conversations about life. Thanks to Natalie and Ali for sharing their home, and to Carmen and Tim for sharing their porch. A special thanks is needed for Leah Segui, Brian Tanis, Kyle Coblentz, Jenna and Joe Stack, Danielle Tom, Syl Wyant, Ian Morelan, and Shannon Hennessey. Another special thanks is needed for Javier Tabima, who brought me into a tremendously supportive community which I can't even begin to thank enough. Finally, thanks and good luck to Katie Dzeidzic, who has shared so many experiences with me including our defense date.

Lastly, I'd like to thank my family for their support over the years. I thank my parents, Meg and Maurice, and my sister Kristen. You each continue to provide me with love and inspiration no matter where I go. I also thank my other family, Jen, Andy, and Eliza for their love and unwavering of support. In addition, I wouldn't have enjoyed this journey without the love from pets past and present, especially Kelpie and Peregrin. Finally, I am eternally grateful to my wife Aurora. She is an amazing, one-of-a-kind human being and I couldn't have done any of this without her love and support.

CONTRIBUTIONS OF AUTHORS

Chapter 2: Sandra Loesgen and Virginia Weis helped to design the experiments and provided significant contributions to chapter revisions. Paige Mandelare and Donovon Adpressa provided reagents, prepared figures, and helped with experiments. Paige Mandelare and John Parkinson also provided significant contributions to chapter revisions.

Chapter 3: Virginia Weis and John Parkinson made significant contributions to the design of experiments and the revision of this chapter and the work within the appendices. Mamo Waianuhea helped with the initial experimental design and data collection of Aiptasia under different symbiotic and nutritional states.

Chapter 4: Tyler Coleman made significant contributions to the method development, experimental design, data collection, and data analysis. Milan Sengthrep and Debbie Kim also helped with data collection. Virginia Weis provided significant contributions to chapter revisions.

TABLE OF CONTENTS

TABLE OF CONTENTS (Continued)

Page

TABLE OF CONTENTS (Continued)

Page

TABLE OF CONTENTS (Continued)

Page

TABLE OF CONTENTS (Continued)

Page

LIST OF FIGURES

LIST OF TABLES

LIST OF APPENDIX FIGURES

LIST OF APPENDIX TABLES

Cellular Recognition, Division, and Proliferation in the Cnidarian-Dinoflagellate Symbiosis.

1. Introduction

Many essential and charismatic biological partnerships fall under the category of symbiosis, defined as the relationship between organisms living in close and sustained proximity (Douglas, 2010). These associations range from parasitism to mutualism, and the continued success of each partner in the relationship relies on a dynamic balancing act between organisms. Within even mutualistic symbioses, many partners exert forms of control over the other so as to gain the most out of the interaction (Sachs et al., 2018). A substantial proportion of these symbiotic relationships are endosymbioses, where a microbial symbiont lives inside of a larger host. Endosymbiosis is fundamental to biological systems; it has critically provided the biological basis for the evolution of eukaryotes through the incorporation of bacterial symbionts into the mitochondria and plastids of their hosts (Sagan, 1967; Schwartz and Dayhoff, 1978). Many current endosymbiotic partnerships serve as the foundations of ecosystems: mycorrhizal fungi directly shape plant community structure, chemoautotrophic bacteria enable nutrient acquisition in deep-sea invertebrates, and microbial communities expand the diets of animals and shape their evolutionary history (Cavanaugh et al., 1981; Heijden et al., 1998; McFall-Ngai et al., 2013). The intimate nature of these relationships expedites the transfer of nutrients and metabolites between partners, which allows for the survival of both partners in nutrient poor environments (Douglas, 2010). However this intimacy can also lock partners into evolutionary spirals consisting of genome degeneration and reduction in their capacity to adapt to new environmental or ecological challenges, thus increasing the risk of extinction (Bennett and Moran, 2015). Though resilience exists in many mutualisms, the majority of mutualistic symbioses are increasingly threatened from rapidly changing environments due to human processes (Toby Kiers et al., 2010). It is

imperative that we understand the dynamic interactions that regulate these symbioses in order to predict their responses in our changing world.

One important type of endosymbiosis forms between photoautotrophic microbial symbionts and heterotrophic host partners (Johnson, 2011). In these relationships, carbon is fixed by the symbiotic algae and moved to their hosts in return for metabolites and a high light environment (Muscatine and Lenhoff, 1963). Many members from the phylum Cnidaria have evolved these types of symbiotic relationships with photosynthetic algae. These nutritional relationships have enabled cnidarians to thrive and create biologically diverse ecosystems such as coral reefs. The formation of these reefs originates from their symbiosis; cnidarian hosts use photosynthetically fixed carbon from their dinoflagellate symbionts to deposit calcium carbonate and create a skeleton (Pearse and Muscatine, 1971). Unfortunately, coral-dinoflagellate symbioses are among the most threatened mutualisms as a consequence of rapidly increasing sea surface temperature maxima (Carpenter et al., 2008; Hughes et al., 2018). As these coral reef ecosystems continue to decline, it is more essential than ever to study the cellular regulation in the cnidarian-dinoflagellate symbiosis so that we can expand our toolset to better predict and mitigate ecosystem loss (Davy et al., 2012; Fransolet et al., 2012; Goldstein and King, 2016; Weis et al., 2008). The following sections aim to further describe the cnidarian-dinoflagellate partnership and to summarize current understanding of their cellular regulation during important phases of symbiosis.

1.1 Cnidarian-dinoflagellate symbiosis: the players

Many cnidarians rely on symbiotic relationships with the dinoflagellate family Symbiodiniacea, formerly the genus *Symbiodinium* (LaJeunesse et al., 2018). Species from this family can either be free-living or reside in hosts from diverse phyla including sponges, cnidarians, molluscs, and foraminifera (Kirk and Weis, 2016). In some groups, the dependence of hosts on algal symbionts has evolved over a substantial period of time. For example, reef-building scleractinian corals have had associations with photo-symbionts since they appeared over 200 million years ago (Muscatine et al., 2005). The Symbiodiniaceae are thought to have appeared 160 million years ago, and there is molecular evidence of speciation in co-occurrence with the Jurassic adaptive radiation of

scleractinian corals as well as the Paleogene adaptive radiation of soritid foraminifera (LaJeunesse et al., 2018; Pochon et al., 2006). The Symbiodiniacea family is currently composed of functionally diverse genera, organized from previous alphabetically-named clades (LaJeunesse et al., 2018). Evidence of host-symbiont specificity exists at the genus level: a restricted set of Symbiodiniacea genera form associations with cnidarians, and another restricted set form associations with foraminifera, including the most recently discovered Clade I (genus not yet named) (Pochon and Gates, 2010). Within these genera there is further host-symbiont specificity. There is no shortage of cnidarian host diversity; a large variety of hydroids, jellyfish, sea anemones, and corals are able to host particular Symbiodiniacea species. These associations with a particular species of symbiont can be general to many hosts or specific to a restricted set of host cnidarian taxa. This range of host-symbiont specificity is thought to derive from a combination of factors including host-symbiont recognition, symbiont genetic composition and physiology, and host-symbiont ecological processes such as biogeography and thermal history (Baker, 2003; Rodriguez-Lanetty et al., 2004; Weis et al., 2001).

Cnidarian-Symbiodiniaceae symbioses are abundant across tropical and some temperate marine environments, and provide ecologically and economically significant biotic, structural, biogeochemical, and cultural services (Moberg and Folke, 1999). The coral reef environments that they construct serve as important havens for biodiversity, fisheries, tourism, and ocean productivity (Hughes et al., 2003). Today, many of these unique relationships are under stress because of a rapidly changing environment (Hoegh-Guldberg et al., 2007; Maynard et al., 2015; van Hooidonk et al., 2013). Under environmental stress, particularly elevated temperature, the symbiosis turns to dysbiosis in a process is known as bleaching: cnidarian hosts visibly lose color as their populations of brown algal symbionts are lost. As coral reefs continue to bleach worldwide at an alarming rate, the destruction of reef habitat also further hinders the establishment of new reefs and possibly results in a bottleneck for biodiversity (Chaves-Fonnegra et al., 2018; Hughes et al., 2019). To understand how the host and symbiont partners function together and why cnidarian-Symbiodiniaceae associations are under stress, we must understand the mechanisms that underlie initiation, maintenance, and breakdown of symbiosis.

1.2 Establishment of symbiosis

The onset of cnidarian-dinoflagellate symbiosis can occur throughout cnidarian development but generally occurs during cnidarian larval stages. Cnidarian larvae can inherit Symbiodiniaceae populations from a parent (vertical transmission), or they can acquire symbionts from the environment (horizontal transmission) (del C. Gomez-Cabrera et al., 2008; Schwarz et al., 2002). Symbiodiniaceae cells are housed in nutritive phagocytic cells which line the host gastrovascular cavity in a tissue layer known as the gastrodermis. In most cnidarian-dinoflagellate symbioses, Symbiodiniaceae cells reside in vacuoles known as symbiosomes and proliferate within host gastrodermal cells (Wakefield et al., 2000; Wakefield and Kempf, 2001). When Symbiodiniaceae cells enter the cnidarian gastrovascular cavity they are phagocytosed into an endosomal vacuole within endodermal cells. Unlike food particles or recognized pathogens, however, the symbionts avoid degradation and persist (Fitt and Trench, 1983a).

There are many molecular interactions that occur between host and symbiont surfaces during the onset of symbiosis. These inter-partner signaling events are hypothesized to be involved in recognition, specificity, and maintenance of the symbiosis (Meyer and Weis, 2012; Nyholm and McFall-Ngai, 2004; Weis et al., 2001). Cnidarians they have a conserved innate immune system which governs recognition of foreign invaders through a variety of molecular pathways (Dunn, 2009; Miller et al., 2007). During the colonization of hosts, many of these recognition pathways are differentially expressed, including complement pathway genes and thrombospondin-type1 repeat domain genes (Neubauer et al., 2017; Poole et al., 2016). Disruption of other immune pathways, such as scavenger receptors, have resulted in decreased colonization (Neubauer et al., 2016). These pathways work together to keep out pathogens, but importantly they can also be modulated to allow acceptance and tolerance the presence of their symbionts (Bosch, 2013).

1.2.1 Glycan-lectin interactions

An important subset of host-symbiont interactions involves the recognition of symbiont glycans (carbohydrates composed of glycosidically-linked monosaccharides)

by host surface lectins (carbohydrate-binding proteins). Host recognition of symbiont glycome characteristics can provide host cells with information about symbiont identity. This information is critical for host cells involved in cell-trafficking, cell-cell adhesion, and pathogen recognition, but it can also be used by invading cells to mask and protect themselves from host immunity (Varki, 2017). Glycans can either be covalently attached to proteins through amino acid attachments to form a variety of glycoproteins and proteoglycans, or to lipids to form glycolipids and GPI anchors. Out of the many types of glycans that constitute the glycome, the glycosylation of proteins has been studied the most thoroughly in the cnidarian-Symbiodiniaceae symbiosis. Through lectin-binding experiments, significant differences between cell surface glycan abundances have been described across diverse Symbiodiniacea species (Logan et al., 2010). Unlike the relatively simple and restricted glycomes found in other protists, the Symbiodiniacea family appears to have rich and diverse sets of glycans (Hashimoto et al., 2009). Though studies have demonstrated the negative effect of altering symbiont glycans on host colonization, it remains unclear how specific glycan-lectin interactions mediate symbiont-host recognition and engulfment (Lin et al., 2000; Wood-Charlson et al., 2006).

1.2.2 Colonization through proliferation

Several molecular pathways have been examined in the context of the initial recognition and uptake of Symbiodiniaceae, however we have limited understanding of the spatial and temporal nature of subsequent symbiont colonization within the cnidarian host gastrodermal tissue. The proliferation of symbionts takes place within host cells and their distribution throughout the cnidarian gastrodermal tissue is probably dependent on host cell proliferation. Space is especially limited within the small, gastrodermal cells of anthozoan host cells. As a result, the number of symbiont cells per host cell tends to be low, on average one to two symbionts cells (Muscatine et al., 1998). In other cnidarians such as hydroids, the number of symbiont cells per host is increased, due to the larger host cell sizes (Fitt, 2000; McAuley and Cook, 1994; Muscatine et al., 1998). Studies examining the effect of host nutrients on the number of symbionts per host cell and the coordination of cell division have mostly utilized these larger cells found in hydroids and non-cnidarian hosts that house different types of algal partners (Fitt, 2000; Kadono et al.,

2004; McAuley, 1985, 1986; Takahashi, 2016). There are a few studies that provide mixed evidence for the coordination of cell cycle timing between Symbiodiniacea symbionts and anthozoan hosts. These studies have described diel symbiont patterns within tropical but not temperate anthozoans, as well as loose correlations between some anthozoan hosts and their symbiont G_2M-phase cell cycle populations (Dimond et al., 2013; Wilkerson et al., 1983). With only a handful of studies, it is still unclear whether there is coordination between host and symbiont cell proliferation during periods of growth and colonization in anthozoan symbioses.

Another factor that continues to influence colonization success after recognition and uptake during the proliferative phase is host-symbiont specificity (Belda-Baillie et al., 2002; Gabay et al., 2018). In many experiments, colonization with homologous symbionts results in rapid increases in symbiont density, whereas colonization with foreign symbionts tend to have mixed success (Belda-Baillie et al., 2002; Gabay et al., 2018; Schoenberg and Trench, 1980; Weis et al., 2001). Since most of these colonization studies have relied on symbiont cell counts from host homogenates, we have limited information that detail mechanisms underlying the spatial and temporal dynamics of symbiont populations. Symbiont colonization dynamics therefore require a more thorough understanding of the patterning and movement of symbionts to disentangle the relative contributions of symbiont uptake and symbiont proliferation within the gastrodermal tissue layer.

1.3 Maintenance of symbiosis

In a stable, healthy symbiosis, hosts and symbionts have coordinated biomass regulation (Muscatine and Pool, 1979). Symbiodiniaceae cell populations are maintained at a dense level in gastrodermal tissue in order to efficiently transfer nutrients from photosynthesis (Jones and Yellowlees, 1997). The additional nutrients expedite cnidarian growth, especially in nutrient poor environments (Wang and Douglas, 1998). Calcifying cnidarians then use these nutrients to deposit calcium carbonate skeletons (Goreau, 1959). Despite the clear function and output of the symbiosis, the cellular mechanisms for how Symbiodiniaceae cells persist and proliferate within cnidarians during this symbiotic homeostasis are only partially understood.

1.3.1 Pre-mitotic biomass regulation: cell cycles in symbiosis

As stated previously, coordination of cell division may occur between partners but there is limited evidence for this type of regulation in cnidarian-dinoflagellate symbioses (Dimond et al., 2013; Fitt, 2000). The regulation of the cell cycles in these symbiotic partners is presumed to be similar to other eukaryotic systems, remains largely unexplored (Davy et al., 2012). The cnidarian cell cycle has been most thoroughly characterized in *Hydra* (Bosch and David, 1984; David and Campbell, 1972). Many studies have further examined cnidarian cell proliferation in anthozoans, but few have focused on the cnidarian cell cycle during stable algal symbiosis (Dimond et al., 2013; Fransolet et al., 2013; Lecointe et al., 2016; Passamaneck and Martindale, 2012). The Symbiodiniacea cell cycle is especially of interest, since dinoflagellates have unique DNA organization among eukaryotes (Wisecaver and Hackett, 2011; Wong and Kwok, 2005). They lack nucleosomes and functional histones, and instead rely on histone-like proteins to organize chromatin (Bodansky et al., 1979; Rizzo, 2003). The timing of cell cycle events is also unique in dinoflagellates. Chromosomes remain condensed throughout the cell cycle in a liquid crystalline state, and the nuclear envelope persists throughout mitosis supported by unusual extranuclear spindles (Bhaud et al., 2000; Bouligand and Norris, 2001).

Many studies have examined Symbiodiniaceae proliferation through mitosis within cnidarian host cells (i.e., *in hospite*) under different host conditions. Symbiodiniaceae cell growth and division has been shown to increase with higher light intensity (Drew, 1972; Muscatine and Pool, 1979). Their photosynthetic machinery is also driven by a diel light-dark cycle (Fitt and Trench, 1983b) which correlates with cell division patterns in culture but not necessarily *in hospite* (Dimond et al., 2013; Fitt, 2000; Wilkerson et al., 1983). The consistent evidence of nitrogen limitation in Symbiodiniaceae species *in hospite* suggests that some cnidarian hosts are able to keep their symbionts in a non-proliferative G_0/G_1 state as a form of pre-mitotic control (Dagenais-Bellefeuille and Morse, 2013; Fitt and Cook, 2001; McAuley and Cook, 1994; Wiedenmann et al., 2013). Increased host nutrition appears to positively affect not only symbiont nutrition but also proliferation rate (Davy et al., 2006; Smith and Muscatine,

1999). This expansion of symbiont proliferation in a space-limited host often results in other mechanisms of host-symbiont regulation.

1.3.2 Post-mitotic biomass regulation

Host-symbiont biomass regulation can take a variety of forms (Jones and Yellowlees, 1997; Parrin et al., 2012; Santos et al., 2009). Hosts can remove symbionts through cellular processes of expulsion or digestion (Dunn and Weis, 2009; McCloskey et al., 1996). Evidence for symbiont expulsion exists *via* a variety of pathways including exocytosis, host apoptosis, host necrosis, and host cell detachment (Dunn et al., 2002; Gates et al., 1992; Steen and Muscatine, 1987; Strychar et al., 2004). Host cells also have the capacity for symbiont digestion through autophagy (Dunn et al., 2007). These forms of symbiont regulation by the host have been predominantly studied under environmental change, and the primary mechanism of symbiont regulation tends to be dependent on the type and degree of stress involved (Dani et al., 2016; Dunn et al., 2007; Weis, 2008). In many symbiotic cnidarians however, symbiont expulsion occurs during a healthy stable symbiosis, presumably as a homeostatic biomass regulatory mechanism (Dimond and Carrington, 2008; McCloskey et al., 1996; Smith and Muscatine, 1999). Analysis of these expelled symbionts found that the Symbiodiniaceae populations contained increased percentages of dividing cells (Baghdasarian and Muscatine, 2000). Further studies are needed to better describe this mechanism of targeted regulation by the cnidarian host.

1.4 Symbiosis dysfunction and breakdown

To maintain symbiosis in a dynamic homeostasis, host and symbiont cells must respond to environmental flux such as changes in nutrients, temperature, light, and infectious disease (Gustafsson et al., 2014; Muscatine et al., 1989). Each of these factors has the potential to create a stressful cellular environment. High light and temperature inhibit the photosynthetic machinery of Symbiodiniaceae cells resulting in the creation of reactive oxygen species (ROS) (Iglesias-Prieto et al., 1992; Venn et al., 2008). ROS trigger a range of responses that result in cellular damage. Both the symbiont and host are susceptible to these responses, and a variety of downstream mechanisms including host nitric oxide production induces a bleaching response (Perez and Weis, 2006). Under these

stressful conditions, Symbiodiniaceae are not maintained within their host cnidarian cells (Gates et al., 1992; Lesser, 1996). In response to this stress, symbionts exit the host *en masse* through a variety of mechanisms including apoptosis, necrosis, and cell detachment. (Brown et al., 1995; Dunn et al., 2002; Gates et al., 1992; Hawkins et al., 2013; Perez et al., 2001). Host cells are left with depleted populations of symbionts, which can result in starvation in nutrient-limited environments. When this cellular dysbiosis happens on a worldwide scale across coral reef ecosystems, this process is known as a mass bleaching event. In the past few decades there has been a dramatic increase in the number of mass bleaching events, correlated with elevated sea surface temperature (Ainsworth et al., 2016; Baker et al., 2008). We are currently recovering from the longest and most extensive mass bleaching event ever known, but the shorter time periods between these mass bleaching events does not leave enough time for coral reef recovery (Hughes et al., 2018). The precipitous decline of coral reefs has led many to begin to rethink how we can protect reefs (van Oppen et al., 2017). The resulting ideas of coral restoration and assisted evolution require firm understanding of cnidarian-dinoflagellate biology and appropriate experimental testing within cnidarian hosts in order to take advantage of the molecular and cellular techniques that have led to some success in transforming other biological systems (Laikre et al., 2010; Mittler and Blumwald, 2010; van Oppen et al., 2015).

1.5 Cellular study of symbiosis

The cellular study of coral-Symbiodiniaceae associations is challenging; corals are slow-growing, difficult to maintain in culture, and many species are endangered from anthropogenic change. To circumvent these problems, an international community of research and teaching labs are studying the symbiosis between the tropical Symbiodiniacea species *Breviolum minutum* (LaJeunesse et al., 2018) and the cosmopolitan sea anemone *Exaiptasia pallida* Aiptasia, a sea anemone in the same subclass (Hexacorallia) as corals. *E. pallida*, commonly known as Aiptasia, has been adopted as a cnidarian model system for studying the cellular and molecular biology of coral symbiosis, since they are easy to maintain and can be cultured symbiont free in an aposymbiotic state (Gladfelter, 2015; Goldstein and King, 2016; Weis et al., 2008).

Studies in the Aiptasia-*Breviolum* symbiosis are supported by an extensive body of research, including the genomes and transcriptomes of both symbiotic partners (Baumgarten et al., 2015; Lehnert et al., 2014; Shoguchi et al., 2013; Sunagawa et al., 2009). The cellular study of symbiosis has provided precise mechanisms for broad ecological concerns such as coral bleaching, and the Aiptasia model system offers a tractable symbiosis in which to interpret and explore hypotheses generated from recent genomic studies.

The cnidarian-dinoflagellate symbiosis relies on the critical cellular interactions that govern onset and regulation of the partnership. In this dissertation I used the Aiptasia-Symbiodiniaceae symbiosis to investigate cellular mechanisms of host-symbiont interactions during the establishment, maintenance, and breakdown of symbiosis. I first examined the role of glycan-lectin interactions in symbiont recognition and uptake by cnidarian hosts (Chapter 2). I then examined host and symbiont proliferation under different symbiotic states and measured the cell cycles and colonization patterns of Symbiodiniaceae symbionts with Aiptasia hosts (Chapter 3). Finally, I examined the cellular patterns of proliferation for different symbiont species under different temperature regimes during recolonization of Aiptasia hosts (Chapter 4).

1.6 References

Ainsworth, T. D., Heron, S. F., Ortiz, J. C., Mumby, P. J., Grech, A., Ogawa, D., et al. (2016). Climate change disables coral bleaching protection on the Great Barrier Reef. *Science* 352, 338–342. doi:10.1017/CBO9781107415324.004.

Baghdasarian, G., and Muscatine, L. (2000). Preferential expulsion of dividing algal cells as a mechanism for regulating algal-cnidarian symbiosis. *Biol. Bull.* 199, 278–86.

Baker, A. C. (2003). Flexibility and specificity in coral-algal symbiosis: Diversity, ccology , and biogeography of Symbiodinium. *Annu. Rev. Ecol. Evol. Syst.* 34, 661–689. doi:10.1146/132417.

Baker, A. C., Glynn, P. W., and Riegl, B. (2008). Climate change and coral reef bleaching: An ecological assessment of long-term impacts, recovery trends and future outlook. *Estuar. Coast. Shelf Sci.* 80, 435–471. doi:10.1016/j.ecss.2008.09.003.

Baumgarten, S., Simakov, O., Esherick, L. Y., Liew, Y. J., Lehnert, E. M., Michell, C. T., et al. (2015). The genome of Aiptasia , a sea anemone model for coral symbiosis. *Proc. Natl. Acad. Sci.* 112, 201513318. doi:10.1073/pnas.1513318112.

Belda-Baillie, C. A., Baillie, B. K., and Maruyama, T. (2002). Specificity of a Model Cnidarian-Dinoflagellate Symbiosis. *Biol. Bull.* 202, 74–85. doi:10.2307/1543224.

Bennett, G. M., and Moran, N. A. (2015). Heritable symbiosis: The advantages and perils of an evolutionary rabbit hole. *Proc. Natl. Acad. Sci.* 112, 10169–10176. doi:10.1073/pnas.1421388112.

Bhaud, Y., Guillebault, D., Lennon, J., Defacque, H., Soyer-Gobillard, M. O., and Moreau, H. (2000). Morphology and behaviour of dinoflagellate chromosomes during the cell cycle and mitosis. *J. Cell Sci.* 113, 1231–1239.

Bodansky, S., Mintz, L. B., and Holmes, D. S. (1979). The mesokaryote Gyrodinium cohnii lacks nucleosomes. *Biochem. Biophys. Res. Commun.* 88, 1329–1336. doi:10.1016/0006-291X(79)91126-4.

Bosch, T. C., and David, C. N. (1984). Growth regulation in Hydra: relationship between epithelial cell cycle length and growth rate. *Dev. Biol.* 104, 161–171. doi:10.1016/0012-1606(84)90045-9.

Bosch, T. C. G. (2013). Cnidarian-microbe interactions and the origin of innate immunity in metazoans. *Annu. Rev. Microbiol.* 67, 499–518. doi:10.1146/annurev-micro-092412-155626.

Bouligand, Y., and Norris, V. (2001). Chromosome separation and segregation in dinoflagellates and bacteria may depend on liquid crystalline states. *Biochimie* 83, 187–192. doi:10.1016/S0300-9084(00)01211-6.

Brown, B. E., Le Tissier, M. D. A., and Bythell, J. C. (1995). Mechanisms of bleaching deduced from histological studies of reef corals sampled during a natural bleaching event. *Mar. Biol.* 122, 655–663. doi:10.1007/BF00350687.

Carpenter, K. E., Abrar, M., Aeby, G., Aronson, R. B., Banks, S., Bruckner, A., et al. (2008). One-Third of Reef-Building Corals Face Elevated Extinction Risk from Climate Change and Local Impacts. *Science* 321, 560–563. doi:10.1126/science.1159196.

Cavanaugh, C. M., Gardiner, S. L., Jones, M. L., Jannasch, H. W., and Waterbury, J. B. (1981). Prokaryotic Cells in the Hydrothermal Vent Tube Worm Riftia pachyptila Jones: Possible Chemoautotrophic Symbionts. *Science* 213, 340–342.

Chaves-Fonnegra, A., Riegl, B., Zea, S., Lopez, J. V., Smith, T., Brandt, M., et al. (2018). Bleaching events regulate shifts from corals to excavating sponges in algae-dominated reefs. *Glob. Change Biol.* 24, 773–785. doi:10.1111/gcb.13962.

Dagenais-Bellefeuille, S., and Morse, D. (2013). Putting the N in dinoflagellates. *Front. Microbiol.* 4, 369. doi:10.3389/fmicb.2013.00369.

Dani, V., Priouzeau, F., Pagnotta, S., and Carette, D. (2016). Thermal and menthol stress induce different cellular events during sea anemone bleaching. *Symbiosis*. doi:10.1007/s13199-016-0406-y.

David, C. N., and Campbell, R. D. (1972). Cell cycle kinetics and development of Hydra attenuata. *J. Cell Sci.* 11, 557–568.

Davy, S. K., Allemand, D., and Weis, V. M. (2012). Cell Biology of Cnidarian-Dinoflagellate Symbiosis. *Microbiol. Mol. Biol. Rev.* 76, 229–261. doi:10.1128/MMBR.05014-11.

Davy, S. K., Withers, K. J. T., and Hinde, R. (2006). Effects of host nutritional status and seasonality on the nitrogen status of zooxanthellae in the temperate coral Plesiastrea versipora (Lamarck). *J. Exp. Mar. Biol. Ecol.* 335, 256–265. doi:10.1016/j.jembe.2006.03.019.

del C. Gomez-Cabrera, M., Ortiz, J. C., Loh, W. K. W., Ward, S., and Hoegh-Guldberg, O. (2008). Acquisition of symbiotic dinoflagellates (Symbiodinium) by juveniles of the coral Acropora longicyathus. *Coral Reefs* 27, 219–226. doi:10.1007/s00338-007-0315-x.

Dimond, J., and Carrington, E. (2008). Symbiosis regulation in a facultatively symbiotic temperate coral: zooxanthellae division and expulsion. *Coral Reefs* 27, 601–604. doi:10.1007/s00338-008-0363-x.

Dimond, J. L., Pineda, R. R., Ramos-Ascherl, Z., and Bingham, B. L. (2013). Relationships between host and symbiont cell cycles in sea anemones and their symbiotic dinoflagellates. *Biol. Bull.* 225, 102–12.

Douglas, A. E. (2010). *The symbiotic habit*. Princeton University Press.

Drew, E. A. (1972). The biology and physiology of alga-invertebrate symbioses. II. The density of symbiotic algal cells in a number of hermatypic hard corals and alcyonarians from various depths. *J. Exp. Mar. Biol. Ecol.* 9, 71–75.

Dunn, S. R. (2009). Immunorecognition and immunoreceptors in the Cnidaria. *Invertebr. Surviv. J.* 6, 7–14.

Dunn, S. R., Bythell, J. C., Le Tissier, M. D. A., Burnett, W. J., and Thomason, J. C. (2002). Programmed cell death and cell necrosis activity during hyperthermic stress-induced bleaching of the symbiotic sea anemone Aiptasia sp. *J. Exp. Mar. Biol. Ecol.* 272, 29–53. doi:10.1016/S0022-0981(02)00036-9.

Dunn, S. R., Schnitzler, C. E., and Weis, V. M. (2007). Apoptosis and autophagy as mechanisms of dinoflagellate symbiont release during cnidarian bleaching: every which way you lose. *Proc. R. Soc. B Biol. Sci.* 274, 3079–3085. doi:10.1098/rspb.2007.0711.

Dunn, S. R., and Weis, V. M. (2009). Apoptosis as a post-phagocytic winnowing mechanism in a coral-dinoflagellate mutualism. *Environ. Microbiol.* 11, 268–76. doi:10.1111/j.1462-2920.2008.01774.x.

Fitt, W. K. (2000). Cellular Growth of Host and Symbiont in a Cnidarian-Zooxanthellar Symbiosis. *Biol. Bull.* 198, 110–120.

Fitt, W. K., and Cook, C. B. (2001). The effects of feeding or addition of dissolved inorganic nutrients in maintaining the symbiosis between dinoflagellates and a tropical marine cnidarian. *Mar. Biol.* 139, 507–517. doi:10.1007/s002270100598.

Fitt, W. K., and Trench, R. K. (1983a). Endocytosis of the symbiotic dinoflagellate symbiodinium microadriaticum Freudenthal by endodermal cells of the scyphistomae of Cassiopeia xamachana and resistance of the algae to host digestion. *J. Cell Sci.* 64, 195–212. doi:10.1111/j.1469-8137.1983.tb03456.x.

Fitt, W. K., and Trench, R. K. (1983b). The Relation of Diel Patterns of Cell Division To Diel Patterns of Motility in the Symbiotic Dinoflagellate Symbiodinium microadriaticum Freudenthal in Culture. *New Phytol.* 94, 421–432. doi:10.1111/j.1469-8137.1983.tb03456.x.

Fransolet, D., Roberty, S., Herman, A.-C., Tonk, L., Hoegh-Guldberg, O., and Plumier, J.-C. (2013). Increased cell proliferation and mucocyte density in the sea anemone Aiptasia pallida recovering from bleaching. *PloS ONE* 8, e65015. doi:10.1371/journal.pone.0065015.

Fransolet, D., Roberty, S., and Plumier, J.-C. (2012). Establishment of endosymbiosis: The case of cnidarians and Symbiodinium. *J. Exp. Mar. Biol. Ecol.* 420–421, 1–7. doi:10.1016/j.jembe.2012.03.015.

Gabay, Y., Weis, V. M., and Davy, S. K. (2018). Symbiont Identity Influences Patterns of Symbiosis Establishment, Host Growth, and Asexual Reproduction in a Model Cnidarian-Dinoflagellate Symbiosis. *Biol. Bull.* 234, 1–10. doi:10.1086/696365.

Gates, R. D., Baghdasarian, G., and Muscatine, L. (1992). Temperature stress causes host cell detachment in symbiotic cnidarians: implications for coral bleaching. *Biol. Bull.* 182, 324–332. doi:10.2307/1542252.

Gladfelter, A. S. (2015). How nontraditional model systems can save us. *Mol. Biol. Cell* 26, 3687–3689. doi:10.1091/mbc.E15-06-0429.

Goldstein, B., and King, N. (2016). The Future of Cell Biology: Emerging Model Organisms. *Trends Cell Biol.* 26, 818–824. doi:10.1016/j.tcb.2016.08.005.

Goreau, T. F. (1959). The physiology of skeleton formation in corals. I. A method for measuring the rate of calcium deposition by corals under different conditions. *Biol. Bull.* 116, 59–75. doi:10.2307/1539156.

Gustafsson, M. S. M., Baird, M. E., and Ralph, P. J. (2014). Modeling photoinhibition-driven bleaching in Scleractinian coral as a function of light, temperature, and heterotrophy. *Limnol. Oceanogr.* 59, 603–622. doi:10.4319/lo.2014.59.2.0603.

Hashimoto, K., Tokimatsu, T., Kawano, S., Yoshizawa, A. C., Okuda, S., Goto, S., et al. (2009). Comprehensive analysis of glycosyltransferases in eukaryotic genomes for structural and functional characterization of glycans. *Carbohydr. Res.* 344, 881–887. doi:10.1016/j.carres.2009.03.001.

Hawkins, T. D., Bradley, B. J., and Davy, S. K. (2013). Nitric oxide mediates coral bleaching through an apoptotic-like cell death pathway: evidence from a model sea anemone-dinoflagellate symbiosis. *FASEB J.* 27, 4790–8. doi:10.1096/fj.13-235051.

Heijden, M. G. A. van der, Boller, T., Wiemken, A., and Sanders, I. R. (1998). Different arbuscular mycorrhizal fungal species are potential determinants of plant community structure. *Ecology* 79, 2082–2091.

Hoegh-Guldberg, O., Mumby, P. J., Hooten, A. J., Steneck, R. S., Greenfield, P., Gomez, E., et al. (2007). Coral Reefs Under Rapid Climate Change and Ocean Acidification. *Science* 318, 1737–1742. doi:10.1126/science.1152509.

Hughes, T. P., Anderson, K. D., Connolly, S. R., Heron, S. F., Kerry, J. T., Lough, J. M., et al. (2018). Spatial and temporal patterns of mass bleaching of corals in the Anthropocene. *Science* 359, 80–83. doi:10.1126/science.aan8048.

Hughes, T. P., Baird, A. H., Bellwood, D. R., Card, M., Connolly, S. R., Folke, C., et al. (2003). Climate change, human impacts, and the resilience of coral reefs. *Science* 301, 929–933. doi:10.1126/science.1085046.

Hughes, T. P., Kerry, J. T., Baird, A. H., Connolly, S. R., Chase, T. J., Dietzel, A., et al. (2019). Global warming impairs stock–recruitment dynamics of corals. *Nature* 568, 387–390. doi:10.1038/s41586-019-1081-y.

Iglesias-Prieto, R., Matta, J. L., Robins, W. A., and Trench, R. K. (1992). Photosynthetic response to elevated temperature in the symbiotic dinoflagellate Symbiodinium microadriaticum in culture. *Proc. Natl. Acad. Sci. U. S. A.* 89, 10302–10305. doi:10.1073/pnas.89.21.10302.

Johnson, M. D. (2011). The acquisition of phototrophy: adaptive strategies of hosting endosymbionts and organelles. *Photosynth. Res.* 107, 117–132. doi:10.1007/s11120-010-9546-8.

Jones, R. J., and Yellowlees, D. (1997). Regulation and control of intracellular algae (= zooxanthellae) in hard corals. *Philos. Trans. R. Soc. B Biol. Sci.* 352, 457–468. doi:10.1098/rstb.1997.0033.

Kadono, T., Kawano, T., Hosoya, H., and Kosaka, T. (2004). Flow cytometric studies of the host-regulated cell cycle in algae symbiotic with green paramecium. *Protoplasma* 223, 133–141. doi:10.1007/s00709-004-0046-6.

Kirk, N. L., and Weis, V. M. (2016). "Animal–Symbiodinium Symbioses: Foundations of Coral Reef Ecosystems," in *The Mechanistic Benefits of Microbial Symbionts*, ed. C. J. Hurst (Cham: Springer International Publishing), 269–294. doi:10.1007/978-3-319-28068-4_10.

Laikre, L., Schwartz, M. K., Waples, R. S., and Ryman, N. (2010). Compromising genetic diversity in the wild: unmonitored large-scale release of plants and animals. *Trends Ecol. Evol.* 25, 520–529. doi:10.1016/j.tree.2010.06.013.

LaJeunesse, T. C., Parkinson, J. E., Gabrielson, P. W., Jeong, H. J., Reimer, J. D., Voolstra, C. R., et al. (2018). Systematic Revision of Symbiodiniaceae Highlights the Antiquity and Diversity of Coral Endosymbionts. *Curr. Biol.* 28, 2570-2580.e6. doi:10.1016/j.cub.2018.07.008.

Lecointe, A., Domart-coulon, I., Paris, A., and Meibom, A. (2016). Cell proliferation and migration during early development of a symbiotic scleractinian coral. *Proc. R. Soc. Lond. B* 283, 20160206. doi:10.1098/rspb.2016.0206.

Lehnert, E. M., Mouchka, M. E., Burriesci, M. S., Gallo, N. D., Schwarz, J. A., and Pringle, J. R. (2014). Extensive differences in gene expression between symbiotic and aposymbiotic cnidarians. *G3 Genes Genomes Genet.* 4, 277–295. doi:10.1534/g3.113.009084.

Lesser, M. P. (1996). Elevated temperatures and ultraviolet radiation cause oxidative stress and inhibit photosynthesis in symbiotic dinoflagellates. *Limnol. Oceanogr.* 41, 271–283. doi:10.4319/lo.1996.41.2.0271.

Lin, K., Wang, J., and Fang, L.-S. (2000). Participation of Glycoproteins on Zooxanthellal Cell Walls in the Establishment of a Symbiotic Relationship with the Sea Anemone, Aiptasia pulchella. 39, 172–178.

Logan, D. D. K., LaFlamme, A. C., Weis, V. M., and Davy, S. K. (2010). Flow-Cytometric Characterization of the Cell-Surface Glycans of Symbiotic Dinoflagellates (Symbiodinium Spp.). *J. Phycol.* 46, 525–533. doi:10.1111/j.1529-8817.2010.00819.x.

Maynard, J., van Hooidonk, R., Eakin, C. M., Puotinen, M., Garren, M., Williams, G., et al. (2015). Projections of climate conditions that increase coral disease susceptibility and pathogen abundance and virulence. *Nat. Clim. Change* 5, 688–694. doi:10.1038/nclimate2625.

McAuley, P. J. (1985). The cell cycle of symbiotic Chlorella. I. The relationship between host feeding and algal cell growth and division. *J. Cell Sci.* 77, 225–239.

McAuley, P. J. (1986). The cell cycle of symbiotic Chlorella. III. Numbers of algae in green hydra digestive cells are regulated at digestive cell division. *J. Cell Sci.* 85, 63–71.

McAuley, P. J., and Cook, C. B. (1994). Effects of host feeding and dissolved ammonium on cell division and nitrogen status of zooxanthellae in the hydroid Myrionema amboinense. *Mar. Biol.* 121, 343–348. doi:10.1007/BF00346743.

McCloskey, L. R., Cove, T. G., and Verde, E. A. (1996). Symbiont expulsion from the anemone Anthopleura elegantissima (Brandt) (Cnidaria; Anthozoa). *J. Exp. Mar. Biol. Ecol.* 195, 173–186. doi:10.1016/0022-0981(95)00079-8.

McFall-Ngai, M., Hadfield, M. G., Bosch, T. C. G., Carey, H. V., Domazet-Lošo, T., Douglas, A. E., et al. (2013). Animals in a bacterial world, a new imperative for the life sciences. *Proc. Natl. Acad. Sci.* 110, 3229–3236. doi:10.1073/pnas.1218525110.

Meyer, E., and Weis, V. M. (2012). Study of cnidarian-algal symbiosis in the “omics” age. *Biol. Bull.* 223, 44–65. doi:10.1086/BBLv223n1p44.

Miller, D. J., Hemmrich, G., Ball, E. E., Hayward, D. C., Khalturin, K., Funayama, N., et al. (2007). The innate immune repertoire in Cnidaria - ancestral complexity and stochastic gene loss. *Genome Biol.* 8, R59. doi:10.1186/gb-2007-8-4-r59.

Mittler, R., and Blumwald, E. (2010). Genetic Engineering for Modern Agriculture: Challenges and Perspectives. *Annu. Rev. Plant Biol.* 61, 443–462. doi:10.1146/annurev-arplant-042809-112116.

Moberg, F. F., and Folke, C. (1999). Ecological goods and services of coral reef ecosystems. *Ecol. Econ.* 29, 215–233. doi:10.1016/S0921-8009(99)00009-9.

Muscatine, L., Falkowski, P. G., Dubinsky, Z., Cook, P. A., and McCloskey, L. L. R. (1989). The effect of external nutrient resources on the population dynamics of zooxanthellae in a reef coral. *Proc. R. Soc. Lond. B* 236, 311–324. doi:10.1098/rspb.1989.0025.

Muscatine, L., Ferrier-Pagès, C., Blackburn, A., Gates, R. D., Baghdasarian, G., and Allemand, D. (1998). Cell specific density of symbiotic dinoflagellates in tropical anthozoans. *Coral Reefs* 17, 329–337. doi:Doi 10.1007/S003380050133.

Muscatine, L., Goiran, C., Land, L., Jaubert, J., Cuif, J.-P., and Allemand, D. (2005). Stable isotopes (delta13C and delta15N) of organic matrix from coral skeleton. *Proc. Natl. Acad. Sci. U. S. A.* 102, 1525–1530. doi:10.1073/pnas.0408921102.

Muscatine, L., and Lenhoff, H. M. (1963). Symbiosis: On the Role of Algae Symbiotic with Hydra. *Science* 142, 956–958. doi:10.1126/science.142.3594.956.

Muscatine, L., and Pool, R. R. (1979). Regulation of numbers of intracellular algae. *Proc. R. Soc. Lond. B* 204, 131–139. doi:10.1098/rspb.1979.0018.

Neubauer, E. F., Poole, A. Z., Weis, V. M., and Davy, S. K. (2016). The scavenger receptor repertoire in six cnidarian species and its putative role in cnidarian-dinoflagellate symbiosis. *PeerJ* 4, e2692. doi:10.7717/peerj.2692.

Neubauer, E.-F., Poole, A. Z., Neubauer, P., Detournay, O., Tan, K., Davy, S. K., et al. (2017). A diverse host thrombospondin-type-1 repeat protein repertoire promotes symbiont colonization during establishment of cnidarian-dinoflagellate symbiosis. *eLife* 6. doi:10.7554/eLife.24494.

Nyholm, S. V., and McFall-Ngai, M. J. (2004). The winnowing: establishing the squid-vibrio symbiosis. *Nat. Rev. Microbiol.* 2, 632–42. doi:10.1038/nrmicro957.

Parrin, A. P., Harmata, K. L., Netherton, S. E., Yaeger, M. A., Bross, L. S., and Blackstone, N. W. (2012). Within-colony migration of symbionts during bleaching of octocorals. *Biol. Bull.* 223, 245–256.

Passamaneck, Y. J., and Martindale, M. Q. (2012). Cell proliferation is necessary for the regeneration of oral structures in the anthozoan cnidarian Nematostella vectensis. *BMC Dev. Biol.* 12, 34. doi:10.1186/1471-213X-12-34.

Pearse, V. B., and Muscatine, L. (1971). Role of symbiotic algae (zooxanthellae) in coral calcification. *Biol. Bull.* 141, 350–363. doi:10.2307/1540123.

Perez, S. F., Cook, C. B., and Brooks, W. R. (2001). The role of symbiotic dinoflagellates in the temperature-induced bleaching response of the subtropical sea anemone Aiptasia pallida. *J. Exp. Mar. Biol. Ecol.* 256, 1–14. doi:10.1016/S0022-0981(00)00282-3.

Perez, S., and Weis, V. M. (2006). Nitric oxide and cnidarian bleaching: an eviction notice mediates breakdown of a symbiosis. *J. Exp. Biol.* 209, 2804–10. doi:10.1242/jeb.02309.

Pochon, X., and Gates, R. D. (2010). A new Symbiodinium clade (Dinophyceae) from soritid foraminifera in Hawai'i. *Mol. Phylogenet. Evol.* 56, 492–497. doi:10.1016/j.ympev.2010.03.040.

Pochon, X., Montoya-Burgos, J. I., Stadelmann, B., and Pawlowski, J. (2006). Molecular phylogeny, evolutionary rates, and divergence timing of the symbiotic dinoflagellate genus Symbiodinium. *Mol. Phylogenet. Evol.* 38, 20–30. doi:10.1016/j.ympev.2005.04.028.

Poole, A. Z., Kitchen, S. A., and Weis, V. M. (2016). The Role of Complement in Cnidarian-Dinoflagellate Symbiosis and Immune Challenge in the Sea Anemone Aiptasia pallida. *Front. Microbiol.* 7, 519. doi:10.3389/fmicb.2016.00519.

Rizzo, P. J. (2003). Those amazing dinoflagellate chromosomes. *Cell Res.* 13, 215–217. doi:10.1038/sj.cr.7290166.

Rodriguez-Lanetty, M., Krupp, D. A., and Weis, V. M. (2004). Distinct ITS types of Symbiodinium in Clade C correlate with cnidarian/dinoflagellate specificity during onset of symbiosis. *Mar. Ecol. Prog. Ser.* 275, 97–102. doi:10.3354/meps275097.

Sachs, J. L., Quides, K. W., and Wendlandt, C. E. (2018). Legumes versus rhizobia: a model for ongoing conflict in symbiosis. doi:10.1111/nph.15222.

Sagan, L. (1967). On the origin of mitosing cells. *J. Theor. Biol.* 14, 225-IN6. doi:10.1016/0022-5193(67)90079-3.

Santos, S. R., Toyoshima, J., and Kinzie III, R. A. (2009). Spatial and temporal dynamics of symbiotic dinoflagellates (Symbiodinium : Dinophyta) in the perforate coral Montipora capitata. 139–147.

Schoenberg, D. A., and Trench, R. K. (1980). Genetic Variation in Symbiodinium (=Gymnodinium) microadriaticum Freudenthal, and Specificity in its Symbiosis with Marine Invertebrates. III. Specificity and Infectivity of Symbiodinium microadriaticum. *Proc. R. Soc. Lond. B Biol. Sci.* 207, 445–460.

Schwartz, R. M., and Dayhoff, M. O. (1978). Origins of Prokaryotes, Eukaryotes, Mitochondria, and Chloroplasts. *Science* 199, 395–403.

Schwarz, J. A., Weis, V. M., and Potts, D. C. (2002). Feeding behavior and acquisition of zooxanthellae by planula larvae of the sea anemone Anthopleura elegantissima. *Mar. Biol.* 140, 471–478. doi:10.1007/s00227-001-0736-y.

Shoguchi, E., Shinzato, C., Kawashima, T., Gyoja, F., Mungpakdee, S., Koyanagi, R., et al. (2013). Draft assembly of the Symbiodinium minutum nuclear genome reveals dinoflagellate gene structure. *Curr. Biol. CB* 23, 1399–408. doi:10.1016/j.cub.2013.05.062.

Smith, G. J., and Muscatine, L. (1999). Cell cycle of symbiotic dinoflagellates: variation in G1 phase-duration with anemone nutritional status and macronutrient supply in the Aiptasia pulchella-Symbiodinium pulchrorum symbiosis. *Mar. Biol.* 134, 405–418.

Steen, R., and Muscatine, L. (1987). Low temperature evokes rapid exocytosis of symbiotic algae by a sea anemone. *Biol. Bull.* 172, 246–263. doi:10.2307/1541797.

Strychar, K. B., Sammarco, P. W., and Piva, T. J. (2004). Apoptotic and necrotic stages of Symbiodinium (Dinophyceae) cell death activity: bleaching of soft and scleractinian corals. *Phycologia* 43, 768–777. doi:10.2216/i0031-8884-43-6-768.1.

Sunagawa, S., Wilson, E. C., Thaler, M., Smith, M. L., Caruso, C., Pringle, J. R., et al. (2009). Generation and analysis of transcriptomic resources for a model system on the rise: the sea anemone Aiptasia pallida and its dinoflagellate endosymbiont. *BMC Genomics* 10, 258. doi:10.1186/1471-2164-10-258.

Takahashi, T. (2016). Simultaneous Evaluation of Life Cycle Dynamics between a Host Paramecium and the Endosymbionts of Paramecium bursaria Using Capillary Flow Cytometry. *Sci. Rep.* 6. doi:10.1038/srep31638.

Toby Kiers, E., Palmer, T. M., Ives, A. R., Bruno, J. F., and Bronstein, J. L. (2010). Mutualisms in a changing world: an evolutionary perspective: Mutualism breakdown. *Ecol. Lett.* 13, 1459–1474. doi:10.1111/j.1461-0248.2010.01538.x.

van Hooidonk, R., Maynard, J. a., and Planes, S. (2013). Temporary refugia for coral reefs in a warming world. *Nat. Clim. Change* 3, 508–511. doi:10.1038/nclimate1829.

van Oppen, M. J. H., Gates, R. D., Blackall, L. L., Cantin, N., Chakravarti, L. J., Chan, W. Y., et al. (2017). Shifting paradigms in restoration of the world's coral reefs. *Glob. Change Biol.*, 1–12. doi:10.1111/gcb.13647.

van Oppen, M. J. H., Oliver, J. K., Putnam, H. M., and Gates, R. D. (2015). Building coral reef resilience through assisted evolution. *Proc. Natl. Acad. Sci.* 112, 2307–2313. doi:10.1073/pnas.1422301112.

Varki, A. (2017). Biological roles of glycans. *Glycobiology* 27, 3–49. doi:10.1093/glycob/cww086.

Venn, A. A., Loram, J. E., and Douglas, A. E. (2008). Photosynthetic symbioses in animals. *J. Exp. Bot.* 59, 1069–1080. doi:10.1093/jxb/erm328.

Wakefield, T. S., Farmer, M. A., and Kempf, S. C. (2000). Revised description of the fine structure of in situ "Zooxanthellae" genus Symbiodinium. *Biol. Bull.* 199, 76–84. doi:10.2307/1542709.

Wakefield, T. S., and Kempf, S. C. (2001). Development of host- and symbiont-specific monoclonal antibodies and confirmation of the origin of the symbiosome membrane in a cnidarian-dinoflagellate symbiosis. *Biol. Bull.* 200, 127–143. doi:10.2307/1543306.

Wang, J., and Douglas, A. E. (1998). Nitrogen recycling or nitrogen conservation in an alga-invertebrate symbiosis? *J. Exp. Biol.* 201, 2445–2453.

Weis, V. M. (2008). Cellular mechanisms of Cnidarian bleaching: stress causes the collapse of symbiosis. *J. Exp. Biol.* 211, 3059–66. doi:10.1242/jeb.009597.

Weis, V. M., Davy, S. K., Hoegh-Guldberg, O., Rodriguez-Lanetty, M., and Pringle, J. R. (2008). Cell biology in model systems as the key to understanding corals. *Trends Ecol. Evol.* 23, 369–76. doi:10.1016/j.tree.2008.03.004.

Weis, V. M., Reynolds, W. S., DeBoer, M. D., and Krupp, D. A. (2001). Host-symbiont specificity during onset of symbiosis between the dinoflagellates Symbiodinium spp. and planula larvae of the scleractinian coral Fungia scutaria. *Coral Reefs* 20, 301–308. doi:10.1007/s003380100179.

Wiedenmann, J., D'Angelo, C., Smith, E. G., Hunt, A. N., Legiret, F.-E., Postle, A. D., et al. (2013). Nutrient enrichment can increase the susceptibility of reef corals to bleaching. *Nat. Clim. Change* 3, 160–164. doi:10.1038/nclimate1661.

Wilkerson, F. P., Muller, G., and Muscatine, L. (1983). Temporal patterns of cell division in natural populations of endosymbiotic algae. *Limnol. Oceanogr.* 28, 1009–1014.

Wisecaver, J. H., and Hackett, J. D. (2011). Dinoflagellate genome evolution. *Annu. Rev. Microbiol.* 65, 369–87. doi:10.1146/annurev-micro-090110-102841.

Wong, J. T. Y., and Kwok, A. C. M. (2005). Proliferation of dinoflagellates: blooming or bleaching. *BioEssays News Rev. Mol. Cell. Dev. Biol.* 27, 730–40. doi:10.1002/bies.20250.

Wood-Charlson, E. M., Hollingsworth, L. L., Krupp, D. A., and Weis, V. M. (2006). Lectin/glycan interactions play a role in recognition in a coral/dinoflagellate symbiosis. *Cell. Microbiol.* 8, 1985–1993. doi:10.1111/j.1462-5822.2006.00765.x.

2. Inhibition of glycan biosynthesis reveals symbiont glycome composition and abundance modulate onset of cnidarian-dinoflagellate symbiosis

Trevor R. Tivey[1*], John E. Parkinson[1,2], Paige E. Mandelare[3], Donovon A. Adpressa[3], Virginia M. Weis[1], Sandra Loesgen[3*]

[1]Department of Integrative Biology, Oregon State University, Corvallis, OR, United States
[2]SECORE International, Miami, FL, United States
[3]Department of Chemistry, Oregon State University, Corvallis, OR, United States

2.1 Abstract

The success of cnidarian-dinoflagellate symbiosis hinges on the molecular interactions that govern the establishment and maintenance of intracellular mutualisms. As a fundamental component of innate immunity, glycan-lectin interactions impact the onset of such endosymbioses. In coral-algal associations, the presence and abundance of symbiont glycans play a role in governing host-symbiont specificity, but our understanding of the effects of glycome composition on symbiosis establishment remains limited. In this study, we examined the canonical N-glycan biosynthesis pathway in the genome of the dinoflagellate symbiont *Breviolum minutum* and found it to be conserved with the exception of the transferase GlcNAc-TII (MGAT2). We confirmed the importance of N-glycans for *B. minutum's* colonization of the model sea anemone Aiptasia (*Exaiptasia pallida*) through specific removal of these moieties by N-glycosidase treatment. Finally, we used the biosynthesis inhibitors kifunensine and swainsonine to alter *B. minutum's* glycome composition by increasing the percentages of high-mannose and hybrid glycans, respectively. Successful high-mannose enrichment via kifunensine treatment resulted in a significant decrease in colonization of hosts by *B. minutum*. However, hybrid glycan enrichment via swainsonine treatment could not be confirmed and did not impact colonization. We conclude that functional Golgi processing of N-glycans is critical for maintaining appropriate cell surface glycan composition and for ensuring colonization success by *B. minutum*.

2.2 Introduction

The biodiversity and productivity of coral reef ecosystems relies on the interactions of cnidarian hosts with dinoflagellates in the family Symbiodiniaceae, formerly the genus *Symbiodinium* (LaJeunesse et al., 2018). These unicellular endosymbionts provide photosynthate to their hosts, which enables the partners to thrive in nutrient-limited waters. Each cnidarian generation has to first engulf potential symbionts, select algae for productive symbiosis in the symbiosome (a modified vacuole), and allow for proliferation within its tissue. The biological steps that regulate this colonization process are therefore critical to symbiosis establishment and homeostasis. Innate immunity pathways govern the onset of symbiosis when algae first come into contact with their future host cells (Davy et al., 2012). Cnidarians rely on expanded innate immune repertoires for defense against pathogens and selection of microbes (Bosch, 2013; Dunn, 2009; Hamada et al., 2013; Neubauer et al., 2017; Poole and Weis, 2014). These immune pathways are often co-opted targets for microorganisms looking to benefit from a host, and therefore offer potential avenues for symbiont coevolution and entry into hosts (McGuinness et al., 2003).

The study of glycan-protein interactions has been critical in characterizing the structure and function of glycans, especially regarding cell surface glycans and the role they play in cell-cell communication (Varki, 2017). Cell surface glycans are recognized by carbohydrate-binding proteins, known as lectins, to mediate events such as cell homing, sperm-egg binding, and microbial interactions (Collins and Paulson, 2004; Gallatin et al., 1983; Pang et al., 2011). Lectins have the ability to either promote microbial attachment and colonization or to block the interactions required for entry into the host (Baum et al., 2014; Kachko et al., 2013; Kvennefors et al., 2008; Zhou et al., 2017). These glycan-lectin interactions form a critical component of host innate immunity that functions in cell adhesion, self/non-self discrimination, and pathway activation against potential pathogens (Ip et al., 2009; van Kooyk and Rabinovich, 2008). Glycans constitute a major category of microbe-associated molecular patterns (MAMPs) that function to regulate innate immunity and symbiosis (Davy et al., 2012; Lannoo and Van Damme, 2014). Their role in communication in host-microbe associations renders

glycans critical to the mediation and evolution of many symbioses (Chu and Mazmanian, 2013; Gust et al., 2012; Schwartzman et al., 2015).

While the importance of glycan recognition has been well documented in some host-symbiont associations, still little progress has been made in the characterization of surface glycans in the family Symbiodiniaceae on the molecular level and on their function in symbiosis. Other alveolates offer insight into the importance of glycan-lectin interactions in Symbiodiniaceae mutualisms (Schwarz, 2008). For example, the well-studied apicomplexan parasites *Plasmodium falciparum* and *Toxoplasma gondii* have simplified glycomes that lack the longer immunogenic glycans often detected by host immunity (Bushkin et al., 2010; Fauquenoy et al., 2008; Samuelson et al., 2005). The alveolate parasite *Perkinsus marinus*, a member of the sister phylum to dinoflagellates, has glycans that are recognized during shellfish infection by a host galectin receptor (Tasumi and Vasta, 2007). The prevalent nature of glycan-lectin interactions in parasitic groups that are closely related to dinoflagellates suggests that the glycomes of Symbiodiniaceae may also have coevolved to gain access to the host cnidarian environment.

The strongest evidence that supports glycan-lectin recognition during the onset of Symbiodiniaceae mutualisms comes from experimental manipulations of symbiont cells through enzymatic cleavage of surface glycans. Several species of Symbiodiniaceae have been experimentally de-glycosylated, leading to reduced symbiont uptake in larval, juvenile, and adult aposymbiotic animals (Bay et al., 2011; Kuniya et al., 2015; Lin et al., 2000; Wood-Charlson et al., 2006). Though the effects are not entirely consistent from study to study, the data suggest that N-glycans in particular are an important determinant of host colonization rates by symbionts. It remains uncertain, however, whether disruption in the onset of symbiosis is driven primarily by changes in the overall abundance of N-glycans (i.e. quantity) or by changes in the composition of N-glycans (i.e. complexity), particularly the relative proportions of high-mannose, hybrid, and complex N-glycans.

Although recent advances in the field of glycomics have made the direct chemical analysis of carbohydrates feasible, most studies probing the Symbiodiniaceae cell surface

have relied on indirect lectin binding to characterize glycan type and abundance, and to mask glycan interactions. For example, a variety of fluorescent FITC-labeled lectin probes were used to examine the cell surface of *Cladocopium* sp. (type C1f) isolated from the coral *Fungia scutaria* (Wood-Charlson et al., 2006). *Cladocopium* C1f symbionts were strongly labeled with Concanavalin A (ConA) and Jacalin lectins, which bind α-mannosyl, α-glucosyl and α-galactosyl (Jacalin only) groups. Logan et al. (2010) further examined other genera of Symbiodiniaceae, finding that binding varied by species. *Breviolum minutum* in particular was labeled by a diversity of lectins recognizing mannose, glucose, galactose, N-acetylglucosamine (GlcNAc), and N-acetylgalactosamine (GalNAc) residues. In contrast, Parkinson et al. (2018) used an array of 40 lectins and found only small differences in the glycan profiles between the free-living species *S. pilosum* and the mutualistic species *B. minutum*. Both studies provide evidence that Symbiodiniaceae produce surface glycoproteins containing high-mannose as well as hybrid/complex type N-glycans, but it remains unclear which types of N-glycans specifically contribute to recognition for colonization by mutualistic species.

The N-glycan biosynthesis pathway is well-described in yeast and humans, and a number of natural products have been isolated that serve as inhibitors (**Figure 2.1**) (Helenius and Aebi, 2004; Stanley et al., 2015). If the pathway is conserved in dinoflagellates, it should be possible to use commercially-available inhibitors to alter glycan biosynthesis in Symbiodiniaceae, changing the composition of the glycome without altering the overall abundance of N-glycans. Kifunensine is one such molecule, a plant derived alkaloid, that effectively inhibits the activity of ER Mannosidase I (Elbein et al., 1990). Because blocking cleavage prevents the synthesis of hybrid and complex glycan structures, this inhibition results in an increase in the proportion of high-mannose type glycans (**Figure 2.1**) (Liebminger et al., 2009; Weng and Spiro, 1993). Swainsonine is another small molecule inhibitor that blocks later stage activity of Golgi Mannosidase II (Tulsiani et al., 1982). Therefore, swainsonine treatment increases the proportion of hybrid-type N-glycan content and decreases the proportion of complex-type glycans (**Figure 2.1**) (Petersen et al., 2010; Shah et al., 2008). These two inhibitors can potentially be used to differentially modify symbiont surface glycan composition and

experimentally test for preferential uptake of certain algal cell surfaces by cnidarian hosts.

In this study, we manipulated the glycome of *B. minutum* by changing the number and composition of cell surface glycans using the enzyme PNGase F and the N-glycan biosynthesis inhibitors kifunensine and swainsonine. In addition, we utilize lectins with high binding affinities and selectivity to distinguish between native and manipulated glycoproteins on algal surfaces. Fluorescent probes were conjugated to the cyanobacterial lectin MVL to report the abundance of N-glycans, the cyanobacterial lectin CVN to label high-mannose glycans, and the plant lectin PHA-L to label complex type N-glycans (Kachko et al., 2013). We then explored the effects of these manipulations on colonization by *B. minutum* of aposymbiotic adult polyps of the model cnidarian host Aiptasia (*Exaiptasia pallida*).

2.3 Materials and methods

Raw data and R code for the following analyses can be found in Supplementary File S1. For complete details regarding colonization and image analysis, protocols can be accessed on protocols.io at dx.doi.org/10.17504/protocols.io.j8ucrww.

Identification of N-Glycan Biosynthesis Homologs

Our hypotheses were based on the idea that Symbiodiniaceae share the canonical N-linked glycosylation biosynthesis pathway with other eukaryotes. To strengthen this premise, we first searched for conservation of dolichol-linked precursor oligosaccharide synthesis and ER/Golgi processing pathways in Symbiodiniaceae genomes. We used *Homo sapiens* protein sequences to search for predicted proteins in the Symbiodiniaceae genomes of *Breviolum minutum* (Shoguchi et al., 2013), *Symbiodinium microadriaticum* (Aranda et al., 2016), and *Fugacium kawagutii* (Lin et al., 2015). The genomes of *Perkinsus marinus* strain ATCC 50983 (https://www.ebi.ac.uk/ena/data/view/GCA_000006405.1) (Joseph et al., 2010), *Plasmodium falciparum* strain 3D7 (Gardner et al., 2002), and *Toxoplasma gondii* strain ME49 (Kissinger et al., 2003) were also included as closely-related alveolate comparisons. In total, 34 manually annotated protein sequences from UniProtKB were

used as queries representing proteins involved in N-glycan precursor synthesis and N-glycan processing in the ER and Golgi (The UniProt Consortium, 2017). Enzymes that have similar functions but that are involved in degradation were included as well, such as lysosomal α-mannosidase and β-hexosaminidase 1. Predicted proteins for Symbiodiniaceae species were searched on reefgenomics.org, a platform hosting the genomes of several marine organisms including three Symbiodiniaceae genomes (Liew et al., 2016). Predicted proteins for the three other alveolate genomes were searched on protists.ensembl.org, a browser for protist genomes (Kersey et al., 2018). Homologous proteins were considered to be present in a genome if the top protein BLAST hit exceeded the following cutoff: eval < 1×10^{-5}, bitscore > 50, identity score > 25%. T-Coffee was used to align amino acid sequences of putative α-mannosidases from Symbiodiniaceae against α-mannosidase 2 and lysosomal α-mannosidase (Di Tommaso et al., 2011; Notredame et al., 2000). Sequences were chosen from *Drosophila melanogaster*, *Homo sapiens*, *Mus musculus*, and *Arabidopsis thaliana* to allow for comparison to previous studies characterizing the active sites of α-mannosidase (Park et al., 2005; Shah et al., 2008).

Treatment of Algal Cultures

Breviolum minutum (strain Mf1.05b), a homologous symbiont found in Aiptasia, was used for all experiments. Algal cultures were maintained in f/2 media in an incubator at 26˚C under a 12:12 light:dark cycle and a light intensity of 50 µmol quanta • m^{-2} • s^{-2}. For experimental treatment, algal cultures were reconstituted at 1×10^6 cells • mL^{-1} in f/2 media. For enzymatic treatment, cultures were treated with Peptide:N-glycosidase F for 48 h (50 U PNGase F • mL^{-1} f/2 media). Kifunensine and swainsonine stocks were prepared at concentrations of 50 mM in 100% dimethyl sulfoxide (DMSO) solvent. For biosynthesis inhibition treatment, cultures were incubated for one week in 1 mM kifunensine or swainsonine in 2% DMSO in f/2 (a 1:50 dilution) or in a 2% DMSO in f/2 vehicle control which was well tolerated. (Pilot experiments tested a range of inhibitor concentrations from 10 µM to 10 mM and tested a range of DMSO concentrations from 2-10%; data not shown.)

Lectin Labeling and Flow Cytometry

After treatment, 100 µL algal samples were taken from each treatment, rinsed in 3 mL of filtered artificial seawater (FSW) and centrifuged in 75 mm borosilicate glass tubes (500 RCF for 5 min). Pellets were resuspended in 50 µL of 3.3X PBS, prepared from a 10X PBS stock solution (0.02 M NaH_2PO_4, 0.077 M Na_2PO_4, 1.4 M NaCl, pH 7.4). Subsequently, 50 µL of 2X labeling solution containing lectins conjugated to phycoerythrin (PE) fluorophores was added to each sample at a final concentration of 5 µg lectin • mL^{-1} PBS. Lectins were coupled to PE using the Lightning-Link R-PE Antibody Labeling Kit (Novus Biologicals #703-0010), PE was chosen in order to avoid any overlap with algal autofluorescence. Cyanovirin-N lectin (CVN-PE) was used to label high-mannose N-glycans. *Microcystis viridis* lectin (MVL-PE) was used to label core N-glycan residues composed of GlcNAc and mannose (Shahzad-ul-Hussan et al., 2009). *Phaseolus vulgaris* Phytohaemagglutinin lectin (PHA-L-PE) was used to label complex glycans. Their respective glycan recognition profiles summarized from publicly available glycan array data are shown in **Appendix Figure A1** (http://www.functionalglycomics.org). These lectins were chosen for their micromolar binding affinities and comparatively greater selectivity and cleaner binding profiles. The surface glycan composition of labeled algal symbionts was measured on a CytoFLEX 5L flow cytometer. Algal populations were identified using forward and side scatter, and doublets were removed using FSC-Width in order to avoid overestimating fluorescent intensities of cells. A minimum of 20,000 cells labeled with PE-conjugated lectins were excited at 561 nm and emission was captured with a 585/42 nm bandpass filter. Detection gates were adjusted to measure phycoerythrin labeling by using unstained *B. minutum* cells to set a negative control population gate. The percentage of positive PE labeled cells was calculated out of the total *B. minutum* cell population in the FSC-Width population gate.

Colonization Experiments

Aposymbiotic adult Aiptasia polyps were obtained after repeated menthol bleaching (Matthews et al., 2016) and maintenance in the dark. Prior to the beginning of experiments, polyps were individually plated in 24-well plates and exposed to the same 12:12 light:dark cycle as algal cultures for one week. Animals were then visually checked under an inverted compound fluorescence microscope for the presence of any contaminating symbionts, and only those completely lacking symbionts were used in colonization experiments. Algae from each treatment were rinsed in FSW and resuspended to 2 x 10^6 cells • mL^{-1}. Each anemone was inoculated with 1 x 10^6 cells (0.5 mL of algal treatment) in a total volume of 1 mL FSW. After 48 h, the wells were rinsed three times with FSW, and left for 24 h before overnight fixation in 4% paraformaldehyde in 1X PBS. To prepare for imaging symbiont density, the oral discs with tentacles were dissected from the columns of each polyp and mounted on slides in a mounting solution (90% glycerol, 10% 1X PBS) as described previously (Parkinson et al., 2018).

Image Analysis

To normalize symbiont density to host surface area, epifluorescence microscopy was used to capture autofluorescence from the symbionts and the host anemone tissue as detailed previously (Parkinson et al., 2018). Symbiont chlorophyll autofluorescence was captured under the Cy3 (red) filter, whereas autofluorescence from host green fluorescence was captured using the GFP (green) filter. Images of symbiont density after colonization of hosts were captured with a Zeiss AxioObserver A1 microscope and an Axiovert ICm1 camera (Carl Zeiss AG, Jena, Germany). Algal cell numbers were automatically quantified by setting a predetermined cell radius for the ITCN plugin for Fiji (ImageJ2). To calculate algal density as a proxy for symbiont colonization, the total algal cell number was divided by the surface area of host autofluorescence.

2.4 Results and Discussion

N-Glycan Biosynthesis Pathway Conservation in Alveolates

We hypothesized that the pathways underlying N-linked glycoprotein production in Symbiodiniaceae are similar to those in humans and other well-studied eukaryotes; indeed, we found a large degree of conservation among members of these groups using BLASTP searches for homologous proteins. We found strong evidence for N-glycan biosynthesis conservation up to MGAT1, an N-acetylglucosaminyltransferase essential for hybrid and complex type glycan processing (**Table 2.1**, **Figure 2.1**). Golgi α-mannosidase 2, the next step in the N-glycan pathway, also appears in a BLASTP search of Symbiodiniaceae genomes, however the sequence hits were more similar to lysosomal α-mannosidase, especially in conserved regions (**Appendix A Figure A2, A3**). Without functional or subcellular location data, it is difficult to discern whether this α-mannosidase functions during N-glycan biosynthesis or only during degradation; regardless, it should be inhibited by swainsonine based on conserved residues (**Appendix A Table A1**) (Shah et al., 2008). Although all Symbiodiniaceae appear to be missing GlcNAc-TII (MGAT2), *B. minutum*'s genome includes transferases GlcNAc-TIII (MGAT 3), GlcNAc-TIV (MGAT 4) and GlcNAc-TV (MGAT5) required for bisecting, tri-, and tetra-antennary N-glycans (**Table 2.1**). The presence of these transferases supports the existence of hybrid glycan biosynthesis in Symbiodiniaceae. With the absence of MGAT2, it remains unclear whether the α-1-6 branch required for complex glycans can be formed (Stanley et al., 2015). In addition to the majority of enzymes required for N-glycan branching, Symbiodiniaceae genomes contain N-glycan transferases for xylose, fucose, and galactose. These moieties are possible targets for the expanded set of cnidarian ficolin-like proteins, fucolectins, and c-type lectins found in Aiptasia (Baumgarten et al., 2015; Sunagawa et al., 2009). There is limited evidence for sialic acid transferases in the N-glycan biosynthesis of these Symbiodiniaceae genomes (**Table 2.1**), but in general these Symbiodiniaceae species appear to have the capacity to create high-mannose, hybrid, and potentially complex glycans.

The N-glycan biosynthesis pathway BLASTP protein hits for the Symbiodiniaceae species (*B. minutum*, *S. microadriaticum*, and *F. kawagutii*) were most similar in identity to the closely related *Perkinsus marinus*, an endoparasite of oysters

(**Table 2.1**). Among the Symbiodiniaceae, we found *F. kawagutii*'s N-glycan biosynthesis pathway to be the least conserved, which agreed with the initial, less stringent analysis of the N-glycan pathway from the *F. kawagutii* draft genome (Lin et al., 2015). This lack of conservation could reflect its phylogenetic position (one of the most derived lineages within the group) and/or its ecology (of the three species, it is the only one that is nonsymbiotic). If hybrid and/or complex N-glycan production is a key to symbiosis establishment and maintenance, there may be less selective pressure to retain these genes in nonsymbiotic species. However, as Symbiodiniaceae genomes are still in draft states, pathway absences may result from differences in genome completeness, especially considering the decreased number and shorter length of gene models in the *F. kawagutii* genome (Lin et al., 2015; Liu et al., 2017). In examining more evolutionarily distant comparisons, *B. minutum* and *S. microadriaticum* appear to have a greater capacity for N glycan biosynthesis than many other algal protists, including other dinoflagellates, chlorophytes, diatoms, and haptophytes (Lin et al., 2015).

The degree of conservation in the N-glycan biosynthesis pathway of Symbiodiniaceae is striking when compared to the degenerate pathways of the alveolate parasites *Plasmodium falciparum* and *Toxoplasma gondii*. In contrast to Symbiodiniaceae, *P. falciparum* has severely limited N-glycosylation and O-glycosylation, and is only able to produce the chitobiose core using ALG13 and ALG14 (**Table 2.1**) (Bushkin et al., 2010; Davidson and Gowda, 2001). Instead *P. falciparum* relies on GPI anchors (glycolipids) to stabilize proteins, and uses its own lectins to bind to host cells (von Itzstein et al., 2008). The *T. gondii* glycome is composed predominantly of high-mannose ($Man_{5–8}(GlcNAc)_2$) and shorter paucimannose ($Man_{3–4}(GlcNAc)_2$) glycans (Fauquenoy et al., 2008). These degenerate N-glycans are partially a consequence of a loss of ALG glycosyltransferases in both parasites (Samuelson et al., 2005) (**Table 2.1**). The general conservation of precursor synthesis and ER/Golgi processing in Symbiodiniaceae and *P. marinus* suggests strong differences in N-glycan processing between apicomplexans and Dinozoans (containing dinoflagellates and their sister phylum Perkinsozoa), supporting the hypothesis that among alveolates, only apicomplexans have undergone secondary loss of ALG enzymes (Bushkin et al., 2010).

N-Glycan Enzymatic Cleavage in Breviolum minutum

We expected that glycosidase treatment with PNGase F would decrease the total number of N-linked glycans on the cell surface of *B. minutum* and subsequently reduce colonization success. We measured changes to the algal cell surfaces using fluorescently tagged lectin (CVN-PE) that recognized glycans highly enriched with α(1-2)-linked dimannosides. After exposure to PNGase F, CVN-PE labeling intensities decreased, indicating that fewer high-mannoside glycans were present on algal cell surfaces after treatment (**Figure 2.2A;** ANOVA, $p < 0.001$). Aiptasia polyps were then inoculated with the glycosidase-treated or untreated cells. After initial colonization, symbiont density was lower in hosts exposed to the cells with reduced N-glycan abundances (**Figure 2.2B;** t-test, $p < 0.05$).

These results support the importance of N-glycans in host-symbiont interactions during the onset of symbiosis and are consistent with previous studies in Aiptasia and coral larvae. N-glycosidase treatments of algal symbionts blocked colonization by algae of Aiptasia adults, as did treatments with O-glycosidase, trypsin, and α-amylase (Lin et al., 2000). Similarly, N-glycosidase and trypsin treatments inhibited symbiont colonization in the larvae of the coral *Fungia scutaria* (Wood-Charlson et al., 2006). In contrast, α-amylase had no effect on the percentage of *F. scutaria* larvae colonized or in algal density within individual larvae. In another coral larval study using *Acropora tenuis*, α-amylase and trypsin instead increased the number of symbiont cells taken up by larvae (Bay et al., 2011). Across all enzymatic treatments to date, N-glycosidases have had the most consistent negative effect on colonization rates of Symbiodiniaceae in cnidarian hosts. Enzymatic treatment with trypsin and PNGase F has also been used to decrease affinity of isolated cnidarian lectins to their glycan binding sites on Symbiodiniaceae, supporting the hypothesized function of glycan-lectin interactions in symbiosis (Jimbo et al., 2013; Kita et al., 2015). This consistency across many studies suggests that the overall abundance of N-glycans on the Symbiodiniaceae cell surface impacts the rate of symbiont uptake by cnidarian cells.

N-Glycan Biosynthesis Inhibition in Breviolum minutum

After confirming the effect of glycan abundance on colonization success, we were interested in understanding how the composition of different types of N-glycans affected onset of symbiosis. To alter glycan composition, we inhibited the N-glycan biosynthesis pathway at ER and golgi mannosidase enzymatic steps using small molecule inhibitors kifunensine and swainsonine (**Figure 2.1**). To confirm that the manipulations altered the composition rather than the abundance of N-glycans, we labeled cells with MVL-PE, which binds to structures consisting of Manβ(1-4)GlcNAcβ(1-4), a common core found in all three N-glycan types (**Figure 2.3A**). MVL-PE labeling did not differ between groups (**Figure 2.3B;** ANOVA, $p > 0.05$), suggesting similar glycan abundances between all treatments. This stability in glycan abundance allowed us to analyze the remaining lectin binding data as representative of differences in glycan composition.

Kifunensine blocks MAN1, the enzyme responsible for converting high-mannose glycans to hybrid glycans featuring less mannose. To confirm that kifunensine treatment increased the proportion of high-mannose glycans, symbiont cells were labeled with CVN-PE, which binds with α(1-2)-linked dimannosides residing at the branch tips of mannose-rich glycans (**Figure 2.3A**). Cells treated with kifunensine had the highest intensity of CVN-PE labeling as expected, significantly greater than both swainsonine-treated and untreated cells (**Figure 2.3C;** ANOVA, $p < 0.05$). Swainsonine-treated cells also exhibited significantly greater labeling by CVN for mannosides than untreated cells. This was expected, as hybrid glycan structures induced by swainsonine should have more abundant mannose moieties than untreated cells that feature a greater proportion of complex, low-mannose glycans (**Figure 2.1**). The increase in lectin-binding in treated symbionts supports the presence of active N-glycan biosynthesis inhibition from kifunensine and swainsonine incubation.

Swainsonine blocks MAN2, the enzyme responsible for converting hybrid glycans to complex glycans featuring even less mannose. To confirm that swainsonine treatment decreased the proportion of complex glycans (and therefore increased the

proportion of hybrid glycans), symbiont cells were labeled with PHA-L-PE, which binds Galβ(1-4)GlcNAc linkages from the 2,6 branch found mainly in complex glycans (Fabre et al., 1998). Symbiont cells exhibited low levels of labeling with PHA-L-PE overall. Opposite to the expectation that swainsonine blocks complex glycan formation, cells treated with swainsonine showed increased, rather than decreased PHA-L-PE labeling compared to untreated cells (**Figure 2.3D;** ANOVA, $p < 0.05$). The low levels of staining combined with an absence of complex glycan inhibition suggests differences in later steps of canonical N-glycan biosynthesis. It is possible that *B. minutum* has alternative pathways to build N-glycans besides the late stage processing in the Golgi apparatus, known in eukaryotes to create N-glycoproteins that can be recognized by PHA-L. Additionally, since the MAN2 found in *B. minutum* is most similar to lysosomal mannosidases (**Appendix A Figure A2**), swainsonine may have instead inhibited lysosomal catabolism, contributing to glycan dysregulation (Dorling et al., 1980). It is also possible that while the treatment failed to decrease complex glycan proportion, it nevertheless may have increased hybrid glycan proportion, as we did not measure hybrid glycans directly. This outcome would be consistent with the greater mannose-binding we observed directly with CVN-PE in swainsonine-treated cells.

Kifunensine-treated cells were also expected to have a lower proportion of complex glycans, however kifunensine showed no difference in PHA-L-PE labeling compared to untreated cells (**Figure 2.3D;** ANOVA, $p = 0.84$). This may indicate that the naturally occurring glycans on the Symbiodiniaceae cell surface are not primarily composed of complex N-glycans. Earlier studies on Symbiodiniaceae cell surface glycans found strong PHA-L lectin binding in the family (Logan et al., 2010). However, compared to other genera, *B. minutum* exhibited the least amount of binding from PHA-L and ConA, recognizing complex N-glycans and high-mannose glycans specifically. It is therefore possible that *B. minutum* does not have the ability to produce complex N-glycans. However, the presence of additional N-glycan transferases for moieties such as xylose, fucose, and galactose, support the potential for glycan complexity, and it cannot be ruled out that *B. minutum* and other Symbiodiniaceae have alternate pathways for producing complex glycans. The O-glycan pathway is currently uncharacterized in

Symbiodiniaceae, but it may allow for similar variation in complexity and subsequently play a role in host recognition.

N-Glycan Biosynthesis Inhibition Decreases Symbiont Colonization Rates

Finally, we inoculated aposymbiotic Aiptasia with *B. minutum* cultures treated with the N-glycan biosynthesis inhibitors to determine whether glycan composition has an effect on symbiont colonization rates in naïve hosts. After a fixed exposure period, Aiptasia polyps inoculated with kifunensine-treated cells had a lower symbiont density compared to those inoculated with untreated control cells (**Figure 2.4**; ANOVA, Dunnett's test, $p < 0.05$). However, animals colonized by swainsonine-treated cells had symbiont densities equivalent to controls (**Figure 2.4**; ANOVA, Dunnett's test $p = 0.295$). Although previous studies have shown that low abundances of high-mannose glycans on symbiont cell surfaces inhibit colonization, our data indicate that elevated proportions of high-mannose glycans can also inhibit colonization, suggesting that glycan composition is a key factor modulating symbiosis establishment.

Our results provide further support for the role of N-glycan recognition during symbiosis establishment. Decreasing mannose through the cleavage and masking of N-glycans decreases colonization success (this study; Parkinson et al., 2018), findings that are consistent with previous studies (Bay et al., 2011; Kuniya et al., 2015; Lin et al., 2000; Wood-Charlson et al., 2006). In addition, this study is the first to increase the proportion of high-mannose glycans without changing the overall abundance of N-linked glycans and show that mannose overabundance also decreases colonization success. These findings suggest that successful symbiosis establishment depends on an appropriate symbiont glycome composition. Abnormal abundances (either too high or too low) of high-mannose N-glycans could signal the presence of an inappropriate symbiont. An additional possibility is that hybrid glycan-lectin interactions are selective at a later step in the recognition process after initial recognition of mannose, which would support the observed difference in colonization success between swainsonine-treated cells (i.e. more high-mannose and hybrid N-glycans) and kifunensine-treated cells (i.e. more high-mannose N-glycans only). This potential multi-step glycan recognition could be part of a

"winnowing" process of host-symbiont selection such as those found in other symbioses (Nyholm and McFall-Ngai, 2004).

In cnidarians, mannose recognition includes a variety of highly conserved mechanisms (Kimura et al., 2009; Meyer and Weis, 2012; Wood-Charlson and Weis, 2009). For example, the lectin-complement pathway is functional in the gastroderm and expression is upregulated in response to bacterial pathogens and algal symbionts (Kimura et al., 2009; Poole et al., 2016). The binding of pattern recognition receptors (PRRs), such as the coral mannose-binding lectin millectin, to both pathogenic bacteria and members of Symbiodiniaceae suggests a dual role of mannose glycan recognition in cnidarian immunity and symbiosis (Kvennefors et al., 2008, 2010). Indeed, the activation of host innate immunity during colonization contrasts with the repression of host innate immunity under stable symbiosis conditions (Detournay et al., 2012; Mansfield et al., 2017; Merselis et al., 2018; Poole et al., 2016). Therefore, the response of host cells to symbiont N-glycan abundance and composition may differ depending on symbiotic state and life history stage.

Implications and Future Directions

Our results reflect an important albeit limited role for N-glycans in symbiont recognition during initiation of symbiosis establishment. The direct approach of manipulating N-glycans (through cleavage with PNGase or through biosynthetic manipulation) had a stronger effect than previous glycan masking on colonization. Nevertheless, colonization success was highly variable in a clonal adult host, possibly due to small differences in polyp size or states of innate immunity in aposymbiotic adults. Challenging naïve, aposymbiotic larvae may be a more fruitful approach in the Aiptasia system when investigating symbiosis establishment, since larvae allow for greater sample sizes and thus more statistical power to detect subtle differences in colonization (Parkinson et al., 2018). Despite this limitation, the differences observed in glycan characterization and symbiont recolonization support the further use of aposymbiotic Aiptasia adults as a model for understanding processes involved in bleaching recovery. Most glycan-lectin studies of cnidarians (this one included) make use of fluorescent lectin proxies for

describing Symbiodiniaceae glycan profiles. It is noteworthy that the choice and quality of selected lectins is important, and for this study we chose lectins with high binding affinities and specific glycan recognition motifs to decipher subtle differences in the Symbiodiniaceae glycome. Though we have learned about the characterization and role of glycans through this indirect approach, a holistic understanding of the symbiont glycome and its functional importance will require direct characterization of the glycome on the molecular level using mass-spectrometry combined with hypothesis-driven colonization experiments. The potential for variation in N-glycan biosynthesis among Symbiodiniaceae could provide a basis for host-symbiont recognition as well as recolonization dynamics after bleaching events. Experimental manipulation of these glycan biosynthesis pathways in different symbiont species will help us to map the range of interactions possible between host cnidarians and symbiont cells, and to better describe glycan-lectin interactions under the dynamic environmental conditions that accompany periods of dysbiosis.

2.5 Acknowledgements

This research was funded by the National Science Foundation (NSF IOS-1557804 to V.M.W and S.L.). We thank Shumpei Maruyama, Sarah Howey, Milan Sengthrep, Tyler Coleman, Kyle Petersen, Darian Thompson, and Kenneth Moller for their assistance in algal and animal maintenance. In addition, we thank Allison Ehrlich, Jamie Pennington, and the Environmental and Molecular Toxicology Department at Oregon State University for technical support in flow cytometry.

2.6 References

Aranda, M., Li, Y., Liew, Y. J., Baumgarten, S., Simakov, O., Wilson, M. C., et al. (2016). Genomes of coral dinoflagellate symbionts highlight evolutionary adaptations conducive to a symbiotic lifestyle. *Sci. Rep.* 6, 39734. doi:10.1038/srep39734.

Baum, L. G., Garner, O. B., Schaefer, K., and Lee, B. (2014). Microbe-host interactions are positively and negatively regulated by galectin-glycan interactions. *Front. Immunol.* 5, 1–8. doi:10.3389/fimmu.2014.00284.

Baumgarten, S., Simakov, O., Esherick, L. Y., Liew, Y. J., Lehnert, E. M., Michell, C. T., et al. (2015). The genome of Aiptasia , a sea anemone model for coral symbiosis. *Proc. Natl. Acad. Sci.* 112, 11893–11898. doi:10.1073/pnas.1513318112.

Bay, L. K., Cumbo, V. R., Abrego, D., Kool, J. T., Ainsworth, T. D., and Willis, B. L. (2011). Infection Dynamics Vary between Symbiodinium Types and Cell Surface Treatments during Establishment of Endosymbiosis with Coral Larvae. *Diversity* 3, 356–374. doi:10.3390/d3030356.

Bosch, T. C. G. (2013). Cnidarian-microbe interactions and the origin of innate immunity in metazoans. *Annu. Rev. Microbiol.* 67, 499–518. doi:10.1146/annurev-micro-092412-155626.

Bushkin, G. G., Ratner, D. M., Cui, J., Banerjee, S., Duraisingh, M. T., Jennings, C. V., et al. (2010). Suggestive evidence for Darwinian selection against asparagine-linked glycans of Plasmodium falciparum and Toxoplasma gondii. *Eukaryot. Cell* 9, 228–241. doi:10.1128/EC.00197-09.

Chu, H., and Mazmanian, S. K. (2013). Innate immune recognition of the microbiota promotes host-microbial symbiosis. *Nat. Immunol.* 14, 668–675. doi:10.1038/ni.2635.

Collins, B. E., and Paulson, J. C. (2004). Cell surface biology mediated by low affinity multivalent protein–glycan interactions. *Curr. Opin. Chem. Biol.* 8, 617–625. doi:10.1016/j.cbpa.2004.10.004.

Davidson, E. A., and Gowda, D. C. (2001). Glycobiology of Plasmodium falciparum. *Biochimie* 83, 601–604. doi:10.1016/S0300-9084(01)01316-5.

Davy, S. K., Allemand, D., and Weis, V. M. (2012). Cell Biology of Cnidarian-Dinoflagellate Symbiosis. *Microbiol. Mol. Biol. Rev.* 76, 229–261. doi:10.1128/MMBR.05014-11.

Detournay, O., Schnitzler, C. E., Poole, A., and Weis, V. M. (2012). Regulation of cnidarian–dinoflagellate mutualisms: Evidence that activation of a host TGFB

innate immune pathway promotes tolerance of the symbiont. *Dev. Comp. Immunol.* 38, 525–537. doi:10.1016/j.dci.2012.08.008.

Di Tommaso, P., Moretti, S., Xenarios, I., Orobitg, M., Montanyola, A., Chang, J.-M., et al. (2011). T-Coffee: a web server for the multiple sequence alignment of protein and RNA sequences using structural information and homology extension. *Nucleic Acids Res.* 39, W13–W17. doi:10.1093/nar/gkr245.

Dorling, P. R., Huxtable, C. R., and Colegate, S. M. (1980). Inhibition of lysosomal alpha-mannosidase by swainsonine, an indolizidine alkaloid isolated from Swainsona canescens. *Biochem. J.* 191, 649–651. doi:10.1042/BJ1910649.

Dunn, S. R. (2009). Immunorecognition and immunoreceptors in the Cnidaria. *Invertebr. Surviv. J.* 6, 7–14.

Elbein, A. D., Tropea, J. E., Mitchell, M., and Kaushal, G. P. (1990). Kifunensine, a potent inhibitor of the glycoprotein processing mannosidase I. *J. Biol. Chem.* 265, 15599–15605.

Fabre, C., Causse, H., Mourey, L., Koninkx, J., Rivière, M., Hendriks, H., et al. (1998). Characterization and sugar-binding properties of arcelin-1, an insecticidal lectin-like protein isolated from kidney bean (Phaseolus vulgaris L. cv. RAZ-2) seeds. *Biochem. J.* 329, 551–560.

Fauquenoy, S., Morelle, W., Hovasse, A., Bednarczyk, A., Slomianny, C., Schaeffer, C., et al. (2008). Proteomics and Glycomics Analyses of N-Glycosylated Structures Involved in Toxoplasma gondii-Host Cell Interactions. *Mol. Cell. Proteomics* 7, 891–910. doi:10.1074/mcp.M700391-MCP200.

Gallatin, W. M., Weissman, I. L., and Butcher, E. C. (1983). A cell-surface molecule involved in organ-specific homing of lymphocytes. *Nature* 304, 30–34. doi:10.1038/304030a0.

Gardner, M. J., Hall, N., Fung, E., White, O., Berriman, M., Hyman, R. W., et al. (2002). Genome sequence of the human malaria parasite Plasmodium falciparum. *Nature* 419. doi:10.1038/nature01097.

Gust, A. A., Willmann, R., Desaki, Y., Grabherr, H. M., and Nürnberger, T. (2012). Plant LysM proteins: modules mediating symbiosis and immunity. *Trends Plant Sci.* 17, 495–502. doi:10.1016/j.tplants.2012.04.003.

Hamada, M., Shoguchi, E., Shinzato, C., Kawashima, T., Miller, D. J., and Satoh, N. (2013). The complex NOD-like receptor repertoire of the coral Acropora digitifera includes novel domain combinations. *Mol. Biol. Evol.* 30, 167–76. doi:10.1093/molbev/mss213.

Helenius, A., and Aebi, M. (2004). Roles of N-Linked Glycans in the Endoplasmic Reticulum. *Annu. Rev. Biochem.* 73, 1019–1049. doi:10.1146/annurev.biochem.73.011303.073752.

Ip, W. K., Takahashi, K., Alan Ezekowitz, R., and Stuart, L. M. (2009). Mannose-binding lectin and innate immunity. *Immunol. Rev.* 230, 9–21. doi:10.1111/j.1600-065X.2009.00789.x.

Jimbo, M., Suda, Y., Koike, K., Nakamura-Tsuruta, S., Kominami, J., Kamei, M., et al. (2013). Possible involvement of glycolipids in lectin-mediated cellular transformation of symbiotic microalgae in corals. *J. Exp. Mar. Biol. Ecol.* 439, 129–135. doi:10.1016/j.jembe.2012.10.022.

Joseph, S. J., Fernández-Robledo, J. A., Gardner, M. J., El-Sayed, N. M., Kuo, C.-H., Schott, E. J., et al. (2010). The Alveolate Perkinsus marinus: Biological Insights from EST Gene Discovery. *BMC Genomics* 11, 228. doi:10.1186/1471-2164-11-228.

Kachko, A., Loesgen, S., Shahzad-Ul-Hussan, S., Tan, W., Zubkova, I., Takeda, K., et al. (2013). Inhibition of hepatitis C virus by the cyanobacterial protein Microcystis viridis lectin: mechanistic differences between the high-mannose specific lectins MVL, CV-N, and GNA. *Mol. Pharm.* 10, 4590–602. doi:10.1021/mp400399b.

Kersey, P. J., Allen, J. E., Allot, A., Barba, M., Boddu, S., Bolt, B. J., et al. (2018). Ensembl Genomes 2018: an integrated omics infrastructure for non-vertebrate species. *Nucleic Acids Res.* 46, D802–D808. doi:10.1093/nar/gkx1011.

Kimura, A., Sakaguchi, E., and Nonaka, M. (2009). Multi-component complement system of Cnidaria: C3, Bf, and MASP genes expressed in the endodermal tissues of a sea anemone, Nematostella vectensis. *Immunobiology* 214, 165–178. doi:10.1016/j.imbio.2009.01.003.

Kissinger, J. C., Gajria, B., Li, L., Paulsen, I. T., and Roos, D. S. (2003). ToxoDB: accessing the Toxoplasma gondii genome. *Nucleic Acids Res.* 31, 234–236. doi:10.1093/nar/gkg072.

Kita, A., Jimbo, M., Sakai, R., Morimoto, Y., and Miki, K. (2015). Crystal structure of a symbiosis-related lectin from octocoral. *Glycobiology* 25, 1016–1023. doi:10.1093/glycob/cwv033.

Kuniya, N., Jimbo, M., Tanimoto, F., Yamashita, H., Koike, K., Harii, S., et al. (2015). Possible involvement of Tachylectin-2-like lectin from Acropora tenuis in the process of Symbiodinium acquisition. *Fish. Sci.* 81, 473–483. doi:10.1007/s12562-015-0862-y.

Kvennefors, E. C. E., Leggat, W., Hoegh-Guldberg, O., Degnan, B. M., and Barnes, A. C. (2008). An ancient and variable mannose-binding lectin from the coral

Acropora millepora binds both pathogens and symbionts. *Dev. Comp. Immunol.* 32, 1582–1592. doi:10.1016/j.dci.2008.05.010.

Kvennefors, E. C. E., Leggat, W., Kerr, C. C., Ainsworth, T. D., Hoegh-Guldberg, O., and Barnes, A. C. (2010). Analysis of evolutionarily conserved innate immune components in coral links immunity and symbiosis. *Dev. Comp. Immunol.* 34, 1219–29. doi:10.1016/j.dci.2010.06.016.

LaJeunesse, T. C., Parkinson, J. E., Gabrielson, P. W., Jeong, H. J., Reimer, J. D., Voolstra, C. R., et al. (2018). Systematic Revision of Symbiodiniaceae Highlights the Antiquity and Diversity of Coral Endosymbionts. *Curr. Biol.* 28, 2570-2580.e6. doi:10.1016/j.cub.2018.07.008.

Lannoo, N., and Van Damme, E. J. M. (2014). Lectin domains at the frontiers of plant defense. *Front. Plant Sci.* 5. doi:10.3389/fpls.2014.00397.

Liebminger, E., Hüttner, S., Vavra, U., Fischl, R., Schoberer, J., Grass, J., et al. (2009). Class I alpha-mannosidases are required for N-glycan processing and root development in Arabidopsis thaliana. *Plant Cell* 21, 3850–3867. doi:10.1105/tpc.109.072363.

Liew, Y. J., Aranda, M., and Voolstra, C. R. (2016). Reefgenomics.Org - a repository for marine genomics data. *Database* 2016. doi:10.1093/database/baw152.

Lin, K., Wang, J., and Fang, L.-S. (2000). Participation of Glycoproteins on Zooxanthellal Cell Walls in the Establishment of a Symbiotic Relationship with the Sea Anemone, Aiptasia pulchella. 39, 172–178.

Lin, S., Cheng, S., Song, B., Zhong, X., Lin, X., Li, W., et al. (2015). The Symbiodinium kawagutii genome illuminates dinoflagellate gene expression and coral symbiosis. *Science* 350, 691–694. doi:10.1126/science.aad0408.

Liu, H., Stephens, T. G., González-pech, R. A., Beltran, V. H., Bongaerts, P., Cooke, I., et al. (2017). Symbiodinium genomes reveal adaptive evolution of functions related to symbiosis.

Logan, D. D. K., LaFlamme, A. C., Weis, V. M., and Davy, S. K. (2010). Flow-Cytometric Characterization of the Cell-Surface Glycans of Symbiotic Dinoflagellates (Symbiodinium Spp.). *J. Phycol.* 46, 525–533. doi:10.1111/j.1529-8817.2010.00819.x.

Mansfield, K. M., Carter, N. M., Nguyen, L., Cleves, P. A., Alshanbayeva, A., Williams, L. M., et al. (2017). Transcription factor NF-κB is modulated by symbiotic status in a sea anemone model of cnidarian bleaching. *Sci. Rep.* 7, 1–14. doi:10.1038/s41598-017-16168-w.

Matthews, J. L., Sproles, A. E., Oakley, C. A., Grossman, A. R., Weis, V. M., and Davy, S. K. (2016). Menthol-induced bleaching rapidly and effectively provides experimental aposymbiotic sea anemones (Aiptasia sp.) for symbiosis investigations. *J. Exp. Biol.* 219, 306–310. doi:10.1242/jeb.128934.

McGuinness, D. H., Dehal, P. K., and Pleass, R. J. (2003). Pattern recognition molecules and innate immunity to parasites. *Trends Parasitol.* 19, 312–319. doi:10.1016/S1471-4922(03)00123-5.

Merselis, D. G., Lirman, D., and Rodriguez-Lanetty, M. (2018). Symbiotic immuno-suppression: is disease susceptibility the price of bleaching resistance? *PeerJ* 6, e4494. doi:10.7717/peerj.4494.

Meyer, E., and Weis, V. M. (2012). Study of cnidarian-algal symbiosis in the "omics" age. *Biol. Bull.* 223, 44–65. doi:10.1086/BBLv223n1p44.

Neubauer, E.-F., Poole, A. Z., Neubauer, P., Detournay, O., Tan, K., Davy, S. K., et al. (2017). A diverse host thrombospondin-type-1 repeat protein repertoire promotes symbiont colonization during establishment of cnidarian-dinoflagellate symbiosis. *eLife* 6. doi:10.7554/eLife.24494.

Notredame, C., Higgins, D. G., and Heringa, J. (2000). T-Coffee: A novel method for fast and accurate multiple sequence alignment. *J. Mol. Biol.* 302, 205–217. doi:10.1006/jmbi.2000.4042.

Nyholm, S. V., and McFall-Ngai, M. J. (2004). The winnowing: establishing the squid-vibrio symbiosis. *Nat. Rev. Microbiol.* 2, 632–42. doi:10.1038/nrmicro957.

Pang, P.-C., Chiu, P. C. N., Lee, C.-L., Chang, L.-Y., Panico, M., Morris, H. R., et al. (2011). Human Sperm Binding Is Mediated by the Sialyl-Lewisx Oligosaccharide on the Zona Pellucida. *Science* 333, 1761–1764. doi:10.1126/science.1207438.

Park, C., Meng, L., Stanton, L. H., Collins, R. E., Mast, S. W., Yi, X., et al. (2005). Characterization of a Human Core-specific Lysosomal α1,6-Mannosidase Involved in *N* -Glycan Catabolism. *J. Biol. Chem.* 280, 37204–37216. doi:10.1074/jbc.M508930200.

Parkinson, J. E., Tivey, T. R., Mandelare, P. E., Adpressa, D. A., Loesgen, S., and Weis, V. M. (2018). Subtle Differences in Symbiont Cell Surface Glycan Profiles Do Not Explain Species-Specific Colonization Rates in a Model Cnidarian-Algal Symbiosis. *Front. Microbiol.* 9. doi:10.3389/fmicb.2018.00842.

Petersen, L., Ardèvol, A., Rovira, C., and Reilly, P. J. (2010). Molecular Mechanism of the Glycosylation Step Catalyzed by Golgi α-Mannosidase II: A QM/MM Metadynamics Investigation. *J. Am. Chem. Soc.* 132, 8291–8300. doi:10.1021/ja909249u.

Poole, A. Z., Kitchen, S. A., and Weis, V. M. (2016). The Role of Complement in Cnidarian-Dinoflagellate Symbiosis and Immune Challenge in the Sea Anemone Aiptasia pallida. *Front. Microbiol.* 7, 519. doi:10.3389/fmicb.2016.00519.

Poole, A. Z., and Weis, V. M. (2014). TIR-domain-containing protein repertoire of nine anthozoan species reveals coral-specific expansions and uncharacterized proteins. *Dev. Comp. Immunol.* 46, 480–488. doi:10.1016/j.dci.2014.06.002.

Samuelson, J., Banerjee, S., Magnelli, P., Cui, J., Kelleher, D. J., Gilmore, R., et al. (2005). The diversity of dolichol-linked precursors to Asn-linked glycans likely results from secondary loss of sets of glycosyltransferases. *Proc. Natl. Acad. Sci.* 102, 1548–1553. doi:10.1073/pnas.0409460102.

Schwartzman, J. A., Koch, E., Heath-Heckman, E. A. C., Zhou, L., Kremer, N., McFall-Ngai, M. J., et al. (2015). The chemistry of negotiation: Rhythmic, glycan-driven acidification in a symbiotic conversation. *Proc. Natl. Acad. Sci.* 112, 201418580. doi:10.1073/pnas.1418580112.

Schwarz, J. A. (2008). Understanding the intracellular niche in cnidarian-Symbiodinium symbioses: parasites lead the way. *Vie Milieu - Life Environ.* 58, 141–151.

Shah, N., Kuntz, D. A., and Rose, D. R. (2008). Golgi -mannosidase II cleaves two sugars sequentially in the same catalytic site. *Proc. Natl. Acad. Sci.* 105, 9570–9575. doi:10.1073/pnas.0802206105.

Shahzad-ul-Hussan, S., Cai, M., and Bewley, C. A. (2009). Unprecedented Glycosidase Activity at a Lectin Carbohydrate-Binding Site Exemplified by the Cyanobacterial Lectin MVL. doi:10.1021/ja905929c.

Shoguchi, E., Shinzato, C., Kawashima, T., Gyoja, F., Mungpakdee, S., Koyanagi, R., et al. (2013). Draft assembly of the Symbiodinium minutum nuclear genome reveals dinoflagellate gene structure. *Curr. Biol. CB* 23, 1399–408. doi:10.1016/j.cub.2013.05.062.

Stanley, P., Taniguchi, N., and Aebi, M. (2015). "N-Glycans," in *Essentials of Glycobiology*, eds. A. Varki, R. D. Cummings, J. D. Esko, P. Stanley, G. W. Hart, M. Aebi, et al. (Cold Spring Harbor (NY): Cold Spring Harbor Laboratory Press). Available at: http://www.ncbi.nlm.nih.gov/books/NBK453020/ [Accessed December 17, 2018].

Sunagawa, S., Wilson, E. C., Thaler, M., Smith, M. L., Caruso, C., Pringle, J. R., et al. (2009). Generation and analysis of transcriptomic resources for a model system on the rise: the sea anemone Aiptasia pallida and its dinoflagellate endosymbiont. *BMC Genomics* 10, 258. doi:10.1186/1471-2164-10-258.

Tasumi, S., and Vasta, G. R. (2007). A Galectin of Unique Domain Organization from Hemocytes of the Eastern Oyster (Crassostrea virginica) Is a Receptor for the

Protistan Parasite Perkinsus marinus. *J. Immunol.* 179, 3086–3098. doi:10.4049/jimmunol.179.5.3086.

The UniProt Consortium (2017). UniProt: the universal protein knowledgebase. *Nucleic Acids Res.* 45, D158–D169. doi:10.1093/nar/gkw1099.

Tulsiani, D. R., Harris, T. M., and Touster, O. (1982). Swainsonine inhibits the biosynthesis of complex glycoproteins by inhibition of Golgi mannosidase II. *J. Biol. Chem.* 257, 7936–7939.

van Kooyk, Y., and Rabinovich, G. a (2008). Protein-glycan interactions in the control of innate and adaptive immune responses. *Nat. Immunol.* 9, 593–601. doi:10.1038/ni.f.203.

Varki, A. (2017). Biological roles of glycans. *Glycobiology* 27, 3–49. doi:10.1093/glycob/cww086.

von Itzstein, M., Plebanski, M., Cooke, B. M., and Coppel, R. L. (2008). Hot, sweet and sticky: the glycobiology of Plasmodium falciparum. *Trends Parasitol.* 24, 210–218. doi:10.1016/j.pt.2008.02.007.

Weng, S., and Spiro, R. G. (1993). Demonstration that a kifunensine-resistant alpha-mannosidase with a unique processing action on N-linked oligosaccharides occurs in rat liver endoplasmic reticulum and various cultured cells. *J Biol Chem* 268, 25656–25663.

Wood-Charlson, E. M., Hollingsworth, L. L., Krupp, D. A., and Weis, V. M. (2006). Lectin/glycan interactions play a role in recognition in a coral/dinoflagellate symbiosis. *Cell. Microbiol.* 8, 1985–1993. doi:10.1111/j.1462-5822.2006.00765.x.

Wood-Charlson, E. M., and Weis, V. M. (2009). The diversity of C-type lectins in the genome of a basal metazoan, Nematostella vectensis. *Dev. Comp. Immunol.* 33, 881–9. doi:10.1016/j.dci.2009.01.008.

Zhou, Z., Yu, X., Tang, J., Zhu, Y., Chen, G., Guo, L., et al. (2017). Dual recognition activity of a rhamnose-binding lectin to pathogenic bacteria and zooxanthellae in stony coral Pocillopora damicornis. *Dev. Comp. Immunol.* 70, 88–93. doi:10.1016/j.dci.2017.01.009.

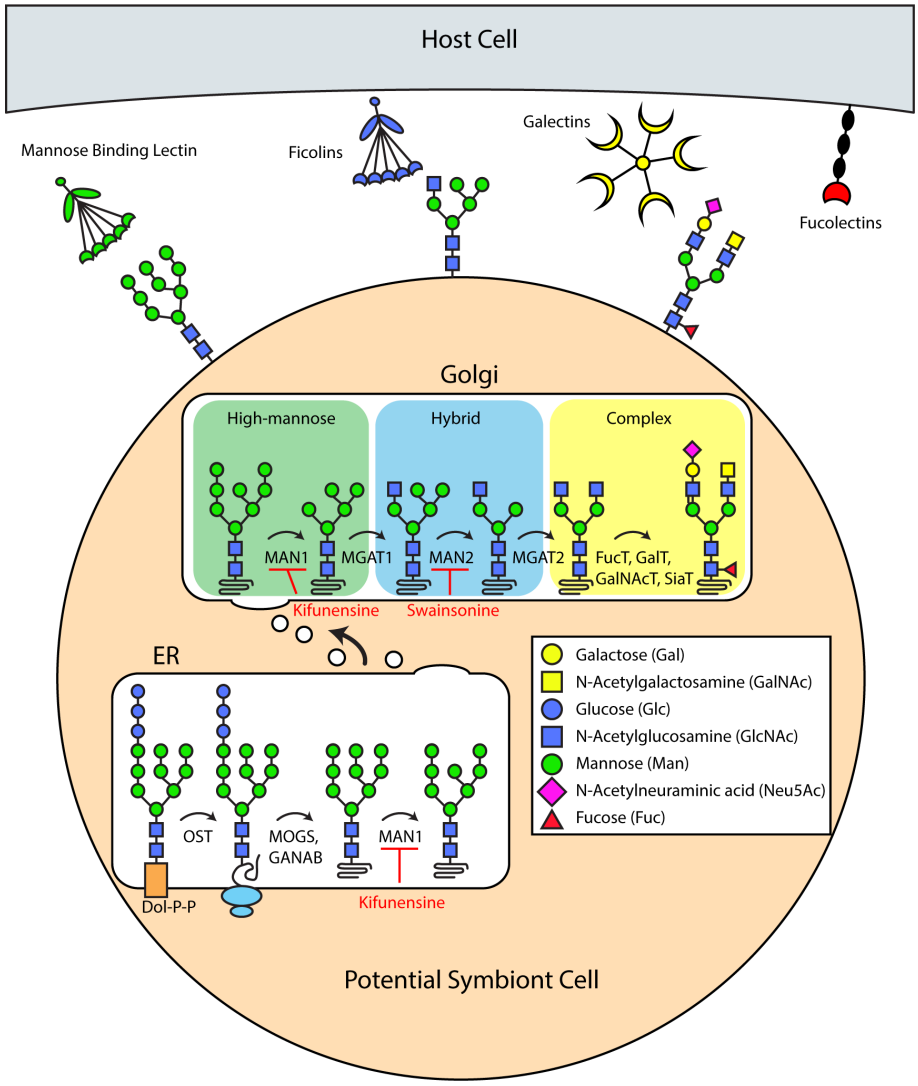

Figure 2.1 N-glycan biosynthesis and recognition.
The biosynthesis of N-glycans begins with the transfer of a nucleoside activated N-acetylglucosamine (GlcNAc) to a dolichol membrane anchor (Dol-P-P). A fourteen-sugar precursor structure is created by elongation, in the ER lumen. This structure is then mass-transferred to an Asn residue of a protein undergoing synthesis and aids in protein folding. N-glycans are further processed by glucosidases (MOGS, GANAB) to remove glucose, and then by ER mannosidase I (MAN1) to remove mannose residues. MAN1 enzymes act in both the ER and the Golgi to transform oligomannoside into hybrid glycans by N-acetylglucosaminyltransferase 1 (MGAT1). To create complex glycans, glycoproteins in the Golgi are further cleaved by mannosidase II (MAN2), then a series of transferases add GlcNAc, galactose, and other sugar residues to create complex N-glycans. Small molecules that act as enzymatic inhibitors can be used to block parts of this pathway, for example kifunensine and swainsonine. Pattern recognition receptors (PRRs) from host cells (Mannose-binding lectin, ficolins, etc.) interact with surface glycans on target cells to mediate immunity. N-glycan biosynthesis pathway adapted from Helenius and Aebi (Helenius and Aebi, 2001).

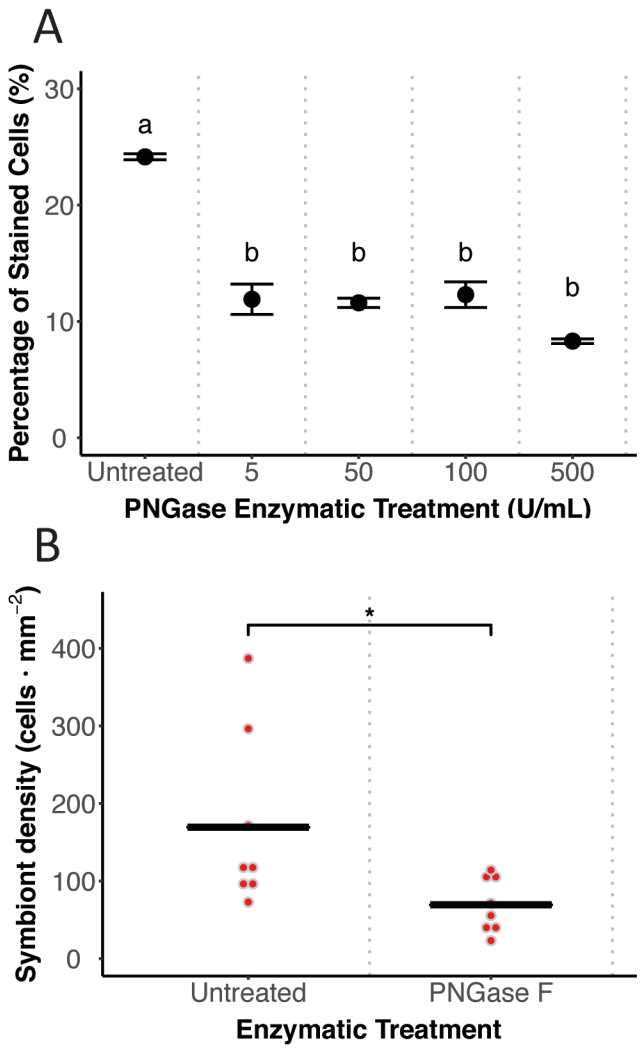

Figure 2.2 Effect of PNGase F treatment on *Breviolum minutum*.
(A) Cell surface N-glycan removal. After 48 h of PNGase treatment at different concentrations, glycan abundance on cell surfaces was measured through the binding of fluorescently tagged lectin CVN. Different letters represent significant differences in staining percentages following ANOVA ($p < 0.001$; n = 2 replicates per treatment). Error bars indicate range. **(B)** Colonization rates of untreated and PNGase F treated algae in adult polyps. Dots represent data from replicate polyps. Asterisk indicates a significant difference (t-test, $p < 0.05$).

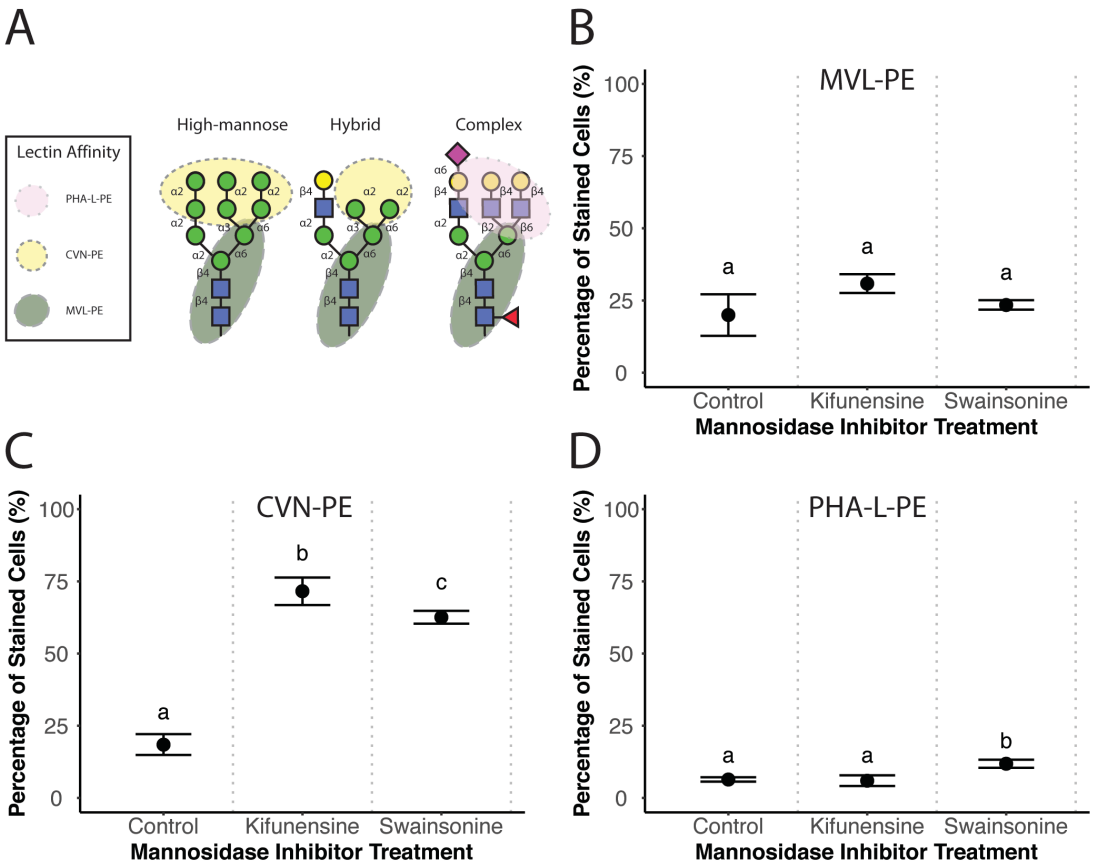

Figure 2.3 Inhibition of N-glycan biosynthesis in *Breviolum minutum*.
(A) Glycan recognition sites of the respective lectins within the three types of N-glycans (high-mannose, hybrid, and complex). MVL-PE was used to confirm the core of N-glycans, whereas CVN-PE and PHA-L-PE were used to determine the high-mannose and complex glycan composition, respectively. **(B)** MVL-PE labeling of core N-glycans. Algae that were incubated for one week with kifunensine, swainsonine, or DMSO (control) were labeled with MVL-PE to quantify N-glycan abundance. No significant differences were found between samples (n = 3). **(C)** CVN-PE labeling of high-mannose N-glycans. Treated algae were labeled with CVN-PE to quantify percentage of oligomannosidic N-glycan composition (n = 3). **(D)** PHA-L-PE labeling of complex N-glycans. Treated algae were labeled with PHA-L-PE to quantify percentage of complex N-glycan composition (n = 4). Different letters represent significant differences in staining percentages (ANOVA, $p < 0.05$).

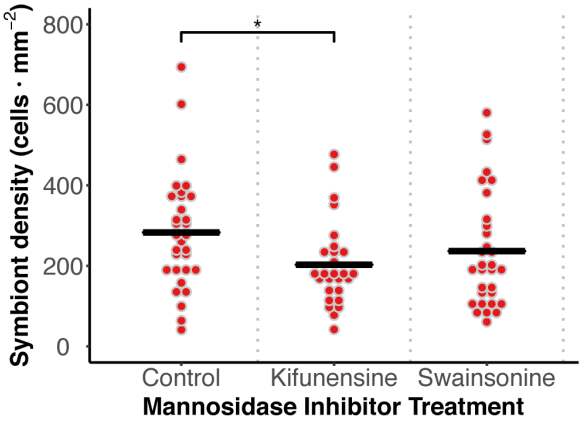

Figure 2.4 Effect on symbiont colonization by kifunensine and swainsonine. Effect of N-glycan biosynthesis inhibition on colonization by *B. minutum* in bleached adult Aiptasia polyps (n = 30). Asterisk indicates a significant difference between treatments (ANOVA, Dunnett's test $p < 0.05$).

Table 2.1: N-glycan biosynthesis in alveolates

Description	Protein	B. min.	S. mic.	F. kaw.	P. mar.	T. gon.	P. fal.
Dol-P precursor synthesis							
UDP-N-acetylglucosaminyltransferase subunit	ALG13	+	+	+		+	+
UDP-N-acetylglucosaminyltransferase subunit	ALG14	+	+		+	+	+
Mannosyltransferase-1	ALG1	+	+		+	+	
α-1,3-mannosyltransferase	ALG2	+	+	+	+	+	
α-1,2-mannosyltransferase	ALG11	+	+		+	+	
α-1,3-mannosyltransferase	ALG3	+	+		+		
α-1,2-mannosyltransferase	ALG9	+	+	+	+		
α-1,6-mannosyltransferase	ALG12		+	+	+		
DolP-glucosyltransferase	ALG5	+	+		+	+	
α-1,3-glucosyltransferase	ALG6	+	+	+	+	+	
α-1,3-glucosyltransferase	ALG8	+	+	+	+	+	
α-1,2-glucosyltransferase	ALG10	+	+	+		+	
Oligosaccharyl transferase subunit STT3	STT3	+	+	+	+	+	+
ER Processing							
Mannosyl-oligosaccharide glucosidase	GCS1	+	+		+	+	
Neutral α-glucosidase AB	GANAB	+	+	+	+	+	
ER α-1,2-mannosidase	MAN1B1	+	+	+	+		
Golgi Processing							
α-1,2-mannosidase IA	MAN1A1	+	+	+	+		
α-1,2-mannosidase IB	MAN1A2	+	+	+	+		
(α-1,3) 2-β-GlcNAc transferase I	MGAT1	+	+	+	+		
α-mannosidase 2	MAN2A1						
Lysosomal α-mannosidase	MAN2B1	+	+	+	+		
(α-1,6) β-1,2-GlcNAc transferase II	MGAT2						
(β-1,4) β-1,4-GlcNAc transferase III	MGAT3	+			+		
(α-1,3) β-1,4-GlcNAc transferase IVC	MGAT4C	+	+				
(α-1,6) β-1,6-GlcNAc transferase V	MGAT5	+	+				
Complex							
Xylosyltransferase 1	XYLT1	+	+				
α-1,6-fucosyltransferase 8	FUT8		+	+			
α-1,3-fucosyltransferase 11	FUT11	+	+		+		
α-1,4-fucosyltransferase 13	FUT13	+	+				
β-1,4-galactosyltransferase 1	B4GALT1	+	+	+			
β-1,3-galactosyltransferase 1	B3GALT1	+	+	+	+		
β-galactoside α-2,6-sialyltransferase 1	SIAT1						
β-galactoside α-2,6-sialyltransferase 2	SIAT2						
Paucimannose							
β-hexosaminidase 1	HEXO1	+	+	+	+		

3. Symbiotic state regulates host and symbiont cell cycles in a sea anemone-dinoflagellate association, a model for coral symbiosis

Trevor R. Tivey[1*], John E. Parkinson[2], Virginia M. Weis[1]

[1]Department of Integrative Biology, Oregon State University, Corvallis, OR, United States

[2]SECORE International, Miami, FL, United States

[3]Department of Chemistry, Oregon State University, Corvallis, OR, United States

3.1 Abstract

The cell cycle is a critical process in the regulation of proliferation, differentiation, and stress, yet its role in the regulation of symbiosis is not well understood. Host and symbiont coordination is essential to maintain mutualistic endosymbiosis in which one cell resides and proliferates within another. To gain greater understanding of the dynamic regulation of endosymbiosis, we examined the cell proliferation of the sea anemone Aiptasia (*Exaiptasia pallida*) and its algal symbionts *Breviolum minutum* and *Breviolum psygmophilum* as a response to symbiotic state. During recolonization of aposymbiotic adult hosts, host cells predominantly proliferated near clusters of proliferating symbionts. These proliferation rates found in anemone tissue undergoing colonization were increased compared to similar tissue from aposymbiotic anemones. These differences in replicating cell populations were general to both gastrodermal and epidermal tissue layers, indicating that the presence of a symbiont may not only slow the immediate cell cycle progression of its host cell but also contribute to a decrease in whole organism proliferation rates. In comparison to the host cell cycle, symbiont cell cycle progression was slowed when in the host (*in hospite*) and under nutrient-poor conditions. Populations of *B. psygmophilum in hospite* exhibited an unusual strong S-phase peak and a low G_2M population, indicating potential species-specific regulation of the symbiont cell cycle in Aiptasia. These results support the hypothesis that symbiotic state affects both host and symbiont cell cycles, but nutritional state predominantly affects symbiont cell cycles. These fundamental cellular regulatory mechanisms that govern host and symbiont proliferation are major forces that can shape cnidarian-dinoflagellate symbioses under rapid acclimation and selection pressure from changing environments. As cnidarian biodiversity continues to experience global declines, further exploration is needed to predict the basic cellular responses of both host and symbionts to changing environmental drivers.

3.2 Introduction

Mutualistic endosymbiotic relationships occupy foundational positions in both terrestrial and marine ecosystems. In these intracellular relationships, where symbionts grow and proliferate within host cells, host and symbiont coordination is essential to maintaining a dynamic, balanced biomass ratio. The cnidarian-Symbiodiniaceae symbiosis (formerly genus *Symbiodinium*; LaJeunesse et al., 2018) provides a dramatic example of the importance of this homeostasis. Under environmental stress, cnidarian hosts lose their photosynthetic symbionts in a process known as bleaching. Without symbiont-produced photosynthate, cnidarians have reduced ability to thrive and often die. Coral reefs, composed of corals and their resident endosymbiont dinoflagellate from the family Symbiodiniaceae, are gravely threatened by bleaching episodes from rising sea surface temperatures (Hughes et al., 2017). It is crucial, therefore, to understand how the cnidarian-dinoflagellate symbiosis is regulated. In a healthy cnidarian-Symbiodiniaceae symbiosis, there are a variety of mechanisms that maintain balanced host-symbiont ratios (Muscatine and Pool, 1979), including (1) symbiont expulsion *via* exocytosis, host cell apoptosis, host cell necrosis, and host cell detachment (Gates et al., 1992), (2) symbiont degradation *via* host autophagic degradation, symbiont apoptosis or necrosis (Dunn et al., 2007), and (3) host and symbiont cell cycle regulation. Although host and symbiont cell division and proliferation are fundamental aspects of symbiosis, the role of the cell cycle in the regulation of symbiosis remains largely unexplored (Davy et al., 2012).

The cell cycle is central to the regulation of mitosis and cell proliferation. In eukaryotes, cells are either quiescent or undergoing a pattern of cell growth, DNA replication, and cell division known as the cell cycle. Cells form two daughter cells through the steps of G_1-phase (cell growth and replication preparation), S-phase (DNA replication), G_2-phase (cell growth and DNA damage checkpoint), and M-phase (mitosis). Though many factors influence cell cycle progression and subsequent proliferation rate, certain conditions, such as nutritional state, commonly arrest and augment cell growth in G_1-phase prior to DNA replication (Fingar and Blenis, 2004; Pardee, 1989). In photoautotrophic cells, the light:dark cycle generally synchronizes DNA replication and cell division. The symbiotic state adds complexity to the regulation

of host and symbiont cell cycles. Hosts and symbionts may modulate the nutrients, growth factors, and/or toxins they provide one another, which will influence cell cycle progression (Dagenais-Bellefeuille and Morse, 2013; Login et al., 2011; Oswald et al., 2005). For example, in the *Rhizobium*-legume symbiosis, the plant host develops nodules where plant peptides allow DNA replication but block cell division of its own nodule cells and the endosymbiotic nitrogen-fixing bacteria residing within (Mergaert et al., 2006; Van de Velde et al., 2010). In the cnidarian-Symbiodiniaceae symbiosis, direct cell cycle modulators have not been discovered, and the mechanisms that govern cell cycle regulation remain unclear.

Cnidarians and dinoflagellates have significant differences in cell division and proliferation. In cnidarians, populations of diploid cells progress through the cell cycle at different rates according to their cell type. Studies have characterized the cell cycles of cnidarian cell populations (Bosch and David, 1984; David and Campbell, 1972) and examined proliferation during development and regeneration (Lecointe et al., 2016; Passamaneck and Martindale, 2012). For example, gastrodermal cells are slower to proliferate compared to epidermal cells, which must rapidly regenerate new mucocytes and venomous cnidocytes for defense and prey capture. In contrast to the multicellular cnidarians, dinoflagellates are haploid single-celled photosynthetic alveolate protists that divide in response to the diel light:dark cycle. These algae exhibit their own complexity in the unique way that their DNA is structured: chromosomes remain condensed throughout the cell cycle, lack nucleosomes and functional histones, and the cells use extranuclear spindles to accommodate the unusual persistence of the nuclear envelope during mitosis (Bouligand and Norris, 2001; Rizzo, 2003; Wisecaver and Hackett, 2011). The cell cycles of cnidarians and dinoflagellates have been most closely examined in nonsymbiotic taxa such as the hydrozoan *Hydra* (Bosch and David, 1984; Otto and Campbell, 1977; Scheurlen et al., 1996) and the heterotrophic dinoflagellate *Crypthecodinium cohnii* (Barbier et al., 1998; Bhaud et al., 1991, 1994, 2000; Wong and Kwok, 2005). Since the cnidarian-Symbiodiniaceae mutualism occupies a foundational role in shaping coral reef ecosystems, we need to understand not only the organisms in isolation but also the interactions of the cell cycles of these two very different partners.

The Aiptasia-Symbiodiniaceae symbiosis is a model system for the study of coral-dinoflagellate cell biology. The sea anemone Aiptasia (*Exaiptasia pallida*) is in Class Anthozoa with corals, and it has been used extensively to study cnidarian cellular and molecular processes involved in the onset, maintenance, and breakdown of symbiosis (Gladfelter, 2015; Goldstein and King, 2016; Weis et al., 2008). Similar to corals, Aiptasia forms nutritional endosymbioses with several species of Symbiodiniaceae whereby the unicellular algae reside inside host gastrodermal cells within vesicles called symbiosomes. Unlike many corals, Aiptasia can be maintained symbiont free (aposymbiotic), which enables comparisons between hosts with and without symbionts and their photosynthetic nutrients. Smith and Muscatine examined the nutritional regulation of G_1-phase in *Breviolum minutum* (formerly *Symbiodinium minutum*) *in hospite* in Aiptasia, and found that the transfer of nutrients such as nitrogen and phosphorus from host to symbiont constrains symbiont cell progression (Smith and Muscatine, 1999). They also found that the host cell environment removes the light:dark cell division patterns found in cultured Symbiodiniaceae cells. A variety of studies have characterized Symbiodiniaceae cultures and isolates under different growth conditions, along with their proliferation and growth (Cook et al., 1988; Fujise et al., 2018; Wang et al., 2013; Wilkerson et al., 1983, 1988). The cell division and proliferation of Aiptasia cells have also been studied previously (Fransolet et al., 2013, 2014; Singer, 1971), however the relationship between the two partners requires further investigation.

Here we aim to describe the cell proliferation of the cnidarian host Aiptasia and its dinoflagellate symbiont under different symbiotic states and nutritional regimes. We compared anemones under two symbiotic conditions: during recolonization of hosts by symbionts and during the stable aposymbiotic state. We first investigated whether the presence of symbionts had an effect on the cell cycle and proliferation of Aiptasia host cells using fluorescent labeling and confocal microscopy (**Figure 3.1A**). We then further explored the interaction effect between stable symbiotic states and host nutritional state on the cell cycles of two *Breviolum* species of Symbiodiniaceae that are found naturally in Aiptasia, *B. minutum* (type B1; formerly *S. minutum*) and *B. psygmophilum* (type B2; formerly *S. psygmophilum*) (Lajeunesse et al., 2012). Our results suggest that Aiptasia not

only alters its cell cycle progression based on its host-symbiont biomass ratios, but also houses symbionts that experience cell cycle regulation in a nutritional and species-specific manner. These results together form a broad understanding of how cell populations in hosts and symbionts respond to each other and to the environment *via* their cell cycle dynamics.

3.3 Methods

Maintenance of anemones and algae

Symbiotic Aiptasia strains and Symbiodiniaceae cultures were maintained on a 12 h:12 h light:dark cycle (approximately 40 µmol photons m^{-2} s^{-1}) at room temperature. Aposymbiotic anemones were generated by menthol bleaching (Matthews et al., 2016). Menthol was added from a stock 20 g/L menthol in ethanol to a final concentration of 0.58 mM in filtered artificial sea water (FSW). Anemones were treated for repeated three-day time periods until no autofluorescence from algal chlorophyll was detected, and they remained in the dark for at least one month prior to experiments. All anemones used in experiments had an oral disc diameter of approximately 0.5 cm, were fed brine shrimp nauplii three times per week, and then starved one week prior to the beginning of experiments unless otherwise indicated. The clonal host strain H2 (containing *Breviolum minutum* [B1]) was used in experiments (**Appendix B Table B1**). Additional experiments on cell cycle phenotypes of symbionts *in hospite* were performed to confirm observations made from symbionts in the above two host strains. These experiments were performed on symbionts from VWB9 and VWA12 containing *B. minutum*, and JK containing *B. psygmophilum*. Cell cultures of *B. minutum* (CCMP830, FLAp2, and Mf1.05b) and *B. psygmophilum* (HIAp) were grown in f/2 media (**Appendix B Table B1**). All Symbiodiniaceae isolates and cultures were genotyped using the ITS2 loci to confirm species identification.

Fluorescent labeling of host Aiptasia during recolonization by symbionts

Aposymbiotic H2 anemones were plated in 24-well plates and inoculated with *B. minutum* (strain Mf1.05b) at a dose of 1 x 10^5 cells in 1 mL FSW for two days, and then

anemones were moved to fresh plates in new FSW. Hosts exhibited a low level of symbiont recolonization for two months, until *B. minutum* recolonization rapidly accelerated. Hosts were monitored for two weeks of rapid symbiont proliferation until recolonization reached 50% of the tentacle area. Hosts were then incubated in 10 μM EdU (added at the beginning of incubation only) in FSW for 24 h to measure host cell proliferation (Click-iT EdU Alexa Fluor 555 Imaging Kit, Life Technologies, Eugene, Oregon, USA). Shorter EdU incubations were used to approximate S-phase duration in the epidermis and gastrodermis (data not shown). In EdU incubations of 4 h, there were low S-phase and G_2/M phase (labeled using anti-pSer10-H3 conjugated to AF488) populations within the gastrodermis (**Appendix Figure D1**, **Appendix Figure D2**). At 6 h incubations, a few epidermal nuclei in confocal tentacle sections exhibited double-labeling with EdU-AF555 and anti-pSer10-H3-AF488, a marker for G_2/M phase, whereas at shorter incubations this was rarely observed (data not shown). We therefore chose to sample anemones after 24 h of incubation in EdU to examine all proliferating gastrodermal cells, not just those cells undergoing DNA replication at the time of EdU addition (**Figure 3.1A**). Samples for host analysis were rinsed in phosphate-buffered saline (1X PBS) prepared from a 10X PBS stock solution (0.02 M NaH_2PO_4, 0.077 M Na_2PO_4, 1.4 M NaCl, pH 7.4) and fixed in 1X PBS + 4% paraformaldehyde overnight at 4ºC. Samples were then rinsed in 1X PBS and blocked in 1X PBST (0.05% Triton-X100) for 30 min. Tentacles were incubated for 1 h in the reaction mix of the Click-iT EdU Alexa Fluor 555 Imaging Kit, which labeled only EdU+ host nuclei. Finally, all host cells were labeled with Hoechst 33342, which brightly labeled only host nuclei. Tentacles were washed three final times in 1X PBS and mounted on slides for confocal microscopy (Prolong Anti-Fade Diamond Mountant, Life Technologies) (**Figure 3.1B**). Samples were recorded on a Zeiss LSM 780 NLO Confocal Microscope System. Symbiodiniaceae autofluorescence was detected using excitation at 633 nm and an emission of 684 nm (**Figure 3.1C**). Host nuclei labeled with Hoechst were detected with excitation at 405 nm and an emission of 443 nm (**Figure 3.1D**). Proliferating host nuclei labeled with EdU-AF555 were excited at 555 nm and an emission of 588 nm (**Figure 3.1E**). Confocal Z-stack images were analyzed using Fiji (ImageJ2).

An image analysis pipeline was developed to quantify the relationship between symbionts and regions of host containing proliferating host nuclei. Images were split into separate channels and the 3D object counter plugin (Bolte and Cordelieres, 2006) was used to detect the centers of masses of host nuclei (Hoechst) and proliferating nuclei (EdU-AF555). Likewise, *B. minutum* cells were detected with the same plugin after smoothing objects using a Gaussian blur and background subtraction. *B. minutum* cells were subjected to two rounds of watershedding using 3D Watershed to segment potential cell clusters into single cells (Ollion et al., 2013). Objects were then re-counted and parameters, including centers of mass and the volumes surrounding each symbiont (minimum bounding box: x-min, y-min, z-min, x-max, y-max, z-max) were recorded. Centers of mass of host nuclei, proliferating nuclei, and symbionts were further analyzed using the R package *spatstat* (Baddeley et al., 2015). Nearest neighbor distances (k = 1-12) were generated between host cells, proliferating host cells, and symbionts. To generate the NN-distance distributions, the Euclidean distances from each point in the symbiont point pattern to the k^{th} - nearest neighbors of the point pattern of either host cells or proliferating host cells. These distances were then aggregated into distributions, and two-sample t-tests were used to determine differences in nearest neighbor distributions at each distance (k = 1-12). The minimum bounding box regions containing each individual symbiont cluster were then aggregated and compared to the spatial location of host nuclei centers of mass. A Boolean test was used on the x-, y-, and z-coordinates of host nuclei to determine whether they were found inside or outside of the bounding box regions containing *B. minutum* cells. To estimate *B. minutum* density, the total volume of these symbiont bounding box regions was calculated and compared to the total volume of each tentacle. Regions of symbiont bounding box overlap were subtracted to avoid overestimation of symbiont density. All image processing pipelines, scripts, and statistical analyses are available as a supplemental data file.

Symbiodiniaceae cell cycle dynamics in culture and in hospite under different nutritional states

To assess the effect of nutritional state on Symbiodiniaceae cell cycles in culture and *in hospite*, two *Breviolum* strains (FLAp2 and HIAp) were sampled during stable growth

conditions (after twelve weeks in f/2 media at 1 x 10^6 cells / mL) or during predicted log-growth phase (after two weeks in f/2 media at 2.5 x 10^5 cells / mL). Hosts (H2 harboring *B. minutum* and JK harboring *B. psygmophilum*) were starved or fed, as previously described, for two weeks prior to symbiont isolation. To obtain Symbiodiniaceae from host anemones, hosts were homogenized in FSW using a BioSpec Tissue-Tearor and centrifuged at 500 g for 5 min to pellet the algae. Pellets were rinsed in 1X PBS twice, forced through a syringe, and fixed in 2 mL of ice-cold 70% ethanol, which was slowly added as samples were vortexed. Samples were kept at 4 ºC for up to one week, then 1 mL of ice-cold 70% ethanol was added and samples were photo-bleached for 1 h under high light. Samples were rinsed in 1X PBS prior to staining in 500 mL of 1X PBS with 10 µg / mL propidium iodide, 0.01% Triton X-100 and 150 µg / mL RNase A. The cells were analyzed using the Cytoflex 4L flow cytometer at a flow rate of 10 µL / min. Cells were excited at 488 nm and detected using a 585/42 bandpass filter. Symbiodiniacea populations were identified from cnidarian cell populations using forward and side-scatter, and then screened for doublet discrimination using FSC-A and FSC-W. At least 20,000 cells were collected per sample. Cell cycle analysis was performed using FlowJo software. Cell cycle gates were determined using the Dean-Jett-Fox model in order to best model S-phase distribution. Once cell proportions of G_1, S, and G_2M-phases were identified from each sample, samples underwent an arcsine transformation to stabilize variance of percentage data. A two-way ANOVA was used to identify differences between nutritional and symbiotic states, followed by a Tukey post-hoc test. All statistical analyses were performed in R.

3.4 Results

Host cells proliferate when in close proximity to invading symbionts during recolonization

To test for localized host cell cycle patterns and their relationship to the presence of symbionts, we analyzed partially-colonized Aiptasia tentacles to examine differences between regions with and those without symbionts (**Figure 3.2**). We hypothesized that larger populations of proliferating host nuclei would be found within the areas containing

high symbiont density compared to those areas with low symbiont density. To determine this relationship, we imaged cells using three fluorescent markers: Hoechst (blue) to label all host nuclei, Click-IT EdU-AF555 (yellow) to label host nuclei that have undergone S-phase DNA replication, a proxy for progression through the cell cycle, and chlorophyll autofluorescence (red) to label symbiont cells (**Figure 3.2A**). The centers of mass of the labeled objects were located for each tentacle (**Figure 3.2B**), and the distances were measured from each object's center of mass to its nearest neighbors (k = 1-12) of another group. When these distances between the labeled host cell groups (Hoechst or EdU) and the symbiont centers of mass were measured, the nearest neighbor distances from both host cell groups were found to be an average of 10 μm from the symbionts (k = 1) (**Figure 3.2C**). To provide context for the proximity of this distance, we measured distances from each symbiont center of mass to their symbiont cell surface and found the average and median distance to be 7 μm, therefore a large proportion of EdU-positive nuclei were within 3 μm of at least one symbiont. At every subsequent neighbor pair tested (k = n [up to n = 12]), the nearest neighbor distances of EdU-positive nuclei were closer than distances of all nuclei to the symbiont centers (Mann-Whitney *U* test, $p < 0.0004$). To determine if this assessment of correlation was accurate, we used the locations of symbionts (**Figure 3.2D**) to divide the tentacle area into aposymbiotic and symbiotic regions (**Figure 3.2E**) and compared the number of proliferating nuclei within aposymbiotic tissue to the number within symbiotic tissue (n = 95 Z-stack images, 33 tentacles, 11 anemones). EdU-positive host nuclei appeared predominantly within symbiotic regions (**Figure 3.2F**). Compared to the null hypothesis of neutral location, the enrichment of EdU-positive nuclei near symbiont clusters was highly significant (Chi-square test, $p < 1 \times 10^{-5}$; paired t-test, $p < 1 \times 10^{-5}$), indicating that host cells are undergoing replication more when in proximity of colonizing symbionts. Not surprisingly, symbiont density had a strong positive correlation to the number of proliferating host cells found within symbiont-containing regions ($F = 135.2$, $p < 2.2 \times 10^{-16}$, $R = 0.5986$). Increased symbiont density correlated with a larger positive difference between the observed and the expected number of host nuclei under the null hypothesis of neutral location ($F = 43.04$, $p = 3.44 \times 10^{-9}$, $R = 0.3184$) (**Figure 3.2F**). Compared to

this correlation between symbiont density and locally proliferating host cells, symbiont density only weakly correlated with the total density of proliferative host cells ($F = 4.49$, $p < 0.037$, $R = 0.037$) and did not correlate with the total number of proliferating host cells found in both symbiont and non-symbiont containing regions ($F = 0.07$ $p = 0.779$, $R = -0.0105$ and respectively). Together, these results indicate a strong correlation of localized proliferating host cells and symbionts during the recolonization process.

Aposymbiotic anemones have lower proliferation rates than anemones undergoing recolonization

To examine differences between symbiotic states on whole organism level, we further analyzed cell populations in aposymbiotic anemones (**Figure 3.3A**). Compared to symbiotic anemone tentacles, aposymbiotic tentacles had a significantly lower density and percentage of EdU-positive proliferating host nuclei (two sample t-test, $p = 0.02$; two sample t-test, $p = 8.7 \times 10^{-5}$) (**Figure 3.3B**). This decrease in proliferating cells was not a result of decreased host cell density, as symbiotic anemones had the lower total nuclei density and overall increase in host cell size (two sample t-test, $p = 0.002$) (**Figure 3.3C**). To examine the distribution of proliferating cells, we compared the nearest-neighbor relationships between nonproliferating host nuclei and EdU-positive proliferating nuclei. Compared to symbiotic anemones, proliferating nuclei were found further away from nonproliferating host nuclei in aposymbiotic anemones (**Figure 3.3D**). Significant decreases in median nearest-neighbor distances in aposymbiotic anemones suggested a change in proliferating tissue distribution (**Figure 3.3E,** Mann-Whitney *U* test, $p < 2.2 \times 10^{-16}$). To determine whether or not this extra space between proliferating nuclei was a result of a shift in tissue layer proliferation, we examined the location of each cell population using the z-coordinate of each object. For each tentacle, we found the median z-coordinate location of each cell population and plotted the resulting density plots (**Figure 3.3F-G**). To delineate tissue layers, we used the presence of Symbiodiniaceae cells to approximate the gastrodermal layer and used the left side of the peak of host nuclei which did not overlap with the gastrodermis to approximate the epidermis. As shown in the two density plots, proliferating nuclei were enriched in the symbiotic gastrodermis compared to the aposymbiotic gastrodermis (**Figure 3.3F-G**). To test for

significance, proliferating nuclei were normalized to the host nuclei median for each tentacle. Normalized proliferating nuclei were significantly shifted towards the gastrodermis in symbiotic tentacles ($p < 7 \times 10^{-5}$, two-sample t-test) (**Figure 3.3H**).

Species-specific responses of Symbiodiniaceae cell cycles to symbiotic and nutritional state

We examined symbiont cell cycle dynamics in two species of Symbiodiniacea in culture and *in hospite* and by analyzing their response to nutritional state using flow cytometry. In culture, we hypothesized that Symbiodiniaceae would have increased S-phase and G_2M-phase cell populations under nutrient-rich conditions. We first compared culture cell cycles in older and newer f/2 media, representing stable culture conditions compared to log-phase growth. As expected, S-phase and G_2M-phase cell populations were significantly higher in treatments with freshly replaced f/2 media in cultures from both *Breviolum* species (**Figure 3.4A, B**, **Appendix B Table B2**; t-test, $p < 0.05$). We then compared the cell cycle response of cultured *B. minutum* and *B. psygmophilum* to nitrogen-limitation, specifically using f/2 media with no added nitrate ($NaNO_3$). In both nitrogen-limited treatments, S-phase cell populations increased and G_2M-phase cell populations decreased significantly compared to their respective control treatments (**Figure 3.4D, E**; t-test, $p < 0.05$). However, the effect was much stronger in *B. psygmophilum* cultures. In addition, *B. psygmophilum* culture under nitrogen limitation had a G_1-phase peak distribution coefficient of variation (CV) more than double the width of the control treatment (**Figure 3.4D, E**). *B. minutum* cultures also exhibited wider G_1 peaks with increased CVs under nitrogen-limitation, albeit only a 50% increase compared to control treatments.

B. minutum and *B. psygmophilum* isolates from Aiptasia had noticeably different cell cycle populations compared to their cultures (**Figure 3.4A-C**; t-test, $p < 0.05$). In addition, *B. psygmophilum* had a distinct S-phase population peak which was absent in *B. minutum* cell populations (**Figure 3.4C**). In both species, symbionts isolated from hosts had similar G_1-phase populations, elevated S-phase populations, and decreased G_2M-phase populations compared to their respective log-phase algal cultures (**Figure 3.4A-C**, **Appendix B Table B2**). To test how nutrition of the holobiont affected these symbionts

in hospite, we examined the cell cycles of *B. minutum* isolates from Aiptasia that were either starved for two weeks or fed *Artemia* nauplii. G_1-phase populations increased and S-phase populations decreased significantly in starved treatments compared to fed treatments whereas G_2M-phase populations only slightly decreased (**Figure 3.4F**; t-test, $p < 0.05$).

3.5 Discussion

Spatial coordination of host cell and symbiont cell proliferation occurs during recolonization

The spatial correlation between symbionts and replicating host nuclei during recolonization suggests that the presence of symbionts strongly affects the regulation of the host cell cycle on a localized scale. This relationship between host and symbiont proliferation during recolonization appears to be density dependent: proliferating host nuclei are observed near symbiont clusters more than expected by chance, especially as symbiont density in the tentacle increased (**Figure 3.2F**). This localized proliferation of host cells enables recolonizing anemones to accommodate their growing population of symbionts. Compared to aposymbiotic anemones, anemones with colonizing symbiont cells increase overall host cell proliferation rates and promote an increase in cell host size in localized groups of host cells.

To-date there has been no direct evidence of cell cycle regulation between cnidarian gastrodermal cells and symbionts. In our spatial examination of recolonizing anemone tissues, the nearest neighbor distributions (**Figure 3.2C, Figure 3.3D**) and z-axis locations (**Figure 3.3F-G**) of proliferating nuclei and symbiont centers of mass locate a majority of proliferating cells within 10µm of a symbiont center and inside the gastrodermis. Considering that both *Breviolum* symbionts range from 8-10 µm in diameter (LaJeunesse et al., 2012), this co-localization provides strong evidence for localized gastrodermal proliferation and suggests direct host-symbiont signaling. Host-cell to symbiont-cell signaling would align with differences that past studies have uncovered between anemones with different symbiont states. For example, symbiotic Aiptasia have altered gene expression compared to aposymbiotic animals, including the

upregulation of genes involved in nutrient transport and fatty acid oxidation (Lehnert et al., 2014). Further studies have shown that hosts harboring different symbiont types have differential expression of genes involved in nutrient metabolism and signal transduction of G protein coupled receptors (Matthews et al., 2017). Though several genes involved in the cell cycle and DNA regulation are differentially expressed in these studies, there is no clear evidence yet of direct stimulation or inhibition of the cell cycle of one partner by the other. These effects have been described in other systems. Both plants and aphids inhibit division of endosymbiotic bacteria by using specific peptides (Login et al., 2011; Van de Velde et al., 2010), whereas the bacteria *Algoriphagus* sp. and *Vibrio fischeri* use lipids and enzymes to stimulate cell division and mating, respectively, of the choanoflagellate *Salpingoeca rosetta* (Fairclough et al., 2010; Woznica et al., 2017). To find evidence of similar pathways in Aiptasia-Symbiodiniaceae system, the continuous interactions between cnidarian hosts and their symbiont need examination at a high resolution within the gastrodermal layer during coordinated proliferation.

Whereas localized gastrodermal proliferation hints of direct host-symbiont regulation, epidermal proliferation is likely a result of cell communication between host cells. Based on the Z-stack position of total host nuclei and proliferating host nuclei, a large number of proliferating host cells were localized in the epidermal layer. It is likely that this epidermal proliferation is needed to accommodate expanding gastrodermal tissue and growth in the overall size of tentacles. Gastrodermal host cells with nutrients provided from symbionts could signal locally *via* growth factors. Examples of conserved cell-cell signaling pathways in cnidarians include Wnt, FGF and TGFβ signaling (Lee et al., 2006; Miller et al., 2007; Rentzsch et al., 2008; Technau et al., 2005). Though Wnt and FGF signaling have been primarily described during cnidarian development, TGFβ signaling has been shown to contribute to innate immunity and symbiosis in Aiptasia (Berthelier et al., 2017; Detournay et al., 2012). Differential expression of cnidarian genes comparing colonized cnidarians to aposymbiotic cnidarians has also revealed increased expression of growth factors such as Wnt and IGF in colonization conditions (Yuyama et al., 2018). These cell-cell signaling pathways are commonly used to promote

localized host growth and proliferation, and in cnidarians they may be acting in response to local increased nutrient exchange from colonizing symbionts.

The cellular coordination of proliferation that we observe in Aiptasia has also been explored in other dinoflagellate symbioses, including many partnerships with other cnidarians. In the sea anemone *Anthopleura elegantissima*, host sea anemones with increased G_2M-phase populations contained symbiont populations with corresponding increased G_2M-phase proportions (Dimond et al., 2013). During dynamic periods of change such as host development and colonization, this coordination between host and symbiont proliferation may be even more important. For example, during the primary polyp development of the coral *Stylophora pistillata*, the coordinated proliferation of gastrodermal cells and their symbionts resulted in a dramatic increase in Symbiodiniaceae cell density and a switch to apoptotic post-mitotic control (Lecointe et al., 2016). As polyps became fully-developed adults, the proliferation rate of gastrodermal and symbiont cells significantly slowed, possibly as a result of space-limitation. Evidence for cellular space-dependent proliferation exists in other cnidarian symbioses, including the *Hydra*-*Chlorella* symbiosis and the *Myrionema*-Symbiodiniaceae symbiosis (Douglas and Smith, 1984; Fitt, 2000; McAuley, 1986; McAuley and Cook, 1994). In these hydroids, one gastrovascular cell contains larger populations of symbiont cells than those populations found in smaller anthozoan cells, and these symbiont populations respond to changes in host cell size and division rate by growing and dividing themselves. There is also evidence of coordinated proliferation of host and symbiont cells by diel-phased cell division (Fitt, 2000). Similarly in the *Paramecium*-green alga symbiosis, symbionts proliferate only upon host cell division (Kadono et al., 2004). The cellular coordination between these large cells and their endosymbionts is easier to study than the relationships in coral-algal and anemone-algal associations with tiny host cells. The small host size found within anthozoans such as corals and anemones has made detection of coordinated proliferation much harder to observe and measure, therefore we cannot rule out that this lack of evidence comes from biases in detection (Davy et al., 2012). Looking forward, the degree of coordination in the Aiptasia-Symbiodiniaceae symbiosis could be targeted by analyzing symbiotic Aiptasia

gastrodermal cells *via* single-cell analysis to obtain simultaneous host and symbiont measurements. In general, coordinated division between partners seems to take place during periods of colonization and dynamic growth of the host.

Recolonization of anemones by algae is associated with enriched host gastrodermis proliferation

The positive effect of symbiont proliferation on host cell proliferation was evident not only between symbiotic and aposymbiotic regions (**Figure 3.2**), but also between symbiotic and aposymbiotic organisms (**Figure 3.3**). Gastrodermal proliferation was increased in colonizing Aiptasia. The shift of proliferation location toward the epidermis in the aposymbiotic state suggests either enrichment or more rapid cellular turnover in the epidermal tissue layer (**Figure 3.3F**). In the tentacles of Aiptasia and other anthozoans, the epidermal tissue layer of cnidarians proliferates at a faster rate than the gastrodermal layer (Fransolet et al., 2013; Passamaneck and Martindale, 2012; Singer, 1971). The aposymbiotic state is further associated with an enrichment in epidermal proliferation rates. In Aiptasia, Fransolet et al. (2013) measured elevated epidermal proliferation and an increase in mucocyte density in the three weeks after thermal bleaching (Fransolet et al., 2013). The authors posited that with the absence of symbionts, the expanded epidermal cell population equipped the anemones for a heterotrophic feeding strategy. They found similar results when they further tested this hypothesis by treating symbiotic anemones with the photosynthetic inhibitor DCMU, which caused the anemones to bleach (Fransolet et al., 2014). In our study, the closer NN distances and epidermal Z-stack location of aposymbiotic proliferating nuclei support this localized host proliferation.

Nutritional state directly regulates symbiont cell cycles

Nutrition had a strong effect on the cell cycles of both *Breviolum* species. In Symbiodiniacea cultures, the increased G_1-phase arrest and cell size of algal cell populations in both nutrient-poor media and nitrogen-limited media (**Figure 3.4A, D**) was similar to previous work examining Symbiodiniacea culture growth rate and cell size in stationary and log-phase growth (Domotor and D'Elia, 1984, 1986). Nitrogen

limitation has caused G_1-phase arrest and wide CVs in a range of other microalgae, including other dinoflagellates (Dagenais-Bellefeuille and Morse, 2013; Olson et al., 1986; Vaulot et al., 1987). Though the similar trends in both *Breviolum* cultures indicate a common cell cycle response, the difference in magnitude suggest that the cell cycle of *B. psygmophilum* is more sensitive to nutrient dynamics than the cell cycle of *B. minutum*. This sensitivity may explain differences observed between *B. psygmophilum* and *B. minutum in hospite* (**Figure 3.4A, C**).

In hospite, increased G_1-phase populations of *B. minutum* in starved compared to fed hosts matched the G_1-phase arrest phenotype found in nutrient-limited cultures (**Figure 3.4F**). These results are similar to previous studies of Aiptasia, where mitotic populations of Symbiodiniacea isolates were higher and G_1-phase arrested populations lower when fed or supplemented with either nitrogen or phosphorus (Cook et al., 1988; Smith and Muscatine, 1999). Other aspects of symbiont physiology have been shown to change with the nutritional state of hosts; starved Aiptasia have Symbiodiniacea phenotypes which include increased cell sizes, and starch and lipids stores (Muller-Parker et al., 1996; Rosset et al., 2017). Symbiodiniacea cell cycle arrest phenotypes have been observed as a result of cerulenin treatment, an inhibitor of free fatty acid synthesis (Wang et al., 2013). Nutrient balance therefore appears to strongly affect the regulation of symbiont proliferation, and is of consequence when considering the effect of nutrient enrichment from agricultural run-off on the vulnerable cnidarian-dinoflagellate symbioses that compose coral reefs (Wiedenmann et al., 2013).

Decreased G_2M-phase mitotic state of Breviolum species is associated with symbiotic state

The cell cycle progression of *Breviolum* in culture was similar to those described in other studies of Symbiodiniaceae (Fujise et al., 2018; Wang et al., 2008), whereas when *in hospite*, both species had increased S-phase and decreased G_2M-phase populations compared to log-phase cultures. Though it is possible that the wider CVs observed in hospite arise as an artifact from sample preparation of homogenized isolates compared to single cell cultures, the increased G_1-phase variation also could represent biological variation in DNA abundance similar to the wider CVs found in nitrogen-depleted cultures

(Darzynkiewicz et al., 2010). Nitrogen stress has been shown in previous studies to have a measured effect (Cook et al., 1988; McAuley and Cook, 1994). These decreased symbiotic G_2M populations observed in Aiptasia lend further evidence to the idea of nutrient limitation by the host as a strategy for symbiont regulation in nutrient-starved cnidarian hosts (Cook et al., 1994; Muscatine et al., 1989). In fed hosts, however, the observed S-phase increase and G_2M-phase decrease is more consistent with other mechanisms of pre-mitotic control such as increased expulsion of late S-phase and G_2M-phase cell populations (Baghdasarian and Muscatine, 2000).

Symbiodiniaceae cell cycles are regulated in a species-specific manner in hospite

Though both *B. minutum* and *B. psygmophilum* were arrested in G_1-phase under nutrient-limiting conditions, the two species differed in their cell cycle states *in hospite*. Compared to their respective cell cycles in culture, *B. psygmophilum* isolates had a more substantial increase in S-phase population than the minimal increase observed in *B. minutum* isolates (**Figure 3.4C**). These cell cycle differences may result from a change in biomass regulation due to different host and symbiont genetic background. Symbiodiniaceae species are nutritionally limited in the host and tend to have faster growth rates in hosts with higher nutrient concentrations in the environment (Muscatine et al., 1989; Wilkerson et al., 1983). *B. psygmophilum* occurs in animals in temperate regions which typically have higher available nutrients than do those in tropical regions (Muller-Parker and Davy, 2001). Indeed, nitrogen sufficiency has been measured in temperate coral associations compared to nitrogen limitation in tropical symbioses (Davy et al., 2006). This difference in nutrient exchange and the possibility for nitrogen storage in temperate symbionts may be an important difference in how host cell cycle dynamics are regulated, but this topic requires further experimentation.

3.6 Conclusions

This study provides evidence of regulation of host and symbiont cell cycles during the establishment and maintenance of cnidarian-dinoflagellate symbiosis. Host cells and colonizing symbionts experienced coordinated localized proliferation during recolonization of hosts by symbionts. This host cell proliferation rate was higher in

colonizing anemones compared to aposymbiotic anemones, and originated from the expansion of gastrodermal proliferation with a growing symbiont population. In addition, we found differences in the S-phase populations of cell cycles of two different species of Symbiodiniaceae *in hospite*, indicating differential cell cycle regulation depending on symbiont species. A basic understanding of host and symbiont cell cycle dynamics is critical to a complete picture of the cellular mechanisms that regulate cnidarian-dinoflagellate symbioses. This foundational information will help us predict how these symbioses will cope with a rapidly changing planet.

3.7 Acknowledgments

This work was funded by award IOB1529059 from the National Science Foundation awarded to VMW. Support for the confocal microscope was from award 1337774 from the National Science Foundation, *MI: Acquisition of Confocal and Two-Photon Excitation Microscope*. The authors wish to acknowledge the Confocal Microscopy Facility of the Center for Genome Research and Biocomputing at Oregon State University. Technical support for flow cytometry was provided by Allison Ehrlich and the Department of Environmental and Molecular Toxicology at Oregon State University.

3.8 References

Baddeley, A., Rubak, E., and Turner, R. (2015). *Spatial Point Patterns: Methodology and Applications with R*. Boca Raton: Chapman & Hall/CRC Press doi:10.18637/jss.v075.b02.

Baghdasarian, G., and Muscatine, L. (2000). Preferential expulsion of dividing algal cells as a mechanism for regulating algal-cnidarian symbiosis. *Biol. Bull.* 199, 278–86.

Barbier, M., Géraud, M. L., Nicolas, G., and Soyer-Gobillard, M. O. (1998). Colocalization of the cyclin B homologue P56 and β-tubulin during the cell cycle in a unicellular eucaryote dinoflagellate. *Biol. Cell* 90, 63–76. doi:10.1016/S0248-4900(98)80233-5.

Berthelier, J., Schnitzler, C. E., Wood-Charlson, E. M., Poole, A. Z., Weis, V. M., and Detournay, O. (2017). Implication of the host TGFB pathway in the onset of symbiosis between larvae of the coral Fungia scutaria and the dinoflagellate Symbiodinium sp. (clade C1f). *Coral Reefs* 36, 1263–1268. doi:10.1007/s00338-017-1621-6.

Bhaud, Y., Barbier, M., and Soyer-Gobillard, M. O. (1994). A detailed study of the complex cell cycle of the dinoflagellate Crypthecodinium cohnii Biecheler and evidence for variation in histone H1 kinase activity. *J. Eukaryot. Microbiol.* 41, 519–526.

Bhaud, Y., Guillebault, D., Lennon, J., Defacque, H., Soyer-Gobillard, M. O., and Moreau, H. (2000). Morphology and behaviour of dinoflagellate chromosomes during the cell cycle and mitosis. *J. Cell Sci.* 113 (Pt 7, 1231–1239.

Bhaud, Y., Salmon, J., and Soyer-Gobillard, M. (1991). The complex cell cycle of the dinoflagellate protoctist Crypthecodinium cohnii as studied in vivo and by cytofluorimetry. *J. Cell Sci.* 100, 675–682.

Bolte, S., and Cordelieres, F. P. (2006). A guided tour into subcellular colocalization analysis in light microscopy. *J. Microsc.* 224, 213–232.

Bosch, T. C., and David, C. N. (1984). Growth regulation in Hydra: relationship between epithelial cell cycle length and growth rate. *Dev. Biol.* 104, 161–171. doi:10.1016/0012-1606(84)90045-9.

Bouligand, Y., and Norris, V. (2001). Chromosome separation and segregation in dinoflagellates and bacteria may depend on liquid crystalline states. *Biochimie* 83, 187–192. doi:10.1016/S0300-9084(00)01211-6.

Cook, C. B., D'Elia, C. F., and Muller-Parker, G. (1988). Host feeding and nutrient sufficiency for zooxanthellae in the sea anemone Aiptasia pallida. *Mar. Biol.* 98, 253–262. doi:10.1007/BF00391203.

Cook, C. B., Muller-Parker, G., and Orlandini, C. D. (1994). Ammonium enhancement of dark carbon fixation and nitrogen limitation in zooxanthellae symbiotic with the reef corals Madracis mirabilis and Montastrea annularis. *Mar. Biol.* 118, 157–165. doi:10.1007/BF00699230.

Dagenais-Bellefeuille, S., and Morse, D. (2013). Putting the N in dinoflagellates. *Front. Microbiol.* 4, 369. doi:10.3389/fmicb.2013.00369.

Darzynkiewicz, Z., Halicka, H. D., and Zhao, H. (2010). Analysis of Cellular DNA Content by Flow and Laser Scanning Cytometry. *Adv. Exp. Med. Biol.* 676, 137–147.

David, C. N., and Campbell, R. D. (1972). Cell cycle kinetics and development of Hydra attenuata. *J. Cell Sci.* 11, 557–568.

Davy, S. K., Allemand, D., and Weis, V. M. (2012). Cell Biology of Cnidarian-Dinoflagellate Symbiosis. *Microbiol. Mol. Biol. Rev.* 76, 229–261. doi:10.1128/MMBR.05014-11.

Davy, S. K., Withers, K. J. T., and Hinde, R. (2006). Effects of host nutritional status and seasonality on the nitrogen status of zooxanthellae in the temperate coral Plesiastrea versipora (Lamarck). *J. Exp. Mar. Biol. Ecol.* 335, 256–265. doi:10.1016/j.jembe.2006.03.019.

Detournay, O., Schnitzler, C. E., Poole, A., and Weis, V. M. (2012). Regulation of cnidarian–dinoflagellate mutualisms: Evidence that activation of a host TGFB innate immune pathway promotes tolerance of the symbiont. *Dev. Comp. Immunol.* 38, 525–537. doi:10.1016/j.dci.2012.08.008.

Dimond, J. L., Pineda, R. R., Ramos-Ascherl, Z., and Bingham, B. L. (2013). Relationships between host and symbiont cell cycles in sea anemones and their symbiotic dinoflagellates. *Biol. Bull.* 225, 102–12.

Domotor, S. L., and D'Elia, C. F. (1984). Nutrient uptake kinetics and growth of zooxanthellae maintained in laboratory culture. *Mar. Biol.* 80, 93–101. doi:10.1007/BF00393132.

Domotor, S. L., and D'Elia, C. F. (1986). Cell-size distributions of zooxanthellae in culture and symbiosis. *Biol. Bull.* 170, 519–525. doi:10.2307/1541859.

Douglas, A., and Smith, D. (1984). The green hydra symbiosis. VIII. Mechanisms in symbiont regulation. *Proc. R. Soc. B Biol. Sci.* 221, 291–319.

Dunn, S. R., Schnitzler, C. E., and Weis, V. M. (2007). Apoptosis and autophagy as mechanisms of dinoflagellate symbiont release during cnidarian bleaching: every which way you lose. *Proc. R. Soc. Lond. B* 274, 3079–3085. doi:10.1098/rspb.2007.0711.

Fairclough, S. R., Dayel, M. J., and King, N. (2010). Multicellular development in a choanoflagellate. *Curr. Biol.* 20, 875–876. doi:10.1016/j.cub.2010.09.014.References.

Fingar, D. C., and Blenis, J. (2004). Target of rapamycin (TOR): An integrator of nutrient and growth factor signals and coordinator of cell growth and cell cycle progression. *Oncogene* 23, 3151–3171. doi:10.1038/sj.onc.1207542.

Fitt, W. K. (2000). Cellular Growth of Host and Symbiont in a Cnidarian-Zooxanthellar Symbiosis. *Biol. Bull.* 198, 110–120.

Fransolet, D., Roberty, S., Herman, A.-C., Tonk, L., Hoegh-Guldberg, O., and Plumier, J.-C. (2013). Increased cell proliferation and mucocyte density in the sea anemone Aiptasia pallida recovering from bleaching. *PloS ONE* 8, e65015. doi:10.1371/journal.pone.0065015.

Fransolet, D., Roberty, S., and Plumier, J. C. (2014). Impairment of symbiont photosynthesis increases host cell proliferation in the epidermis of the sea anemone Aiptasia pallida. *Mar. Biol.*, 1735–1743. doi:10.1007/s00227-014-2455-1.

Fujise, L., Nitschke, M. R., Frommlet, J. C., Serôdio, J., Woodcock, S., Ralph, P. J., et al. (2018). Cell cycle dynamics of cultured coral endosymbiotic microalgae (Symbiodinium) across different types (species) under alternate light and temperature conditions. *J. Eukaryot. Microbiol.* 0, 1–13. doi:10.1111/jeu.12497.

Gates, R. D., Baghdasarian, G., and Muscatine, L. (1992). Temperature stress causes host cell detachment in symbiotic cnidarians: implications for coral bleaching. *Biol. Bull.* 182, 324–332. doi:10.2307/1542252.

Gladfelter, A. S. (2015). How nontraditional model systems can save us. *Mol. Biol. Cell* 26, 3687–3689. doi:10.1091/mbc.E15-06-0429.

Goldstein, B., and King, N. (2016). The Future of Cell Biology: Emerging Model Organisms. *Trends Cell Biol.* 26, 818–824. doi:10.1016/j.tcb.2016.08.005.

Hughes, T. P., Kerry, J. T., Álvarez-Noriega, M., Álvarez-Romero, J. G., Anderson, K. D., Baird, A. H., et al. (2017). Global warming and recurrent mass bleaching of corals. *Nature* 543, 373–377. doi:10.1038/nature21707.

Kadono, T., Kawano, T., Hosoya, H., and Kosaka, T. (2004). Flow cytometric studies of the host-regulated cell cycle in algae symbiotic with green paramecium. *Protoplasma* 223, 133–141. doi:10.1007/s00709-004-0046-6.

LaJeunesse, T. C., Parkinson, J. E., Gabrielson, P. W., Jeong, H. J., Reimer, J. D., Voolstra, C. R., et al. (2018). Systematic Revision of Symbiodiniaceae Highlights

the Antiquity and Diversity of Coral Endosymbionts. *Curr. Biol.* 28, 2570-2580.e6. doi:10.1016/j.cub.2018.07.008.

Lajeunesse, T. C., Parkinson, J. E., and Reimer, J. D. (2012). A genetics-based description of Symbiodinium minutum sp. nov. and S. psygmophilum sp. nov. (Dinophyceae), two dinoflagellates symbiotic with cnidaria. *J. Phycol.* 48, 1380–1391. doi:10.1111/j.1529-8817.2012.01217.x.

Lecointe, A., Domart-coulon, I., Paris, A., and Meibom, A. (2016). Cell proliferation and migration during early development of a symbiotic scleractinian coral. *Proc. R. Soc. Lond. B* 283, 20160206. doi:10.1098/rspb.2016.0206.

Lee, P. N., Pang, K., Matus, D. Q., and Martindale, M. Q. (2006). A WNT of things to come : Evolution of Wnt signaling and polarity in cnidarians. *Semin. Cell Dev. Biol.* 17, 157–167. doi:10.1016/j.semcdb.2006.05.002.

Lehnert, E. M., Mouchka, M. E., Burriesci, M. S., Gallo, N. D., Schwarz, J. A., and Pringle, J. R. (2014). Extensive differences in gene expression between symbiotic and aposymbiotic cnidarians. *G3 Genes Genomes Genet.* 4, 277–295. doi:10.1534/g3.113.009084.

Login, F. H., Balmand, S., Vallier, A., Vincent-Monegat, C., Vigneron, A., Weiss-Gayet, M., et al. (2011). Antimicrobial peptides keep insect endosymbionts under control. *Science* 334, 362–365. doi:10.1126/science.1209728.

Matthews, J. L., Crowder, C. M., Oakley, C. A., Lutz, A., Roessner, U., Meyer, E., et al. (2017). Optimal nutrient exchange and immune responses operate in partner specificity in the cnidarian-dinoflagellate symbiosis. *Proc. Natl. Acad. Sci. U. S. A.* 114, 13194–13199. doi:10.1073/pnas.1710733114.

Matthews, J. L., Sproles, A. E., Oakley, C. A., Grossman, A. R., Weis, V. M., and Davy, S. K. (2016). Menthol-induced bleaching rapidly and effectively provides experimental aposymbiotic sea anemones (Aiptasia sp.) for symbiosis investigations. *J. Exp. Biol.* 219, 306–310. doi:10.1242/jeb.128934.

McAuley, P. J. (1986). The cell cycle of symbiotic Chlorella. III. Numbers of algae in green hydra digestive cells are regulated at digestive cell division. *J. Cell Sci.* 85, 63–71.

McAuley, P. J., and Cook, C. B. (1994). Effects of host feeding and dissolved ammonium on cell division and nitrogen status of zooxanthellae in the hydroid Myrionema amboinense. *Mar. Biol.* 121, 343–348. doi:10.1007/BF00346743.

Mergaert, P., Uchiumi, T., Alunni, B., Evanno, G., Cheron, A., Catrice, O., et al. (2006). Eukaryotic control on bacterial cell cycle and differentiation in the Rhizobium-legume symbiosis. *Proc. Natl. Acad. Sci. U. S. A.* 103, 5230–5235. doi:10.1073/pnas.0600912103.

Miller, D. J., Hemmrich, G., Ball, E. E., Hayward, D. C., Khalturin, K., Funayama, N., et al. (2007). The innate immune repertoire in Cnidaria - Ancestral complexity and stochastic gene loss. *Genome Biol.* 8, R59. doi:10.1186/gb-2007-8-4-r59.

Muller-Parker, G., and Davy, S. K. (2001). Temperate and Tropical Algal-Sea Anemone Symbioses. *Invertebr. Biol.* 120, 104–123.

Muller-Parker, G., Lee, K. W., and Cook, C. B. (1996). Changes in the ultrastructure of symbiotic zooxanthellae (Symbiodinium Sp., Dinophyceae) in fed and starved sea anemones maintained under high and low light. *J. Phycol.* 32, 987–994. doi:10.1111/j.1529-8817.1996.tb02206.x.

Muscatine, L., Falkowski, P. G., Dubinsky, Z., Cook, P. A., and McCloskey, L. L. R. (1989). The effect of external nutrient resources on the population dynamics of zooxanthellae in a reef coral. *Proc. R. Soc. Lond. B* 236, 311–324. doi:10.1098/rspb.1989.0025.

Muscatine, L., and Pool, R. R. (1979). Regulation of numbers of intracellular algae. *Proc. R. Soc. Lond. B* 204, 131–139. doi:10.1098/rspb.1979.0018.

Ollion, J., Cochennec, J., Loll, F., Escudé, C., and Boudier, T. (2013). TANGO: A generic tool for high-throughput 3D image analysis for studying nuclear organization. *Bioinformatics* 29, 1840–1841. doi:10.1093/bioinformatics/btt276.

Olson, R. J., Vaulot, D., and Chisholm, S. W. (1986). Effects of Environmental Stresses on the Cell Cycle of Two Marine Phytoplankton Species. *Plant Physiol.* 80, 918–925.

Oswald, E., Nougayrède, J. P., Taieb, F., and Sugai, M. (2005). Bacterial toxins that modulate host cell-cycle progression. *Curr. Opin. Microbiol.* 8, 83–91. doi:10.1016/j.mib.2004.12.011.

Otto, J. J., and Campbell, R. D. (1977). Tissue economics of hydra: regulation of cell cycle, animal size and development by controlled feeding rates. *J. Cell Sci.* 28, 117–132.

Pardee, A. B. (1989). G1 events and regulation of cell proliferation. *Science* 246, 603–608.

Passamaneck, Y. J., and Martindale, M. Q. (2012). Cell proliferation is necessary for the regeneration of oral structures in the anthozoan cnidarian Nematostella vectensis. *BMC Dev. Biol.* 12, 34. doi:10.1186/1471-213X-12-34.

Rentzsch, F., Fritzenwanker, J. H., Scholz, C. B., and Technau, U. (2008). FGF signalling controls formation of the apical sensory organ in the cnidarian Nematostella vectensis. *Development* 135, 1761–1769. doi:10.1242/dev.020784.

Rizzo, P. J. (2003). Those amazing dinoflagellate chromosomes. *Cell Res.* 13, 215–217. doi:10.1038/sj.cr.7290166.

Rosset, S., Wiedenmann, J., Reed, A. J., and D'Angelo, C. (2017). Phosphate deficiency promotes coral bleaching and is reflected by the ultrastructure of symbiotic dinoflagellates. *Mar. Pollut. Bull.* 118, 180–187. doi:10.1016/j.marpolbul.2017.02.044.

Scheurlen, I., Hoffmeister, S. a, and Schaller, H. C. (1996). Presence and expression of G2 cyclins in the coelenterate hydra. *J. Cell Sci.* 109, 1063–1069.

Singer, I. (1971). Tentacular and oral-disc regeneration in the sea anemone, Aiptasia diaphana. *J. Embryol. Exp. Morphol.* 26, 253–270.

Smith, G. J., and Muscatine, L. (1999). Cell cycle of symbiotic dinoflagellates: variation in G1 phase-duration with anemone nutritional status and macronutrient supply in the Aiptasia pulchella-Symbiodinium pulchrorum symbiosis. *Mar. Biol.* 134, 405–418.

Technau, U., Rudd, S., Maxwell, P., Gordon, P. M. K., Saina, M., Grasso, L. C., et al. (2005). Maintenance of ancestral complexity and non-metazoan genes in two basal cnidarians. *Trends Genet.* 21, 633–639. doi:10.1016/j.tig.2005.09.007.

Van de Velde, W., Zehirov, G., Szatmari, A., Debreczeny, M., Ishihara, H., Kevei, Z., et al. (2010). Plant peptides govern terminal differentiation of bacteria in symbiosis. *Science* 327, 1122–1126. doi:10.1126/science.1184057.

Vaulot, D., Olson, R. J., Merkel, S., and Chisholm, S. W. (1987). Cell-cycle response to nutrient starvation in two phytoplankton species, Thalassiosira weissflogii and Hymenomonas carterae. *Mar. Biol.* 95, 625–630. doi:10.1007/BF00393106.

Wang, L.-H., Lee, H.-H., Fang, L.-S., Mayfield, A. B., and Chen, C.-S. (2013). Fatty acid and phospholipid syntheses are prerequisites for the cell cycle of Symbiodinium and their endosymbiosis within sea anemones. *PloS ONE* 8, e72486. doi:10.1371/journal.pone.0072486.

Wang, L.-H., Liu, Y. H., Ju, Y. M., Hsiao, Y. Y., Fang, L.-S., and Chen, C. S. (2008). Cell cycle propagation is driven by light-dark stimulation in a cultured symbiotic dinoflagellate isolated from corals. *Coral Reefs* 27, 823–835. doi:10.1007/s00338-008-0434-z.

Weis, V. M., Davy, S. K., Hoegh-Guldberg, O., Rodriguez-Lanetty, M., and Pringle, J. R. (2008). Cell biology in model systems as the key to understanding corals. *Trends Ecol. Evol.* 23, 369–76. doi:10.1016/j.tree.2008.03.004.

Wiedenmann, J., D'Angelo, C., Smith, E. G., Hunt, A. N., Legiret, F.-E., Postle, A. D., et al. (2013). Nutrient enrichment can increase the susceptibility of reef corals to bleaching. *Nat. Clim. Change* 3, 160–164. doi:10.1038/nclimate1661.

Wilkerson, F. P., Kobayashi, D., and Muscatine, L. (1988). Mitotic index and size of symbiotic algae in Caribbean Reef corals. *Coral Reefs* 7, 29–36.

Wilkerson, F. P., Muller, G., and Muscatine, L. (1983). Temporal patterns of cell division in natural populations of endosymbiotic algae. *Limnol. Oceanogr.* 28, 1009–1014.

Wisecaver, J. H., and Hackett, J. D. (2011). Dinoflagellate genome evolution. *Annu. Rev. Microbiol.* 65, 369–87. doi:10.1146/annurev-micro-090110-102841.

Wong, J. T. Y., and Kwok, A. C. M. (2005). Proliferation of dinoflagellates: blooming or bleaching. *BioEssays News Rev. Mol. Cell. Dev. Biol.* 27, 730–40. doi:10.1002/bies.20250.

Woznica, A., Gerdt, J. P., Hulett, R. E., Clardy, J., and King, N. (2017). Mating in the closest living relatives of animals is induced by a bacterial chondroitinase. *Cell* 170, 1175–1183. doi:10.1016/j.cell.2017.08.005.

Yuyama, I., Ishikawa, M., Nozawa, M., Yoshida, M., and Ikeo, K. (2018). Transcriptomic changes with increasing algal symbiont reveal the detailed process underlying establishment of coral-algal symbiosis. *Sci. Rep.* 8, 16802. doi:10.1038/s41598-018-34575-5.

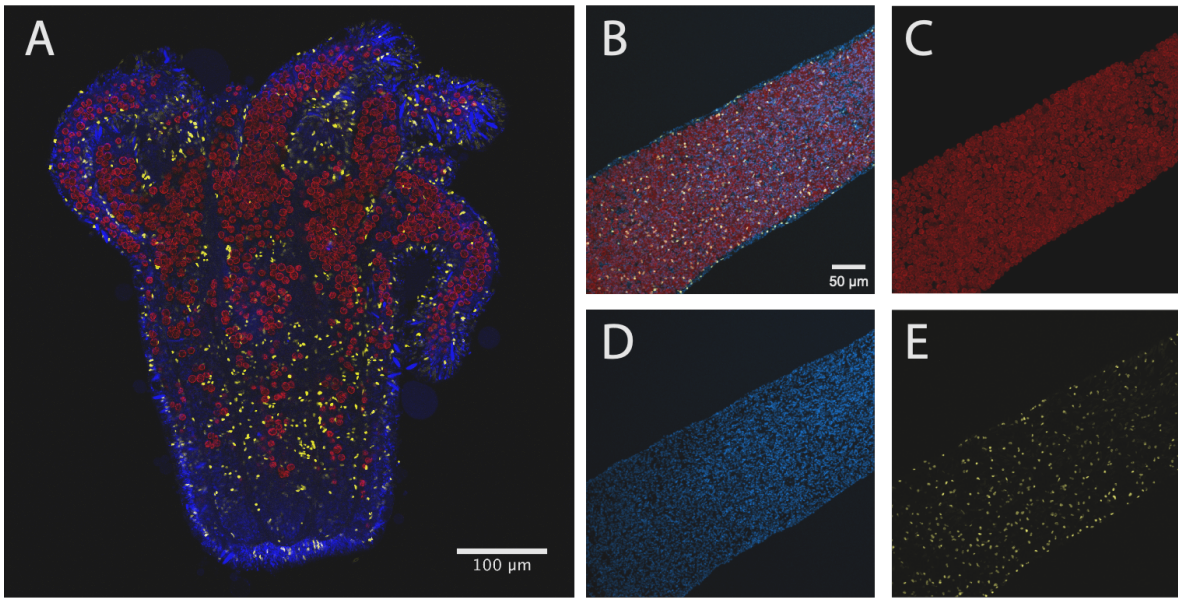

Figure 3.1 Fluorescent labeling of *Aiptasia pallida*.
(A) Tiled section of a symbiotic *A. pallida* sea anemone labeled with EdU-AF555 (yellow). Host cell proliferation analyses were done using fluorescently labeled Aiptasia tentacles (**B**). Symbiont location was captured using chlorophyll autofluorescence shown in red (**C**). Cnidarian host nuclei were labeled with Hoechst (**D**) and proliferative host nuclei were labeled with EdU-AF555 (**E**) to capture cell populations that have incorporated new DNA during S-phase.

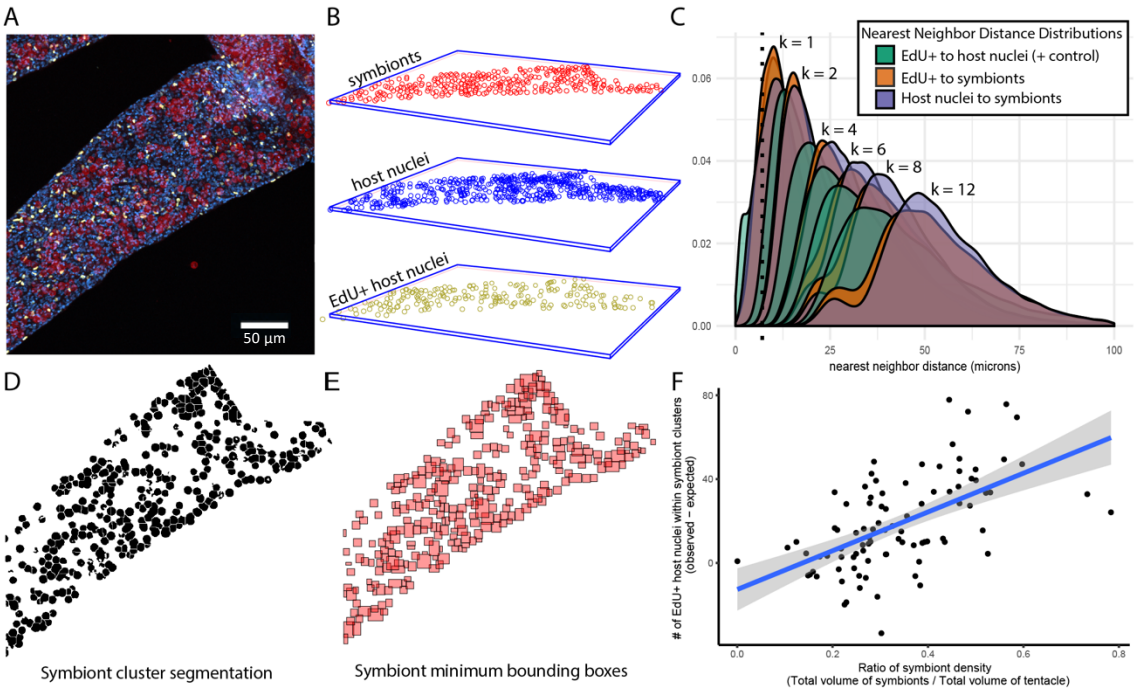

Figure 3.2 Intersection analysis of host EdU-positive nuclei and symbionts during colonization.
Confocal images were taken of host tentacles during colonization by symbionts **(A)**. Host cells were differentiated with Hoechst (blue) to label nuclei, with EdU-AF555 (yellow) to label proliferating nuclei, and symbiont cells by chlorophyll autofluorescence (red). The centers of masses of host nuclei (blue), proliferating host nuclei (green), and symbionts (red) were located for each tentacle **(B)**. In each tentacle, the distances from each center of mass to the nearest neighbor (NN) of another group were determined. NN distances were combined across tentacles and density plots of these distances was plotted in **(C)** for the 1st NN k = 1 up to the 12th closest NN k = 12. The NN distances from EdU-positive nuclei to Hoechst-stained nuclei were used as an indicator of a strong positive relationship (green). The NN distances of EdU-positive nuclei to symbionts (orange) were on average closer than non-proliferating nuclei to symbionts (purple). The dotted vertical line indicates the mean and median distance from a symbiont center of mass to its cell surface. Segmented symbiont objects **(**shown in **D)** were used to determine the presence / absence of symbionts in specific locations of the tentacle. The number of EdU-positive nuclei were quantified inside and outside of corresponding symbiont-containing locations (**E**) and compared to a null hypothesis where one would expect proliferating nuclei to be found in equal proportion inside and outside of these symbiont-containing volumes **(F)**. The number of proliferating nuclei within symbiont-containing locations increased with symbiont density.

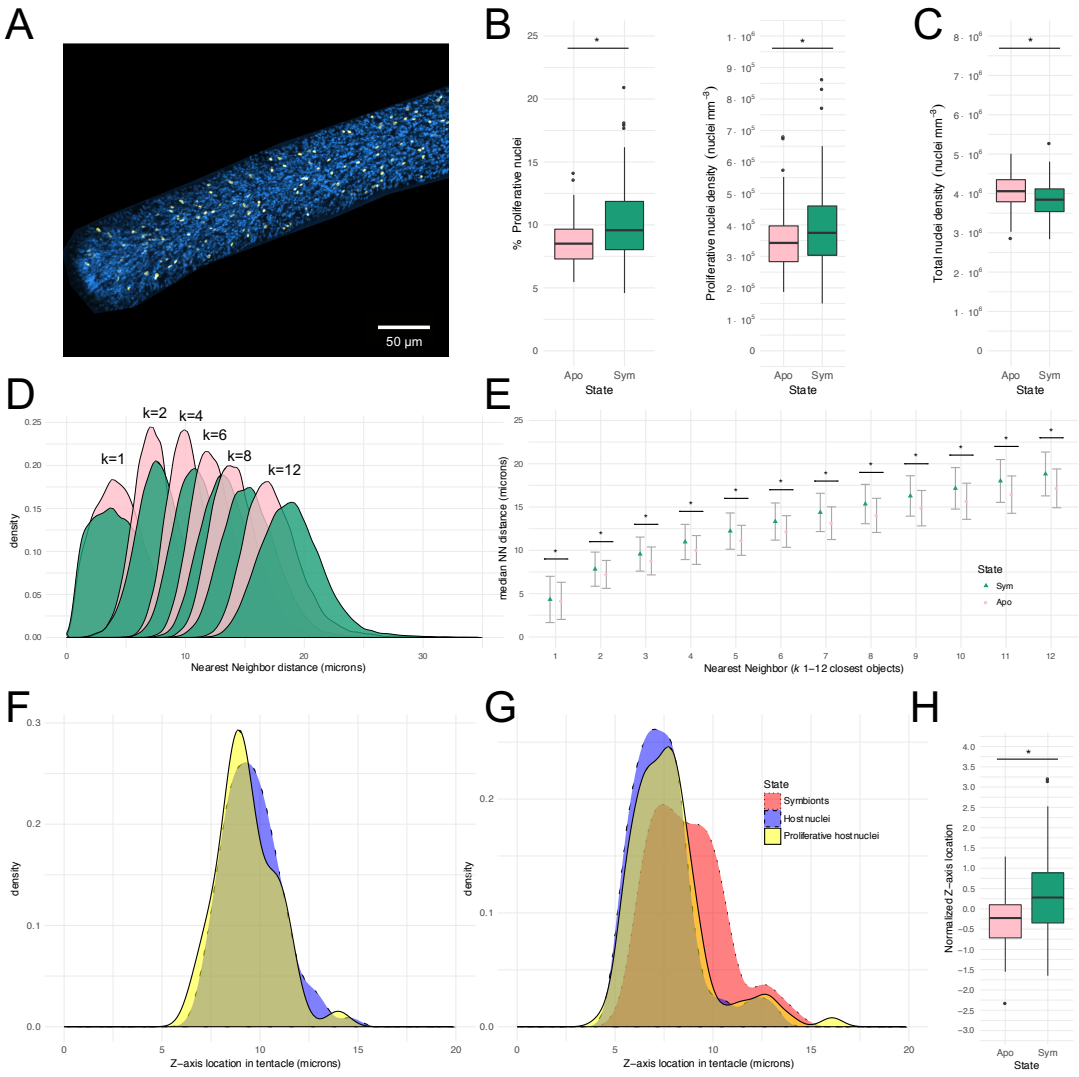

Figure 3.3 Comparative analysis of host EdU-positive nuclei in aposymbiotic and symbiotic sea anemones.
Confocal z-stack images were taken of aposymbiotic tentacles **(A)** in order to compare to proliferation colonization by symbionts. Host cells were differentiated with Hoechst (blue) to label nuclei, with EdU-AF555 (yellow) to label proliferating nuclei. The percentage and density of host proliferative nuclei (**B**) and total host nuclei (**C**) were compared across symbiotic state. Asterisks indicate significant differences (two-sample t-test, $p < 0.05$). (**D**) For each tentacle, the distances from each center of mass of a proliferative cell were measured to the nearest neighbor (NN) non-proliferative cell. A density plot compares the distributions of NN distances in aposymbiotic (pink) and symbiotic (green) Aiptasia tentacles. Median NN distances of these NN distributions are shown in (**E**), with error bars representing median absolute deviation. Asterisks indicate significant differences (MannWhitney *U* test, $p < 2.2 \times 10^{-16}$). Finally, cell center of mass distributions were plotted to visualize Z-axis location in aposymbiotic (**F**) and symbiotic (**G**) tentacles. Epidermal tissue layer is represented by the left peak of Hoechst-labeled host cells (blue) whereas the gastrodermal tissue layer is right-shifted as evident by the location of symbionts (red) in symbiotic tentacles (**G**). To compare proliferative nuclei Z-axis location, distributions were normalized for each tentacle by subtracting the distribution medians of host nuclei from the medians of proliferative nuclei (**H**). A positive normalized Z-axis location (**H**) therefore represents a rightward shift towards the gastrodermis for proliferative nuclei. Asterisk indicate significant differences (two-sample t-test, $p < 1 \times 10^{-6}$).

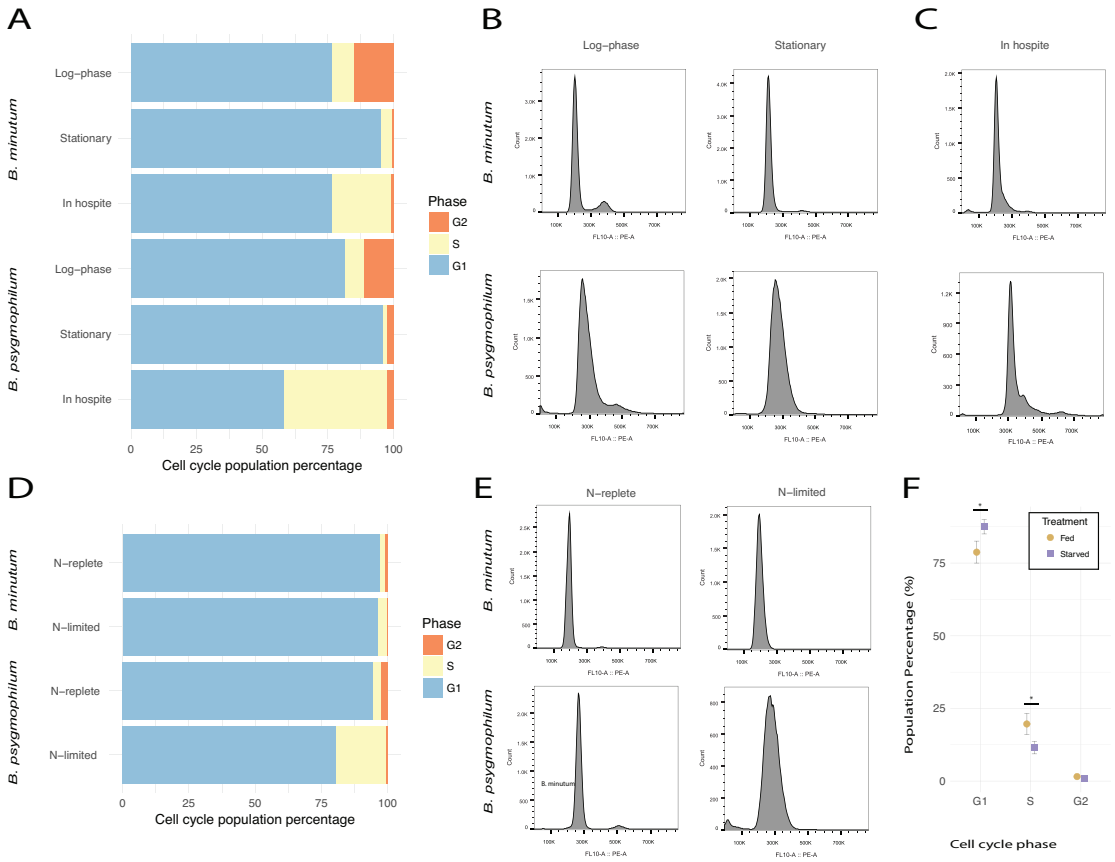

Figure 3.4 Cell cycles of *B. minutum* and *B. psygmophilum* in culture and *in hospite*. The cell cycles of two *Breviolum* species in culture and *in hospite* were analyzed under different nutritional states using propidium iodide staining of DNA and flow cytometry. Stacked horizontal bar graphs represent cell cycle percentages (blue = G_1, yellow = S, orange = G_2M) of *Breviolum* cultures and isolates. (**A**) The log-phase and stationary cell cultures of *B. minutum* and *B. psygmophilum* were compared to their respective cell cycles *in hospite*. Representative cell cycle profiles are shown for (**B**) log-phase and stationary *Breviolum* cultures and (**C**) *Breviolum* populations isolated from host Aiptasia strains H2 (*B. minutum*) and JK (*B. psygmophilum*). Cellular DNA content was measured using propidium iodide and fluorescence was captured in the FL10: PE-A emission channel after doublet discrimination. Units represent relative propidium iodide fluorescence. *B. psygmophilum* had right-shifted G_1 peaks representing increased DNA content compared to *B. minutum*. G_2 peaks for both species were found at double the fluorescence (i.e. 2x DNA content) of the G_1 peaks. (**D**) To test for the effect of nitrogen limitation, *Breviolum* cultures were placed in nitrogen-replete and nitrogen-limited cultures and their cell cycles were compared with each other. (**E**) Representative cell cycle profiles of nitrogen-replete and nitrogen-limited cultures are shown for both *Breviolum* cultures. (**F**) To examine the effect of nutrition on *Breviolum* populations *in hospite*, cell cycle percentages of *B. minutum* symbionts were measured from fed (brown circles) and starved (purple squares) Aiptasia. The population percentages are shown for each cell cycle phase (G_1, S, and G_2). Asterisks represent significant differences (two-sample t-test, $p < 0.05$).

4. Spatial and temporal patterns of symbiont colonization in the model sea anemone Aiptasia

Trevor R. Tivey[1*], Virginia M. Weis[1]

[1]Department of Integrative Biology, Oregon State University, Corvallis, OR, United States

4.1 Abstract

The ability of symbionts to recolonize their hosts after a period of dysbiosis is essential for the maintenance of a resilient partnership. Many cnidarians rely on the photosynthate provided from a substantial symbiont population density. Under periods of thermal stress, symbiont densities in cnidarians decline, and the recovery of susceptible cnidarians is dependent on the re-establishment of symbiosis. The cellular patterns and mechanisms that govern this process of colonization are not well-defined and require further exploration. To study these colonization patterns in Aiptasia, we developed a noninvasive, efficient method of imaging and analysis that measured the abundance and location of local symbiont proliferation clusters within host tentacles. With this method we were also able to estimate the cell cluster size to measure the occurrence of singlets, doublets, and so on up to much larger clusters. Our results support the combined mechanisms of locally clustered symbiont growth and continuous new symbiont establishment during recolonization. A consistent minimum threshold of singlet and doublet symbiont populations was observed during recolonization, as well as increased bleaching susceptibility of large symbiont clusters to heat stress. The role of host-symbiont specificity was evident in the rapid recolonization by homologous symbiont *Breviolum minutum*. However, under thermal stress *B. minutum* populations exited their hosts at a rapid pace compared to the persistence of *Symbiodinium microadriaticum* and *Durusdinium trenchii* populations. Though these thermally tolerant populations remained at low levels under constant elevated temperature, their ability to persist during periods of stress may be a mechanism that increases their colonization success during subsequent periods of recovery.

4.2 Introduction

Coral reefs worldwide face an uphill battle against the threat of warming sea surface temperatures and global climate change (Frieler et al., 2013; Hughes et al., 2018). The vulnerable cnidarians that comprise these reefs rely on their partnership with endosymbiotic algae to provide nutrient-rich photosynthate in relatively nutrient-poor environments (Muscatine and Porter, 1977). Upon sustained elevated temperature stress, this intracellular relationship breaks down, causing rapid decreases of algal populations in host gastrodermal tissues in a process known as bleaching (Brown, 1997). Although the overall symbiont population dynamics during bleaching are well-documented, mechanisms for how algal populations decrease and subsequently recover in hosts are not well-understood (Bieri et al., 2016; Gates et al., 1992; Weis, 2008). It is therefore critical to examine cellular mechanisms of population depletion and re-establishment within cnidarians in order to predict host and symbiont response to rapidly changing ocean environments (Davy et al., 2012).

The establishment of algal symbiosis within cnidarians can occur through either initial colonization or through recolonization after symbiont depletion. During initial colonization, symbioses are acquired during the larval stage or after settlement and metamorphosis into a juvenile polyp (Schwarz et al., 1999). Major disruptions in symbiont population dynamics occur during cnidarian bleaching, when a host loses its algae under environmental stress. Recolonization occurs after a bleaching episode. It is still not clear whether recolonizing symbionts originate from the water column or if recovery is solely from those algae remaining within the depleted host (Coffroth et al., 2006). These colonization and recolonization events are fundamental to the survival of cnidarians at key vulnerable life stages.

After initial symbiont uptake, colonizing symbionts must proliferate via many cycles of cell division to form a stable symbiosis with their cnidarian host. Symbiont proliferation takes place within host cnidarian cells, which are also undergoing cell division. The dispersal of Symbiodiniaceae cells through the gastrodermal layer of cnidarians can therefore occur primarily through localized cnidarian cell division. However the rapid increase in patchy symbiotic tissue supports the additional the

presence of cnidarian cell migration or the release and re-uptake of a Symbiodiniaceae cell into another host cell from the gastrovascular cavity (Gabay et al., 2018). Similar redistribution of Symbiodiniaceae has occurred within *Montipora capitata* in response to light intensity (Santos et al., 2009). In the more distantly related octocorals, symbiotic host cells detach and accumulate in stolons during bleaching events (Parrin et al., 2012, 2016). Though equivalent refugia for Symbiodiniaceae generally do not exist in hexacorallians such as corals and sea anemones, host cell detachment and expelled symbiont migration within the gastrovascular cavity may play a role in symbiont proliferation or bleaching processes. Time-lapse imaging of cnidarians may be able to capture both symbiont and detached host cell movement within the gastrovascular cavity.

Despite the focus on symbiont colonization and bleaching, spatial and temporal patterns of colonization are often limited to population density snapshots in time. The symbiotic sea anemone *Exaiptasia pallida*, commonly called Aiptasia, provides a tractable model to understand these fundamental cellular mechanisms in depth (Weis et al., 2008). Aiptasia is readily culturable in a laboratory setting and can be maintained indefinitely in an aposymbiotic state after rapid bleaching from either thermal stress or menthol treatment (Belda-Baillie et al., 2002; Matthews et al., 2016). Aposymbiotic Aiptasia are competent to symbiont inoculation with native and non-native members (i.e. those not observed in nature) of the family Symbiodiniaceae, and many previous studies have used adult Aiptasia to test the effects of symbiont surface manipulation and species specificity on symbiont uptake and colonization (Belda-Baillie et al., 2002; Detournay et al., 2012; Lin et al., 2000; Parkinson et al., 2018; Schoenberg and Trench, 1980). In this study, we aimed to quantify symbiont proliferation dynamics in individual sea anemones over periods of recolonization and bleaching. We developed and compared two noninvasive methods for tracking symbiont population patterns throughout the tentacles of Aiptasia. We further used this methodology to compare the patterning and population dynamics of native symbiont species (*Breviolum minutum*) and non-native species (*Symbiodinium microadriaticum* and *Durusdinium trenchii*) under ambient and elevated temperatures.

4.3 Methods

Animal and algal culturing

Experimental Aiptasia hosts were generated from animal stocks of the clonal Aiptasia strain H2 containing their native symbiont species *Breviolum minutum*, originally isolated from a single individual collected from Coconut Island, Kaneohe, Hawaii (Xiang et al., 2013). For comparisons between host strains, the strain VWA12 (also containing *B. minutum*) was created from asexual cloning of a single individual from Weis Lab population VWA, collected from multiple sources dating from the 2002. Aposymbiotic sea anemones were generated using a menthol bleaching protocol (Matthews et al., 2016). Sea anemones were maintained in an aposymbiotic state for longer than two months prior to use in experiments and fed *Artemia* nauplii three times per week until one week prior to experiments. Anemones were individually plated one week in advance of experiments, kept under 12:12 L:D cycle and checked for symbionts using epifluorescence microscopy, to make sure that the animals remained symbiont-free. Sea anemones and algal cultures were maintained in incubators at 26˚C under 12:12 L:D cycle. Algal cultures of Symbiodiniaceae were grown in f/2 media at a light intensity of 50 µmol quanta • m^{-2} • s^{-1}. The native symbiont of Aiptasia, *B. minutum* (culture IDs: FLAp2 Mf1.05b). Competent non-native symbionts of Aiptasia, *Symbiodinium microadriaticum* (CCMP 2467) and *Durusdinium trenchii* (Ap2). All cultures were genotyped prior to experiments to verify the identification of symbionts (data not shown).

Recolonization of two strains of aposymbiotic Aiptasia with native symbionts

Tiny (1 mm oral disc) aposymbiotic anemones (strains H2 and VWA12) were selected and plated into 24-well plates. Sea anemones were visually checked to determine absence of any algal symbionts. Sea anemones were then inoculated with 1 x 10^4 cells • mL^{-1} of *B. minutum* (Culture FLAp2). After 24 h of exposure, sea anemones were rinsed and moved to a 96-well plate and imaged. The same sea anemones were imaged for up to seven days after recolonization (n = 10). For imaging, sea anemones were placed in a relaxing solution of 1:1 FSW mixed with 0.37M $MgCl_2$ in FSW. After 5 minutes, the

animal was plated onto a depression slide for confocal imaging at 10x magnification on a Zeiss LSM 780 NLO Confocal Microscope System (Carl Zeiss AG, Jena, Germany) in the Center for Genomic Research and Biocomputing at Oregon State University. Z-stack images were taken of the entire anemone under bright light only (**Figure 4.1**). Quantification of the number of singlet, doublet, triplet, and quadruplet algal cells was performed for each Z-stack image using Fiji (ImageJ2) (Rueden et al., 2017; Schindelin et al., 2012).

Recolonization of anemone by native symbionts under elevated temperature conditions

Medium-sized (0.25 cm oral disc) menthol-bleached sea anemones (strain H2) were selected and plated into 24-well plates. To examine residual symbiont populations, sea anemones were visually inspected under bright light and under laser excitation using the Cy3 red filter to capture symbiont autofluorescence. Low densities of singlet algal cells (approximately 5-15 cells per tentacle) were found to have persisted in Aiptasia tentacles after six months of darkness post-menthol bleaching. To better understand how cnidarians rebound after losing the vast majority of their symbionts, we inoculated these Aiptasia with their native symbiont *B. minutum* and examined proliferation patterns under two temperature regimes, 26˚C and 32˚C. All anemones were initially inoculated with 5 x 10^4 cells • mL^{-1} of *B. minutum* culture. After 24 h, Aiptasia were rinsed with FSW (d = 0). Anemones were imaged and maintained at 26˚C for one week before dividing them into an ambient treatment (26˚C) and an elevated heat treatment (32˚C) (n = 24 anemones per treatment). Since heat and ambient treatment of anemones required incubation in two separate incubators, each 24-well plate was housed in identical chambers with LED lighting strips covered with nylon mesh for a final light intensity of 10 µmol quanta • m^{-2} • s^{-1} across the entire plate. An inverted epifluorescence Zeiss AxioObserver A1 microscope with an Axiovert ICm1 camera (Carl Zeiss AG, Jena, Germany) was used for three weeks to take videos of three tentacles per anemone at 35 ms exposure under bright light and under laser excitation (Cy3 red filter) to capture algal cell chlorophyll autofluorescence (**Figure 4.2**). For each tentacle, videos were taken by scrolling through the focus from the tip to the base of a tentacle using a 10x objective, simulating a

confocal Z-stack. Brightfield video was taken first to determine the depth of the tentacle, and a video was taken immediately after using darkfield laser excitation.

Comparisons of non-native symbiont colonization and bleaching

To understand differences between colonization patterns of different symbionts, we inoculated Aiptasia with three species of Symbiodiniaceae: native *B. minutum*, and non-native *S. microadriaticum*, and *D. trenchii*. Prior to inoculations, all anemones were examined using epifluorescence microscopy to verify the absence of residual algal symbionts. Inoculations were performed using 5 x 10^5 cells • mL^{-1} for all species over two days. After 48 h of inoculation, anemones were rinsed and moved to new 24-well plates. Sea anemones were maintained at 26˚C for two weeks before separating into an ambient treatment (26˚C) and an elevated heat treatment (32˚C) (n = 12 each). Environmental conditions and epifluorescence imaging were identical to the previous experiment.

Image Analysis

For experiments performed on the epifluorescence microscope, videos were saved and exported into jpeg stacks using the batch export function in the ZEN software package (Black Edition v. 3.0). Photo stacks with more than 50 images were flagged and truncated to delete images that were out of focus at the top and bottom of the image stack. Image stacks were then imported into Adobe Photoshop CC 2019 (v. 20.0.3) to undergo autoblend in order to merge the image stack into one 2D image of a tentacle (**Figure 4.2**). Once all of the stacks were merged into single tentacles containing all symbionts, these merged images were separated into two different folders, one containing brightfield merged images and one containing fluorescent merged images. Image lists were verified to determine that both folders contained the same order of sample tentacles. Custom Fiji (ImageJ2) macros (available on protocols.io at https://www.protocols.io/groups/weis-lab-osu) were used to determine the area and region of interest from the brightfield image and to estimate the number of symbiont clusters and individual symbionts within the corresponding fluorescent merged image. This concurrent measurement provided information with both the abundance and density of symbionts within Aiptasia tentacles.

4.4 Results

Sustained singlet inoculation and doublet formation is critical in first week of symbiont recolonization in tiny Aiptasia

Using brightfield confocal microscopy, we took repeated measurements and tracked symbiont populations over one week of recolonization in two strains of Aiptasia. At relatively low symbiont inoculation concentration (1 x 10^4 cells • mL^{-1}), tentacles were slowly populated with low levels of singlet symbionts in the host tentacles (**Figure 4.3**). The columns of inoculated Aiptasia had much lower symbiont density which remained low through the duration of the experiment. Over the course of one week of inoculation, singlet cells remained in tentacles at a constant rate, whereas doublet presence grew exponentially (**Figure 4.3**). Though the presence of triplets was recorded as early as two days post-inoculation, multiple triplets and quadruplets only began to appear at day seven of the experiment. This colonization pattern in Aiptasia strain H2 was compared to a simultaneous recolonization experiment using Aiptasia strain VWA12. Despite undergoing an identical inoculation, *B. minutum* failed to colonize VWA12 anemones (**Figure 4.3**). In contrast to the increased symbiont population in H2 tentacles, the total number of symbiont cells in VWA12 tentacles was as low as the number of cells in their pharynges and body columns. In VWA12 anemone tentacles, singlet populations remained at a density five times lower than those in H2 tentacles, and doublets showed no trend in growth. Triplets and quadruplets were absent in VWA12 strain inoculations, indicative of low early colonization.

Detailed spatial and temporal patterns of B. minutum recolonization in Aiptasia

Epifluorescence microscopy and automated imaging processes allowed us to more efficiently collect and analyze symbiont patterns within host Aiptasia. With these methods, we were able to capture symbiont proliferation dynamics in Aiptasia tentacles over an extended period of recolonization (**Figure 4.4A**). We inoculated Aiptasia with a concentration of 5 x 10^4 cells • mL^{-1}, which was increased from the previous experiment in order to be able to image rapid symbiont proliferation within the tentacles of larger-sized Aiptasia polyps. Initial symbiont recolonization occurred throughout the length of

the tentacle (**Figure 4.4B**). Singlet and doublets were present in host tissue within the first week (**Figure 4.4C**). Larger clusters appeared earlier than they did with 1 x 10^4 cells • mL^{-1} concentration inoculation, with triplets seen as early as two days post-inoculation. After an additional four days of growth, mean cluster size grew dramatically towards 5-8 cells. The percentage of cells in clusters of triplets or higher began to compose the majority of tentacle patterning after six days post-inoculation. Despite this change in growth, singlet populations remained the most observed cell pattern for the duration of the experiment. These single cell populations could be persisting either through a lack of cell division in this population, or more likely a continual influx of new colonization events. After three weeks, singlet cells finally dropped down to levels consistent with other cluster size groups (**Figure 4.4C**). The number of individual isolated clusters rose linearly within the first week but plateaued soon after.

Heat stress predominantly affects larger symbiont clusters

After one week of recolonization, heat stress was applied to half of the colonizing anemones. After one day at 32˚C, the overall number of symbiont cells decreased significantly (**Figure 4.4A**; two-sample t-test, $p < 3.6 \times 10^{-7}$). Cell clusters also decreased from a mean of 80 clusters to 65 clusters per tentacle (two-sample t-test, $p < 2.1 \times 10^{-6}$). All larger cluster sizes decreased in abundance (**Figure 4.4C**). Each cluster group underwent a 50% decrease in abundance, with the exception of singlet populations, which increased by 40%., and After one week of heat treatment, all cell cluster sizes declined dramatically, and after two weeks of heat treatment, only the occasional singlet or doublet symbiont cluster was found in tentacles. There was no locational difference in recolonization or bleaching along the length of the tentacle (**Figure 4.4**).

Symbiont thresholds of inoculation are barriers to initial recolonization in non-native species

To understand how recolonization patterns of hosts by symbionts differ across symbiont species, we compared recolonization of Aiptasia using three species of Symbiodiniaceae: *B. minutum*, *S. microadriaticum*, and *D. trenchii* (**Figure 4.5**). We inoculated Aiptasia with a concentration of 5 x 10^5 cells • mL^{-1}, which was increased from the previous

experiment in order to be able to ensure successful symbiont uptake of heterologous species. Aiptasia inoculations with *B. minutum* had the strongest and least variable colonization rates. Average symbiont volume in hosts grew at a linear rate over one month in ambient temperature conditions (26˚C), similar to recolonization pattern in the prior experiment (**Figures 4.4 and 4.5**). Singlets declined after three weeks post-inoculation, whereas larger clusters increased more slowly but did so steadily throughout the experiment (**Figure 4.5**). Inoculations with *S. microadriaticum* and *D. trenchii* had much higher variation between anemones. Increased singlet and doublet population clusters in animals inoculated with *S. microadriaticum* and *D. trenchii* was predictive of successful recolonization and appeared to drive overall recolonization. With all colonizing symbiont species, once tentacles contained over 50 clusters, they remained colonized for the duration of the experiment (**Figure 4.5**).

Native and non-native symbionts in host anemones differ in response to elevated temperature stress

After two weeks of recolonization, heat stress was applied to half of the colonizing anemones. Inoculations with *B. minutum* declined in density and cluster number immediately after the temperature was increased (**Figure 4.6A**). After one week, most tentacles had no clusters of symbionts present in their tentacles (**Figure 4.6B**). In contrast, inoculations with *S. microadriaticum* and *D. trenchii* remained relatively constant (**Figure 4.6A**). Symbiont clusters were present in non-native species, albeit at low numbers, throughout the heat treatment (**Figure 4.6B**). Because of this prolonged presence, there was noticeably higher variation in *S. microadriaticum* and *D. trenchii* after elevated temperature treatment (**Figure 4.6**).

4.5 Discussion

Successful cluster establishment is vital to support rapid recolonization

The first weeks of inoculation appear to be the critical time of symbiosis establishment prior to log-phase growth of symbionts within hosts. This early proliferation within two weeks by native symbionts has been a common indicator of recolonization success in

many studies (Belda-Baillie et al., 2002; Davy et al., 1997; Gabay et al., 2018; Schoenberg and Trench, 1980). For example, in one Aiptasia recolonization study, the initial symbiont density at two weeks appeared predictive of overall length and intensity of infection (Belda-Baillie et al., 2002). We found a similar predictive pattern across our experiments; recolonization success was contingent on a threshold of symbiont density. In low-density symbiont inoculation of tiny anemones (**Figure 4.3**), symbiont populations only grew if there were at least two symbiont cells per tentacle. Though both VWA12 and H2 tentacles had the same number of doublets in their tentacles initially, later doublet population growth and consequent recolonization did not occur in VWA12, presumably because of low singlet density. In the larger-sized Aiptasia used in the subsequent experiments, approximately ten unique clusters seemed to be necessary for rapid symbiont proliferation. Increased density of both singlet and doublet populations within the first two weeks post-inoculation with symbionts were important predictors of colonization success. Rapid recolonization of Aiptasia tentacles by invading symbionts was crucial to consistently establishing symbiosis in our experiments.

Host-symbiont specificity is predictive of recolonization rate of symbionts in hosts

Host-symbiont specificity was observed in our experiments, as symbiont species *S. microadriaticum* and *D. trenchii* recolonized aposymbiotic Aiptasia adults more slowly and with significantly higher variation across animals than did *B. minutum*. Slower rates of host recolonization with these non-native species was expected and consistent with previous Aiptasia studies (Belda-Baillie et al., 2002; Gabay et al., 2018; Schoenberg and Trench, 1980). Gabay et al. specifically examined the recolonization patterns of symbionts within adult aposymbiotic Aiptasia to find that unsuccessful recolonizations fail from the beginning, and that those with competent but non-native symbionts *S. microadriaticum* and *D. trenchii* start slowly and take twice as long to recolonize hosts compared to recolonizations with native *B. minutum*. In our experiments, the majority of *D. trenchii* inoculations began substantial proliferation of symbiont clusters after three weeks, and only a handful of inoculations of *S. microadriaticum* proliferated with a similar pattern. These slower rates of colonization of a cnidarian host by non-native symbiont species have been observed in the colonization of aposymbiotic scyphozoan

Cassiopeia xamachana and *Cereus pedunculatus*, another sea anemone (Colley and Trench, 1983; Davy et al., 1997).

Effect of elevated heat stress on symbiont populations colonizing host tissue

The reduction of symbiont populations in Aiptasia as a result of increased temperature created consistent local symbiont cluster patterns across all symbiont inoculations, but differed in magnitude between hosts harboring native and non-native symbiont species. The pattern of symbiont cluster size reduction was the same across species, and it involved a rapid reduction in the size of symbiont clusters in host tentacles. The winnowing away of larger symbiont clusters may be a function of local tissue stress, which would result from local effects of reactive oxygen species production from both high algal densities and the host cells that contain these multiple algal cells (Hawkins and Davy, 2012; Lesser, 1996; Perez and Weis, 2006). As a consequence of environmental stress, there are many cellular mechanisms that may be acting to decrease symbiont density, including symbiont expulsion, host cell detachment, and apoptosis; however the prevalence and co-occurrence of these mechanisms are not clear (Gates et al., 1992; Weis, 2008). When inoculated Aiptasia were subjected to 32˚C, larger clusters left the host tissue after only one day (**Figure 4.4D**). During this timepoint, there was an unusual circulation of large symbiont clusters, evidenced by autofluorescence of the clusters, within the gastrovascular cavity of the column and tentacles (**Appendix C Figure C1**). These observations, coupled with the observed decrease in large clusters from the anemone tissue, suggests mechanisms such as host cell detachment or exocytosis. After this short period, the rapid disappearance of *B. minutum* singlet populations indicated the relatively poor tolerance of the *B. minutum* – Aiptasia symbiosis to heat stress.

In contrast to the poor resilience of native *B. minutum* populations to heat stress, *S. microadriaticum* and *D. trenchii* populations did not change in abundance as a result of heat stress, but instead remained at low population densities composed of singlet and doublet cells. The continued presence of these non-native species under elevated temperatures is consistent with their physiology in culture. These symbiont species differ significantly in their production of nitric oxide (NO) and tolerance to heat stress; *B. minutum* produces increased NO and experiences high photoinhibition under heat stress,

whereas *S. microadriaticum* is a much more thermally tolerant species (Hawkins and Davy, 2012). In addition, coral monitoring during elevated temperatures has shown that thermally tolerant symbiont species such as *D. trenchii* are able to opportunistically recolonize coral hosts during and after bleaching events (Berkelmans and van Oppen, 2006; Boulotte et al., 2016; Cunning et al., 2018; LaJeunesse et al., 2009). In Aiptasia, it appears that during ambient conditions, these opportunistic thermally tolerant symbionts are either unproductive or selfish, requiring hosts to upregulate their own catabolism of lipids and carbohydrates (Matthews et al., 2017, 2018). Host transcriptional responses also included upregulated innate immunity and stress pathways. The lower inoculation rates of *S. microadriaticum* and *D. trenchii* during ambient conditions supports these partnerships, and the lack of bleaching response during thermal stress supports their hypothesized role as opportunistic, weedy, and less-productive symbionts (Stat et al., 2008). Despite these thermal tolerant phenotypes, heterologous species seem to have limited colonization success when attempting inoculation during periods of thermal stress (Gabay et al., 2019). Further exploration is needed to better understand how thermal stress limits uptake of heterologous species but not their persistence within hosts.

Parsing the population dynamics of cluster growth vs. movement

Initial symbiont recolonization within Aiptasia has been described as a patchy process (Gabay et al., 2018), with a pattern characterized by small symbiont clusters appearing and locally proliferating in a stochastic nature along the length of a tentacle. In order to track this patterning, our study initially attempted to repeatedly image the exact same tentacles on inoculated Aiptasia. However, problems with rapid wound healing and tentacle movement during live imaging made this process impractical. Our study of cell populations therefore lacks the ability to trace cell origin, and although we have been able to label algal symbionts with fluorescent dye labels such as DiI and DiO, we have not been able to establish successful colonization with these fluorescently-labeled cells (**Appendix C Figure C2**). Despite this missing causative step in our studies of symbiont population dynamics, our results indicate that we need to account for cluster growth from at least two mechanisms: 1. individual local cluster proliferation and 2. either establishment of new symbiont clusters *via* the gastrovascular cavity, or migration of

symbiont-containing host cells within the gastroderm. The linear trend in cluster establishment periods is suggestive of continuous reuptake from the gastrovascular cavity during early recolonization, but further exploration is needed to determine the viability of exocytosed symbionts. Though migration of epidermal host cells can occur during cnidarian development and wound healing (Denker et al., 2008; DuBuc et al., 2014; Lecointe et al., 2016), symbiont-containing gastrodermal cells have not been tracked to determine if migration within the gastrodermis is a process that occurs during recolonization. Movement of symbionts certainly happens in the gastrodermis, especially under colonization or environmental perturbation (Santos et al., 2009), but whether this occurs within the gastrodermis or through the gastrovascular cavity remains unclear.

Benefits and limitations of using confocal vs epifluorescence microscopy to track symbiont population dynamics in Aiptasia

Imaging small Aiptasia using confocal microscopy provided highly accurate data within the first week of inoculation. By analyzing brightfield confocal Z-stacks, we were able to capture symbiont cell proliferation in hosts with high resolution. Despite this fidelity, imaging symbiont autofluorescence was slow and unreliable using this method. In general, confocal imaging took much longer than did epifluorescence imaging. In addition, repeated anesthetic $MgCl_2$ treatment for confocal imaging appeared detrimental to anemones. At the end of the experiment, $MgCl_2$-relaxed Aiptasia tentacles appeared to unhealthy as evidenced by permanently contracted tentacles columns (data not shown). Finally, manual counting of symbionts within brightfield image stacks was needed to quantify symbiont cluster number and size. Though manual counts provided accurate symbiont cluster data, after one week of symbiont recolonization the increased abundance of symbionts made counting infeasible without automation for groups of successfully colonized anemones.

Imaging the recolonization of Aiptasia by symbionts using epifluorescence microscopy provided consistent repeatable measurements across all samples. Animals were minimally disrupted during imaging; the brightfield and epifluorescence imaging process was rapid and samples experienced no photobleaching as a result of fluorescent excitation. Videos and their representative photo stacks did require considerable storage

space, however. Time-intensive steps occurred primarily during image analysis, specifically during image stitching into a single merged photo. Image analysis steps required thresholding and tentacle gating but was otherwise automated. In general, the collapse of 3D information into 2D information lost information on tentacle depth and likely resulted in overlap between symbiont clusters at higher symbiont densities during later weeks of recolonization. This method is therefore probably most useful during the initial few weeks of infection before cluster analysis of dense symbiont populations requires 3D imaging.

4.6 References

Belda-Baillie, C. A., Baillie, B. K., and Maruyama, T. (2002). Specificity of a Model Cnidarian-Dinoflagellate Symbiosis. *Biol. Bull.* 202, 74–85. doi:10.2307/1543224.

Berkelmans, R., and van Oppen, M. J. H. (2006). The role of zooxanthellae in the thermal tolerance of corals: a 'nugget of hope' for coral reefs in an era of climate change. *Proc. R. Soc. B Biol. Sci.* 273, 2305–2312. doi:10.1098/rspb.2006.3567.

Bieri, T., Onishi, M., Xiang, T., Grossman, A. R., and Pringle, J. R. (2016). Relative contributions of various cellular mechanisms to loss of algae during cnidarian bleaching. *PLoS ONE* 11, 1–24. doi:10.1371/journal.pone.0152693.

Boulotte, N. M., Dalton, S. J., Carroll, A. G., Harrison, P. L., Putnam, H. M., Peplow, L. M., et al. (2016). Exploring the Symbiodinium rare biosphere provides evidence for symbiont switching in reef-building corals. *ISME J.* 10, 2693–2701. doi:10.1038/ismej.2016.54.

Brown, B. E. (1997). Coral bleaching: causes and consequences. *Coral Reefs* 16, S129–S138. doi:10.1007/s003380050249.

Coffroth, M. A., Lewis, C. F., Santos, S. R., and Weaver, J. L. (2006). Environmental populations of symbiotic dinoflagellates in the genus Symbiodinium can initiate symbioses with reef cnidarians. *Curr. Biol.* 16, 985–987. doi:10.1016/j.cub.2006.10.049.

Colley, N. J., and Trench, R. K. (1983). Selectivity in Phagocytosis and Persistence of Symbiotic Algae by the Scyphistoma Stage of the Jellyfish Cassiopeia xamachana. *Proc. R. Soc. Lond. B Biol. Sci.* 219, 61–82.

Cunning, R., Silverstein, R. N., and Baker, A. C. (2018). Symbiont shuffling linked to differential photochemical dynamics of Symbiodinium in three Caribbean reef corals. *Coral Reefs* 37, 145–152. doi:10.1007/s00338-017-1640-3.

Davy, S. K., Allemand, D., and Weis, V. M. (2012). Cell Biology of Cnidarian-Dinoflagellate Symbiosis. *Microbiol. Mol. Biol. Rev.* 76, 229–261. doi:10.1128/MMBR.05014-11.

Davy, S. K., Lucas, I. a. N., and Turner, J. R. (1997). Uptake and Persistence of Homologous and Heterologous Zooxanthellae in the Temperate Sea Anemone Cereus pedunculatus (Pennant). *Biol. Bull.* 192, 208–216. doi:10.2307/1542715.

Denker, E., Manuel, M., Leclère, L., Le Guyader, H., and Rabet, N. (2008). Ordered progression of nematogenesis from stem cells through differentiation stages in the tentacle bulb of Clytia hemisphaerica (Hydrozoa, Cnidaria). *Dev. Biol.* 315, 99–113. doi:10.1016/j.ydbio.2007.12.023.

Detournay, O., Schnitzler, C. E., Poole, A., and Weis, V. M. (2012). Regulation of cnidarian–dinoflagellate mutualisms: Evidence that activation of a host TGFB innate immune pathway promotes tolerance of the symbiont. *Dev. Comp. Immunol.* 38, 525–537. doi:10.1016/j.dci.2012.08.008.

DuBuc, T. Q., Traylor-Knowles, N., and Martindale, M. Q. (2014). Initiating a regenerative response; cellular and molecular features of wound healing in the cnidarian Nematostella vectensis. *BMC Biol.* 12, 24. doi:10.1186/1741-7007-12-24.

Frieler, K., Meinshausen, M., Golly, A., Mengel, M., Lebek, K., Donner, S. D., et al. (2013). Limiting global warming to 2 °C is unlikely to save most coral reefs. *Nat. Clim. Change* 3, 165–170. doi:10.1038/nclimate1674.

Gabay, Y., Parkinson, J. E., Wilkinson, S. P., Weis, V. M., and Davy, S. K. (2019). Inter-partner specificity limits the acquisition of thermotolerant symbionts in a model cnidarian-dinoflagellate symbiosis. *IMSE J.*, 1. doi:10.1038/s41396-019-0429-5.

Gabay, Y., Weis, V. M., and Davy, S. K. (2018). Symbiont Identity Influences Patterns of Symbiosis Establishment, Host Growth, and Asexual Reproduction in a Model Cnidarian-Dinoflagellate Symbiosis. *Biol. Bull.* 234, 1–10. doi:10.1086/696365.

Gates, R. D., Baghdasarian, G., and Muscatine, L. (1992). Temperature stress causes host cell detachment in symbiotic cnidarians: implications for coral bleaching. *Biol. Bull.* 182, 324–332. doi:10.2307/1542252.

Hawkins, T. D., and Davy, S. K. (2012). Nitric oxide production and tolerance differ among symbiodinium types exposed to heat stress. *Plant Cell Physiol.* 53, 1889–1898. doi:10.1093/pcp/pcs127.

Hughes, T. P., Anderson, K. D., Connolly, S. R., Heron, S. F., Kerry, J. T., Lough, J. M., et al. (2018). Spatial and temporal patterns of mass bleaching of corals in the Anthropocene. *Science* 359, 80–83. doi:10.1126/science.aan8048.

LaJeunesse, T. C., Smith, R. T., Finney, J., and Oxenford, H. (2009). Outbreak and persistence of opportunistic symbiotic dinoflagellates during the 2005 Caribbean mass coral 'bleaching' event. *Proc. R. Soc. B Biol. Sci.* 276, 4139–4148. doi:10.1098/rspb.2009.1405.

Lecointe, A., Domart-coulon, I., Paris, A., and Meibom, A. (2016). Cell proliferation and migration during early development of a symbiotic scleractinian coral. *Proc. R. Soc. Lond. B* 283, 20160206. doi:10.1098/rspb.2016.0206.

Lesser, M. P. (1996). Elevated temperatures and ultraviolet radiation cause oxidative stress and inhibit photosynthesis in symbiotic dinoflagellates. *Limnol. Oceanogr.* 41, 271–283. doi:10.4319/lo.1996.41.2.0271.

Lin, K., Wang, J., and Fang, L.-S. (2000). Participation of Glycoproteins on Zooxanthellal Cell Walls in the Establishment of a Symbiotic Relationship with the Sea Anemone, Aiptasia pulchella. 39, 172–178.

Matthews, J. L., Crowder, C. M., Oakley, C. A., Lutz, A., Roessner, U., Meyer, E., et al. (2017). Optimal nutrient exchange and immune responses operate in partner specificity in the cnidarian-dinoflagellate symbiosis. *Proc. Natl. Acad. Sci. U. S. A.* 114, 13194–13199. doi:10.1073/pnas.1710733114.

Matthews, J. L., Oakley, C. A., Lutz, A., Hillyer, K. E., Roessner, U., Grossman, A. R., et al. (2018). Partner switching and metabolic flux in a model cnidarian–dinoflagellate symbiosis. *Proc. R. Soc. B Biol. Sci.* 285, 20182336. doi:10.1098/rspb.2018.2336.

Matthews, J. L., Sproles, A. E., Oakley, C. A., Grossman, A. R., Weis, V. M., and Davy, S. K. (2016). Menthol-induced bleaching rapidly and effectively provides experimental aposymbiotic sea anemones (Aiptasia sp.) for symbiosis investigations. *J. Exp. Biol.* 219, 306–310. doi:10.1242/jeb.128934.

Muscatine, L., and Porter, J. W. (1977). Reef Corals : Mutualistic Symbioses Adapted to Nutrient-Poor Environments. *BioScience* 27, 454–460. doi:10.2307/1297526.

Parkinson, J. E., Tivey, T. R., Mandelare, P. E., Adpressa, D. A., Loesgen, S., and Weis, V. M. (2018). Subtle Differences in Symbiont Cell Surface Glycan Profiles Do Not Explain Species-Specific Colonization Rates in a Model Cnidarian-Algal Symbiosis. *Front. Microbiol.* 9. doi:10.3389/fmicb.2018.00842.

Parrin, A. P., Goulet, T. L., Yaeger, M. A., Bross, L. S., McFadden, C. S., and Blackstone, N. W. (2016). Symbiodinium migration mitigates bleaching in three octocoral species. *J. Exp. Mar. Biol. Ecol.* 474, 73–80. doi:10.1016/j.jembe.2015.09.019.

Parrin, A. P., Harmata, K. L., Netherton, S. E., Yaeger, M. A., Bross, L. S., and Blackstone, N. W. (2012). Within-colony migration of symbionts during bleaching of octocorals. *Biol. Bull.* 223, 245–256.

Perez, S., and Weis, V. M. (2006). Nitric oxide and cnidarian bleaching: an eviction notice mediates breakdown of a symbiosis. *J. Exp. Biol.* 209, 2804–10. doi:10.1242/jeb.02309.

Rueden, C. T., Schindelin, J., Hiner, M. C., DeZonia, B. E., Walter, A. E., Arena, E. T., et al. (2017). ImageJ2: ImageJ for the next generation of scientific image data. *BMC Bioinformatics* 18. doi:10.1186/s12859-017-1934-z.

Santos, S. R., Toyoshima, J., and Kinzie III, R. A. (2009). Spatial and temporal dynamics of symbiotic dinoflagellates (Symbiodinium : Dinophyta) in the perforate coral Montipora capitata. 139–147.

Schindelin, J., Arganda-carreras, I., Frise, E., Kaynig, V., Longair, M., Pietzsch, T., et al. (2012). Fiji: an open-source platform for biological-image analysis. *Nat. Methods N. Y.* 9, 676–82. doi:http://dx.doi.org.ezproxy.proxy.library.oregonstate.edu/10.1038/nmeth.2019.

Schoenberg, D. A., and Trench, R. K. (1980). Genetic Variation in Symbiodinium (=Gymnodinium) microadriaticum Freudenthal, and Specificity in its Symbiosis with Marine Invertebrates. III. Specificity and Infectivity of Symbiodinium microadriaticum. *Proc. R. Soc. Lond. B Biol. Sci.* 207, 445–460.

Schwarz, J. A., Krupp, D. A., and Weis, V. M. (1999). Late larval development and onset of symbiosis in the scleractinian coral Fungia scutaria. *Biol. Bull.* 196, 70–79. doi:10.2307/1543169.

Stat, M., Morris, E., and Gates, R. D. (2008). Functional diversity in coral-dinoflagellate symbiosis. *Proc. Natl. Acad. Sci. U. S. A.* 105, 9256–61. doi:10.1073/pnas.0801328105.

Weis, V. M. (2008). Cellular mechanisms of Cnidarian bleaching: stress causes the collapse of symbiosis. *J. Exp. Biol.* 211, 3059–66. doi:10.1242/jeb.009597.

Weis, V. M., Davy, S. K., Hoegh-Guldberg, O., Rodriguez-Lanetty, M., and Pringle, J. R. (2008). Cell biology in model systems as the key to understanding corals. *Trends Ecol. Evol.* 23, 369–76. doi:10.1016/j.tree.2008.03.004.

Xiang, T., Hambleton, E. a., DeNofrio, J. C., Pringle, J. R., and Grossman, A. R. (2013). Isolation of clonal axenic strains of the symbiotic dinoflagellate Symbiodinium and their growth and host specificity 1. *J. Phycol.* 49, 447–458. doi:10.1111/jpy.12055.

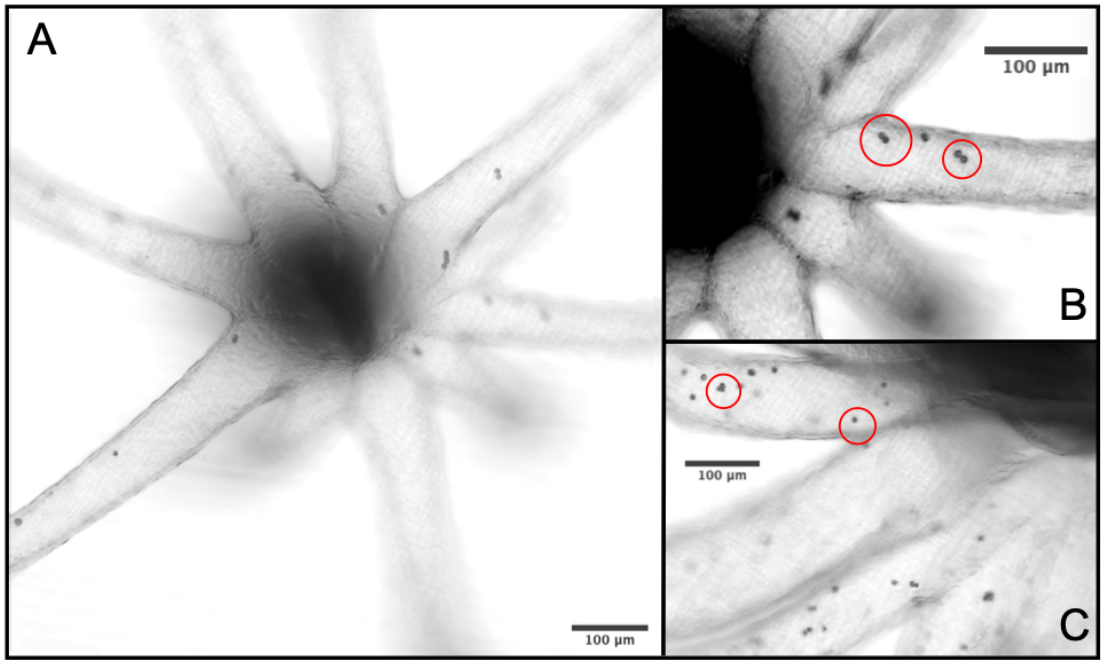

Figure 4.1 Colonization dynamics of *B. minutum* in Aiptasia polyps using confocal microscopy.
Aiptasia polyps (**A**) were imaged using confocal microscopy. Z-stack images were taken of the tentacles and column of Aiptasia host strains recolonized with *B. minutum*. Representative Z-sections are shown with examples of single cells, doublet cell, and triplet cell symbiont clusters circled in red (**B** and **C**).

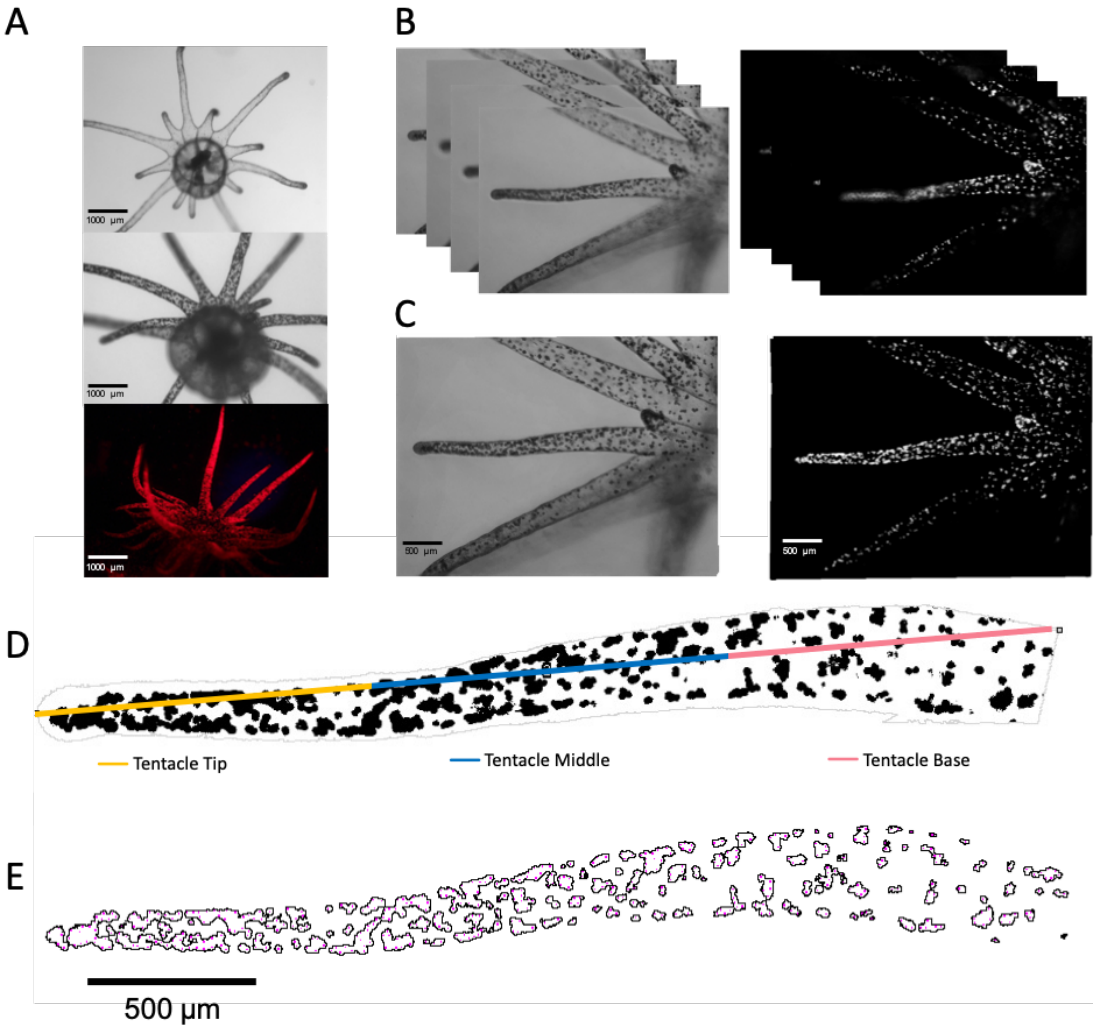

Figure 4.2 Colonization dynamics in Aiptasia polyps using epifluorescence microscopy.
Bleached Aiptasia polyps were colonized with algal symbionts over a period of four weeks and imaged (**A**) under brightfield and epifluorescence to track symbiont autofluorescence. Videos were taken as representative Z-stack images (**B**) under brightfield and laser excitation. Videos were merged into 2D images (**C**), and processed in Fiji (ImageJ2) to determine symbiont cluster location (**D**) and cluster size (**E**) within each tentacle.

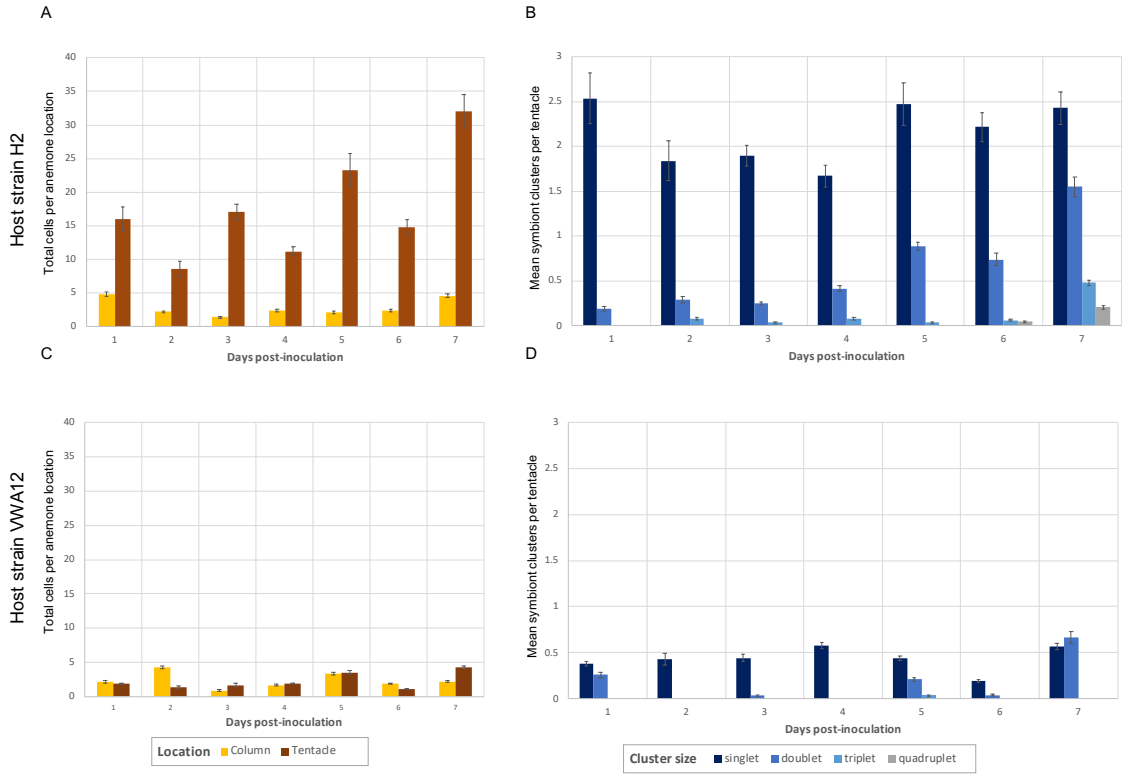

Figure 4.3 Native symbiont colonization in two host strains of Aiptasia.
The total number of colonizing symbionts were tracked within the tentacles and columns of tiny Aiptasia polyps with the genetic host strain background of H2 (**A**) and VWA12 (**C**) (n = 7 anemones per host strain). Aiptasia were inoculated with a concentration of 1 x 10^4 cells • mL^{-1}. Cluster sizes of singlets, doublets, triplets and quadruplets were tracked within tentacles to find mean cluster abundances over time in strains H2 (**B**) and VWA12 (**D**).

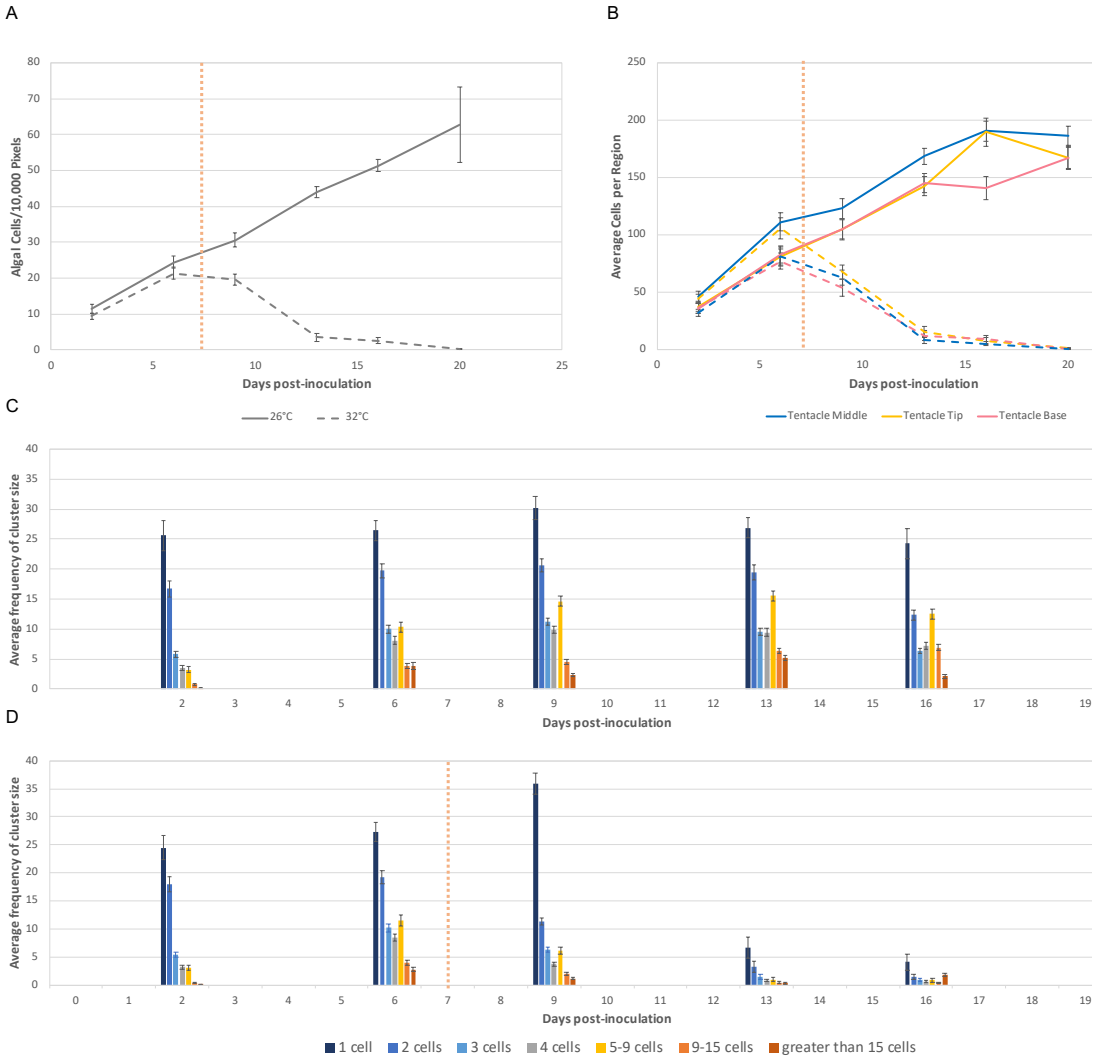

Figure 4.4 Native symbiont colonization in Aiptasia polyps during ambient and elevated temperature.
The relative density (**A**), abundance (**B**), and location (**B**) of symbiont cells was tracked over time in the tentacles of Aiptasia polyps under ambient and elevated temperature regimes (26˚C and 32˚C, respectively). Aiptasia were inoculated with a concentration of 5 x 10^4 cells • mL^{-1}. Initial movement of polyps to elevated temperature conditions for the 32˚C treatment is indicated by a vertical dotted line at 7 days post-inoculation (n = 24 anemones per treatment). The abundances of cell cluster sizes were monitored throughout the experiment in both ambient (**C**) and elevated (**D**) temperature treatments.

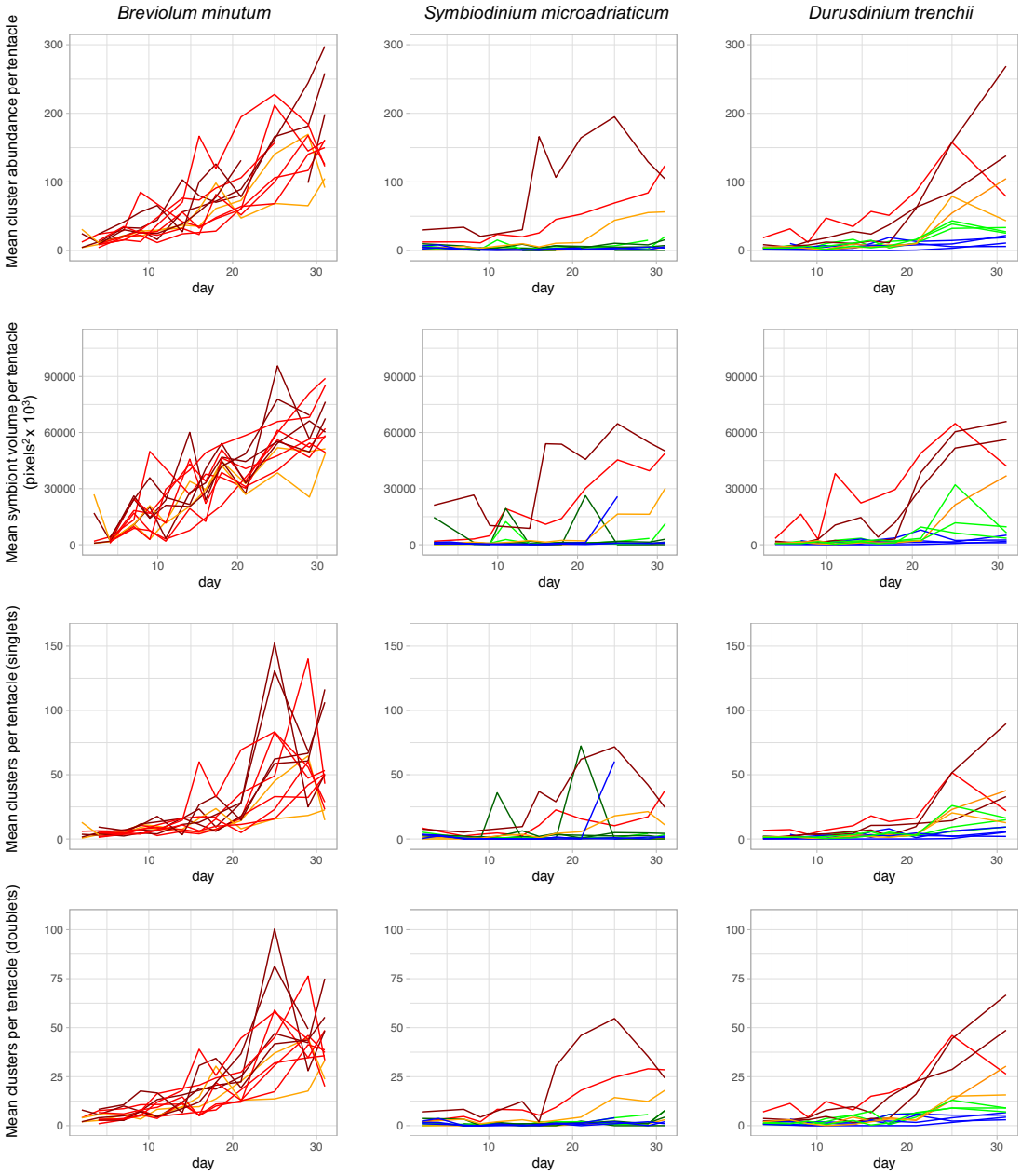

Figure 4.5 Colonization dynamics of native and non-native species in Aiptasia polyps under ambient temperature.

Bleached Aiptasia polyps were colonized with three species of algal symbionts: *B. minutum*, *S. microadriaticum*, and *D. trenchii*. Aiptasia were inoculated with a concentration of 5 x 10^5 cells • mL^{-1}. Mean cluster abundance and volume of symbiont occupation per tentacle was observed over four weeks. Clusters were groups according to size, only the abundances of singlets and doublets are shown in this figure. Colors are for sample visualization only, with red indicating increased colonization and blue indicating decreased colonization. Each line is representative of sample tentacle means from one anemone (n = 12 anemones per treatment).

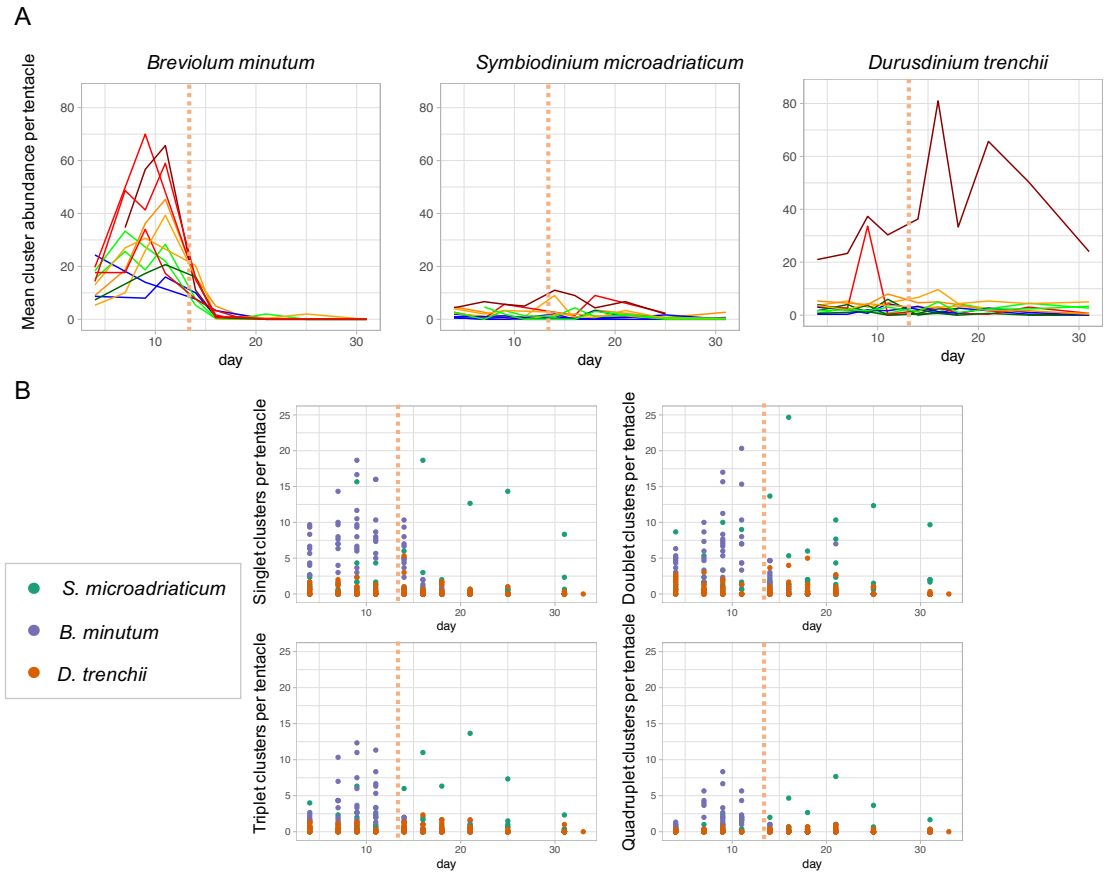

Figure 4.6: Colonization dynamics of native and non-native species in Aiptasia polyps under elevated temperature stress. After two weeks of colonization by one of three species of algal symbionts (B. minutum, S. microadriaticum, and D. trenchii), Aiptasia polyps were moved to constant elevated temperature of 32˚C. Mean cluster abundance (**A**) was observed over four weeks. Colors are for sample visualization only, with red indicating increased colonization and blue indicating decreased colonization. Each line is representative of sample tentacle means from one anemone (n = 12 anemones per treatment). Symbiont clusters were also analyzed according to size (**B**), with the abundances of the four most common groups (singlets, doublets, triplets, and quadruplets) shown across species for comparison. Each dot is representative of the sample tentacle mean from one anemone at an individual timepoint (n = 12 anemones per treatment). For all graphs, a vertical dotted line represents the beginning of elevated temperature treatment.

5. General conclusions and future directions

5.1 Summary of research

In the chapters and appendices of this dissertation I have provided experimental evidence that informs our understanding of the cellular regulation of symbioses. These results indicate that the many processes which govern symbiotic relationships are context-dependent. Symbiosis is a dynamic process, and we still have much to understand with respect to its regulation under different conditions. In this dissertation I revealed the importance of glycan complexity in symbiont recognition. I found evidence of coordination between local symbiont and host proliferation during colonization. In addition, I showed differences between multiple Symbiodiniaceae cell cycles in culture and *in hospite* under different nutritional states. I also examined the patterning of cell proliferation during colonization and bleaching, which revealed evidence of species specificity.

5.2 N-glycan complexity is utilized by hosts during symbiont uptake

In Chapter 2, I characterized and manipulated the N-glycan biosynthesis pathway within *Breviolum minutum*. I validated the importance of glycan abundance on symbiont uptake through specific enzymatic cleavage of N-glycans. I then found evidence of conservation in the N-glycan biosynthesis pathway in Symbiodiniacea species, but failed to find evidence of a Golgi alpha-Mannosidase II protein that was distinct from the putative Lysosomal alpha-mannosidase II protein. Despite this absence and the additional absence of MGAT2, Symbiodiniacea species retained nearly all other transferases. Symbiodiniaceae therefore appear to have the ability to produce both high-mannose and hybrid glycans. This biosynthesis pathway was successfully tested using an alpha-mannosidase I inhibitor, kifunensine, which blocked the creation of hybrid glycans and resulted in higher levels of high-mannose glycans on the cell surface. This increase in high-mannose was higher than the increase from mannosidase 2 inhibitor, swainsonine. Despite having an intermediate effect, we were not able to directly show that swainsonine

treatment resulted in predominantly hybrid glycans. It is possible that swainsonine treatment also blocked the lysosomal alpha-mannosidase but because of the lack of consistent phenotype the effect of swainsonine on Symbiodiniaceae cultures remains unclear. The uptake of symbionts from kifunensine treated cultures was significantly lower than the uptake of untreated cells. Simplified high-mannose glycomes appear to impact colonization at a level similar to total N-glycan removal. It therefore appears that the abundance and complexity of N-glycans equally matters during symbiont recognition and uptake.

5.3 Evidence of regulation in host and symbiont proliferation

In Chapter 3 and the appendices I teased apart the relationships between symbionts and their host cells during periods of different symbiotic and nutritional states. I found evidence for coordination between the cell proliferation of hosts and symbionts that depends on symbiotic state, probably due to space availability. Host and symbiont cells proliferate in coordination during initial colonization in localized tissue areas. This host cell proliferation during colonization is more abundant than host proliferation found in the aposymbiotic host tissue regions of partially symbiotic and aposymbiotic anemones. In comparisons between colonizing symbiotic and aposymbiotic hosts, proliferative nuclei shift median tissue locations. Aposymbiotic hosts have increased proliferation within the epidermis, whereas symbiotic hosts have increased proliferation within the gastrodermis.

When hosts and symbionts are in a stable symbiosis (See Appendix D), there is stronger evidence for pre-mitotic regulation. Fully symbiotic hosts experience decreased proliferative populations compared to aposymbiotic hosts. Nutrition has little effect on these proliferative populations in the gastrodermis. Despite this lower amount of proliferation, host cells in symbiotic hosts appear to significantly grow in size in response to added nutrients. The cell cycles of symbionts responded much more directly to feeding, starvation, and nitrogen limitation. Cell cycles in culture exhibited low G_2M-phase populations under starvation, and wider G_1-phase CVs under nitrogen limitation. *In hospite*, symbiont cell cycles also had low G_2M-phase populations but much higher S-phase populations compared to their respective cultures. In addition, there were species-

specific differences; *B. psygmophilum* exhibited increased S-phase populations *in hospite* compared to *B. minutum* populations. These differences in symbiont cell cycle and proliferation were demonstrated in competition in culture and *in hospite*. Under fed conditions, *B. minutum* cell populations appeared to be more competitive compared to *B. minutum* populations, based on the populations of representative cells. Starvation had a stronger impact on *B. psygmophilum* than *B. minutum*. These cell cycle differences in response to nutrition may be evolutionarily linked to the nutritional differences between the temperate and tropical locations from which each Symbiodiniaceae species is found.

5.4 Symbiont population dynamics during colonization and thermal stress

In Chapter 4 I undertook a series of experiments to design and implement a fast and noninvasive method to capture symbiont population dynamics within the Aiptasia host. Successful colonization of hosts within the first week was composed of both sustained inoculation from circulating symbionts and also doublet formation through symbiont proliferation within the tissue. Proliferation of symbionts within the tentacles specifically was critical to overall symbiont colonization. After establishment of symbiosis, the introduction of heat stress affected predominantly larger clusters of symbionts within colonizing tissue. These proliferation and colonization patterns were dependent on the species of symbiont. Different symbiont species colonized Aiptasia tentacles with different success rates. Homologous symbionts resulted in the most consistent successful establishment of symbiosis, whereas heterologous symbiont species either were successful immediately or more often took a while to establish even low levels of colonization. Despite the variation in inoculation with heterologous symbiont species, these non-native Symbiodiniaceae species persisted longer at low levels under heat stress compared to more thermally sensitive homologous symbionts.

5.5 Future Research

Chapter 2: Future directions for glycan work

The conclusions of Chapter 2 support the role of both glycan abundance and complexity in host-symbiont interactions during symbiont recognition and uptake. More

specific interrogation of glycan-lectin interactions is required to isolate the multiple functions of Symbiodiniaceae glycan complexity. There are many tools available for characterizing the variation and binding affinities of glycans, including lectin microarrays and mass spectrometry (Cummings and Pierce, 2014; Paulson et al., 2006). The use of mass spectrometry and confirmation from lectin probes has the potential to further reveal the diversity and abundance of specific glycan structures on a variety of Symbiodiniaceae species. The comparison of Symbiodiniaceae species to other dinoflagellates also may reveal differences in cell surface glycans and possibly glycan biosynthesis. The data collected from this chapter and from previous studies provide limited evidence for complex glycans in Symbiodiniaceae, and the presence of glycan modification such as sialic acid needs to be further investigated (Lin et al., 2015; Logan et al., 2010; Parkinson et al., 2018; Stephens et al., 2018). Specific glycosidic linkages can be targeted using either enzymes or even addition of synthetic derivatives to understand glycan biosynthesis and cell surface glycan processes. Further research should also address the recognition pathways of host lectins. Targeted host gene expression studies may be able to be combined with symbiont glycan manipulation to disentangle the molecular pathways involved in recognition and uptake processes of cnidarian-dinoflagellate symbiosis. Finally, the glycans present on host membrane proteins have not been properly examined, and characterization of the host glycome may reveal function during the recognition of symbionts.

Chapter 3: Future directions for cell cycle regulation and proliferation

This dissertation has demonstrated that the evidence for coordinated local proliferation in cnidarians exists, however we still lack information on cell-cell interactions at a cellular level. Cell maceration and cell sorting offer an avenue to examine host and symbiont cell cycles on a single-cell scale, possibly together. This would provide us with a much more complete understanding of the regulation of cell cycles within cnidarian-dinoflagellate symbiosis. Tied to these cellular and physiological studies needs to be molecular characterization. Transcriptional regulation of genes is central to the regulation of proliferation, and so future research would benefit from examining the activity of transcription factors and state of chromatin, as well as the gene

expression of cyclins, cyclin-dependent kinases, and growth factors. We also are missing information about the duration of cell cycles and the variety of host cell types. Pulse-chase labeling with multiple fluorescent indicators would enable such measurement and hopefully help identify different cell types and their turnover rates. In addition, the concurrent measurement of apoptosis would also help to understand the regulation of host cells and their symbionts under different environmental conditions.

Chapter 4: Future directions for the imaging of colonization and symbiont proliferation

The current protocol developed in Chapter 4 of this thesis is a useful, noninvasive, and inexpensive imaging method that can be used alongside many types of Aiptasia experiments. The protocol images sample tentacles in the same host over many weeks, and there is some information lost by not imaging the entire anemone. Imaging whole anemones required more time-intensive reconstruction of photographs and lowered the quality of autofluorescence signal when using a wider 5x objective. In addition, 3D reconstruction from manually captured videos results in dramatic loss in quality compared to slower Z-stack capture from confocal imaging, which can only be done well if the cnidarian host is properly anaesthetized. Future studies can take advantage of faster imaging capture of newer microscope technology. For example, light sheet microscopy enables a much more complete picture of spatial and temporal organization of microbial communities (Strobl et al., 2017; Taormina et al., 2012).

The colonization experiments from Chapter 4 presented an additional important limitation: the past locations of symbionts in a tentacle could not readily be identified. The study lacks symbiont colonization history that could enable us to show how new clusters form, how older clusters proliferate, and if there are certain patterns of symbiont migration or reuptake into host gastrodermal tissue. Currently the only method of tracking Symbiodiniaceae within host is through genotyping *via* qPCR (Gabay et al., 2019). Attempts at labeling Symbiodiniaceae with CM-DiI, DiI, and DiO have been marginally successful, but there has been no success imaging uptake of labeled cells. Despite this limited success, there is still a need for competitive cellular assays to help understand how host-symbiont specificity plays a role in symbiont colonization. Other

live cell tracker dyes or genetic transformation of Symbiodiniaceae provides a way forward to create hypothesis-testing experiments on the subject of symbiont colonization.

5.6 Conclusions

In summary, the work presented here focused on the cellular regulation of symbiosis and provides a platform for further exploration. Looking forward, future directions for this work would benefit from the unification of cellular and molecular experiments in order to better understand the molecular pathways of both partners that provide the cellular phenotypes measured in this study. With the development of predictable larval reproduction, future studies have the ability to compare the processes of larval colonization and adult recolonization to examine the relative contributions of pathways involved in the establishment of symbiosis (Grawunder et al., 2015; Hambleton et al., 2014; Wolfowicz et al., 2016). The genetic transformation of Aiptasia and *B. minutum* is also on the horizon. These new methods will provide a mechanistic approach to understanding these basic questions of symbiosis emphasized within this dissertation.

5.7 Bibliography

Cummings, R. D., and Pierce, J. M. (2014). The Challenge and Promise of Glycomics. *Chem. Biol.* 21, 1–15. doi:10.1016/j.chembiol.2013.12.010.

Gabay, Y., Parkinson, J. E., Wilkinson, S. P., Weis, V. M., and Davy, S. K. (2019). Inter-partner specificity limits the acquisition of thermotolerant symbionts in a model cnidarian-dinoflagellate symbiosis. *IMSE J.*, 1. doi:10.1038/s41396-019-0429-5.

Grawunder, D., Hambleton, E. A., Bucher, M., Wolfowicz, I., Bechtoldt, N., and Guse, A. (2015). Induction of Gametogenesis in the Cnidarian Endosymbiosis Model Aiptasia sp. *Sci. Rep.* 5, 15677. doi:10.1038/srep15677.

Hambleton, E. a, Guse, A., and Pringle, J. R. (2014). Similar specificities of symbiont uptake by adults and larvae in an anemone model system for coral biology. *J. Exp. Biol.* 217, 1613–9. doi:10.1242/jeb.095679.

Lin, S., Cheng, S., Song, B., Zhong, X., Lin, X., Li, W., et al. (2015). The Symbiodinium kawagutii genome illuminates dinoflagellate gene expression and coral symbiosis. *Science* 350, 691–694. doi:10.1126/science.aad0408.

Logan, D. D. K., LaFlamme, A. C., Weis, V. M., and Davy, S. K. (2010). Flow-Cytometric Characterization of the Cell-Surface Glycans of Symbiotic Dinoflagellates (Symbiodinium Spp.)1. *J. Phycol.* 46, 525–533. doi:10.1111/j.1529-8817.2010.00819.x.

Parkinson, J. E., Tivey, T. R., Mandelare, P. E., Adpressa, D. A., Loesgen, S., and Weis, V. M. (2018). Subtle Differences in Symbiont Cell Surface Glycan Profiles Do Not Explain Species-Specific Colonization Rates in a Model Cnidarian-Algal Symbiosis. *Front. Microbiol.* 9. doi:10.3389/fmicb.2018.00842.

Paulson, J. C., Blixt, O., and Collins, B. E. (2006). Sweet spots in functional glycomics. *Nat. Chem. Biol.* 2, 238–248. doi:10.1038/nchembio785.

Stephens, T. G., Ragan, M. A., Bhattacharya, D., and Chan, C. X. (2018). Core genes in diverse dinoflagellate lineages include a wealth of conserved dark genes with unknown functions. *Sci. Rep.* 8. doi:10.1038/s41598-018-35620-z.

Strobl, F., Schmitz, A., and Stelzer, E. H. K. (2017). Improving your four-dimensional image: traveling through a decade of light-sheet-based fluorescence microscopy research. *Nat. Protoc.* 12, 1103–1109. doi:10.1038/nprot.2017.028.

Taormina, M. J., Jemielita, M., Stephens, W. Z., Burns, A. R., Troll, J. V., Parthasarathy, R., et al. (2012). Investigating Bacterial-Animal Symbioses with Light Sheet Microscopy. *Biol. Bull.* 223, 7–20. doi:10.1086/BBLv223n1p7.

Wolfowicz, I., Baumgarten, S., Voss, P. A., Hambleton, E. A., Voolstra, C. R., Hatta, M., et al. (2016). Aiptasia sp. larvae as a model to reveal mechanisms of symbiont selection in cnidarians. *Sci. Rep.* 6. doi:10.1038/srep32366.

6. Combined Bibliography

Ainsworth, T. D., Heron, S. F., Ortiz, J. C., Mumby, P. J., Grech, A., Ogawa, D., et al. (2016). Climate change disables coral bleaching protection on the Great Barrier Reef. *Science* 352, 338–342. doi:10.1017/CBO9781107415324.004.

Aranda, M., Li, Y., Liew, Y. J., Baumgarten, S., Simakov, O., Wilson, M. C., et al. (2016). Genomes of coral dinoflagellate symbionts highlight evolutionary adaptations conducive to a symbiotic lifestyle. *Scientific Reports* 6, 39734. doi:10.1038/srep39734.

Baddeley, A., Rubak, E., and Turner, R. (2015). *Spatial Point Patterns: Methodology and Applications with R*. Boca Raton: Chapman & Hall/CRC Press doi:10.18637/jss.v075.b02.

Baghdasarian, G., and Muscatine, L. (2000a). Preferential expulsion of dividing algal cells as a mechanism for regulating algal-cnidarian symbiosis. *The Biological bulletin* 199, 278–86.

Baghdasarian, G., and Muscatine, L. (2000b). Preferential expulsion of dividing algal cells as a mechanism for regulating algal-cnidarian symbiosis. *The Biological bulletin* 199, 278–86.

Baker, A. C. (2003). Flexibility and specificity in coral-algal symbiosis: Diversity, ccology , and biogeography of Symbiodinium. *Annual Review of Ecology, Evolution, and Systematics* 34, 661–689. doi:10.1146/132417.

Baker, A. C., Glynn, P. W., and Riegl, B. (2008). Climate change and coral reef bleaching: An ecological assessment of long-term impacts, recovery trends and future outlook. *Estuarine, Coastal and Shelf Science* 80, 435–471. doi:10.1016/j.ecss.2008.09.003.

Barbier, M., Géraud, M. L., Nicolas, G., and Soyer-Gobillard, M. O. (1998). Colocalization of the cyclin B homologue P56 and β-tubulin during the cell cycle in a unicellular eucaryote dinoflagellate. *Biology of the Cell* 90, 63–76. doi:10.1016/S0248-4900(98)80233-5.

Baum, L. G., Garner, O. B., Schaefer, K., and Lee, B. (2014). Microbe-host interactions are positively and negatively regulated by galectin-glycan interactions. *Frontiers in Immunology* 5, 1–8. doi:10.3389/fimmu.2014.00284.

Baumgarten, S., Simakov, O., Esherick, L. Y., Liew, Y. J., Lehnert, E. M., Michell, C. T., et al. (2015a). The genome of Aiptasia , a sea anemone model for coral symbiosis. *Proceedings of the National Academy of Sciences* 112, 201513318. doi:10.1073/pnas.1513318112.

Baumgarten, S., Simakov, O., Esherick, L. Y., Liew, Y. J., Lehnert, E. M., Michell, C. T., et al. (2015b). The genome of Aiptasia , a sea anemone model for coral symbiosis. *Proceedings of the National Academy of Sciences* 112, 11893–11898. doi:10.1073/pnas.1513318112.

Bay, L. K., Cumbo, V. R., Abrego, D., Kool, J. T., Ainsworth, T. D., and Willis, B. L. (2011). Infection Dynamics Vary between Symbiodinium Types and Cell Surface Treatments during Establishment of Endosymbiosis with Coral Larvae. *Diversity* 3, 356–374. doi:10.3390/d3030356.

Belda-Baillie, C. A., Baillie, B. K., and Maruyama, T. (2002). Specificity of a Model Cnidarian-Dinoflagellate Symbiosis. *The Biological Bulletin* 202, 74–85. doi:10.2307/1543224.

Bennett, G. M., and Moran, N. A. (2015). Heritable symbiosis: The advantages and perils of an evolutionary rabbit hole. *Proceedings of the National Academy of Sciences* 112, 10169–10176. doi:10.1073/pnas.1421388112.

Berkelmans, R., and van Oppen, M. J. H. (2006). The role of zooxanthellae in the thermal tolerance of corals: a 'nugget of hope' for coral reefs in an era of climate change. *Proceedings of the Royal Society B: Biological Sciences* 273, 2305–2312. doi:10.1098/rspb.2006.3567.

Berthelier, J., Schnitzler, C. E., Wood-Charlson, E. M., Poole, A. Z., Weis, V. M., and Detournay, O. (2017). Implication of the host TGFB pathway in the onset of symbiosis between larvae of the coral Fungia scutaria and the dinoflagellate Symbiodinium sp. (clade C1f). *Coral Reefs* 36, 1263–1268. doi:10.1007/s00338-017-1621-6.

Bhaud, Y., Barbier, M., and Soyer-Gobillard, M. O. (1994). A detailed study of the complex cell cycle of the dinoflagellate Crypthecodinium cohnii Biecheler and evidence for variation in histone H1 kinase activity. *Journal of Eukaryotic Microbiology* 41, 519–526.

Bhaud, Y., Guillebault, D., Lennon, J., Defacque, H., Soyer-Gobillard, M. O., and Moreau, H. (2000). Morphology and behaviour of dinoflagellate chromosomes during the cell cycle and mitosis. *Journal of cell science* 113, 1231–1239.

Bhaud, Y., Salmon, J., and Soyer-Gobillard, M. (1991). The complex cell cycle of the dinoflagellate protoctist Crypthecodinium cohnii as studied in vivo and by cytofluorimetry. *Journal of Cell Science* 100, 675–682.

Bieri, T., Onishi, M., Xiang, T., Grossman, A. R., and Pringle, J. R. (2016). Relative contributions of various cellular mechanisms to loss of algae during cnidarian bleaching. *PLoS ONE* 11, 1–24. doi:10.1371/journal.pone.0152693.

Bodansky, S., Mintz, L. B., and Holmes, D. S. (1979). The mesokaryote Gyrodinium cohnii lacks nucleosomes. *Biochemical and Biophysical Research Communications* 88, 1329–1336. doi:10.1016/0006-291X(79)91126-4.

Bolte, S., and Cordelieres, F. P. (2006). A guided tour into subcellular colocalization analysis in light microscopy. *Journal of Microscopy* 224, 213–232.

Bosch, T. C., and David, C. N. (1984). Growth regulation in Hydra: relationship between epithelial cell cycle length and growth rate. *Developmental biology* 104, 161–171. doi:10.1016/0012-1606(84)90045-9.

Bosch, T. C. G. (2013). Cnidarian-microbe interactions and the origin of innate immunity in metazoans. *Annual review of microbiology* 67, 499–518. doi:10.1146/annurev-micro-092412-155626.

Bouligand, Y., and Norris, V. (2001). Chromosome separation and segregation in dinoflagellates and bacteria may depend on liquid crystalline states. *Biochimie* 83, 187–192. doi:10.1016/S0300-9084(00)01211-6.

Boulotte, N. M., Dalton, S. J., Carroll, A. G., Harrison, P. L., Putnam, H. M., Peplow, L. M., et al. (2016). Exploring the Symbiodinium rare biosphere provides evidence for symbiont switching in reef-building corals. *The ISME Journal* 10, 2693–2701. doi:10.1038/ismej.2016.54.

Brown, B. E. (1997). Coral bleaching: causes and consequences. *Coral Reefs* 16, S129–S138. doi:10.1007/s003380050249.

Brown, B. E., Le Tissier, M. D. A., and Bythell, J. C. (1995). Mechanisms of bleaching deduced from histological studies of reef corals sampled during a natural bleaching event. *Marine Biology* 122, 655–663. doi:10.1007/BF00350687.

Bushkin, G. G., Ratner, D. M., Cui, J., Banerjee, S., Duraisingh, M. T., Jennings, C. V., et al. (2010). Suggestive evidence for Darwinian selection against asparagine-linked glycans of Plasmodium falciparum and Toxoplasma gondii. *Eukaryotic Cell* 9, 228–241. doi:10.1128/EC.00197-09.

Carpenter, K. E., Abrar, M., Aeby, G., Aronson, R. B., Banks, S., Bruckner, A., et al. (2008). One-Third of Reef-Building Corals Face Elevated Extinction Risk from Climate Change and Local Impacts. *Science* 321, 560–563. doi:10.1126/science.1159196.

Cavanaugh, C. M., Gardiner, S. L., Jones, M. L., Jannasch, H. W., and Waterbury, J. B. (1981). Prokaryotic Cells in the Hydrothermal Vent Tube Worm Riftia pachyptila Jones: Possible Chemoautotrophic Symbionts. *Science* 213, 340–342.

Chaves-Fonnegra, A., Riegl, B., Zea, S., Lopez, J. V., Smith, T., Brandt, M., et al. (2018). Bleaching events regulate shifts from corals to excavating sponges in algae-dominated reefs. *Global Change Biology* 24, 773–785. doi:10.1111/gcb.13962.

Chu, H., and Mazmanian, S. K. (2013). Innate immune recognition of the microbiota promotes host-microbial symbiosis. *Nat Immunol* 14, 668–675. doi:10.1038/ni.2635.

Coffroth, M. A., Lewis, C. F., Santos, S. R., and Weaver, J. L. (2006). Environmental populations of symbiotic dinoflagellates in the genus Symbiodinium can initiate symbioses with reef cnidarians. *Current Biology* 16, 985–987. doi:10.1016/j.cub.2006.10.049.

Colley, N. J., and Trench, R. K. (1983). Selectivity in Phagocytosis and Persistence of Symbiotic Algae by the Scyphistoma Stage of the Jellyfish Cassiopeia xamachana. *Proceedings of the Royal Society of London. Series B, Biological Sciences* 219, 61–82.

Collins, B. E., and Paulson, J. C. (2004). Cell surface biology mediated by low affinity multivalent protein–glycan interactions. *Current Opinion in Chemical Biology* 8, 617–625. doi:10.1016/j.cbpa.2004.10.004.

Cook, C. B., D'Elia, C. F., and Muller-Parker, G. (1988). Host feeding and nutrient sufficiency for zooxanthellae in the sea anemone Aiptasia pallida. *Marine Biology* 98, 253–262. doi:10.1007/BF00391203.

Cook, C. B., Muller-Parker, G., and Orlandini, C. D. (1994). Ammonium enhancement of dark carbon fixation and nitrogen limitation in zooxanthellae symbiotic with the reef corals Madracis mirabilis and Montastrea annularis. *Marine Biology* 118, 157–165. doi:10.1007/BF00699230.

Cummings, R. D., and Pierce, J. M. (2014). The Challenge and Promise of Glycomics. *Chemistry & Biology* 21, 1–15. doi:10.1016/j.chembiol.2013.12.010.

Cunning, R., Silverstein, R. N., and Baker, A. C. (2018). Symbiont shuffling linked to differential photochemical dynamics of Symbiodinium in three Caribbean reef corals. *Coral Reefs* 37, 145–152. doi:10.1007/s00338-017-1640-3.

Dagenais-Bellefeuille, S., and Morse, D. (2013). Putting the N in dinoflagellates. *Frontiers in microbiology* 4, 369. doi:10.3389/fmicb.2013.00369.

Dani, V., Priouzeau, F., Pagnotta, S., and Carette, D. (2016). Thermal and menthol stress induce different cellular events during sea anemone bleaching. *Symbiosis*. doi:10.1007/s13199-016-0406-y.

Darzynkiewicz, Z., Bruno, S., Del Bino, G., Gorczyca, W., Hotz, M. A., Lassota, P., et al. (1992). Features of apoptotic cells measured by flow cytometry. *Cytometry* 13, 795–808. doi:10.1002/cyto.990130802.

Darzynkiewicz, Z., Halicka, H. D., and Zhao, H. (2010). Analysis of Cellular DNA Content by Flow and Laser Scanning Cytometry. *Adv Exp Med Biol* 676, 137–147.

David, C. N., and Campbell, R. D. (1972). Cell cycle kinetics and development of Hydra attenuata. *Journal of cell science* 11, 557–568.

Davidson, E. A., and Gowda, D. C. (2001). Glycobiology of Plasmodium falciparum. *Biochimie* 83, 601–604. doi:10.1016/S0300-9084(01)01316-5.

Davy, S. K., Allemand, D., and Weis, V. M. (2012). Cell Biology of Cnidarian-Dinoflagellate Symbiosis. *Microbiology and Molecular Biology Reviews* 76, 229–261. doi:10.1128/MMBR.05014-11.

Davy, S. K., Lucas, I. a. N., and Turner, J. R. (1997). Uptake and Persistence of Homologous and Heterologous Zooxanthellae in the Temperate Sea Anemone Cereus pedunculatus (Pennant). *The Biological Bulletin* 192, 208–216. doi:10.2307/1542715.

Davy, S. K., Withers, K. J. T., and Hinde, R. (2006). Effects of host nutritional status and seasonality on the nitrogen status of zooxanthellae in the temperate coral Plesiastrea versipora (Lamarck). *Journal of Experimental Marine Biology and Ecology* 335, 256–265. doi:10.1016/j.jembe.2006.03.019.

del C. Gomez-Cabrera, M., Ortiz, J. C., Loh, W. K. W., Ward, S., and Hoegh-Guldberg, O. (2008). Acquisition of symbiotic dinoflagellates (Symbiodinium) by juveniles of the coral Acropora longicyathus. *Coral Reefs* 27, 219–226. doi:10.1007/s00338-007-0315-x.

Denker, E., Manuel, M., Leclère, L., Le Guyader, H., and Rabet, N. (2008). Ordered progression of nematogenesis from stem cells through differentiation stages in the tentacle bulb of Clytia hemisphaerica (Hydrozoa, Cnidaria). *Developmental Biology* 315, 99–113. doi:10.1016/j.ydbio.2007.12.023.

Detournay, O., Schnitzler, C. E., Poole, A., and Weis, V. M. (2012). Regulation of cnidarian–dinoflagellate mutualisms: Evidence that activation of a host TGFB innate immune pathway promotes tolerance of the symbiont. *Developmental and Comparative Immunology* 38, 525–537. doi:10.1016/j.dci.2012.08.008.

Di Tommaso, P., Moretti, S., Xenarios, I., Orobitg, M., Montanyola, A., Chang, J.-M., et al. (2011). T-Coffee: a web server for the multiple sequence alignment of protein and RNA sequences using structural information and homology extension. *Nucleic Acids Res* 39, W13–W17. doi:10.1093/nar/gkr245.

Dimond, J., and Carrington, E. (2008). Symbiosis regulation in a facultatively symbiotic temperate coral: zooxanthellae division and expulsion. *Coral Reefs* 27, 601–604. doi:10.1007/s00338-008-0363-x.

Dimond, J. L., Holzman, B. J., and Bingham, B. L. (2012). Thicker host tissues moderate light stress in a cnidarian endosymbiont. *Journal of Experimental Biology* 215, 2247–2254. doi:10.1242/jeb.067991.

Dimond, J. L., Pineda, R. R., Ramos-Ascherl, Z., and Bingham, B. L. (2013). Relationships between host and symbiont cell cycles in sea anemones and their symbiotic dinoflagellates. *The Biological bulletin* 225, 102–12.

Domotor, S. L., and D'Elia, C. F. (1984). Nutrient uptake kinetics and growth of zooxanthellae maintained in laboratory culture. *Marine Biology* 80, 93–101. doi:10.1007/BF00393132.

Domotor, S. L., and D'Elia, C. F. (1986). Cell-size distributions of zooxanthellae in culture and symbiosis. *The Biological Bulletin* 170, 519–525. doi:10.2307/1541859.

Dorling, P. R., Huxtable, C. R., and Colegate, S. M. (1980). Inhibition of lysosomal alpha-mannosidase by swainsonine, an indolizidine alkaloid isolated from Swainsona canescens. *The Biochemical journal* 191, 649–651. doi:10.1042/BJ1910649.

Douglas, A. E. (2010). *The symbiotic habit*. Princeton University Press.

Douglas, A., and Smith, D. (1984). The green hydra symbiosis. VIII. Mechanisms in symbiont regulation. *Proceedings of the Royal Society B: Biological Sciences* 221, 291–319.

Drew, E. A. (1972). The biology and physiology of alga-invertebrate symbioses. II. The density of symbiotic algal cells in a number of hermatypic hard corals and alcyonarians from various depths. *Journal of Experimental Marine Biology and Ecology* 9, 71–75.

DuBuc, T. Q., Traylor-Knowles, N., and Martindale, M. Q. (2014). Initiating a regenerative response; cellular and molecular features of wound healing in the cnidarian Nematostella vectensis. *BMC Biology* 12, 24. doi:10.1186/1741-7007-12-24.

Dunn, S. R. (2009). Immunorecognition and immunoreceptors in the Cnidaria. *Invertebrate Survival Journal* 6, 7–14.

Dunn, S. R., Bythell, J. C., Le Tissier, M. D. A., Burnett, W. J., and Thomason, J. C. (2002). Programmed cell death and cell necrosis activity during hyperthermic stress-induced bleaching of the symbiotic sea anemone Aiptasia sp. *Journal of*

Experimental Marine Biology and Ecology 272, 29–53. doi:10.1016/S0022-0981(02)00036-9.

Dunn, S. R., Schnitzler, C. E., and Weis, V. M. (2007). Apoptosis and autophagy as mechanisms of dinoflagellate symbiont release during cnidarian bleaching: every which way you lose. *Proceedings of the Royal Society B: Biological Sciences* 274, 3079–3085. doi:10.1098/rspb.2007.0711.

Dunn, S. R., and Weis, V. M. (2009). Apoptosis as a post-phagocytic winnowing mechanism in a coral-dinoflagellate mutualism. *Environmental microbiology* 11, 268–76. doi:10.1111/j.1462-2920.2008.01774.x.

Elbein, A. D., Tropea, J. E., Mitchell, M., and Kaushal, G. P. (1990). Kifunensine, a potent inhibitor of the glycoprotein processing mannosidase I. *J. Biol. Chem.* 265, 15599–15605.

Fabre, C., Causse, H., Mourey, L., Koninkx, J., Rivière, M., Hendriks, H., et al. (1998). Characterization and sugar-binding properties of arcelin-1, an insecticidal lectin-like protein isolated from kidney bean (Phaseolus vulgaris L. cv. RAZ-2) seeds. *Biochem J* 329, 551–560.

Fairclough, S. R., Dayel, M. J., and King, N. (2010). Multicellular development in a choanoflagellate. *Current Biology* 20, 875–876. doi:10.1016/j.cub.2010.09.014.References.

Fauquenoy, S., Morelle, W., Hovasse, A., Bednarczyk, A., Slomianny, C., Schaeffer, C., et al. (2008). Proteomics and Glycomics Analyses of N-Glycosylated Structures Involved in Toxoplasma gondii-Host Cell Interactions. *Molecular & Cellular Proteomics* 7, 891–910. doi:10.1074/mcp.M700391-MCP200.

Fingar, D. C., and Blenis, J. (2004). Target of rapamycin (TOR): An integrator of nutrient and growth factor signals and coordinator of cell growth and cell cycle progression. *Oncogene* 23, 3151–3171. doi:10.1038/sj.onc.1207542.

Fitt, W. K. (2000). Cellular Growth of Host and Symbiont in a Cnidarian-Zooxanthellar Symbiosis. *Biological Bulletin* 198, 110–120.

Fitt, W. K., and Cook, C. B. (2001). The effects of feeding or addition of dissolved inorganic nutrients in maintaining the symbiosis between dinoflagellates and a tropical marine cnidarian. *Marine Biology* 139, 507–517. doi:10.1007/s002270100598.

Fitt, W. K., and Trench, R. K. (1983a). Endocytosis of the symbiotic dinoflagellate symbiodinium microadriaticum Freudenthal by endodermal cells of the scyphistomae of Cassiopeia xamachana and resistance of the algae to host digestion. *Journal of cell science* 64, 195–212. doi:10.1111/j.1469-8137.1983.tb03456.x.

Fitt, W. K., and Trench, R. K. (1983b). The Relation of Diel Patterns of Cell Division To Diel Patterns of Motility in the Symbiotic Dinoflagellate Symbiodinium microadriaticum Freudenthal in Culture. *New Phytologist* 94, 421–432. doi:10.1111/j.1469-8137.1983.tb03456.x.

Fransolet, D., Roberty, S., Herman, A.-C., Tonk, L., Hoegh-Guldberg, O., and Plumier, J.-C. (2013). Increased cell proliferation and mucocyte density in the sea anemone Aiptasia pallida recovering from bleaching. *PloS ONE* 8, e65015. doi:10.1371/journal.pone.0065015.

Fransolet, D., Roberty, S., and Plumier, J. C. (2014). Impairment of symbiont photosynthesis increases host cell proliferation in the epidermis of the sea anemone Aiptasia pallida. *Marine Biology*, 1735–1743. doi:10.1007/s00227-014-2455-1.

Fransolet, D., Roberty, S., and Plumier, J.-C. (2012). Establishment of endosymbiosis: The case of cnidarians and Symbiodinium. *Journal of Experimental Marine Biology and Ecology* 420–421, 1–7. doi:10.1016/j.jembe.2012.03.015.

Frieler, K., Meinshausen, M., Golly, A., Mengel, M., Lebek, K., Donner, S. D., et al. (2013). Limiting global warming to 2 °C is unlikely to save most coral reefs. *Nature Climate Change* 3, 165–170. doi:10.1038/nclimate1674.

Fujise, L., Nitschke, M. R., Frommlet, J. C., Serôdio, J., Woodcock, S., Ralph, P. J., et al. (2018). Cell cycle dynamics of cultured coral endosymbiotic microalgae (Symbiodinium) across different types (species) under alternate light and temperature conditions. *Journal of Eukaryotic Microbiology* 0, 1–13. doi:10.1111/jeu.12497.

Gabay, Y., Parkinson, J. E., Wilkinson, S. P., Weis, V. M., and Davy, S. K. (2019). Inter-partner specificity limits the acquisition of thermotolerant symbionts in a model cnidarian-dinoflagellate symbiosis. *IMSE J.*, 1. doi:10.1038/s41396-019-0429-5.

Gabay, Y., Weis, V. M., and Davy, S. K. (2018). Symbiont Identity Influences Patterns of Symbiosis Establishment, Host Growth, and Asexual Reproduction in a Model Cnidarian-Dinoflagellate Symbiosis. *The Biological Bulletin* 234, 1–10. doi:10.1086/696365.

Gallatin, W. M., Weissman, I. L., and Butcher, E. C. (1983). A cell-surface molecule involved in organ-specific homing of lymphocytes. *Nature* 304, 30–34. doi:10.1038/304030a0.

Gardner, M. J., Hall, N., Fung, E., White, O., Berriman, M., Hyman, R. W., et al. (2002). Genome sequence of the human malaria parasite Plasmodium falciparum. *Nature* 419. doi:10.1038/nature01097.

Gates, R. D., Baghdasarian, G., and Muscatine, L. (1992). Temperature stress causes host cell detachment in symbiotic cnidarians: implications for coral bleaching. *Biological Bulletin* 182, 324–332. doi:10.2307/1542252.

Gladfelter, A. S. (2015). How nontraditional model systems can save us. *Molecular Biology of the Cell* 26, 3687–3689. doi:10.1091/mbc.E15-06-0429.

Goldstein, B., and King, N. (2016). The Future of Cell Biology: Emerging Model Organisms. *Trends in Cell Biology* 26, 818–824. doi:10.1016/j.tcb.2016.08.005.

Goreau, T. F. (1959). The physiology of skeleton formation in corals. I. A method for measuring the rate of calcium deposition by corals under different conditions. *Biological Bulletin* 116, 59–75. doi:10.2307/1539156.

Grawunder, D., Hambleton, E. A., Bucher, M., Wolfowicz, I., Bechtoldt, N., and Guse, A. (2015). Induction of Gametogenesis in the Cnidarian Endosymbiosis Model Aiptasia sp. *Scientific reports* 5, 15677. doi:10.1038/srep15677.

Gust, A. A., Willmann, R., Desaki, Y., Grabherr, H. M., and Nürnberger, T. (2012). Plant LysM proteins: modules mediating symbiosis and immunity. *Trends in Plant Science* 17, 495–502. doi:10.1016/j.tplants.2012.04.003.

Gustafsson, M. S. M., Baird, M. E., and Ralph, P. J. (2014). Modeling photoinhibition-driven bleaching in Scleractinian coral as a function of light, temperature, and heterotrophy. *Limnology and Oceanography* 59, 603–622. doi:10.4319/lo.2014.59.2.0603.

Hamada, M., Shoguchi, E., Shinzato, C., Kawashima, T., Miller, D. J., and Satoh, N. (2013). The complex NOD-like receptor repertoire of the coral Acropora digitifera includes novel domain combinations. *Molecular biology and evolution* 30, 167–76. doi:10.1093/molbev/mss213.

Hambleton, E. a, Guse, A., and Pringle, J. R. (2014). Similar specificities of symbiont uptake by adults and larvae in an anemone model system for coral biology. *The Journal of experimental biology* 217, 1613–9. doi:10.1242/jeb.095679.

Hashimoto, K., Tokimatsu, T., Kawano, S., Yoshizawa, A. C., Okuda, S., Goto, S., et al. (2009). Comprehensive analysis of glycosyltransferases in eukaryotic genomes for structural and functional characterization of glycans. *Carbohydrate Research* 344, 881–887. doi:10.1016/j.carres.2009.03.001.

Hawkins, T. D., Bradley, B. J., and Davy, S. K. (2013). Nitric oxide mediates coral bleaching through an apoptotic-like cell death pathway: evidence from a model sea anemone-dinoflagellate symbiosis. *FASEB journal* 27, 4790–8. doi:10.1096/fj.13-235051.

Hawkins, T. D., and Davy, S. K. (2012). Nitric oxide production and tolerance differ among symbiodinium types exposed to heat stress. *Plant and Cell Physiology* 53, 1889–1898. doi:10.1093/pcp/pcs127.

Heijden, M. G. A. van der, Boller, T., Wiemken, A., and Sanders, I. R. (1998). Different arbuscular mycorrhizal fungal species are potential determinants of plant community structure. *Ecology* 79, 2082–2091.

Helenius, A., and Aebi, M. (2004). Roles of N-Linked Glycans in the Endoplasmic Reticulum. *Annual Review of Biochemistry* 73, 1019–1049. doi:10.1146/annurev.biochem.73.011303.073752.

Hoegh-Guldberg, O., Harvell, C. D., Sale, P. F., Edwards, a J., Caldeira, K., Knowlton, N., et al. (2007). Coral Reefs Under Rapid Climate Change and Ocean Acidification. *Science* 318, 1737–1742. doi:10.1126/science.1152509.

Hughes, T. P., Anderson, K. D., Connolly, S. R., Heron, S. F., Kerry, J. T., Lough, J. M., et al. (2018). Spatial and temporal patterns of mass bleaching of corals in the Anthropocene. *Science* 359, 80–83. doi:10.1126/science.aan8048.

Hughes, T. P., Baird, A. H., Bellwood, D. R., Card, M., Connolly, S. R., Folke, C., et al. (2003). Climate change, human impacts, and the resilience of coral reefs. *Science* 301, 929–933. doi:10.1126/science.1085046.

Hughes, T. P., Kerry, J. T., Álvarez-Noriega, M., Álvarez-Romero, J. G., Anderson, K. D., Baird, A. H., et al. (2017). Global warming and recurrent mass bleaching of corals. *Nature* 543, 373–377. doi:10.1038/nature21707.

Hughes, T. P., Kerry, J. T., Baird, A. H., Connolly, S. R., Chase, T. J., Dietzel, A., et al. (2019). Global warming impairs stock–recruitment dynamics of corals. *Nature* 568, 387–390. doi:10.1038/s41586-019-1081-y.

Iglesias-Prieto, R., Matta, J. L., Robins, W. A., and Trench, R. K. (1992). Photosynthetic response to elevated temperature in the symbiotic dinoflagellate Symbiodinium microadriaticum in culture. *Proceedings of the National Academy of Sciences of the United States of America* 89, 10302–10305. doi:10.1073/pnas.89.21.10302.

Ip, W. K., Takahashi, K., Alan Ezekowitz, R., and Stuart, L. M. (2009). Mannose-binding lectin and innate immunity. *Immunological Reviews* 230, 9–21. doi:10.1111/j.1600-065X.2009.00789.x.

Jimbo, M., Suda, Y., Koike, K., Nakamura-Tsuruta, S., Kominami, J., Kamei, M., et al. (2013). Possible involvement of glycolipids in lectin-mediated cellular transformation of symbiotic microalgae in corals. *Journal of Experimental Marine Biology and Ecology* 439, 129–135. doi:10.1016/j.jembe.2012.10.022.

Johnson, M. D. (2011). The acquisition of phototrophy: adaptive strategies of hosting endosymbionts and organelles. *Photosynthesis Research* 107, 117–132. doi:10.1007/s11120-010-9546-8.

Jones, R. J., and Yellowlees, D. (1997). Regulation and control of intracellular algae (= zooxanthellae) in hard corals. *Philosophical Transactions of the Royal Society B: Biological Sciences* 352, 457–468. doi:10.1098/rstb.1997.0033.

Joseph, S. J., Fernández-Robledo, J. A., Gardner, M. J., El-Sayed, N. M., Kuo, C.-H., Schott, E. J., et al. (2010). The Alveolate Perkinsus marinus: Biological Insights from EST Gene Discovery. *BMC Genomics* 11, 228. doi:10.1186/1471-2164-11-228.

Kachko, A., Loesgen, S., Shahzad-Ul-Hussan, S., Tan, W., Zubkova, I., Takeda, K., et al. (2013). Inhibition of hepatitis C virus by the cyanobacterial protein Microcystis viridis lectin: mechanistic differences between the high-mannose specific lectins MVL, CV-N, and GNA. *Molecular pharmaceutics* 10, 4590–602. doi:10.1021/mp400399b.

Kadono, T., Kawano, T., Hosoya, H., and Kosaka, T. (2004). Flow cytometric studies of the host-regulated cell cycle in algae symbiotic with green paramecium. *Protoplasma* 223, 133–141. doi:10.1007/s00709-004-0046-6.

Kersey, P. J., Allen, J. E., Allot, A., Barba, M., Boddu, S., Bolt, B. J., et al. (2018). Ensembl Genomes 2018: an integrated omics infrastructure for non-vertebrate species. *Nucleic Acids Res* 46, D802–D808. doi:10.1093/nar/gkx1011.

Kimura, A., Sakaguchi, E., and Nonaka, M. (2009). Multi-component complement system of Cnidaria: C3, Bf, and MASP genes expressed in the endodermal tissues of a sea anemone, Nematostella vectensis. *Immunobiology* 214, 165–178. doi:10.1016/j.imbio.2009.01.003.

Kirk, N. L., and Weis, V. M. (2016). “Animal–Symbiodinium Symbioses: Foundations of Coral Reef Ecosystems,” in *The Mechanistic Benefits of Microbial Symbionts*, ed. C. J. Hurst (Cham: Springer International Publishing), 269–294. doi:10.1007/978-3-319-28068-4_10.

Kissinger, J. C., Gajria, B., Li, L., Paulsen, I. T., and Roos, D. S. (2003). ToxoDB: accessing the Toxoplasma gondii genome. *Nucleic Acids Res* 31, 234–236. doi:10.1093/nar/gkg072.

Kita, A., Jimbo, M., Sakai, R., Morimoto, Y., and Miki, K. (2015). Crystal structure of a symbiosis-related lectin from octocoral. *Glycobiology* 25, 1016–1023. doi:10.1093/glycob/cwv033.

Kuniya, N., Jimbo, M., Tanimoto, F., Yamashita, H., Koike, K., Harii, S., et al. (2015). Possible involvement of Tachylectin-2-like lectin from Acropora tenuis in the

process of Symbiodinium acquisition. *Fisheries Science* 81, 473–483. doi:10.1007/s12562-015-0862-y.

Kvennefors, E. C. E., Leggat, W., Hoegh-Guldberg, O., Degnan, B. M., and Barnes, A. C. (2008). An ancient and variable mannose-binding lectin from the coral Acropora millepora binds both pathogens and symbionts. *Developmental & Comparative Immunology* 32, 1582–1592. doi:10.1016/j.dci.2008.05.010.

Kvennefors, E. C. E., Leggat, W., Kerr, C. C., Ainsworth, T. D., Hoegh-Guldberg, O., and Barnes, A. C. (2010). Analysis of evolutionarily conserved innate immune components in coral links immunity and symbiosis. *Developmental and comparative immunology* 34, 1219–29. doi:10.1016/j.dci.2010.06.016.

Laikre, L., Schwartz, M. K., Waples, R. S., and Ryman, N. (2010). Compromising genetic diversity in the wild: unmonitored large-scale release of plants and animals. *Trends in Ecology & Evolution* 25, 520–529. doi:10.1016/j.tree.2010.06.013.

LaJeunesse, T. C., Parkinson, J. E., Gabrielson, P. W., Jeong, H. J., Reimer, J. D., Voolstra, C. R., et al. (2018). Systematic Revision of Symbiodiniaceae Highlights the Antiquity and Diversity of Coral Endosymbionts. *Current Biology* 28, 2570-2580.e6. doi:10.1016/j.cub.2018.07.008.

Lajeunesse, T. C., Parkinson, J. E., and Reimer, J. D. (2012). A genetics-based description of Symbiodinium minutum sp. nov. and S. psygmophilum sp. nov. (Dinophyceae), two dinoflagellates symbiotic with cnidaria. *Journal of Phycology* 48, 1380–1391. doi:10.1111/j.1529-8817.2012.01217.x.

LaJeunesse, T. C., Smith, R. T., Finney, J., and Oxenford, H. (2009). Outbreak and persistence of opportunistic symbiotic dinoflagellates during the 2005 Caribbean mass coral 'bleaching' event. *Proceedings of the Royal Society B: Biological Sciences* 276, 4139–4148. doi:10.1098/rspb.2009.1405.

Lannoo, N., and Van Damme, E. J. M. (2014). Lectin domains at the frontiers of plant defense. *Front. Plant Sci.* 5. doi:10.3389/fpls.2014.00397.

Lecointe, A., Domart-coulon, I., Paris, A., and Meibom, A. (2016). Cell proliferation and migration during early development of a symbiotic scleractinian coral. *Proceedings of the Royal Society of London B* 283, 20160206. doi:10.1098/rspb.2016.0206.

Lee, P. N., Pang, K., Matus, D. Q., and Martindale, M. Q. (2006). A WNT of things to come : Evolution of Wnt signaling and polarity in cnidarians. *Seminars in Cell and Developmental Biology* 17, 157–167. doi:10.1016/j.semcdb.2006.05.002.

Lehnert, E. M., Mouchka, M. E., Burriesci, M. S., Gallo, N. D., Schwarz, J. A, and Pringle, J. R. (2014). Extensive differences in gene expression between symbiotic

and aposymbiotic cnidarians. *G3 (Bethesda, Md.)* 4, 277–95. doi:10.1534/g3.113.009084.

Lesser, M. P. (1996). Elevated temperatures and ultraviolet radiation cause oxidative stress and inhibit photosynthesis in symbiotic dinoflagellates. *Limnology and Oceanography* 41, 271–283. doi:10.4319/lo.1996.41.2.0271.

Liebminger, E., Hüttner, S., Vavra, U., Fischl, R., Schoberer, J., Grass, J., et al. (2009). Class I alpha-mannosidases are required for N-glycan processing and root development in Arabidopsis thaliana. *The Plant cell* 21, 3850–3867. doi:10.1105/tpc.109.072363.

Liew, Y. J., Aranda, M., and Voolstra, C. R. (2016). Reefgenomics.Org - a repository for marine genomics data. *Database (Oxford)* 2016. doi:10.1093/database/baw152.

Lin, K., Wang, J., and Fang, L.-S. (2000). Participation of Glycoproteins on Zooxanthellal Cell Walls in the Establishment of a Symbiotic Relationship with the Sea Anemone, Aiptasia pulchella. 39, 172–178.

Lin, S., Cheng, S., Song, B., Zhong, X., Lin, X., Li, W., et al. (2015). The Symbiodinium kawagutii genome illuminates dinoflagellate gene expression and coral symbiosis. *Science* 350, 691–694. doi:10.1126/science.aad0408.

Liu, H., Stephens, T. G., González-pech, R. A., Beltran, V. H., Bongaerts, P., Cooke, I., et al. (2017). Symbiodinium genomes reveal adaptive evolution of functions related to symbiosis.

Logan, D. D. K., LaFlamme, A. C., Weis, V. M., and Davy, S. K. (2010). Flow-Cytometric Characterization of the Cell-Surface Glycans of Symbiotic Dinoflagellates (Symbiodinium Spp.). *Journal of Phycology* 46, 525–533. doi:10.1111/j.1529-8817.2010.00819.x.

Login, F. H., Balmand, S., Vallier, A., Vincent-Monegat, C., Vigneron, A., Weiss-Gayet, M., et al. (2011). Antimicrobial peptides keep insect endosymbionts under control. *Science* 334, 362–365. doi:10.1126/science.1209728.

Mansfield, K. M., Carter, N. M., Nguyen, L., Cleves, P. A., Alshanbayeva, A., Williams, L. M., et al. (2017). Transcription factor NF-κB is modulated by symbiotic status in a sea anemone model of cnidarian bleaching. *Scientific Reports* 7, 1–14. doi:10.1038/s41598-017-16168-w.

Matthews, J. L., Crowder, C. M., Oakley, C. A., Lutz, A., Roessner, U., Meyer, E., et al. (2017). Optimal nutrient exchange and immune responses operate in partner specificity in the cnidarian-dinoflagellate symbiosis. *Proceedings of the National Academy of Sciences of the United States of America* 114, 13194–13199. doi:10.1073/pnas.1710733114.

Matthews, J. L., Oakley, C. A., Lutz, A., Hillyer, K. E., Roessner, U., Grossman, A. R., et al. (2018). Partner switching and metabolic flux in a model cnidarian–dinoflagellate symbiosis. *Proceedings of the Royal Society B: Biological Sciences* 285, 20182336. doi:10.1098/rspb.2018.2336.

Matthews, J. L., Sproles, A. E., Oakley, C. A., Grossman, A. R., Weis, V. M., and Davy, S. K. (2016). Menthol-induced bleaching rapidly and effectively provides experimental aposymbiotic sea anemones (Aiptasia sp.) for symbiosis investigations. *Journal of Experimental Biology* 219, 306–310. doi:10.1242/jeb.128934.

Maynard, J., van Hooidonk, R., Eakin, C. M., Puotinen, M., Garren, M., Williams, G., et al. (2015). Projections of climate conditions that increase coral disease susceptibility and pathogen abundance and virulence. *Nature Climate Change* 5, 688–694. doi:10.1038/nclimate2625.

McAuley, P. J. (1985). The cell cycle of symbiotic Chlorella. I. The relationship between host feeding and algal cell growth and division. *Journal of cell science* 77, 225–239.

McAuley, P. J. (1986). The cell cycle of symbiotic Chlorella. III. Numbers of algae in green hydra digestive cells are regulated at digestive cell division. *Journal of Cell Science* 85, 63–71.

McAuley, P. J., and Cook, C. B. (1994). Effects of host feeding and dissolved ammonium on cell division and nitrogen status of zooxanthellae in the hydroid Myrionema amboinense. *Marine Biology* 121, 343–348. doi:10.1007/BF00346743.

McCloskey, L. R., Cove, T. G., and Verde, E. A. (1996). Symbiont expulsion from the anemone Anthopleura elegantissima (Brandt) (Cnidaria; Anthozoa). *Journal of Experimental Marine Biology and Ecology* 195, 173–186. doi:10.1016/0022-0981(95)00079-8.

McFall-Ngai, M., Hadfield, M. G., Bosch, T. C. G., Carey, H. V., Domazet-Lošo, T., Douglas, A. E., et al. (2013). Animals in a bacterial world, a new imperative for the life sciences. *Proceedings of the National Academy of Sciences* 110, 3229–3236. doi:10.1073/pnas.1218525110.

McGuinness, D. H., Dehal, P. K., and Pleass, R. J. (2003). Pattern recognition molecules and innate immunity to parasites. *Trends in Parasitology* 19, 312–319. doi:10.1016/S1471-4922(03)00123-5.

Mergaert, P., Uchiumi, T., Alunni, B., Evanno, G., Cheron, A., Catrice, O., et al. (2006). Eukaryotic control on bacterial cell cycle and differentiation in the Rhizobium-legume symbiosis. *Proceedings of the National Academy of Sciences of the United States of America* 103, 5230–5235. doi:10.1073/pnas.0600912103.

Merselis, D. G., Lirman, D., and Rodriguez-Lanetty, M. (2018). Symbiotic immuno-suppression: is disease susceptibility the price of bleaching resistance? *PeerJ* 6, e4494. doi:10.7717/peerj.4494.

Meyer, E., and Weis, V. M. (2012). Study of cnidarian-algal symbiosis in the "omics" age. *The Biological Bulletin* 223, 44–65. doi:10.1086/BBLv223n1p44.

Miller, D. J., Hemmrich, G., Ball, E. E., Hayward, D. C., Khalturin, K., Funayama, N., et al. (2007). The innate immune repertoire in Cnidaria - ancestral complexity and stochastic gene loss. *Genome Biology* 8, R59. doi:10.1186/gb-2007-8-4-r59.

Mittler, R., and Blumwald, E. (2010). Genetic Engineering for Modern Agriculture: Challenges and Perspectives. *Annual Review of Plant Biology* 61, 443–462. doi:10.1146/annurev-arplant-042809-112116.

Moberg, F. F., and Folke, C. (1999). Ecological goods and services of coral reef ecosystems. *Ecological Economics* 29, 215–233. doi:10.1016/S0921-8009(99)00009-9.

Muller-Parker, G., and Davy, S. K. (2001). Temperate and Tropical Algal-Sea Anemone Symbioses. *Invertebrate Biology* 120, 104–123.

Muller-Parker, G., Lee, K. W., and Cook, C. B. (1996). Changes in the ultrastructure of symbiotic zooxanthellae (Symbiodinium Sp., Dinophyceae) in fed and starved sea anemones maintained under high and low light. *Journal of Phycology* 32, 987–994. doi:10.1111/j.1529-8817.1996.tb02206.x.

Muscatine, L., Falkowski, P. G., Dubinsky, Z., Cook, P. A., and McCloskey, L. L. R. (1989). The effect of external nutrient resources on the population dynamics of zooxanthellae in a reef coral. *Proceedings of the Royal Society of London B* 236, 311–324. doi:10.1098/rspb.1989.0025.

Muscatine, L., Ferrier-Pagès, C., Blackburn, A., Gates, R. D., Baghdasarian, G., and Allemand, D. (1998). Cell specific density of symbiotic dinoflagellates in tropical anthozoans. *Coral Reefs* 17, 329–337. doi:Doi 10.1007/S003380050133.

Muscatine, L., Goiran, C., Land, L., Jaubert, J., Cuif, J.-P., and Allemand, D. (2005). Stable isotopes (delta13C and delta15N) of organic matrix from coral skeleton. *Proceedings of the National Academy of Sciences of the United States of America* 102, 1525–1530. doi:10.1073/pnas.0408921102.

Muscatine, L., and Lenhoff, H. M. (1963). Symbiosis: On the Role of Algae Symbiotic with Hydra. *Science (New York, N.Y.)* 142, 956–958. doi:10.1126/science.142.3594.956.

Muscatine, L., and Pool, R. R. (1979). Regulation of numbers of intracellular algae. *Proceedings of the Royal Society of London B* 204, 131–139. doi:10.1098/rspb.1979.0018.

Muscatine, L., and Porter, J. W. (1977). Reef Corals : Mutualistic Symbioses Adapted to Nutrient-Poor Environments. *BioScience* 27, 454–460. doi:10.2307/1297526.

Neubauer, E. F., Poole, A. Z., Weis, V. M., and Davy, S. K. (2016). The scavenger receptor repertoire in six cnidarian species and its putative role in cnidarian-dinoflagellate symbiosis. *PeerJ* 4, e2692. doi:10.7717/peerj.2692.

Neubauer, E.-F., Poole, A. Z., Neubauer, P., Detournay, O., Tan, K., Davy, S. K., et al. (2017). A diverse host thrombospondin-type-1 repeat protein repertoire promotes symbiont colonization during establishment of cnidarian-dinoflagellate symbiosis. *eLife* 6. doi:10.7554/eLife.24494.

Notredame, C., Higgins, D. G., and Heringa, J. (2000). T-Coffee: A novel method for fast and accurate multiple sequence alignment. *J. Mol. Biol.* 302, 205–217. doi:10.1006/jmbi.2000.4042.

Nyholm, S. V., and McFall-Ngai, M. J. (2004). The winnowing: establishing the squid-vibrio symbiosis. *Nature reviews. Microbiology* 2, 632–42. doi:10.1038/nrmicro957.

Ollion, J., Cochennec, J., Loll, F., Escudé, C., and Boudier, T. (2013). TANGO: A generic tool for high-throughput 3D image analysis for studying nuclear organization. *Bioinformatics* 29, 1840–1841. doi:10.1093/bioinformatics/btt276.

Olson, R. J., Vaulot, D., and Chisholm, S. W. (1986). Effects of Environmental Stresses on the Cell Cycle of Two Marine Phytoplankton Species. *Plant Physiology* 80, 918–925.

Oswald, E., Nougayrède, J. P., Taieb, F., and Sugai, M. (2005). Bacterial toxins that modulate host cell-cycle progression. *Current Opinion in Microbiology* 8, 83–91. doi:10.1016/j.mib.2004.12.011.

Otto, J. J., and Campbell, R. D. (1977). Tissue economics of hydra: regulation of cell cycle, animal size and development by controlled feeding rates. *Journal of cell science* 28, 117–132.

Pang, P.-C., Chiu, P. C. N., Lee, C.-L., Chang, L.-Y., Panico, M., Morris, H. R., et al. (2011). Human Sperm Binding Is Mediated by the Sialyl-Lewisx Oligosaccharide on the Zona Pellucida. *Science* 333, 1761–1764. doi:10.1126/science.1207438.

Pardee, A. B. (1989). G1 events and regulation of cell proliferation. *Science* 246, 603–608.

Park, C., Meng, L., Stanton, L. H., Collins, R. E., Mast, S. W., Yi, X., et al. (2005). Characterization of a Human Core-specific Lysosomal α1,6-Mannosidase Involved in *N* -Glycan Catabolism. *Journal of Biological Chemistry* 280, 37204–37216. doi:10.1074/jbc.M508930200.

Parkinson, J. E., Tivey, T. R., Mandelare, P. E., Adpressa, D. A., Loesgen, S., and Weis, V. M. (2018). Subtle Differences in Symbiont Cell Surface Glycan Profiles Do Not Explain Species-Specific Colonization Rates in a Model Cnidarian-Algal Symbiosis. *Frontiers in Microbiology* 9. doi:10.3389/fmicb.2018.00842.

Parrin, A. P., Goulet, T. L., Yaeger, M. A., Bross, L. S., McFadden, C. S., and Blackstone, N. W. (2016). Symbiodinium migration mitigates bleaching in three octocoral species. *Journal of Experimental Marine Biology and Ecology* 474, 73–80. doi:10.1016/j.jembe.2015.09.019.

Parrin, A. P., Harmata, K. L., Netherton, S. E., Yaeger, M. A., Bross, L. S., and Blackstone, N. W. (2012). Within-colony migration of symbionts during bleaching of octocorals. *Biological Bulletin* 223, 245–256.

Passamaneck, Y. J., and Martindale, M. Q. (2012). Cell proliferation is necessary for the regeneration of oral structures in the anthozoan cnidarian Nematostella vectensis. *BMC developmental biology* 12, 34. doi:10.1186/1471-213X-12-34.

Patterson, M. R. (1992). A chemical engineering view of cnidarian symbioses. *American Zoologist* 32, 566–582. doi:10.1093/icb/32.4.566.

Paulson, J. C., Blixt, O., and Collins, B. E. (2006). Sweet spots in functional glycomics. *Nature Chemical Biology* 2, 238–248. doi:10.1038/nchembio785.

Pearse, V. B., and Muscatine, L. (1971). Role of symbiotic algae (zooxanthellae) in coral calcification. *Biological Bulletin* 141, 350–363. doi:10.2307/1540123.

Perez, S. F., Cook, C. B., and Brooks, W. R. (2001). The role of symbiotic dinoflagellates in the temperature-induced bleaching response of the subtropical sea anemone Aiptasia pallida. *Journal of Experimental Marine Biology and Ecology* 256, 1–14. doi:10.1016/S0022-0981(00)00282-3.

Perez, S., and Weis, V. M. (2006). Nitric oxide and cnidarian bleaching: an eviction notice mediates breakdown of a symbiosis. *The Journal of experimental biology* 209, 2804–10. doi:10.1242/jeb.02309.

Petersen, L., Ardèvol, A., Rovira, C., and Reilly, P. J. (2010). Molecular Mechanism of the Glycosylation Step Catalyzed by Golgi α-Mannosidase II: A QM/MM Metadynamics Investigation. *Journal of the American Chemical Society* 132, 8291–8300. doi:10.1021/ja909249u.

Pochon, X., and Gates, R. D. (2010). A new Symbiodinium clade (Dinophyceae) from soritid foraminifera in Hawai'i. *Molecular Phylogenetics and Evolution* 56, 492–497. doi:10.1016/j.ympev.2010.03.040.

Pochon, X., Montoya-Burgos, J. I., Stadelmann, B., and Pawlowski, J. (2006). Molecular phylogeny, evolutionary rates, and divergence timing of the symbiotic dinoflagellate genus Symbiodinium. *Molecular Phylogenetics and Evolution* 38, 20–30. doi:10.1016/j.ympev.2005.04.028.

Poole, A. Z., Kitchen, S. A., and Weis, V. M. (2016). The Role of Complement in Cnidarian-Dinoflagellate Symbiosis and Immune Challenge in the Sea Anemone Aiptasia pallida. *Frontiers in Microbiology* 7, 519. doi:10.3389/fmicb.2016.00519.

Poole, A. Z., and Weis, V. M. (2014). TIR-domain-containing protein repertoire of nine anthozoan species reveals coral-specific expansions and uncharacterized proteins. *Developmental and Comparative Immunology* 46, 480–488. doi:10.1016/j.dci.2014.06.002.

Rentzsch, F., Fritzenwanker, J. H., Scholz, C. B., and Technau, U. (2008). FGF signalling controls formation of the apical sensory organ in the cnidarian Nematostella vectensis. *Development* 135, 1761–1769. doi:10.1242/dev.020784.

Riccardi, C., and Nicoletti, I. (2006). Analysis of apoptosis by propidium iodide staining and flow cytometry. *Nature Protocols* 1, 1458–1461. doi:10.1038/nprot.2006.238.

Rizzo, P. J. (2003). Those amazing dinoflagellate chromosomes. *Cell research* 13, 215–217. doi:10.1038/sj.cr.7290166.

Rodriguez-Lanetty, M., Krupp, D. A., and Weis, V. M. (2004). Distinct ITS types of Symbiodinium in Clade C correlate with cnidarian/dinoflagellate specificity during onset of symbiosis. *Marine Ecology Progress Series* 275, 97–102. doi:10.3354/meps275097.

Rosset, S., Wiedenmann, J., Reed, A. J., and D'Angelo, C. (2017). Phosphate deficiency promotes coral bleaching and is reflected by the ultrastructure of symbiotic dinoflagellates. *Marine Pollution Bulletin* 118, 180–187. doi:10.1016/j.marpolbul.2017.02.044.

Rueden, C. T., Schindelin, J., Hiner, M. C., DeZonia, B. E., Walter, A. E., Arena, E. T., et al. (2017). ImageJ2: ImageJ for the next generation of scientific image data. *BMC Bioinformatics* 18. doi:10.1186/s12859-017-1934-z.

Sachs, J. L., Quides, K. W., and Wendlandt, C. E. (2018). Legumes versus rhizobia: a model for ongoing conflict in symbiosis. doi:10.1111/nph.15222.

Sagan, L. (1967). On the origin of mitosing cells. *Journal of Theoretical Biology* 14, 225-IN6. doi:10.1016/0022-5193(67)90079-3.

Samuelson, J., Banerjee, S., Magnelli, P., Cui, J., Kelleher, D. J., Gilmore, R., et al. (2005). The diversity of dolichol-linked precursors to Asn-linked glycans likely results from secondary loss of sets of glycosyltransferases. *Proceedings of the National Academy of Sciences* 102, 1548–1553. doi:10.1073/pnas.0409460102.

Santos, S. R., Toyoshima, J., and Kinzie III, R. A. (2009). Spatial and temporal dynamics of symbiotic dinoflagellates (Symbiodinium : Dinophyta) in the perforate coral Montipora capitata. 139–147.

Scheurlen, I., Hoffmeister, S. a, and Schaller, H. C. (1996). Presence and expression of G2 cyclins in the coelenterate hydra. *Journal of Cell Science* 109, 1063–1069.

Schindelin, J., Arganda-carreras, I., Frise, E., Kaynig, V., Longair, M., Pietzsch, T., et al. (2012). Fiji: an open-source platform for biological-image analysis. *Nature Methods; New York* 9, 676–82. doi:http://dx.doi.org.ezproxy.proxy.library.oregonstate.edu/10.1038/nmeth.2019.

Schoenberg, D. A., and Trench, R. K. (1980). Genetic Variation in Symbiodinium (=Gymnodinium) microadriaticum Freudenthal, and Specificity in its Symbiosis with Marine Invertebrates. III. Specificity and Infectivity of Symbiodinium microadriaticum. *Proceedings of the Royal Society of London. Series B, Biological Sciences* 207, 445–460.

Schwartz, R. M., and Dayhoff, M. O. (1978). Origins of Prokaryotes, Eukaryotes, Mitochondria, and Chloroplasts. *Science* 199, 395–403.

Schwartzman, J. A., Koch, E., Heath-Heckman, E. A. C., Zhou, L., Kremer, N., McFall-Ngai, M. J., et al. (2015). The chemistry of negotiation: Rhythmic, glycan-driven acidification in a symbiotic conversation. *Proceedings of the National Academy of Sciences* 112, 201418580. doi:10.1073/pnas.1418580112.

Schwarz, J. A. (2008). Understanding the intracellular niche in cnidarian-Symbiodinium symbioses: parasites lead the way. *Vie et Milieu - Life and Environment* 58, 141–151.

Schwarz, J. A., Krupp, D. A., and Weis, V. M. (1999). Late larval development and onset of symbiosis in the scleractinian coral Fungia scutaria. *Biological Bulletin* 196, 70–79. doi:10.2307/1543169.

Schwarz, J. A., Weis, V. M., and Potts, D. C. (2002). Feeding behavior and acquisition of zooxanthellae by planula larvae of the sea anemone Anthopleura elegantissima. *Marine Biology* 140, 471–478. doi:10.1007/s00227-001-0736-y.

Shah, N., Kuntz, D. A., and Rose, D. R. (2008). Golgi -mannosidase II cleaves two sugars sequentially in the same catalytic site. *Proceedings of the National Academy of Sciences* 105, 9570–9575. doi:10.1073/pnas.0802206105.

Shahzad-ul-Hussan, S., Cai, M., and Bewley, C. A. (2009). Unprecedented Glycosidase Activity at a Lectin Carbohydrate-Binding Site Exemplified by the Cyanobacterial Lectin MVL. doi:10.1021/ja905929c.

Shoguchi, E., Shinzato, C., Kawashima, T., Gyoja, F., Mungpakdee, S., Koyanagi, R., et al. (2013). Draft assembly of the Symbiodinium minutum nuclear genome reveals dinoflagellate gene structure. *Current biology : CB* 23, 1399–408. doi:10.1016/j.cub.2013.05.062.

Singer, I. (1971). Tentacular and oral-disc regeneration in the sea anemone, Aiptasia diaphana. *Journal of Embryology and Experimental Morphology* 26, 253–270.

Smith, G. J., and Muscatine, L. (1999). Cell cycle of symbiotic dinoflagellates: variation in G1 phase-duration with anemone nutritional status and macronutrient supply in the Aiptasia pulchella-Symbiodinium pulchrorum symbiosis. *Marine Biology* 134, 405–418.

Stanley, P., Taniguchi, N., and Aebi, M. (2015). "N-Glycans," in *Essentials of Glycobiology*, eds. A. Varki, R. D. Cummings, J. D. Esko, P. Stanley, G. W. Hart, M. Aebi, et al. (Cold Spring Harbor (NY): Cold Spring Harbor Laboratory Press). Available at: http://www.ncbi.nlm.nih.gov/books/NBK453020/ [Accessed December 17, 2018].

Stat, M., Morris, E., and Gates, R. D. (2008). Functional diversity in coral-dinoflagellate symbiosis. *Proceedings of the National Academy of Sciences of the United States of America* 105, 9256–61. doi:10.1073/pnas.0801328105.

Steen, R., and Muscatine, L. (1987). Low temperature evokes rapid exocytosis of symbiotic algae by a sea anemone. *The Biological Bulletin* 172, 246–263. doi:10.2307/1541797.

Stephens, T. G., Ragan, M. A., Bhattacharya, D., and Chan, C. X. (2018). Core genes in diverse dinoflagellate lineages include a wealth of conserved dark genes with unknown functions. *Scientific Reports* 8. doi:10.1038/s41598-018-35620-z.

Strobl, F., Schmitz, A., and Stelzer, E. H. K. (2017). Improving your four-dimensional image: traveling through a decade of light-sheet-based fluorescence microscopy research. *Nature Protocols* 12, 1103–1109. doi:10.1038/nprot.2017.028.

Strychar, K. B., Sammarco, P. W., and Piva, T. J. (2004). Apoptotic and necrotic stages of Symbiodinium (Dinophyceae) cell death activity: bleaching of soft and scleractinian corals. *Phycologia* 43, 768–777. doi:10.2216/i0031-8884-43-6-768.1.

Sunagawa, S., Wilson, E. C., Thaler, M., Smith, M. L., Caruso, C., Pringle, J. R., et al. (2009). Generation and analysis of transcriptomic resources for a model system on the rise: the sea anemone Aiptasia pallida and its dinoflagellate endosymbiont. *BMC genomics* 10, 258. doi:10.1186/1471-2164-10-258.

Takahashi, T. (2016). Simultaneous Evaluation of Life Cycle Dynamics between a Host Paramecium and the Endosymbionts of Paramecium bursaria Using Capillary Flow Cytometry. *Scientific Reports* 6. doi:10.1038/srep31638.

Taormina, M. J., Jemielita, M., Stephens, W. Z., Burns, A. R., Troll, J. V., Parthasarathy, R., et al. (2012). Investigating Bacterial-Animal Symbioses with Light Sheet Microscopy. *The Biological Bulletin* 223, 7–20. doi:10.1086/BBLv223n1p7.

Tasumi, S., and Vasta, G. R. (2007). A Galectin of Unique Domain Organization from Hemocytes of the Eastern Oyster (Crassostrea virginica) Is a Receptor for the Protistan Parasite Perkinsus marinus. *The Journal of Immunology* 179, 3086–3098. doi:10.4049/jimmunol.179.5.3086.

Technau, U., Rudd, S., Maxwell, P., Gordon, P. M. K., Saina, M., Grasso, L. C., et al. (2005). Maintenance of ancestral complexity and non-metazoan genes in two basal cnidarians. *Trends in Genetics* 21, 633–639. doi:10.1016/j.tig.2005.09.007.

The UniProt Consortium (2017). UniProt: the universal protein knowledgebase. *Nucleic Acids Research* 45, D158–D169. doi:10.1093/nar/gkw1099.

Toby Kiers, E., Palmer, T. M., Ives, A. R., Bruno, J. F., and Bronstein, J. L. (2010). Mutualisms in a changing world: an evolutionary perspective: Mutualism breakdown. *Ecology Letters* 13, 1459–1474. doi:10.1111/j.1461-0248.2010.01538.x.

Tulsiani, D. R., Harris, T. M., and Touster, O. (1982). Swainsonine inhibits the biosynthesis of complex glycoproteins by inhibition of Golgi mannosidase II. *J. Biol. Chem.* 257, 7936–7939.

Van de Velde, W., Zehirov, G., Szatmari, A., Debreczeny, M., Ishihara, H., Kevei, Z., et al. (2010). Plant peptides govern terminal differentiation of bacteria in symbiosis. *Science (New York, N.Y.)* 327, 1122–1126. doi:10.1126/science.1184057.

van Hooidonk, R., Maynard, J. a., and Planes, S. (2013). Temporary refugia for coral reefs in a warming world. *Nature Climate Change* 3, 508–511. doi:10.1038/nclimate1829.

van Kooyk, Y., and Rabinovich, G. a (2008). Protein-glycan interactions in the control of innate and adaptive immune responses. *Nature immunology* 9, 593–601. doi:10.1038/ni.f.203.

van Oppen, M. J. H., Gates, R. D., Blackall, L. L., Cantin, N., Chakravarti, L. J., Chan, W. Y., et al. (2017). Shifting paradigms in restoration of the world's coral reefs. *Global Change Biology*, 1–12. doi:10.1111/gcb.13647.

van Oppen, M. J. H., Oliver, J. K., Putnam, H. M., and Gates, R. D. (2015). Building coral reef resilience through assisted evolution. *Proceedings of the National Academy of Sciences* 112, 2307–2313. doi:10.1073/pnas.1422301112.

Varki, A. (2017). Biological roles of glycans. *Glycobiology* 27, 3–49. doi:10.1093/glycob/cww086.

Vaulot, D., Olson, R. J., Merkel, S., and Chisholm, S. W. (1987). Cell-cycle response to nutrient starvation in two phytoplankton species, Thalassiosira weissflogii and Hymenomonas carterae. *Mar. Biol.* 95, 625–630. doi:10.1007/BF00393106.

Venn, A. A., Loram, J. E., and Douglas, A. E. (2008). Photosynthetic symbioses in animals. *Journal of Experimental Botany* 59, 1069–1080. doi:10.1093/jxb/erm328.

von Itzstein, M., Plebanski, M., Cooke, B. M., and Coppel, R. L. (2008). Hot, sweet and sticky: the glycobiology of Plasmodium falciparum. *Trends in Parasitology* 24, 210–218. doi:10.1016/j.pt.2008.02.007.

Wakefield, T. S., Farmer, M. A., and Kempf, S. C. (2000). Revised description of the fine structure of in situ "Zooxanthellae" genus Symbiodinium. *Biological Bulletin* 199, 76–84. doi:10.2307/1542709.

Wakefield, T. S., and Kempf, S. C. (2001). Development of host- and symbiont-specific monoclonal antibodies and confirmation of the origin of the symbiosome membrane in a cnidarian-dinoflagellate symbiosis. *Biological Bulletin* 200, 127–143. doi:10.2307/1543306.

Wang, J., and Douglas, A. E. (1998). Nitrogen recycling or nitrogen conservation in an alga-invertebrate symbiosis? *The Journal of experimental biology* 201, 2445–2453.

Wang, L.-H., Lee, H.-H., Fang, L.-S., Mayfield, A. B., and Chen, C.-S. (2013). Fatty acid and phospholipid syntheses are prerequisites for the cell cycle of Symbiodinium and their endosymbiosis within sea anemones. *PloS ONE* 8, e72486. doi:10.1371/journal.pone.0072486.

Wang, L.-H., Liu, Y. H., Ju, Y. M., Hsiao, Y. Y., Fang, L.-S., and Chen, C. S. (2008). Cell cycle propagation is driven by light-dark stimulation in a cultured symbiotic dinoflagellate isolated from corals. *Coral Reefs* 27, 823–835. doi:10.1007/s00338-008-0434-z.

Weis, V. M. (2008). Cellular mechanisms of Cnidarian bleaching: stress causes the collapse of symbiosis. *The Journal of experimental biology* 211, 3059–66. doi:10.1242/jeb.009597.

Weis, V. M., Davy, S. K., Hoegh-Guldberg, O., Rodriguez-Lanetty, M., and Pringle, J. R. (2008). Cell biology in model systems as the key to understanding corals. *Trends in ecology & evolution* 23, 369–76. doi:10.1016/j.tree.2008.03.004.

Weis, V. M., Reynolds, W. S., DeBoer, M. D., and Krupp, D. A. (2001). Host-symbiont specificity during onset of symbiosis between the dinoflagellates Symbiodinium spp. and planula larvae of the scleractinian coral Fungia scutaria. *Coral Reefs* 20, 301–308. doi:10.1007/s003380100179.

Weng, S., and Spiro, R. G. (1993). Demonstration that a kifunensine-resistant alpha-mannosidase with a unique processing action on N-linked oligosaccharides occurs in rat liver endoplasmic reticulum and various cultured cells. *J Biol Chem* 268, 25656–25663.

Wiedenmann, J., D'Angelo, C., Smith, E. G., Hunt, A. N., Legiret, F.-E., Postle, A. D., et al. (2013). Nutrient enrichment can increase the susceptibility of reef corals to bleaching. *Nature Climate Change* 3, 160–164. doi:10.1038/nclimate1661.

Wilkerson, F. P., Kobayashi, D., and Muscatine, L. (1988). Mitotic index and size of symbiotic algae in Caribbean Reef corals. *Coral Reefs* 7, 29–36.

Wilkerson, F. P., Muller, G., and Muscatine, L. (1983). Temporal patterns of cell division in natural populations of endosymbiotic algae. *Limnology and Oceanography* 28, 1009–1014.

Wisecaver, J. H., and Hackett, J. D. (2011). Dinoflagellate genome evolution. *Annual review of microbiology* 65, 369–87. doi:10.1146/annurev-micro-090110-102841.

Wolfowicz, I., Baumgarten, S., Voss, P. A., Hambleton, E. A., Voolstra, C. R., Hatta, M., et al. (2016). Aiptasia sp. larvae as a model to reveal mechanisms of symbiont selection in cnidarians. *Scientific Reports* 6. doi:10.1038/srep32366.

Wong, J. T. Y., and Kwok, A. C. M. (2005). Proliferation of dinoflagellates: blooming or bleaching. *BioEssays : news and reviews in molecular, cellular and developmental biology* 27, 730–40. doi:10.1002/bies.20250.

Wood-Charlson, E. M., Hollingsworth, L. L., Krupp, D. A., and Weis, V. M. (2006). Lectin/glycan interactions play a role in recognition in a coral/dinoflagellate symbiosis. *Cellular Microbiology* 8, 1985–1993. doi:10.1111/j.1462-5822.2006.00765.x.

Wood-Charlson, E. M., and Weis, V. M. (2009). The diversity of C-type lectins in the genome of a basal metazoan, Nematostella vectensis. *Developmental and comparative immunology* 33, 881–9. doi:10.1016/j.dci.2009.01.008.

Woznica, A., Gerdt, J. P., Hulett, R. E., Clardy, J., and King, N. (2017). Mating in the closest living relatives of animals is induced by a bacterial chondroitinase. *Cell* 170, 1175–1183. doi:10.1016/j.cell.2017.08.005.

Xiang, T., Hambleton, E. a., DeNofrio, J. C., Pringle, J. R., and Grossman, A. R. (2013). Isolation of clonal axenic strains of the symbiotic dinoflagellate Symbiodinium and their growth and host specificity 1. *Journal of Phycology* 49, 447–458. doi:10.1111/jpy.12055.

Yuyama, I., Ishikawa, M., Nozawa, M., Yoshida, M., and Ikeo, K. (2018). Transcriptomic changes with increasing algal symbiont reveal the detailed process underlying establishment of coral-algal symbiosis. *Scientific Reports* 8, 16802. doi:10.1038/s41598-018-34575-5.

Zhou, Z., Yu, X., Tang, J., Zhu, Y., Chen, G., Guo, L., et al. (2017). Dual recognition activity of a rhamnose-binding lectin to pathogenic bacteria and zooxanthellae in stony coral Pocillopora damicornis. *Developmental & Comparative Immunology* 70, 88–93. doi:10.1016/j.dci.2017.01.009.

7. Appendices

7.1 Appendix A: Supplementary materials for Chapter 2

Appendix Figure A1. Lectin specificity of MVL, CVN, and PHA-L.

The lectin specificity of (**A**) MVL, (**B**) CVN, and (**C**) PHA-L. is shown as determined from glycan microarray experiments. MVL shows binding affinity for chitobiose core N-glycan motifs [Man-3 to Man-9; α(1-6) and α(1-3)-dimannoside, Man β(1-4) GlcNAc], CVN shows affinity for high-mannose N-glycan motifs [Man-8 and Man-9 only; α(1-2)-dimannoside], and PHA-L shows affinity for complex type N-glycan motifs [Gal-β(1-4)GlcNAc β(1-6)(GlcNAc β(1-2)Man α(1-3)) Manα(1-3)]. Data provided by the Consortium for Functional Glycomics.

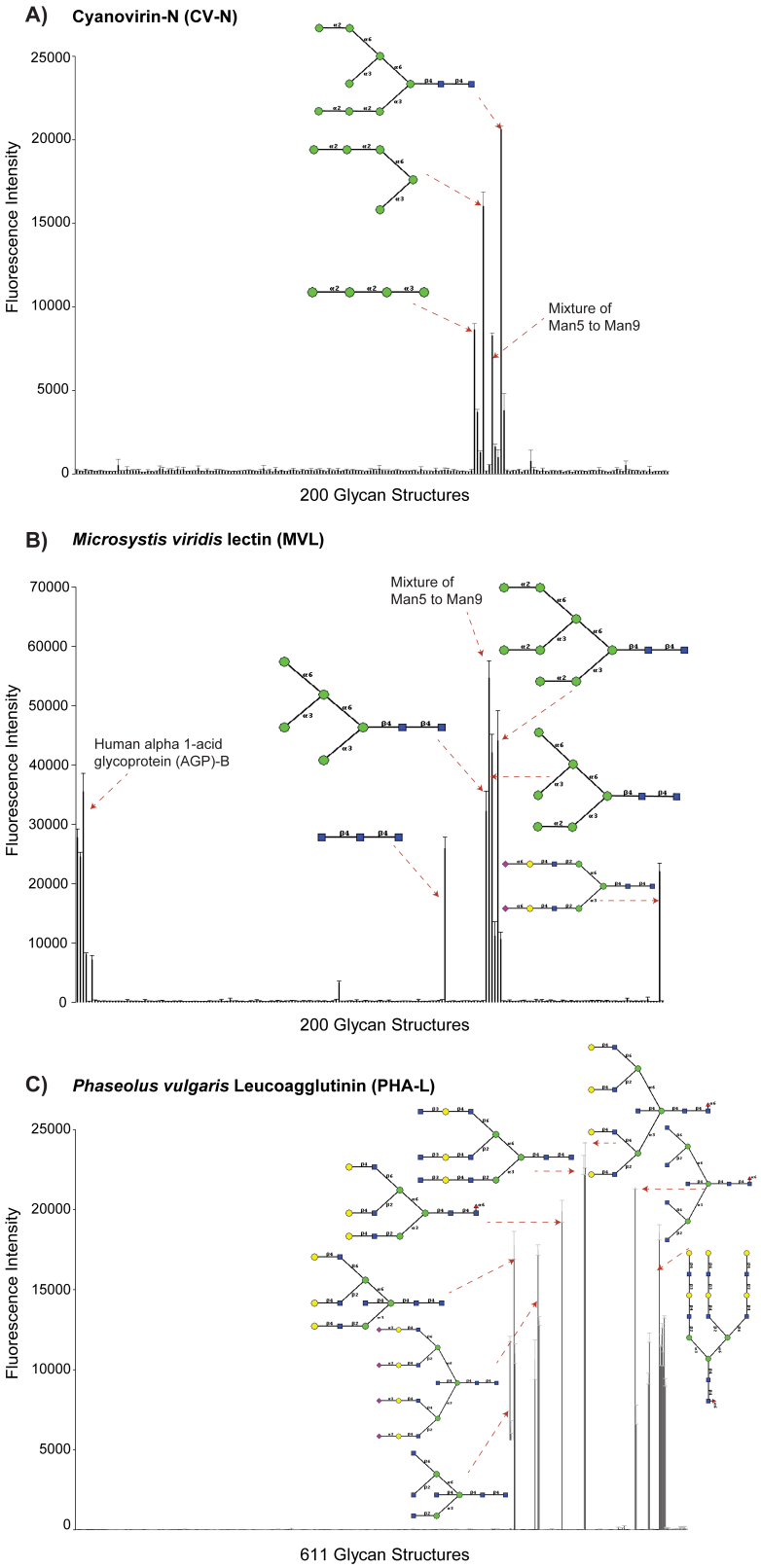
A) Cyanovirin-N (CV-N)
Fluorescence Intensity
25000
20000
15000
10000
5000
0
Mixture of
Man5 to Man9
200 Glycan Structures
B) Microsystis viridis lectin (MVL)
Fluorescence Intensity
70000
60000
50000
40000
30000
20000
10000
0
Mixture of
Man5 to Man9
Human alpha 1-acid
glycoprotein (AGP)-B
200 Glycan Structures
C) Phaseolus vulgaris Leucoagglutinin (PHA-L)
Fluorescence Intensity
25000
20000
15000
10000
5000
0
611 Glycan Structures

Appendix Figure A2. Multiple sequence alignment of Mannosidase II sequences.

A multiple sequence alignment was conducted in T-Coffee using the amino acid sequences of Golgi Mannosidase II (MAN2_DROME, MA2A1_HUMAN, MA2A1_MOUSE, GMAN2_ARATH) and Lysosomal α-Mannosidase (LMANII_DROME, MA2B1_HUMAN, MA2B1_MOUSE, MANA2_ARATH) from *Drosophila melanogaster*, *Homo sapiens*, *Mus musculus*, and *Arabidopsis thaliana* to the α-Mannosidase found in Symbiodiniaceae species *Symbiodinium microadriaticum* (Smic), *Breviolum minutum (*symbB*)*, and *Fugacium kawagutii* (Fkaw).

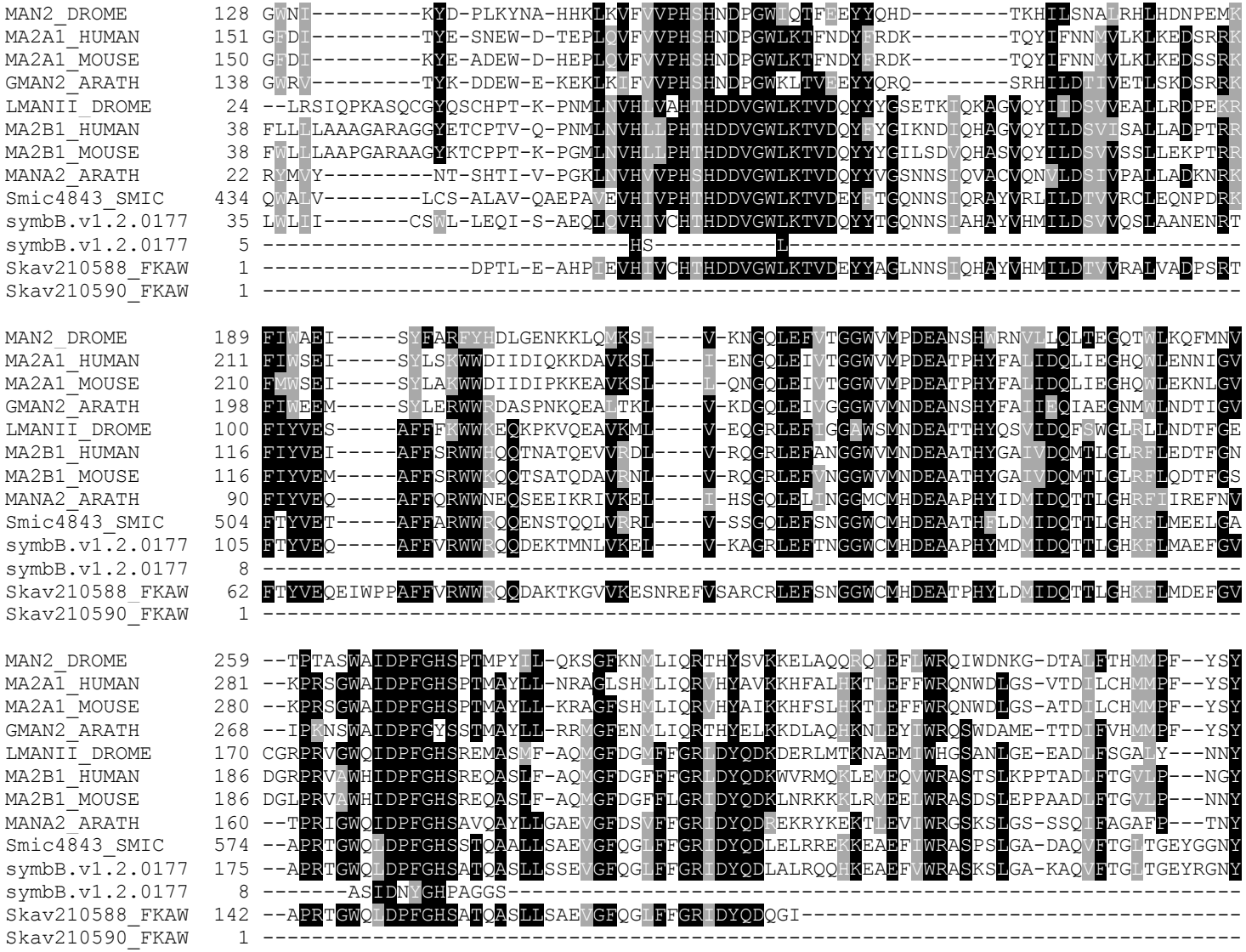
MAN2_DROME
MA2A1_HUMAN
MA2A1_MOUSE
GMAN2_ARATH
LMANII_DROME
MA2B1_HUMAN
MA2B1_MOUSE
MANA2_ARATH
Smic4843_SMIC
symbB.v1.2.0177
symbB.v1.2.0177
Skav210588_FKAW
Skav210590_FKAW
MAN2_DROME
MA2A1_HUMAN
MA2A1_MOUSE
GMAN2_ARATH
LMANII_DROME
MA2B1_HUMAN
MA2B1_MOUSE
MANA2_ARATH
Smic4843_SMIC
symbB.v1.2.0177
symbB.v1.2.0177
Skav210588_FKAW
Skav210590_FKAW
MAN2_DROME
MA2A1_HUMAN
MA2A1_MOUSE
GMAN2_ARATH
LMANII_DROME
MA2B1_HUMAN
MA2B1_MOUSE
MANA2_ARATH
Smic4843_SMIC
symbB.v1.2.0177
symbB.v1.2.0177
Skav210588_FKAW
Skav210590_FKAW

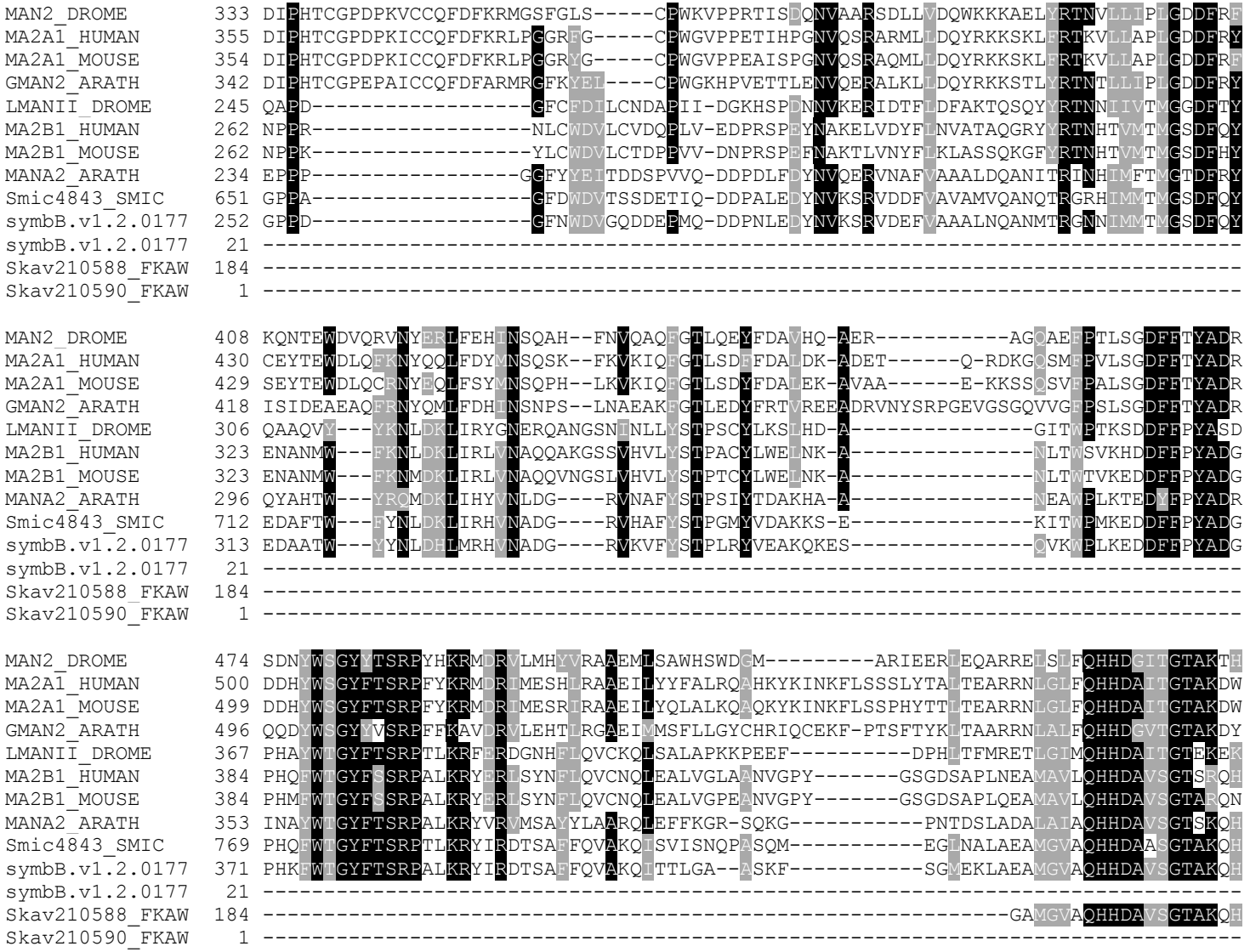
MAN2_DROME 333
MA2A1_HUMAN 355
MA2A1_MOUSE 354
GMAN2_ARATH 342
LMANII_DROME 245
MA2B1_HUMAN 262
MA2B1_MOUSE 262
MANA2_ARATH 234
Smic4843_SMIC 651
symbB.v1.2.0177 252
symbB.v1.2.0177 21
Skav210588_FKAW 184
Skav210590_FKAW 1
MAN2_DROME 408
MA2A1_HUMAN 430
MA2A1_MOUSE 429
GMAN2_ARATH 418
LMANII_DROME 306
MA2B1_HUMAN 323
MA2B1_MOUSE 323
MANA2_ARATH 296
Smic4843_SMIC 712
symbB.v1.2.0177 313
symbB.v1.2.0177 21
Skav210588_FKAW 184
Skav210590_FKAW 1
MAN2_DROME 474
MA2A1_HUMAN 500
MA2A1_MOUSE 499
GMAN2_ARATH 496
LMANII_DROME 367
MA2B1_HUMAN 384
MA2B1_MOUSE 384
MANA2_ARATH 353
Smic4843_SMIC 769
symbB.v1.2.0177 371
symbB.v1.2.0177 21
Skav210588_FKAW 184
Skav210590_FKAW 1

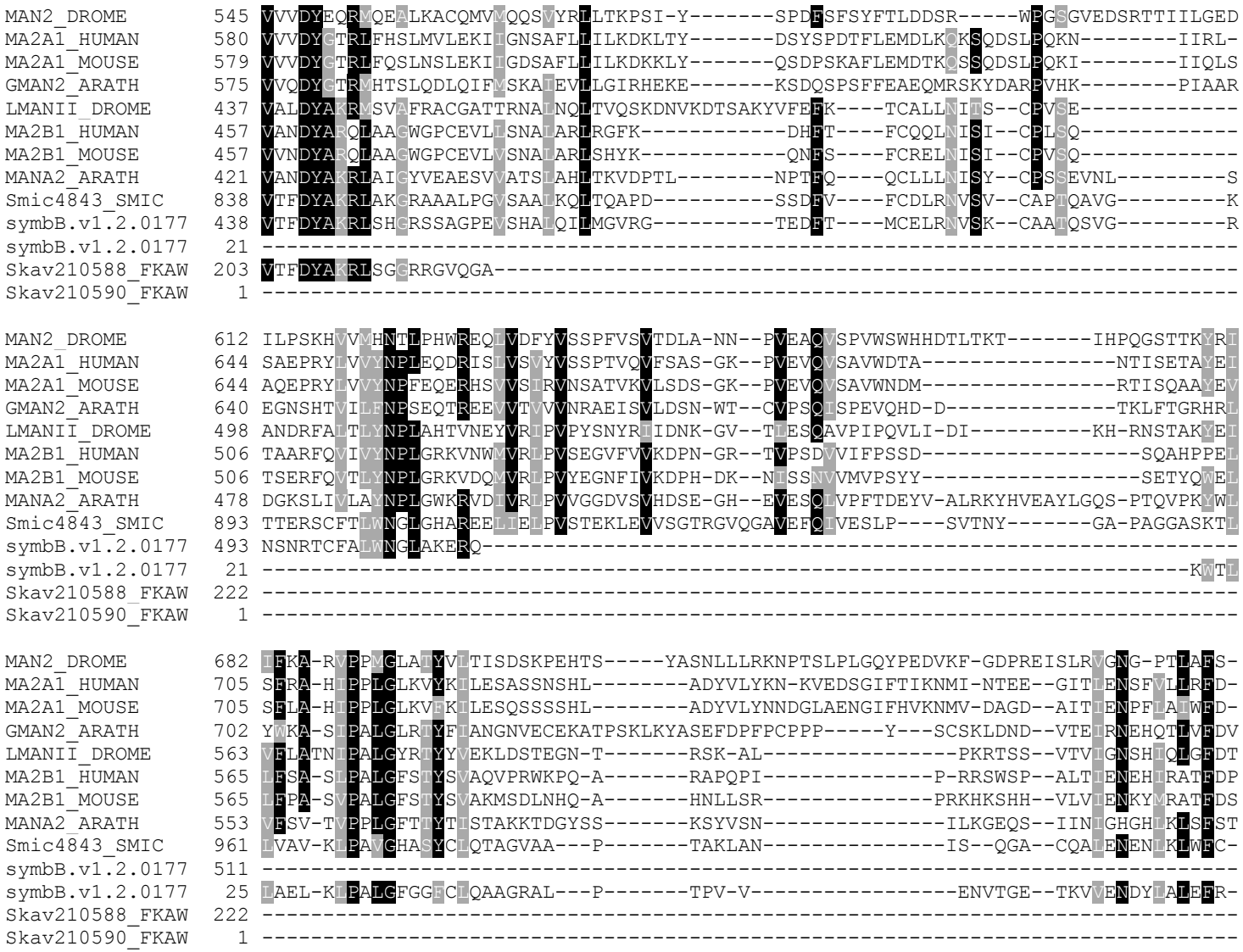
MAN2_DROME 545 VVVDYEQRVQEALKACQMVMQQSVYRLLTKPSI-Y-------SPDFSFSYFTLDDSR-----WPGSGVEDSRTTIILGED
MA2A1_HUMAN 580 VVVDYGTRLFHSLMVLEKIIGNSAFLILKDKLTY-------DSYSPDTFLEMDLKQKSQDSLPQKN--------IIRL-
MA2A1_MOUSE 579 VVVDYGTRLFQSLNSLEKIIGDSAFLILKDKKLY-------QSDPSKAFLEMDTKQSSQDSLPQKI--------IIQLS
GMAN2_ARATH 575 VVQDYGTRVHTSLQDLQIFMSKAIEVLLGIRHEKE-------KSDQSPSFFEAEQMRSKYDARPVHK--------PIAAR
LMANII_DROME 437 VALDYAKRMSVAFRACGATTRNALNQLTVQSKDNVKDTSAKYVFEFK----TCALLNITS--CPVSE-------------
MA2B1_HUMAN 457 VANDYARQLAAGWGPCEVLLSNALARLRGFK----------DHFT----FCQQLNISI--CPLSQ-------------
MA2B1_MOUSE 457 VVNDYARQLAAGWGPCEVLVSNALARLSHYK----------QNFS----FCRELNISI--CPVSQ-------------
MANA2_ARATH 421 VANDYAKRLAIGYVEAESVVATSLAHLTKVDPTL--------NPTFQ----QCLLLNISY--CPSSEVNL---------S
Smic4843_SMIC 838 VTFDYAKRLAKGRAAALPGVSAALKQLTQAPD----------SSDFV----FCDLRNVSV--CAPTQAVG---------K
symbB.v1.2.0177 438 VTFDYAKRLSHGRSSAGPEVSHALQILMGVRG----------TEDFT----MCELRNVSK--CAATQSVG---------R
symbB.v1.2.0177 21 ----------
Skav210588_FKAW 203 VTFDYAKRLSGGRRGVQGA----------
Skav210590_FKAW 1 ----------
MAN2_DROME 612 ILPSKHVVMHNTLPHWREQLVDFYVSSPFVSVTDLA-NN--PVEAQVSPVWSWHHDTLTKT-------IHPQGSTTKYRI
MA2A1_HUMAN 644 SAEPRYLVVYNPLEQDRISLVSVYVSSPTVQVFSAS-GK--PVEVQVSAVWDTA----------------NTISETAYEI
MA2A1_MOUSE 644 AQEPRYLVVYNPFEQERHSVVSIRVNSATVKVLSDS-GK--PVEVQVSAVWNDM----------------RTISQAAYEV
GMAN2_ARATH 640 EGNSHTVILFNPSEQTREEVVTVVVNRAEISVLDSN-WT--CVPSQISPEVQHD-D--------------TKLFTGRHRL
LMANII_DROME 498 ANDRFALTLYNPLAHTVNEYVRIPVPYSNYRIIDNK-GV--TLESQAVPIPQVLI-DI----------KH-RNSTAKYEI
MA2B1_HUMAN 506 TAARFQVIVYNPLGRKVNWMVRLPVSEGVFVVKDPN-GR--TVPSDVVIFPSSD-------------------SQAHPPEL
MA2B1_MOUSE 506 TSERFQVTLYNPLGRKVDQMVRLPVYEGNFIVKDPH-DK--NISSNVVMVPSYY-------------------SETYQWEL
MANA2_ARATH 478 DGKSLIVLAYNPLGWKRVDIVRLPVVGGDVSVHDSE-GH--EVESQLVPFTDEYV-ALRKYHVEAYLGQS-PTQVPKYWL
Smic4843_SMIC 893 TTERSCFTLWNGLGHAREELIELPVSTEKLEVVSGTRGVQGAVEFQIVESLP----SVTNY-------GA-PAGGASKTL
symbB.v1.2.0177 493 NSNRTCFALWNGLAKERQ----------
symbB.v1.2.0177 21 ----------KWTL
Skav210588_FKAW 222 ----------
Skav210590_FKAW 1 ----------
MAN2_DROME 682 IFKA-RVPPVGLATYVLTISDSKPEHTS-----YASNLLLRKNPTSLPLGQYPEDVKF-GDPREISLRVGNG-PTLAFS-
MA2A1_HUMAN 705 SFRA-HIPPLGLKVYKILESASSNSHL--------ADYVLYKN-KVEDSGIFTIKNMI-NTEE--GITIENSFVLLRFD-
MA2A1_MOUSE 705 SFLA-HIPPLGLKVFKILESQSSSSHL--------ADYVLYNNDGLAENGIFHVKNMV-DAGD--AITIENPFLAIWFD-
GMAN2_ARATH 702 YWKA-SIPALGLRTYFIANGNVECEKATPSKLKYASEFDPFPCPPP-----Y---SCSKLDND--VTEIRNEHQTLVFDV
LMANII_DROME 563 VFLATNIPALGYRTYYVEKLDSTEGN-T-------RSK-AL----------------PKRTSS--VTVIGNSHIQLGFDT
MA2B1_HUMAN 565 LFSA-SLPALGFSTYSVAQVPRWKPQ-A-------RAPQPI--------------P-RRSWSP--ALTIENEHIRATFDP
MA2B1_MOUSE 565 LFPA-SVPALGFSTYSVAKMSDLNHQ-A-------HNLLSR--------------PRKHKSHH--VLVIENKYMRATFDS
MANA2_ARATH 553 VFSV-TVPPLGFTTYTISTAKKTDGYSS-------KSYVSN---------------ILKGEQS--IINIGHGHLKLSFST
Smic4843_SMIC 961 LVAV-KLPAVGHASYCLQTAGVAA---P-------TAKLAN---------------IS--QGA--CQAIENENLKLWFC-
symbB.v1.2.0177 511 ----------
symbB.v1.2.0177 25 LAEL-KLPALGFGGFCLQAAGRAL---P-------TPV-V----------------ENVTGE--TKVVENDYLALEFR-
Skav210588_FKAW 222 ----------
Skav210590_FKAW 1 ----------

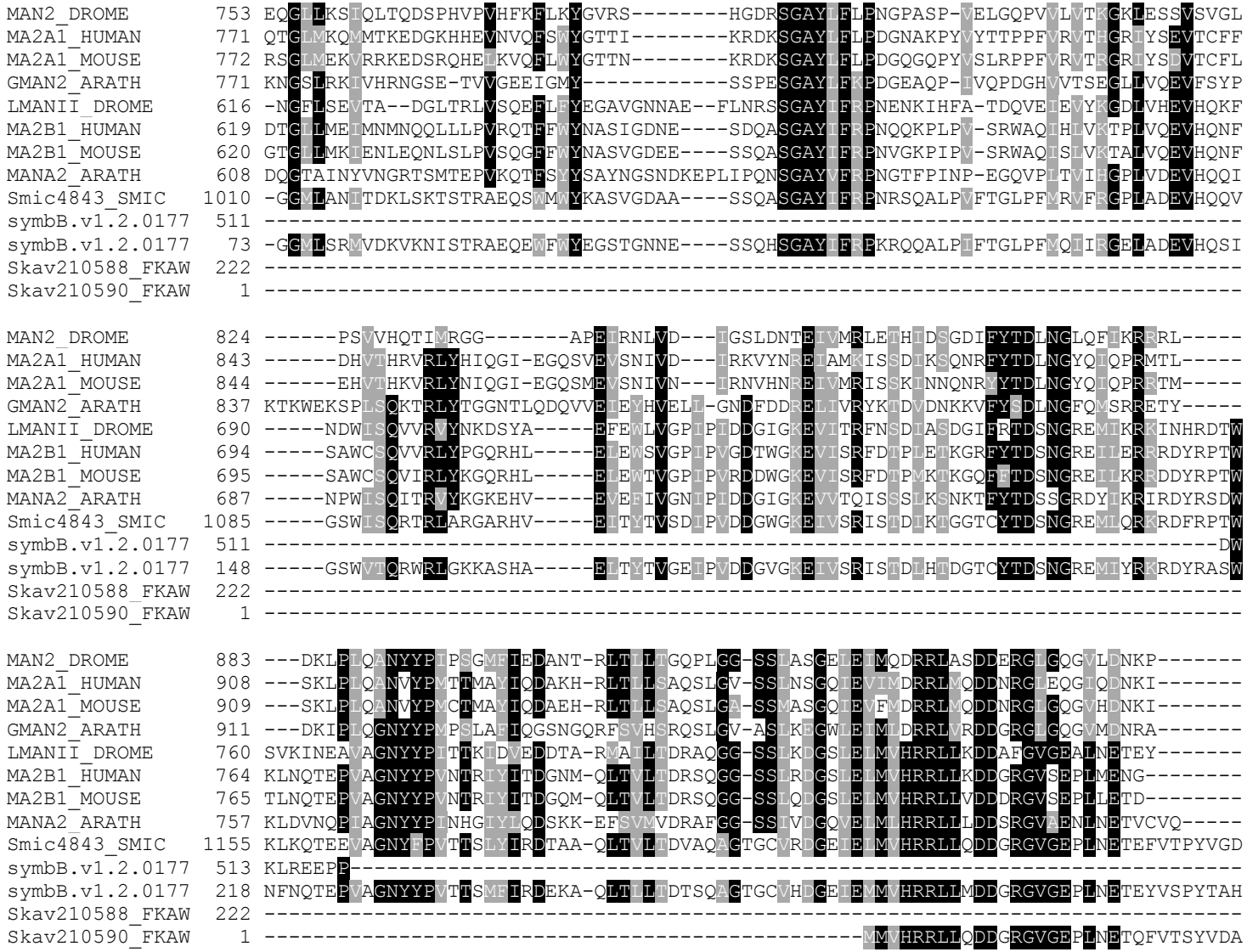
MAN2_DROME 753 EQGLKSIQLTQDSPHVPVHFKFLKYGVRS--------HGDRSGAYLFLPNGPASP-VELGQPVVLVTRGKLESSVSVGL
MA2A1_HUMAN 771 QTGLMKQMMTKEDGKHHEVNVQFSWYGTTI--------KRDKSGAYLFLPDGNAKPYVYTTPPFVRVTRGRIYSEVTCFF
MA2A1_MOUSE 772 RSGLMEKVRRKEDSRQHELKVQFLWYGTTN--------KRDKSGAYLFLPDGQGQPYVSLRPPFVRVTRGRIYSDVTCFL
GMAN2_ARATH 771 KNGSLRKIVHRNGSE-TVVGEEIGMY----------SSPESGAYLFKPDGEAQP-IVQPDGHVVTSEGLLVQEVFSYP
LMANII_DROME 616 -NGFLSEVTA--DGLTRLVSQEFLFYEGAVGNNAE--FLNRSSGAYIFRPNENKIHFA-TDQVEIEVYKGDLVHEVHQKF
MA2B1_HUMAN 619 DTGLLMEIMNMNQQLLLPVRQTFFWYNASIGDNE----SDQASGAYIFRPNQQKPLPV-SRWAQIHIVKTPLVQEVHQNF
MA2B1_MOUSE 620 GTGLLMKIENLEQNLSLPVSQGFFWYNASVGDEE----SSQASGAYIFRPNVGKPIPV-SRWAQISIVKTALVQEVHQNF
MANA2_ARATH 608 DQGTAINYVNGRTSMTEPVKQTFSYYSAYNGSNDKEPLIPQNSGAYVFRPNGTFPINP-EGQVPITVIHGPLVDEVHQQI
Smic4843_SMIC 1010 -GGYLANITDKLSKTSTRAEQSWMWYKASVGDAA----SSQASGAYIFRPNRSQALPVFTGLPFMRVFRGPLADEVHQQV
symbB.v1.2.0177 511 ----------
symbB.v1.2.0177 73 -GGYLSRMVDKVKNISTRAEQEWFWYEGSTGNNE----SSQHSGAYIFRPKRQQALPIFTGLPFMQIIRGELADEVHQSI
Skav210588_FKAW 222 ----------
Skav210590_FKAW 1 ----------
MAN2_DROME 824 ------PSVVHQTIMRGG-------APEIRNLVD---IGSLDNTEIVMRLETHIDSGDIFYTDLNGLQFIKRRRL-----
MA2A1_HUMAN 843 ------DHVTHRVRLYHIQGI-EGQSVEVSNIVD---IRKVYNREIAMKISSDIKSQNRFYTDLNGYQIQPRMTL-----
MA2A1_MOUSE 844 ------EHVTHKVRLYNIQGI-EGQSMEVSNIVN---IRNVHNREIVMRISSKINNQNRYYTDLNGYQIQPRRTM-----
GMAN2_ARATH 837 KTKWEKSPLSQKTRLYTGGNTLQDQVVEIEVHVELL-GNDFDDRELIVRYKTDVDNKKVFYSDLNGFQVSRRETY-----
LMANII_DROME 690 -----NDWISQVVRVYNKDSYA-----EFEWLVGPIPIDDGIGKEVITRFNSDIASDGIFRTDSNGREMIKRKINHRDTW
MA2B1_HUMAN 694 -----SAWCSQVVRLYPGQRHL-----ELEWSVGPIPVGDTWGKEVISRFDTPLETKGRFYTDSNGREIIERRRDYRPTW
MA2B1_MOUSE 695 -----SAWCSQVIRLYKGQRHL-----ELEWTVGPIPVRDDWGKEVISRFDTPMKTKGQFFTDSNGREIIKRRDDYRPTW
MANA2_ARATH 687 -----NPWISQITRVYKGKEHV-----EVEFIVGNIPIDDGIGKEVVTQISSSLKSNKTFYTDSSGRDYIKRIRDYRSDW
Smic4843_SMIC 1085 -----GSWISQRTRLARGARHV-----ELTYTVSDIPVDDGWGKEIVSRISTDIKTGGTCYTDSNGREMIQRKRDFRPTW
symbB.v1.2.0177 511 ----------DW
symbB.v1.2.0177 148 -----GSWVTQRWRLGKKASHA-----ELTYTVGEIPVDDGVGKEIVSRISTDLHTDGTCYTDSNGREMIYRKRDYRASW
Skav210588_FKAW 222 ----------
Skav210590_FKAW 1 ----------
MAN2_DROME 883 ---DKLPLQANYYPIPSGMFIEDANT-RLTLLIGQPLGG-SSLASGELEIMQDRRLASDDERGLGQGVLDNKP-------
MA2A1_HUMAN 908 ---SKLPLQANVYPMTTMAYIQDAKH-RLTLLSAQSLGV-SSINSGQIEVIMDRRLMQDDNRGLEQGIQDNKI-------
MA2A1_MOUSE 909 ---SKLPLQANVYPMCTMAYIQDAEH-RLTLLSAQSLGA-SSMASGQIEVFMDRRLMQDDNRGLGQGVHDNKI-------
GMAN2_ARATH 911 ---DKIPLQGNYYPMPSLAFIQGSNGQRFSVHSRQSLGV-ASIKEGWLEIMLDRRLVRDDGRGLGQGVMDNRA-------
LMANII_DROME 760 SVKINEAVAGNYYPITTKIDVEDDTA-RVAILVDRAQGG-SSLKDGSLELMVHRRLLKDDAFGVGEAINETEY-------
MA2B1_HUMAN 764 KLNQTEPVAGNYYPVNTRIYITDGNM-QLTVLVDRSQGG-SSLRDGSLELMVHRRLLKDDGRGVSEPLMENG--------
MA2B1_MOUSE 765 TLNQTEPVAGNYYPVNTRIYITDGQM-QLTVLVDRSQGG-SSLQDGSLELMVHRRLLVDDDRGVSEPLLETD--------
MANA2_ARATH 757 KLDVNQPIAGNYYPINHGIYLQDSKK-EFSVMVDRAFGG-SSIVDGQVELMLHRRLLLDDSRGVAENLNETVCVQ-----
Smic4843_SMIC 1155 KLKQTEEVAGNYFPVTTSLYIRDTAA-QLTVLVDVAQAGTGCVRDGEIELMVHRRLLQDDGRGVGEPLNETEFVTPYVGD
symbB.v1.2.0177 513 KLREEPP----------
symbB.v1.2.0177 218 NFNQTEPVAGNYYPVTTSMFIRDEKA-QLTLLVDTSQAGTGCVHDGEIEMMVHRRLLMDDGRGVGEPLNETEYVSPYTAH
Skav210588_FKAW 222 ----------
Skav210590_FKAW 1 ----------MMVHRRLLQDDGRGVGEPLNETQFVTSYVDA

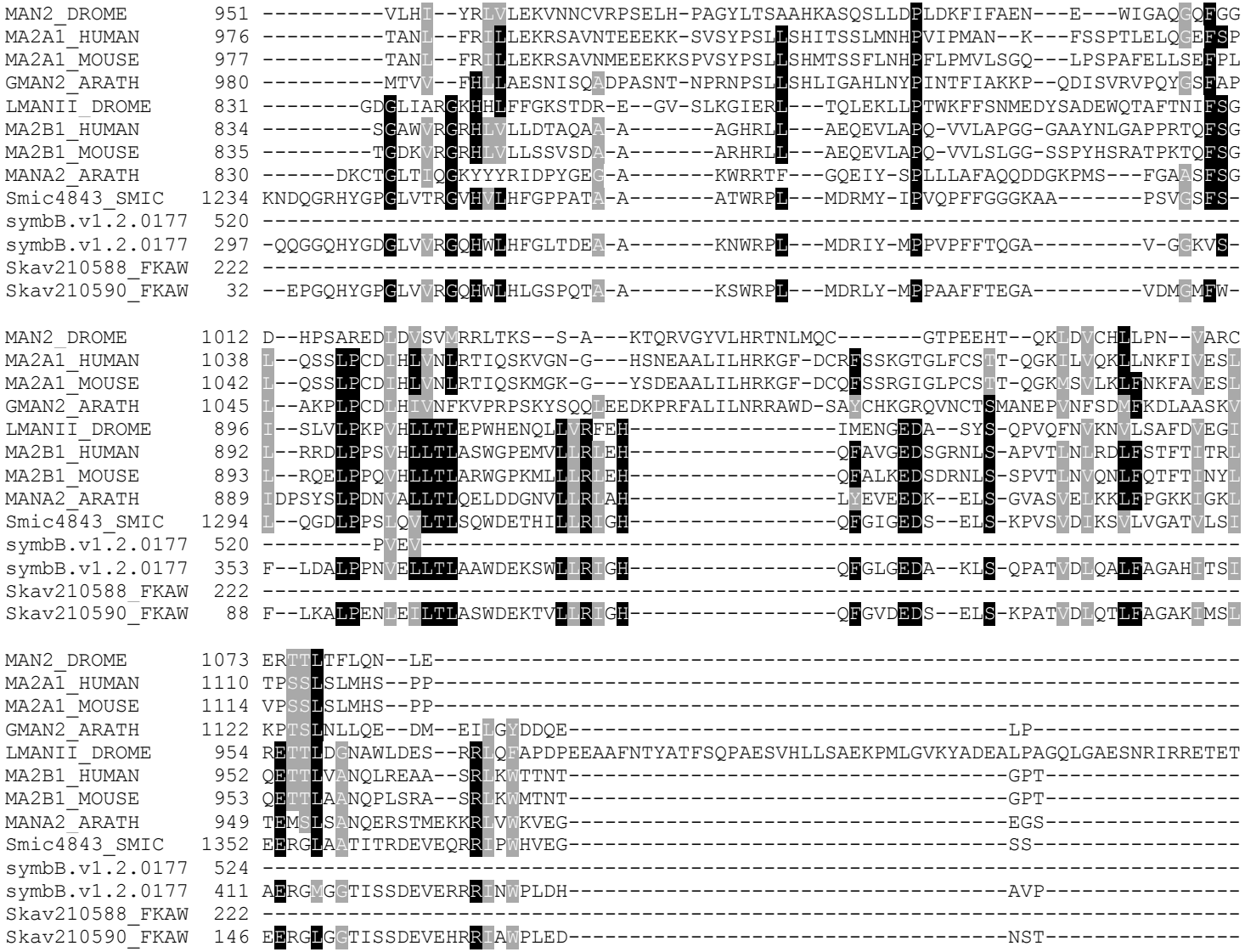
MAN2_DROME 951 ----------VLHI--YRLVLEKVNNCVRPSELH-PAGYLTSAAHKASQSLLDPLDKFIFAEN---E---WIGAQGQFGG
MA2A1_HUMAN 976 ----------TANL--FRILLEKRSAVNTEEEKK-SVSYPSLLSHITSSLMNHPVIPMAN--K---FSSPTLELQGEFSP
MA2A1_MOUSE 977 ----------TANL--FRILLEKRSAVNMEEEKKSPVSYPSLLSHMTSSFLNHPFLPMVLSGQ---LPSPAFELLSEFPL
GMAN2_ARATH 980 ----------MTVV--FHLLAESNISQADPASNT-NPRNPSLLSHLIGAHLNYPINTFIAKKP--QDISVRVPQYGSFAP
LMANII_DROME 831 ---------GDGLIARGKHHLFFGKSTDR-E--GV-SLKGIERL---TQLEKLLPTWKFFSNMEDYSADEWQTAFTNIFSG
MA2B1_HUMAN 834 ---------SGAWVRGRHLVLLDTAQAA-A-------AGHRLL---AEQEVLAPQ-VVLAPGG-GAAYNLGAPPRTQFSG
MA2B1_MOUSE 835 ---------TGDKVRGRHLVLLSSVSDA-A-------ARHRLL---AEQEVLAPQ-VVLSLGG-SSPYHSRATPKTQFSG
MANA2_ARATH 830 ------DKCTGLTIQGKYYYRIDPYGEG-A-------KWRRTF---GQEIY-SPLLLAFAQQDDGKPMS---FGAASFSG
Smic4843_SMIC 1234 KNDQGRHYGPGLVTRGVHVLHFGPPATA-A-------ATWRPL---MDRMY-IPVQPFFGGGKAA-------PSVGSFS-
symbB.v1.2.0177 520 ----------
symbB.v1.2.0177 297 -QQGGQHYGDGLVVRGQHWLHFGLTDEA-A-------KNWRPL---MDRIY-MPPVPFFTQGA---------V-GGKVS-
Skav210588_FKAW 222 ----------
Skav210590_FKAW 32 --EPGQHYGPGLVVRGQHWLHLGSPQTA-A-------KSWRPL---MDRLY-MPPAAFFTEGA---------VDMGMFW-
MAN2_DROME 1012 D--HPSAREDLDVSVMRRLTKS--S-A---KTQRVGYVLHRTNLMQC-------GTPEEHT--QKLDVCHLLPN--VARC
MA2A1_HUMAN 1038 L--QSSLPCDIHLVNLRTIQSKVGN-G---HSNEAALILHRKGF-DCRFSSKGTGLFCSTT-QGKLLVQKLLNKFIVESL
MA2A1_MOUSE 1042 L--QSSLPCDIHLVNLRTIQSKMGK-G---YSDEAALILHRKGF-DCQFSSRGIGLPCSTT-QGKVSVLKLFNKFAVESL
GMAN2_ARATH 1045 L--AKPLPCDLHIVNFKVPRPSKYSQQIEEDKPRFALILNRRAWD-SAYCHKGRQVNCTSMANEPVNFSDMFKDLAASKV
LMANII_DROME 896 I--SLVLPKPVHLLTLEPWHENQLLVRFEH----------------IMENGEDA--SYS-QPVQFNVKNVLSAFDVEGI
MA2B1_HUMAN 892 L--RRDLPPSVHLLTLASWGPEMVLIRIEH----------------QFAVGEDSGRNLS-APVTLNLRDLFSTFTITRL
MA2B1_MOUSE 893 L--RQELPPQVHLLTLARWGPKMLLIRIEH----------------QFALKEDSDRNLS-SPVTLNVQNLFQTFTINYL
MANA2_ARATH 889 IDPSYSLPDNVALLTLQELDDGNVLIRIAH----------------LYEVEEDK--ELS-GVASVELKKLFPGKKIGKL
Smic4843_SMIC 1294 L--QGDLPPSLQVLTLSQWDETHILIRIGH----------------QFGIGEDS--ELS-KPVSVDIKSVLVGATVLSI
symbB.v1.2.0177 520 ---------PVEV----------
symbB.v1.2.0177 353 F--LDALPPNVELLTLAAWDEKSWLIRIGH----------------QFGLGEDA--KLS-QPATVDIQALFAGAHITSI
Skav210588_FKAW 222 ----------
Skav210590_FKAW 88 F--LKALPENLEILTLASWDEKTVLIRIGH----------------QFGVDEDS--ELS-KPATVDIQTLFAGAKIMSL
MAN2_DROME 1073 ERTTLTFLQN--LE----------
MA2A1_HUMAN 1110 TPSSLSLMHS--PP----------
MA2A1_MOUSE 1114 VPSSLSLMHS--PP----------
GMAN2_ARATH 1122 KPTSLNLLQE--DM--EILGYDDQE----------LP----------
LMANII_DROME 954 RETTLDGNAWLDES--RRLQFAPDPEEAAFNTYATFSQPAESVHLLSAEKPMLGVKYADEALPAGQLGAESNRIRRETET
MA2B1_HUMAN 952 QETTLVANQLREAA--SRLKWTTNT----------GPT----------
MA2B1_MOUSE 953 QETTLAANQPLSRA--SRLKWMTNT----------GPT----------
MANA2_ARATH 949 TEMSLSANQERSTMEKKRLVWKVEG----------EGS----------
Smic4843_SMIC 1352 EERGLAATITRDEVEQRRIPWHVEG----------SS----------
symbB.v1.2.0177 524 ----------
symbB.v1.2.0177 411 AERGVGGTISSDEVERRRINWPLDH----------AVP----------
Skav210588_FKAW 222 ----------
Skav210590_FKAW 146 EERGLGGTISSDEVEHRRIAWPLED----------NST----------

ManII Residue	ManII AA	Conserved Sequence	Importance	Bmin AA	Smic AA	Fkav AA	Lysosomal Mannosidase AA
64	Q	DGGVWKQG	m5 stacking	S	M		K/G/W/M/T/L
90	H	VVPHSHNDPGW	Zn coordination	H	H	H	H
92	D	VVPHSHNDPGW	Zn coordination	D	D	D	D
95	W	VVPHSHNDPGW	m5 stacking	W	W	W	W
204	D	WAIDPFG	nucleophile	D	D	D	D
269	YSY	MPFYSYDIPHTCGPE	m5 h-bonding	YRG	YGG	GRR	FSG/FTG/FLG
298,299	P	PP	m5 stacking	DD	DD		DN/DD/ED/DG
340	D	PLGDDFR	m5 stacking	D	D		D
343	R	PLGDDFR	m5 h-bonding	Q	Q		T/Q/H/A
426	R/V	YADR		G	G		G/D/N
431	W	YWS/T		W	W		W
470,471,472	HHD	LFQHHD	Zn coordination, m5 h-bonding	HHD	HHD		HHD
727	Y	GAYLF	m5 h-bonding, stacking	Y	Y		Y

Appendix Table A1: ManII site conservation in Symbiodiniaceae.

The conserved ManII residue in *Drosophila* is shown on the left, with its corresponding amino acid and conserved sequence. The importance of the residue for binding affinity is shown in the center. Symbiodiniaceae residues are shown for *B. minutum*, *S. microadriaticum*, and *F. kawagutii.* Conserved residues for lysosomal mannosidase amino acids are shown on the right.

	Breviolum minutum				Symbiodinium microadriaticum				Fugacium kawagutii				Perkinsus marinus				Toxoplasma gondii				Plasmodium falciparum			
N-Glycan Synthesis	Gene	Score	Eval	Iden	Gene	Score	Eval	Iden	Gene	Score	Eval	Iden	Gene	Score	Eval	Iden	Gene	Score	Eval	Iden	Gene	Score	Eval	Iden
ALG13	symbB.v1.2.008534.t1|scaffold538.1|size242405|1	86	3.25E-16	43	Smic27423	110	4.83E-26	49	Skav20751 6	97	2.36E-20	47	Pmar_PMAR015450	73	0.09	35	TGME49_268340	167	1.20E-14	40.8	PF3D7_0806400	154	4.30E-13	43
ALG14	symbB.v1.2.034275.t1|scaffold4398.1|size40168|2	146	8.76E-42	38	Smic33514	157	4.79E-46	43					Pmar_PMAR000327	105	2.90E-07	52.8	TGME49_207070	290	2.90E-33	43.4	ALG14	156	1.20E-14	44.6
ALG1	symbB.v1.2.027383.t1|scaffold2713.1|size74948|3	137	7.38E-36	38	Smic38965	272	1.38E-78	41	Skav26113	47	1.81E-05	30	Pmar_PMAR020699	239	9.90E-26	55.8	TGME49_230590	285	3.30E-32	47				
ALG2	symbB.v1.2.008675.t1|scaffold539.1|size189864|7	368	3.85E-115	49	Smic41638	355	3.39E-116	49	Skav20521 0	53	1.30E-06	37	Pmar_PMAR013250	190	6.20E-19	55.4	TGME49_227790	172	2.00E-16	53.2	CLAG2	75	0.0056	24
ALG11	symbB.v1.2.001761.t1|scaffold95.1|size600632|9	336	1.02E-104	44	Smic25097	447	2.90E-140	47	Skav20273 1	36	0.07	42	Pmar_PMAR018755	191	4.30E-19	41.8	TGME49_246982	157	2.60E-14	47				
ALG3	symbB.v1.2.013786.t1|scaffold975.1|size153061|1	212	5.66E-59	40	Smic9149	54	3.84E-07	31					Pmar_PMAR023648	140	4.00E-12	53.3								
ALG9	symbB.v1.2.032558.t2|scaffold3923.1|size48286|4	220	6.30E-32	51	Smic34730	311	1.67E-62	38	Skav22546 5	57	6.95E-08	41	Pmar_PMAR019024	106	4.90E-07	54.3	TGME49_321660	89	1.20E-04	42.5	GPI10	78	0.0027	23.8
ALG12	symbB.v1.2.012500.t1|scaffold862.1|size157115|9	39	0.06	31	Smic23540	258	6.22E-74	42	Skav22120 6	235	2.09E-67	35	Pmar_PMAR016091	194	1.20E-19	79.5								
ALG5	symbB.v1.2.007750.t1|scaffold480.1|size253386|12	231	3.09E-72	45	Smic39167	243	4.29E-76	46	Skav20832 3	39	0.01	29	Pmar_PMAR018469	327	3.90E-38	50.8	TGME49_216540	240	5.80E-26	51.8	DPM1	83	3.50E-04	30.2
ALG6	symbB.v1.2.013301.t1|scaffold937.1|size150259|7	297	2.56E-86	39	Smic22253	120	1.80E-27	32	Skav21015 6	174	1.24E-47	32	Pmar_PMAR028409	245	2.80E-27	56.3	TGME49_262030	118	4.60E-09	45				
ALG8	symbB.v1.2.013301.t1|scaffold937.1|size150259|7	129	3.25E-30	31	Smic30006	284	1.97E-82	43	Skav22936 7	62	4.20E-10	55	Pmar_PMAR002960	161	3.60E-15	46.9	TGME49_314730	208	6.20E-22	61.8				
ALG10	symbB.v1.2.021974.t1|scaffold1899.1|size238565|10	208	1.10E-59	33	Smic14123	158	2.43E-40	31	Skav23246 1	210	1.72E-60	32	Pmar_PMAR005103	92	1.90E-05	48.6	TGME49_263690	104	3.30E-07	53.1				
STT	symbB.v1.2.013974.t1|scaffold1001.1|size146904|5	383	1.82E-115	32	Smic38591	377	1.30E-116	34	Skav23448 9	94	1.04E-20	46	Pmar_PMAR025427	514	6.60E-65	62.8	TGME49_231430	520	8.90E-66	63.7	STT3	390	1.60E-47	
GCS1	symbB.v1.2.029725.t1|scaffold3288.1|size59728|1	285	2.35E-55	33	Smic33937	337	1.18E-41	41	Skav21128 2	44	0.001	43	Pmar_PMAR017791	151	7.40E-13	59.1	TGME49_242020	128	1.10E-09	53.2				
GANAB	symbB.v1.2.008520.t1|scaffold527.1|size293072|18	563	0	38	Smic30546	631	0	38	Skav20048 4	116	7.40E-28	35	Pmar_PMAR016665	992	9.5E-130	54.1	TGME49_253030	667	1.40E-84	54.5				
MAN1A1	symbB.v1.2.025226.t1|scaffold2429.1|size79298|6	242	1.69E-70	34	Smic1440	326	6.65E-100	43	Skav22590	112	5.58E-25	39	Pmar_PMAR020391	226	2.30E-23	44.1								

	Breviolum minutum				Symbiodinium microadriaticum				Fugacium kawagutii				Perkinsus marinus				Toxoplasma gondii				Plasmodium falciparum			
N-Glycan Synthesis	Gene	Score	Eval	Iden	Gene	Score	Eval	Iden	Gene	Score	Eval	Iden	Gene	Score	Eval	Iden	Gene	Score	Eval	Iden	Gene	Score	Eval	Iden
MAN1A2	symbB.v1.2.025226.t1|scaffold2429.1|size79298|6	252	1.80E-74	36	Smic1440	306	9.61E-93	35	Skav22590	112	3.40E-25	40	Pmar_PMAR020391	238	3.40E-25	45.1								
MAN1B1	symbB.v1.2.025226.t1|scaffold2429.1|size79298|6	287	3.80E-87	39	Smic1440	302	1.08E-90	39	Skav22590	131	3.53E-31	38	Pmar_PMAR020391	227	2.40E-23	45	TGME49_264450	73	0.045	25.5				
MGAT1	symbB.v1.2.037358.t1|scaffold5495.1|size26502|3	210	9.89E-61	46	Smic24963	230	1.29E-70	30	Skav223442	86	2.65E-19	54	Pmar_PMAR009039	233	5.30E-25	56.3								
MAN2A1	symbB.v1.2.017759.t1|scaffold1355.1|size123688|1	213	8.96E-58	30	Smic4843	282	5.18E-77	28	Skav210588	161	1.01E-29	37	Pmar_PMAR026493	149	1.80E-12	38								
MAN2B1	symbB.v1.2.017759.t1|scaffold1355.1|size123688|1	428	5.71E-137	50	Smic4843	762	0.00E+00	44.5	Skav210588	246	1.55E-56	55	Pmar_PMAR026493	524	1.10E-64	58								
MGAT2	symbB.v1.2.014463.t1|scaffold1055.1|size140776|5	34	1.36E+00	23	Smic19105	40	0.02	26	Skav233648	33	3.17E+00	25												
MGAT3	symbB.v1.2.002545.t1|scaffold103.1|size331058|10	51	4.13E-06	27	Smic3340	40	0.02	25	Skav215135	38	3.00E-02	27	Pmar_PMAR007528	106	5.57E-07	34.3	TGME49_207750	76	0.0089	39.5				
MGAT4A	symbB.v1.2.033022.t1|scaffold4044.1|size45693|5	141	8.27E-36	35	Smic12	174	1.29E-44	30																
MGAT4B	symbB.v1.2.033022.t1|scaffold4044.1|size45693|5	146	2.86E-37	34	Smic12	153	5.41E-38	29																
MGAT4C	symbB.v1.2.033022.t1|scaffold4044.1|size45693|5	174	1.74E-47	36	Smic12	193	2.30E-51	29	Skav211800	30	9.79E+00	26												
MGAT4D	symbB.v1.2.033022.t1|scaffold4044.1|size45693|5	100	1.44E-22	30	Smic12	109	2.03E-24	30	Skav225805	39	1.00E-02	36									PF3D7_041080 0	74	0.0068	26.7
MGAT5	symbB.v1.2.027073.t3|scaffold2751.1|size71576|2	62	4.65E-09	27	Smic31095	57	2.69E-07	26	Skav217085	31.6	2.12E+00	29												
MGAT5B	symbB.v1.2.027073.t3|scaffold2751.1|size71576|2	62	7.04E-09	25	Smic31095	65	6.41E-10	25	Skav221354	36	7.00E-01	27												
XYLT1	symbB.v1.2.020832.t1|scaffold1775.1|size101854|1	81	1.79E-14	26	Smic32875	89	4.74E-17	26									TGME49_309160	75	0.03	25.4	PF3D7_134380 0	70	0.091	28.9
FUT8	symbB.v1.2.027005.t1|scaffold2737.1|size71945|3	49	2.39E-05	23	Smic28583	52	3.86E-06	25	Skav233149	56	4.17E-08	25												

	Breviolum minutum				Symbiodinium microadriaticum				Fugacium kawagutii				Perkinsus marinus				Toxoplasma gondii				Plasmodium falciparum			
N-Glycan Synthesis	Gene	Score	Eval	Iden	Gene	Score	Eval	Iden	Gene	Score	Eval	Iden	Gene	Score	Eval	Iden	Gene	Score	Eval	Iden	Gene	Score	Eval	Iden
FUT11	symbB.v1.2.020659.t1|scaffold1748.1|size222129|7	91	1.12E-18	32	Smic38835	63	1.56E-09	27	Skav21320	32	4.72E+00	50	Pmar_PMAR024081	110	1.90E-07	44.2								
B4GALT1	symbB.v1.2.030619.t1|scaffold3471.1|size56067|7	96	6.25E-22	32	Smic22386	108	2.87E-24	28	Skav21032	52	3.61E-07	47	Pmar_PMAR007565	78	0.0044	43.3	TGME49_314660	83	8.50E-04	42.2	PF3D7_0609900	68	0.065	28.8
B4GALT2	symbB.v1.2.030619.t1|scaffold3471.1|size56067|7	99	6.16E-23	34	Smic22386	104	3.94E-23	33	Skav21032	52	1.65E-07	27	Pmar_PMAR007565	73	0.021	41.2	TGME49_259080	76	0.0056	40.9				
B3GALT1	symbB.v1.2.031248.t1|scaffold3605.1|size53397|2	66	5.32E-11	27	Smic25670	81	7.36E-16	26	Skav26048	65	5.56E-11	26	Pmar_PMAR016328	96	7.60E-06	28.8	TGME49_321570	72	0.018	38.6				
SIAT1	symbB.v1.2.039159.t1|scaffold6378.1|size18592|2	34	1.64E+00	27	Smic2669	33	3.27E+00	33	Skav20734	33	1.55E+00	30												
SIAT2	Smic25787	36	4.30E-01	40	Skav200920	32	5.35E+00	41																
FUT13	symbB.v1.2.020659.t1|scaffold1748.1|size222129|7	75	8.77E-14	26	Smic38835	70	7.01E-12	28					Pmar_PMAR003958	83	9.70E-04	36.6								
HEXO1	symbB.v1.2.034859.t1|scaffold4576.1|size37795|4	330	8.82E-103	38	Smic24332	200	1.47E-54	40	Skav215817	111	1.26E-25	25	Pmar_PMAR009436	152	3.00E-13	47.5								

Appendix Table A2: N-glycan biosynthesis datasheet

N-glycan biosynthesis BLASTp searches were performed in Symbiodiniaceae species and in related alveolates *Perkinsus marinus*, *Toxoplasma gondii*, and *Plasmodium falciparum*. Manually annotated N-glycan protein sequences from humans were collected from Uniprot and queried directly against a target species protein database consisting of gene models. The first result of each successful search (gene) is shown for each protein query, along with its score, eval, and % identity.

7.2 Appendix B: Supplementary materials for Chapter 3

Appendix Table B1: Aiptasia and Symbiodiniaceae strain information

Strain	ITS2 Type of symbiont	Source
Aiptasia		
H2	B1	Collected at Coconut Island in Kaneohe Bay, HI
JK	B2	Population collected at Wilmington, NC in 2016
VWA12	B1	Clone from population collected from an aquarium in Corvallis, OR
VWB9	B1	Clone from population collected at Coconut Island in Kaneohe Bay, HI
B. minutum		
CCMP830	B1	*Exaiptasia pallida* isolate collected at Bermuda Biological Station, Bermuda
FLAp2	B1	*Exaiptasia pallida* isolate collected at Long Key, FL
Mf1.05b	B1	*Orbicella faveolata* isolate collected at the Florida Keys, Florida
B. psygmophilum		
HIAp	B2	*Exaiptasia pallida* isolate collected at Kaneohe Bay, Hawaii

Appendix Table B2: Cell cycle distribution in Symbiodiniaceae cultures and isolates

					Log-Growth Phase			Stationary Phase		
Species Name	**ITS2 Type**	**Strain (ID)**	**Source Organism**	**Culture or isolate**	**G1 (%)**	**S (%)**	**G2 (%)**	**G1 (%)**	**S (%)**	**G2 (%)**
B. minutum	B1	CCMP 830	*Exaiptasia pallida*	Culture	73.4 (2.3)	10.0 (2.3)	14.4 (0.7)	93.6 (1.1)	3.7 (0.8)	2.3 (0.3)
		Ap2	*Exaiptasia pallida*	Culture	79.5 (0.7)	4.1 (0.7)	15.4 (0.3)	93.6 (0.3)	2.2 (1.3)	2.1 (1.9)
		FLAp2	*Exaiptasia pallida*	Culture	76.0 (1.3)	8.4 (1.0)	14.9 (0.5)	94.2 (3.1)	4.1 (2.1)	0.7 (0.6)
		Mf 1.05b	*Orbicella faveolata*	Culture	89.3 (6.4)	2.8 (1.2)	7.4 (7.1)	94.6 (0.2)	3.2 (2.7)	0.1 (0.1)
B. psygmophilum	B2	HIAp	*Exaiptasia pallida*	Culture	81.1 (3.5)	7.5 (3.0)	11.1 (2.9)	96.0 (0.4)	1.4 (0.2)	2.5 (0.4)
					Nitrogen-replete			**Nitrogen-limited**		
B. minutum	B1	Mf 1.05b	*Orbicella faveolata*	Culture	98.7 (1.1)	1.9 (0.5)	0.8 (0.3)	94.3 (1.0)	3.6 (0.2)	0.0 (0.0)
B. psygmophilum	B2	HIAp	*Exaiptasia pallida*	Culture	91 (1.6)	2.9 (0.6)	2.5 (1.1)	81.2 (2.2)	19.3 (1.5)	0.4 (0.1)
					In Symbiosis					
B. minutum	B1	H2 isolate	*Exaiptasia pallida*	Freshly isolated	72.0 (4.3)	21.2 (5.24)	0.8 (0.3)			
		VWA12 isolate	*Exaiptasia pallida*	Freshly isolated	77.9 (11.9)	16.6 (7.8)	3.7 (3.1)			
		VWB9 isolate	*Exaiptasia pallida*	Freshly isolated	82.2 (2.2)	13.0 (3.2)	4.0 (0.6)			
B. psygmophilum	B2	JK isolate	*Exaiptasia pallida*	Freshly isolated	54.1 (7.2)	36.5 (7.7)	2.3 (0.7)			

All numbers represent averaged cell cycle percentages of cultures and isolates as determined by the Dean Jet Fox model (n = 3). Numbers in parentheses represent standard deviation.

7.3 Appendix C: Supplementary materials for Chapter 4

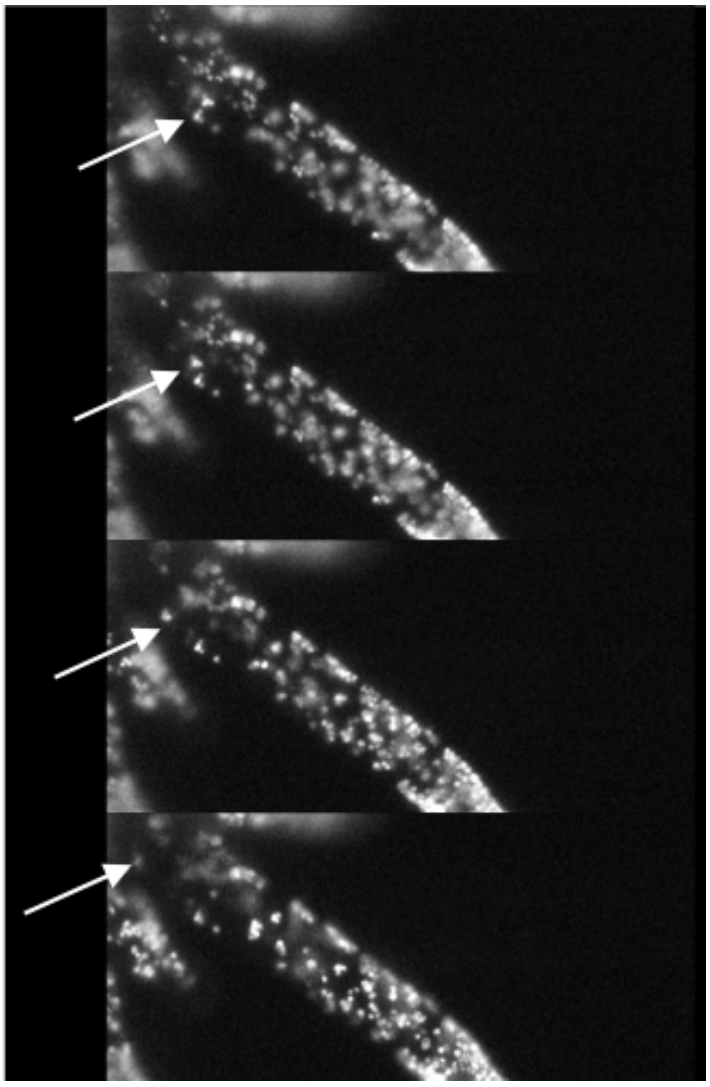

Appendix Figure C1: Gastrovascular circulation of symbiont clusters during bleaching

Directly following thermal stress, *B. minutum* populations were observed to be circulating within the gastrovascular cavity of Aiptasia polyps. An example of one such symbiont cluster is shown above, traveling from the tentacle of an anemone out to the pharynx and body column.

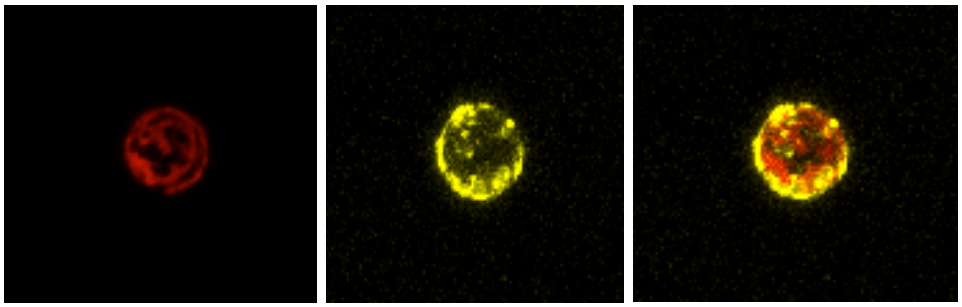

Appendix Figure C2: DiI labeling of Symbiodiniaceae

Symbiodiniaceae species were fluorescently labeled with DiI (middle panel) and DiO (not shown). Cells were imaged to monitor both autofluorescence (left) and dye uptake. Shown above is *Symbiodinium pilosum*. Imaging was performed on a Zeiss LSM 780 NLO Confocal Microscope System in collaboration with John Parkinson.

7.3 Appendix D: Effects of nutritional state and symbiont competition in Aiptasia

The effect of nutritional state on host cell cycle and symbiont competition within the model sea anemone Aiptasia.

Trevor R. Tivey[1*], Virginia M. Weis[1]

[1]Department of Integrative Biology, Oregon State University, Corvallis, OR, USA

Summary

We examined the cell cycles of the sea anemone Aiptasia (*Exaiptasia pallida*) and its algal symbionts *Breviolum minutum* and *Breviolum psygmophilum* as a response to symbiotic state and nutritional state. Hosts in a stable symbiosis contained lower densities of cells undergoing replication compared to densities in aposymbiotic hosts. In nutritional state experiments, starvation had a large negative effect on host size but only a small negative effect on host cell cycle percentages. In comparison to the host cell cycle, symbiont cell cycles under different nutritional states revealed putative competitive shifts between species within the same host.

Introduction

In this appendix chapter we aim to describe the cell cycles of the cnidarian host Aiptasia and its dinoflagellate symbionts *Breviolum minutum* and *Breviolum psygmophilum* under different stable symbiotic states and nutritional regimes. We explored the interaction effect between stable symbiotic states and host nutritional state on the cell cycles of Aiptasia and two species of *Breviolum* that are found naturally in Aiptasia, *B. minutum* (type B1) and *B. psygmophilum* (type B2) (Lajeunesse et al., 2012). Our results suggest that Aiptasia not only alters its cell cycle progression based on its host-symbiont biomass ratios, but also houses symbionts that experience cell cycle regulation in a nutritional and species-specific manner. These results together form a broad understanding of how cell populations in hosts and symbionts respond to each other and the environment *via* their cell cycle dynamics.

Methods

Maintenance of anemones and algae

Aiptasia strains (H2 and EM5) and *Breviolum* cultures were maintained at room temperature on a 12 h:12 h light:dark cycle (40 µmol photons m^{-2} s^{-1}). Aposymbiotic anemones were generated by menthol bleaching as described previously and kept in the dark to avoid symbiont contamination (Matthews et al., 2016). Anemones were fed three

times per week with *Artemia* nauplii unless otherwise indicated. Two clonal host strains were used in experiments: H2 (collected from containing *B. minutum* [B1]) and EM5 (collected from a Texas aquarium and containing a mixture of *B. minutum* [B2] and *B. psygmophilum* [B2]). Additional experiments on cell cycle phenotypes of symbionts *in hospite* were performed to confirm observations made from symbionts in the above two host strains. These experiments were performed on symbionts from VWB9 and VWA12 containing *B. minutum*, and JK containing *B. psygmophilum*. Cell cultures of *B. minutum* (CCMP830, FLAp2, and Mf1.05b) and *B. psygmophilum* (HIAp) were grown in F/2 media as in **Chapter 3**.

Fluorescent labeling of host Aiptasia

Proportions of host cells in the different phases of the cell cycle were estimated using fluorescent labeling. Host cells that had partially or completely undergone S phase DNA-replication were visualized using direct detection of the modified thymidine analog EdU (ethynyl deoxyuridine) and host cells at the G_2/M transition were labeled with a phosphorylated histone antibody. Pilot studies determined an incubation time of 4 h for EdU-positive cells to appear in both epidermal and gastrodermal tissue; longer incubations resulted in double-positive labeled populations for S phase and G_2/M phase (data not shown). Anemones were incubated in 10 μM EdU in FSW (Click-iT EdU Alexa Fluor 555 Imaging Kit, Life Technologies, Eugene, Oregon, USA) for 4 h prior to sampling, then placed in relaxing solution (0.37 M $MgCl_2$ diluted 1:1 with FSW). Samples for host analysis were rinsed in 1X PBS (Phosphate buffered saline, pH 7.4) and placed in 1X PBS + 4% paraformaldehyde at 4ºC for overnight fixation. Fixed samples were rinsed in 1X PBS, blocked in 1X PBST (0.05% Triton-X100) for 30 min, and incubated for 1 h in the reaction mix of the Click-iT EdU Alexa Fluor 555 Imaging Kit. To detect cells in the G_2/M phase transition, tentacles were then washed in 1X PBS and stained with a 1:200 dilution of fluorescent antibody to phosphorylated-histone H3 (anti-phospho-Ser10 histone H3 conjugated to Alexafluor 488, EMD Millipore). After antibody staining, host nuclei were labeled with Hoechst 33342. Finally, tentacles were washed three final times in 1X PBS and mounted (Prolong Anti-Fade Diamond

Mountant, Life Technologies) on slides for confocal analysis using the Zeiss LSM 780 NLO Confocal Microscope System. Host nuclei labeled with Hoechst were detected by excitation at 405 nm and an emission of 443 nm. Histones labeled with anti-pSer10 AF488 were detected by excitation at 488 nm and emission of 527 nm. Nuclei labeled with EdU-AF555 were detected by excitation at 555 nm and an emission of 588 nm. *Breviolum* autofluorescence was detected by excitation at 633 nm and an emission of 684 nm. Confocal images and Z-stacks were then analyzed using Fiji (ImageJ2) with the 3D Objects Counter plugin (Bolte and Cordelieres, 2006).

Host cell cycle dynamics under different symbiotic and nutritional states

To determine the effects and interactions of symbiotic and nutritional state on host and symbiont cell cycles, aposymbiotic and symbiotic EM5 hosts were fed or starved for long- and short-term experiments. Long-term effects were determined in two experiments. For the first experiment, lasting for six weeks, aposymbiotic and symbiotic anemones were divided into two groups. One was fed three times a week and the other was starved for the duration of the experiment (n = 10 anemones per group, n = 3 tentacles per anemone). A confocal 3D Z-stack of entire tentacles was then captured. Three tentacles were imaged per anemone and treated as technical replicates to create average counts for each biological replicate anemone. The total area, host cell density (number of nuclei / mm^2 of tissue), and host cell cycle percentages (S phase: EdU-positive nuclei / total nuclei; G_2/M phase: H3Ser10-positive nuclei / total nuclei) were measured for each epidermal and gastrodermal image using the 3D Object counter plugin in Fiji (ImageJ2). A second experiment with the same four treatments was carried out for 10 weeks to explore differences in division rates between tissue layers. Individual sections (not entire Z-stacks) of representative of tentacle epidermis and gastrodermis were imaged (n = 15 anemones per group, n = 5 tentacles per anemone), and images were processed as in the first experiment.

To test the short-term effect of nutritional state on the host cell cycle in epidermal and gastrodermal tissue, symbiotic anemones were starved for 72 h. Following this, anemones were randomly divided into two groups, those that were either fed for 4 h (time

0-4 h) or left unfed. To measure S phase replication, 10 μM EdU was added to fed or starved anemones for the following incubation periods: 0-4 h, 4-8 h, 12-16 h, and 24-28 h (n = 30 anemones per group of treatment x time period). Epidermal and gastrodermal cell cycle percentages and densities were determined using confocal microscopy and image analysis as described previously.

Breviolum *cell cycle competitive dynamics in culture and* in hospite *under different nutritional states*

To assess the effect of nutritional state on cell cycles in culture and *in hospite*, *B. minutum* and *B. psygmophilum* were analyzed separately under different nutritional states (see **Chapter 3**) and also in competition. Cultures were grown in the presence and absence of a nitrogen source to examine their competitive growth rates. EM5 anemones served as a model for naturally occurring symbiont competition *in hospite*. EM5 hosts were starved or fed as previously described for two weeks prior to symbiont isolation. *Breviolum* symbionts were isolated from hosts and analyzed on a Cytoflex 4L as described in **Chapter 3**.

Results

Host cell cycle is slowed when in stable symbiotic state

The interaction of symbiotic and nutritional state on host and symbiont cell cycles was characterized by feeding or starving symbiotic and aposymbiotic anemones in a set of experiments. We will cover the effect of symbiotic state first. We hypothesized that symbiotic hosts would have a higher proportion of cells progressing through the cell cycle compared to aposymbiotic hosts. In contrast, and to our surprise, hosts in a stable symbiotic state had significantly lower percentages of cells undergoing DNA replication than did aposymbiotic hosts (**Appendix D Figure D1A**; p = 4.94e-9, Two-way ANOVA). To determine tissue-specific trends, we repeated the experiment with an increased sample size and captured images representative of the epidermal and gastrodermal layers (single representative images instead of Z-stacks used in the former experiment). The epidermis from symbiotic animals had a significantly lower percentage

of S phase cells compared to epidermis from aposymbiotic animals (**Appendix D Figure D1B**). There was no difference in percentages of S phase cells between the gastrodermis of symbiotic and aposymbiotic anemones (**Appendix D Figure D1C**). When number of S phase cells was indexed to tentacle area (shown in Figure 2F) however, patterns between aposymbiotic and symbiotic animals changed (**Appendix D Figure D1D, E**). S phase cell density in aposymbiotic tissues, both gastrodermis and epidermis, was higher than those in symbiotic tissues (**Appendix D Figure D1D, E**; $p < 0.05$, ANOVA Tukey post-hoc test). G_2/M-phase density was also higher in aposymbiotic compared to symbiotic anemones, but the difference was not significant (**Appendix D Figure D2B**).

Host cell growth is slowed under starvation but host cell cycle differences with nutritional state are more nuanced

In comparing nutritional states in the same experiments described above, tentacle size and average host cell size was larger in the presence of symbionts and under constant feeding conditions compared to aposymbiotic animals and during starvation **(Appendix D Figure D1F**; $p < 0.05$, ANOVA Tukey post-hoc test**)**. In the epidermis, nuclei density was higher in starved compared to fed hosts, in both symbiotic states, indicating a decreased average cell size in response to starvation (**Appendix D Figure D1G**; $p < 0.05$, ANOVA Tukey post-hoc test). Similar to the epidermis, in the gastrodermis of aposymbiotic hosts, starvation increased host nuclei density and decreased cell size. An opposite pattern occurred only in the gastrodermis of symbiotic hosts where starvation decreased cell density significantly (**Appendix D Figure D1H**; $p < 0.05$, ANOVA Tukey post-hoc test), indicating a larger average cell size in starved symbiotic compared to starved aposymbiotic gastrodermis. Since the changes in total nuclei density had the possibility of affecting S-phase density measurements, we compared the percentages of S-phase cells in each treatment. Starvation decreased S-phase percentages in the epidermis of symbiotic hosts (**Appendix D Figure D1B**; $p < 0.05$, ANOVA Tukey post-hoc test) but did not alter EdU-positive nuclei densities in either host gastrodermis or epidermis (**Appendix D Figure D1D, E**). To test whether there would be a stronger effect on host cell cycle progression immediately following feeding, we performed a

short-term experiment during the first 24 h after feeding (preceded by 72 h of starvation). Despite a large sample size (n = 30 anemones per treatment x time period), the percentage of EdU-positive cells did not change with feeding (**Appendix D Figure D2C, D**). There was a trend of higher percentages post-feeding in the gastrodermis, but the difference was not significant (**Appendix D Figure D2D**; $F = 3.69$, $p = 0.056$, ANOVA). EdU-positive densities were also not significantly different between treatments (data not shown). Overall, the effect of nutritional state on the host cell cycles was more nuanced than the effect of symbiotic state, regardless of treatment duration.

Competition of Breviolum *cell cycles in response to symbiotic and nutritional state*

Since there were measurable differences between symbiont cell cycles and their responses to nutritional state in culture and *in hospite* (**Appendix D Figure D3A, B,** also see **Chapter 3**), we examined symbiont cell cycles in culture together. Nitrogen-rich cultures had roughly equal G_1 population peaks for *B. minutum* and *B. psygmophilum*, indicating that their relative density was about equal (**Appendix D Figure D3C**). In contrast, nitrogen-limited cultures had a strong effect on the G_1 peak of *B. psygmophilum*. As made evident in the combined cell cycle profile panel (**Appendix D Figure D3C**), B. psygmophilum lost its G_2M population and experienced a widening G_1 peak distribution (increased CV). These phenotypes resulted in a lower overall symbiont density compared to the G_1 peak of *B. minutum*, which appeared relatively unaffected by nitrogen-limitation. The cell cycle dynamics of naturally co-occurring symbionts were also measured. Co-occurring symbionts were not expected within Aiptasia strains, therefore the initial symbiont cell cycle analysis of EM5 anemones required confirmation through cell cycle profile comparisons to Aiptasia strains hosting only *B. minutum* and *B. psygmophilum*. Sanger sequencing of the ITS2 locus and Sym15 microsatellite region confirmed the presence of *B. psygmophilum* but not that of *B. minutum*. However, the asymmetric amplification of sequences may mask the sequence of *B. minutum*, therefore denaturing gradient gel electrophoresis (DGGE) may be necessary to resolve symbiont identity. The cell cycles of symbionts from EM5 anemones were further compared under fed and starved conditions. Under fed conditions, the putative G_1 peak of *B.*

psygmophilum was significantly increased (**Appendix D Figure D3D** $p < 1 \times 10^{-7}$, ANOVA Tukey post-hoc test). Isolates from fed anemones also exhibited small G_2M peaks at 2x the DNA content as the *B. psygmophilum* peak. Under starved conditions, the putative peak of *B. minutum* was dominant, whereas the putative G_1 peak of *B. psygmophilum* and its G_2M peak were decreased in population (**Appendix D Figure D3D**).

Discussion

Constraints on the host cell cycle during stable symbiosis is correlated to cellular and tissue space limitations in the gastrodermis

In contrast to the correlation between proliferating host nuclei and symbionts during recolonization, we found that anemone tissues had fewer cells entering S phase during the stable symbiotic state (i.e. when hosts are fully populated with *Breviolum* cells) compared to the stable aposymbiotic state (**Appendix D Figure D3**). The significant difference in S phase populations between symbiotic and aposymbiotic tissues is a strong indicator of comparative restriction during G_1 phase in symbiotic anemones. One reason for this difference may be a cell size requirement for symbiont-containing gastrodermal cells because they are harboring relatively large (~5-10 μm in diameter) symbionts in their cells. In our study, symbiotic gastrodermal cells were larger in size compared to aposymbiotic gastrodermal cells, based on lower nuclei density (**Appendix D Figure D3H)**. Symbiotic cell populations accommodating new symbionts might therefore require longer G_1 phases to grow in size.

In addition, this G_1 restriction in symbiotic compared to aposymbiotic anemones correlates with gastrodermal tissue space availability (**Appendix D Figure D3E, F**). The symbiotic gastrodermis, at least in tentacles (the structures examined in this study), has limited space in which host cells containing symbionts reside. In tentacles, the gastrodermis is a cylinder within a cylinder of epidermis: constrained on the outside and only able to expand on the inside by reducing the gastrodermal cavity space. Without a large population of symbiotic algae, there is little spatial constraint because the gastrodermis is relatively thin, and the gastrovascular cavity is large. In symbiotic

anemones, however, the gastrodermal tissue makes up a much larger percentage of tentacle thickness, dramatically shrinking the gastrovascular cavity. In many cnidarians, tissue layers are limited in thickness in a manner consistent with maximal rates of nutritional and gas exchange (Patterson, 1992). Tissue thickness is important for cnidarian symbioses, and may explain different symbiont assemblages such as the shifted latitudinal gradients between the thinner-walled *Anthopleura elegantissima* and thicker-walled *Anthopleura xanthogrammica* (Dimond et al., 2012). The thickness of the symbiotic gastrodermal layer is limited possibly as a result of self-shading and available nutrition for the symbionts (Jones and Yellowlees, 1997). In contrast, aposymbiotic anemones and those undergoing recolonization are less limited in gastrodermal space than symbiotic anemones since they lack dense populations of algae.

These cell- and tissue-level spatial constraints on symbiotic hosts have been hypothesized to affect the regulation of symbiont populations, through either symbiont expulsion, degradation, or inhibition of population growth (Davy et al., 2012). The G_1 cell cycle arrest of host gastrodermal cells in symbiotic compared to aposymbiotic anemones may be one pre-mitotic control mechanism used to inhibit *Breviolum* cell growth. In this scenario, host gastrodermal cells in G_1 would not undergo division even as algal cells divide, limiting the accessible space and available nutrients for further endosymbiont growth and division. One study uncovered such a scenario: as *Breviolum* cell density increases, *Breviolum* cell size and mitotic index decreases (Jones and Yellowlees, 1997). On the other hand, the host G_1 cell cycle arrest leading to high algal density rates may also prompt post-mitotic control of *Breviolum* cells. For example, Aiptasia has been shown to preferentially expel symbionts undergoing division during stable symbiosis but not during recolonization (Baghdasarian and Muscatine, 2000). This expulsion may be a form of post-mitotic control that is symbiont density-dependent in order to maintain healthy host:symbiont biomass ratios.

G_1 cell cycle arrest is also observed in the epidermal cells of symbiotic hosts compared to aposymbiotic hosts (**Appendix D Figure D3B, D**). Fransolet et al. measured a similar expansion of host epidermal cell proliferation when symbiotic Aiptasia were treated with DCMU, rendering their symbionts unable to photosynthesize. The authors

suggested that higher epidermal proliferation in aposymbiotic state is a form of tissue adaptation that results from the switch in energy sources between the two symbiotic states, since aposymbiotic anemones rely entirely on heterotrophic prey capture for survival (Fransolet et al., 2014). Regardless of the mechanistic explanation for either tissue, there is an organism-wide decrease in cell cycle populations when hosts are maintaining stable symbiont populations, which illustrates the potential role of the host cell cycle in response to symbiotic state.

Starvation predominantly slows host cell growth but subtly affects cell proliferation

The S phase decrease under starvation is more nuanced compared to findings in the sea anemone *Nematostella vectensis*, where S phase percentages were found to significantly decrease corresponding to number of weeks post-feeding (Passamaneck and Martindale, 2012). In *Hydra*, epithelial cell proliferation rate also decreases in response to starvation, but similar to our study, tissue area loss is not fully explained by this reduction in proliferation (Bosch and David, 1984; Otto and Campbell, 1977).

Of note, symbiotic gastrodermal tissue had a unique trend in cell density compared to other tissues. Starved anemones had lower cell densities and increased cell sizes compared to fed anemones in the symbiotic gastrodermis (**Appendix D Figure D2H**). An explanation for this difference could be the preferential retention of cells containing symbionts over those without symbionts, which would increase overall host cell size and lower cell density. To better determine cell fate, future studies should address the role of apoptosis alongside host cell cycle and proliferation.

Co-occurring Breviolum *species continue to exhibit species-specific cell cycles and influence relative population dynamics in culture and* in hospite

Nutrition had a much stronger effect on the cell cycles of *Breviolum* than on their cnidarian hosts (see **Chapter 3**). Breviolum species continued to differ in their responses to nutrition when in competition in culture and *in hospite*. In both environments, *B. minutum* cell cycles are less impacted by limited nutrition than *B. psygmophilum.* Similar to results found in **Chapter 3**, *B. psygmophilum* cultures and isolates appear more

sensitive to changes in nutrition, and take competitive advantage of these dynamics when in nutrient-replete hosts. Overall, the *Breviolum* species in association with their Aiptasia hosts responded to symbiotic and nutritional conditions in a species-specific manner.

Further considerations and possibilities regarding naturally co-occurring symbionts

From our results in the EM5 strain of Aiptasia, it is highly likely that we captured a mixed population of symbionts with two G_1 phase peaks of DNA. However, we saw no evidence of two populations in Sanger sequencing of ITS2 and Sym15 loci. Furthermore, the second G_1 peak was found between the G_1 and G_2/M populations at approximately 1.5 x mean fluorescence intensity of the G_1 population *in hospite*. This peak could hypothetically represent a form of S-phase cell cycle arrest, but the 2x distance between the second G_1 peak and the small G_2M peak does not support this S-phase arrest hypothesis. It is also possible but unlikely that the left-most peak of DNA in isolates from EM5 hosts instead represents a sub-G_1 population of apoptotic cells (Darzynkiewicz et al., 1992; Riccardi and Nicoletti, 2006), however this phenotype was repeatedly measured in EM5 isolates alongside other samples, and no other isolates or cultures had anything resembling apoptotic peaks in our cell cycle analysis (including *B. psygmophilum*-containing JK).

References

Baghdasarian, G., and Muscatine, L. (2000). Preferential expulsion of dividing algal cells as a mechanism for regulating algal-cnidarian symbiosis. *Biol. Bull.* 199, 278–86.

Bolte, S., and Cordelieres, F. P. (2006). A guided tour into subcellular colocalization analysis in light microscopy. *J. Microsc.* 224, 213–232. doi:10.1111/j.1365-2818.2006.01706.x.

Bosch, T. C., and David, C. N. (1984). Growth regulation in Hydra: relationship between epithelial cell cycle length and growth rate. *Dev. Biol.* 104, 161–171. doi:10.1016/0012-1606(84)90045-9.

Darzynkiewicz, Z., Bruno, S., Del Bino, G., Gorczyca, W., Hotz, M. A., Lassota, P., et al. (1992). Features of apoptotic cells measured by flow cytometry. *Cytometry* 13, 795–808. doi:10.1002/cyto.990130802.

Davy, S. K., Allemand, D., and Weis, V. M. (2012). Cell Biology of Cnidarian-Dinoflagellate Symbiosis. *Microbiol. Mol. Biol. Rev.* 76, 229–261. doi:10.1128/MMBR.05014-11.

Dimond, J. L., Holzman, B. J., and Bingham, B. L. (2012). Thicker host tissues moderate light stress in a cnidarian endosymbiont. *J. Exp. Biol.* 215, 2247–2254. doi:10.1242/jeb.067991.

Fransolet, D., Roberty, S., and Plumier, J. C. (2014). Impairment of symbiont photosynthesis increases host cell proliferation in the epidermis of the sea anemone Aiptasia pallida. *Mar. Biol.*, 1735–1743. doi:10.1007/s00227-014-2455-1.

Jones, R. J., and Yellowlees, D. (1997). Regulation and control of intracellular algae (= zooxanthellae) in hard corals. *Philos. Trans. R. Soc. B Biol. Sci.* 352, 457–468. doi:10.1098/rstb.1997.0033.

Lajeunesse, T. C., Parkinson, J. E., and Reimer, J. D. (2012). A genetics-based description of Symbiodinium minutum sp. nov. and S. psygmophilum sp. nov. (Dinophyceae), two dinoflagellates symbiotic with cnidaria. *J. Phycol.* 48, 1380–1391. doi:10.1111/j.1529-8817.2012.01217.x.

Matthews, J. L., Sproles, A. E., Oakley, C. A., Grossman, A. R., Weis, V. M., and Davy, S. K. (2016). Menthol-induced bleaching rapidly and effectively provides experimental aposymbiotic sea anemones (Aiptasia sp.) for symbiosis investigations. *J. Exp. Biol.* 219, 306–310. doi:10.1242/jeb.128934.

Otto, J. J., and Campbell, R. D. (1977). Tissue economics of hydra: regulation of cell cycle, animal size and development by controlled feeding rates. *J. Cell Sci.* 28, 117–132.

Passamaneck, Y. J., and Martindale, M. Q. (2012). Cell proliferation is necessary for the regeneration of oral structures in the anthozoan cnidarian Nematostella vectensis. *BMC Dev. Biol.* 12, 34. doi:10.1186/1471-213X-12-34.

Patterson, M. R. (1992). A chemical engineering view of cnidarian symbioses. *Am. Zool.* 32, 566–582. doi:10.1093/icb/32.4.566.

Riccardi, C., and Nicoletti, I. (2006). Analysis of apoptosis by propidium iodide staining and flow cytometry. *Nat. Protoc.* 1, 1458–1461. doi:10.1038/nprot.2006.238.

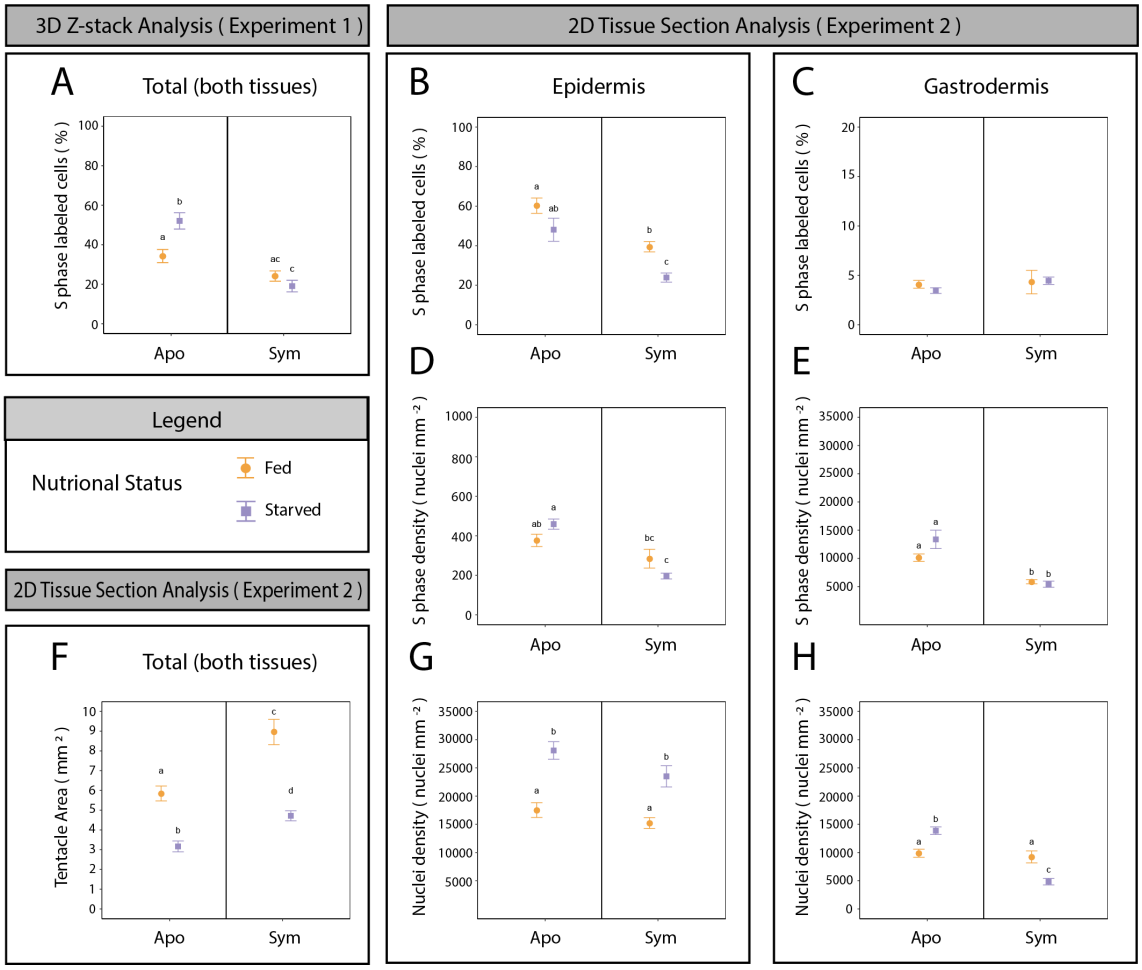

Appendix Figure D1: Host cell cycle and cell density in response to symbiotic and nutritional state.

S-phase percentages and densities were measured as a function of two treatments: symbiotic (aposymbiotic and symbiotic) and nutritional state (fed and starved). For each treatment group, cell populations undergoing S phase incorporated EdU, which was visualized via Click-IT EdU AF555. The percentage of EdU-positive S phase cells (**A**) was first measured in confocal Z-stacks of anemone tentacles (n = 10 anemones, 3 tentacles per anemone). In a second experiment (n = 15 anemones, 5 tentacles per anemone), the percentages of EdU-positive S phase cells in the epidermis **(B)** and the gastrodermis **(C)** were measured, and S phase densities (**D, E**) were determined by normalizing S-phase positive cells to total tissue area of the tentacle (**F**). Total nuclei densities of the epidermis (**G**) and gastrodermis (**H**) were also measured. In all graphs, purple squares represent the mean of fed groups and orange circles represent the mean of starved groups. Error bars represent standard error. Letters indicate significant differences between groups ($p < 0.05$, ANOVA, Tukey's *post-hoc* test).

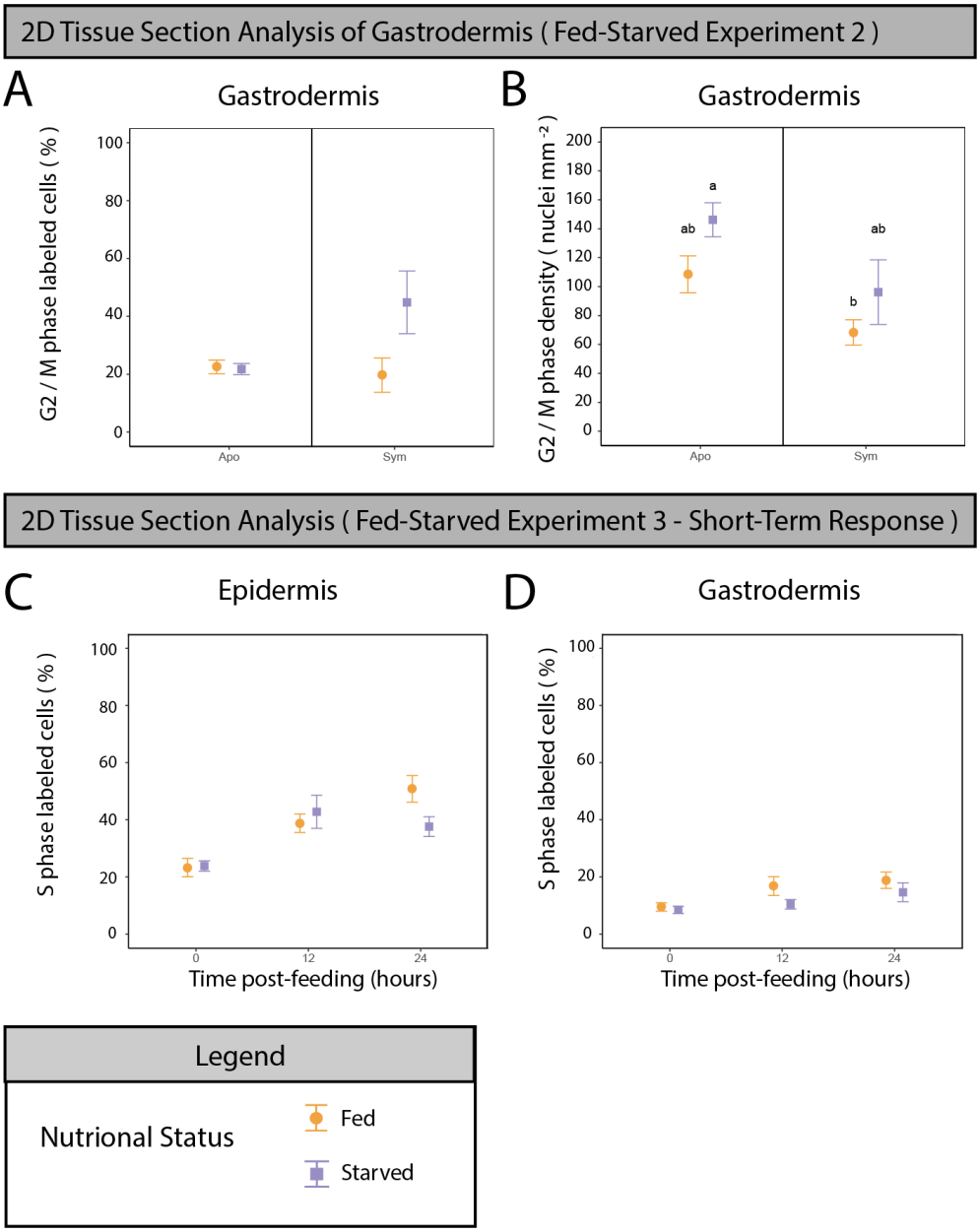

Appendix Figure D2: Additional effects of feeding and starvation on host cell cycle.

G_2M phase percentages (**A**) and densities (**B**) were measured for the gastrodermal tissue in the long-term nutrition experiment (n = 15 anemones, 5 tentacles / anemone). In addition, a short-term feeding experiment was performed after 72 h of starvation for both fed and starved treatments. The host cell cycle was analyzed in the epidermis (**C**) and gastrodermis (**D**) during three timepoints post-feeding compared to unfed anemones (n = 30 anemones per group per timepoint). In all graphs, purple squares represent the mean of fed groups and orange circles represent the mean of starved groups. Error bars represent standard error. Letters indicate significant differences between groups ($p < 0.05$, ANOVA, Tukey's *post-hoc* test).

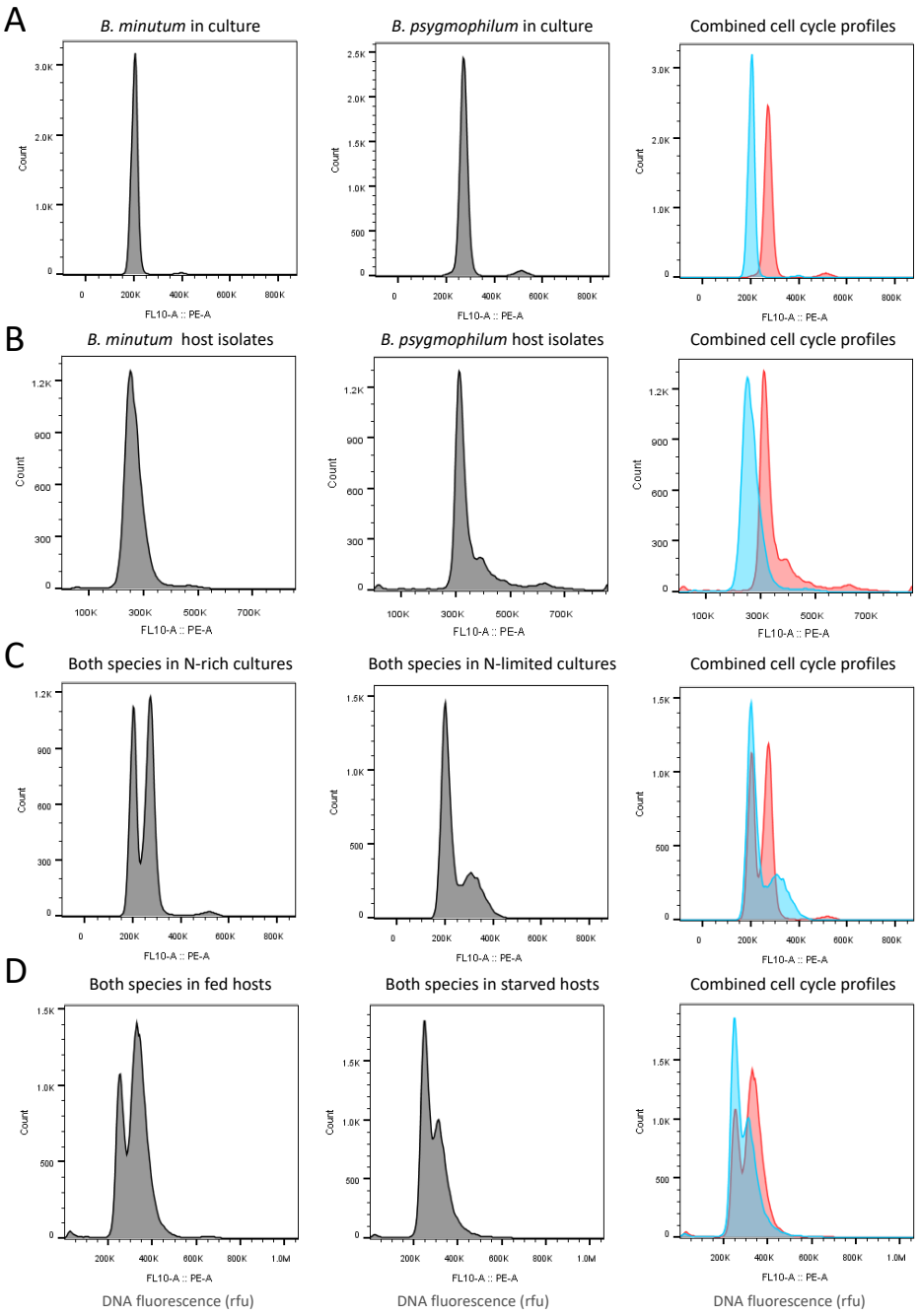

Appendix Figure D3: Cell cycles of *Breviolum* species in competition in culture and *in hospite*

Cell cycle profiles from propidium iodide labeling are show for two *Breviolum* species. The cell cycles of *B. minutum* and *B. psygmophilum* were measured separately in culture (**A**) and in hospite (**B**) to confirm the relative fluorescent intensity of DNA content of the two species. Cell cultures of both species were examined under nitrogen-rich and nitrogen-limited culture conditions (**C**). The cell cycles of Breviolum species were examined in Symbiodiniaceae isolates from fed and starved hosts (**D**).

7.4 Appendix E: Responses of host cell cycles to light and temperature

Methods:

Temperature experiments

To test the effect of thermal stress on host and symbiont cell cycles, symbiotic VWA12 anemones from were plated and exposed to ambient (25ºC) or elevated (33ºC) under the same light conditions (12h:12h light:dark cycle, 40 µmol photons m^{-2} s^{-1}). Anemones were sampled at 4, 8, 16, and 28 hours post-treatment. Samples were incubated for four hours in 10µM EdU prior to collection. Twelve anemones were sampled from each group at each timepoint, and all samples were processed for confocal analysis as described in **Appendix D** and **Chapter 3**.

Light/dark experiments

To examine the effect of light on cnidarian host cell cycle, 30 symbiotic anemones were collected at 6 timepoints (n = 5) over a period of 24 h in a 12:12 light:dark (LD) cycle. Anemones were incubated in 10 µM EdU in FSW for four hours prior to collection and fixation in 4% paraformaldehyde in 1X PBS. Samples were further labeled using the Click-IT EdU 555 kit and a phospho-Ser10-H3 antibody conjugated to Alexafluor 488, which labeled S-phase incorporation and G_2M phase populations respectively (see **Appendix C** for details). Host cell percentages were normalized to total host cells labeled using Hoechst. To test the effect of light cycle on symbiont and host cell cycles, 144 symbiotic VW9 anemones (containing *B. minutum*) were divided into groups of 48 anemones under three light regimes – 24h:0h (LL), 12h:12h (LD), and 0h:24h (DD). Six individual anemones from each treatment were collected at each timepoint beginning in the dark at end of the LD cycle, one hour before the next experimental light cycle was scheduled to begin. To measure S-phase incorporation as a proxy for host cell division, anemones were incubated in 10µM EdU for six hours and collected every six hours for 48 hours. All EdU treatments therefore began six hours prior to collection. Prior to fixation, tentacles were sampled for confocal analysis of host tissues and the rest of the animal was homogenized for symbiont isolation and flow cytometry (as described in **Chapter 3**).

Results:

Thermal stress immediately arrests the host cell cycle

During the first four hours of heat stress, the fraction of host nuclei that were mitotic decreased significantly compared to control treatments, as evidenced by Histone H3ser10 AF488 staining (**Appendix E Figure E1**). This response was immediate but temporary; mitotic cells percentages returned to control treatment levels within 24 hours.

Gastrodermal cells and symbionts may be coordinated only under diel conditions

To examine the effect of the diel cycle on host and symbiont cell cycles, we performed two light cycle experiments. In both experiments, we found high variation across samples and no clear diel patterns. In a one-day experiment examining only hosts, the S-phase cell population percentage was significantly higher in the afternoon (**Appendix E Figure E2**; $p < 0.05$, ANOVA, Tukey's post-hoc test). G_2M percentage was similarly increased during the afternoon but was only significantly higher than the 10 pm-2 am timepoint (**Appendix E Figure E2**; $p < 0.05$, ANOVA, Tukey's post-hoc test). In a subsequent experiment measuring both hosts and symbionts across two days, no significant cell cycle patterns were found. S-phase population trends in *B. minutum* were similar to host gastrodermal S-phase populations trends under normal L:D conditions, indicating possible coordination (**Appendix E Figure E3A,B**). *B. minutum* cells and their host gastrodermal cells lost their synchronization under total dark (DD) or light (LL) conditions. Under total darkness, *B. minutum* cells had the highest S-phase percentages separated by 48 hours, exhibiting a possible two-day cycle, whereas gastrodermal host cell division only decreased. Under constant light conditions, S-phase populations in *B. minutum* showed a nonsignificant increase over two days. In the epidermis, S-phase populations had an opposite trend compared to the gastrodermal cells under LD conditions (**Appendix E Figure E3C.**). Under LL and DD conditions there was no discernible pattern.

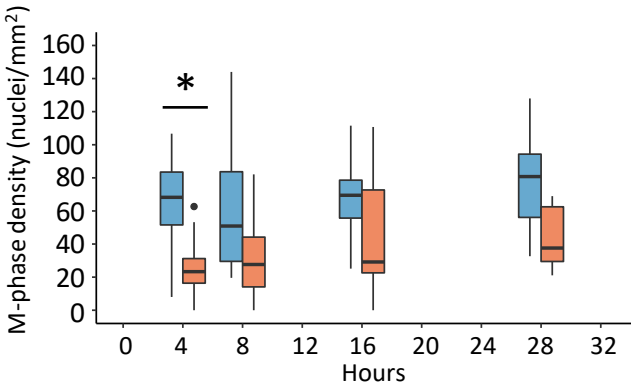

Appendix Figure E1: Host mitotic cell density as a function of temperature stress over 24 hours.

Anemones responded to heat stress immediately by halting the cell cycle, then acclimated over time. Twelve anemones were sampled from control (blue) and heat (orange) treatment at each timepoint post-temperature increase (n = 12, hours of treatment shown at top). Cell density of mitotic cells (Histone H3ser10 AF488 positive) was measured from confocal section images of tentacles. The asterisk indicates a significance difference as evaluated by a two-tailed t test ($p = 0.01$). Boxplot conventions as in previous figures.

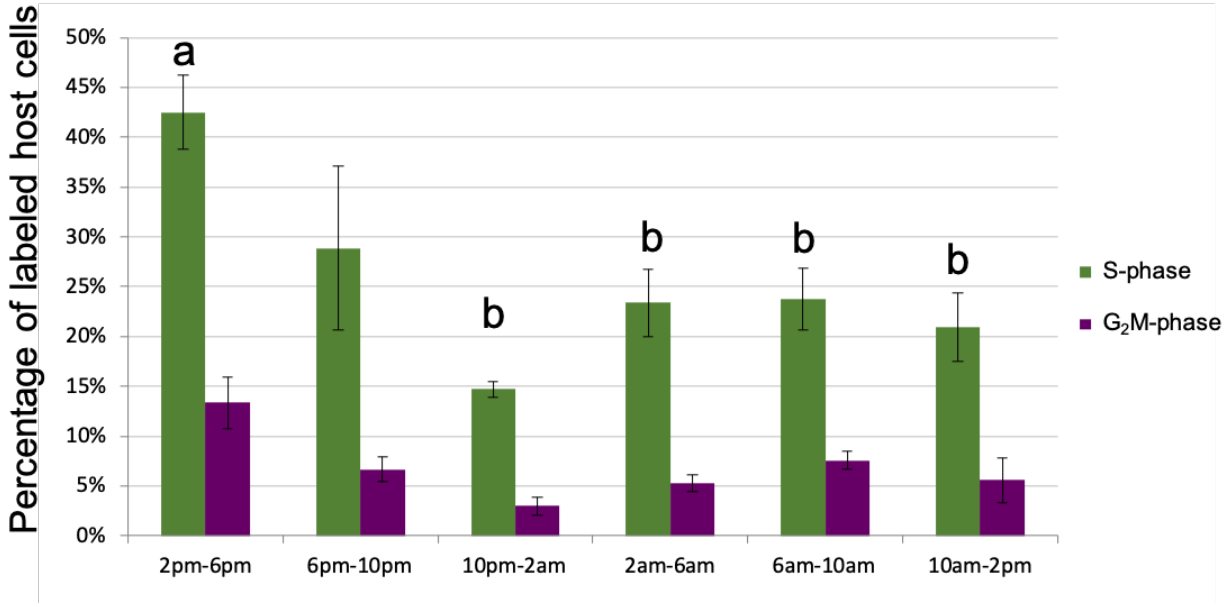

Appendix Figure E2: Host cell cycle over a 24 hour diel period.

The host cell cycles of symbiotic Aiptasia polyps were measured over a 24-hour period. S-phase populations were measured through four hours of EdU incorporation, and G_2M phase populations were measured *via* an antibody to phosphorylated histone H3. Cell population percentages were normalized to total host nuclei using Hoechst staining. Letters represent significant differences between S-phase percentages ($p < 0.05$, ANOVA, Tukey's post-hoc test). There was one significant comparison between G_2M-phase percentages (between 2pm-6pm and 10pm-2am) which is not shown for simplification and figure clarity.

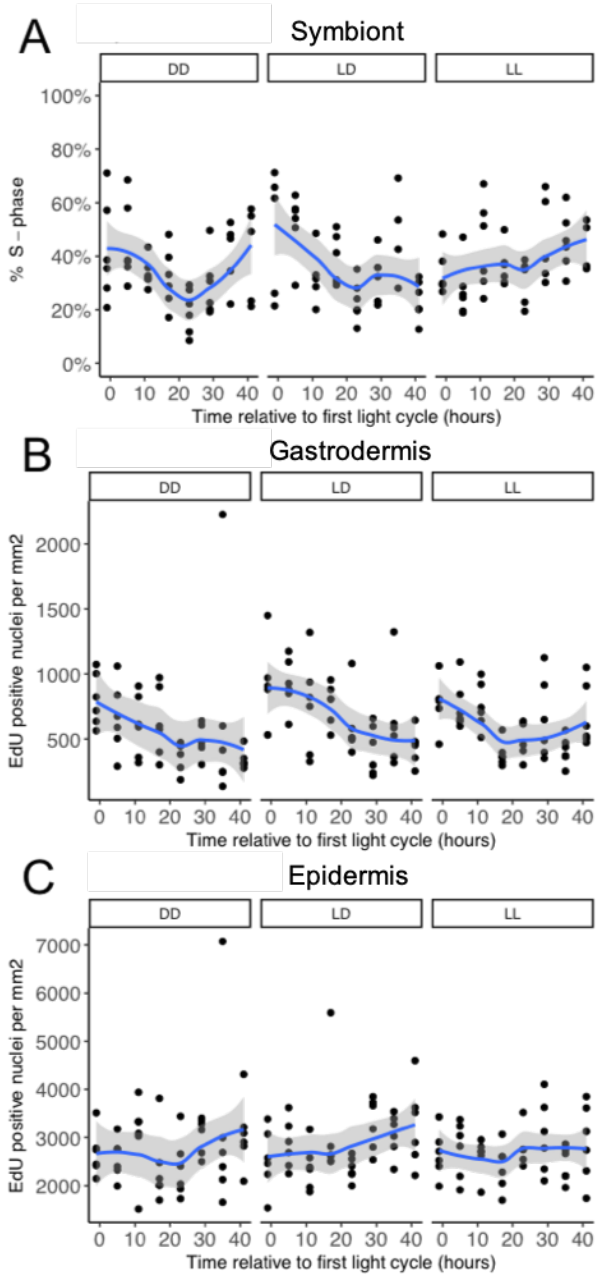

Appendix Figure E3: Diel cell cycle variation in paired hosts and symbionts.

Six anemones were sampled for each six hour timepoint over a 48-hour dark:dark (DD), light:dark (LD), and light:light (LL) treatments. (n = 6, time of day on x-axis). All treatments began during the last hour of the dark phase of a natural LD cycle and continued into their respective treatments. DD treatments therefore had experienced 12h + 42h of darkness. LL treatments experienced 42h of light after their first measurement in darkness. LD treatments experienced light during the collection timepoints ending at hours 5, 11, 29, and 35. Symbiodiniaceae S-phase percentages **(A)** were analyzed via flow cytometry, and host S-phase populations were analyzed via fluorescent microscopy in the gastrodermis **(B)** and epidermis **(C)**. Boxplot conventions as in previous figures.